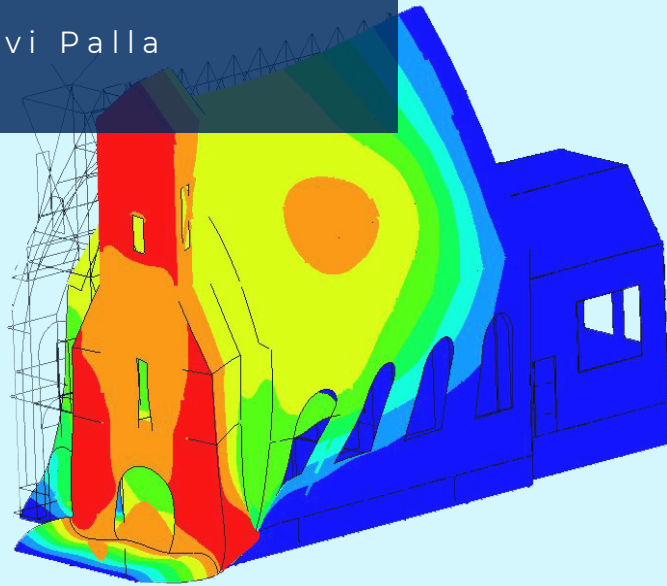# Numerical Prediction of the Dynamic Properties of a Historic Masonry Structure

A Case study of The Old Church in Garrelsweer, Groningen.

Pallavi Palla

TUDelft

NUMERICAL PREDICTION OF THE DYNAMIC PROPERTIES OF A HISTORIC MASONRY STRUCTURE

A Case Study of The Old Church in Garrelsweer, Groningen.

Masters Graduation Thesis

for the partial fulfilment of the Master of Science in Civil Engineering and Geo-Sciences
at Delft University of Technology

by

Pallavi Palla

GRADUATION COMMITTEE

Thesis Committee

Committee Chair
Dr. Rita Esposito
Department of Applied Mechanics

Daily Supervisor
Dr. Francesco Messali
Department of Applied Mechanics

Committee Member
Dr. Giorgia Giardina
Department of Geo-engineering

Committee Member
Michele Mirra, M.Sc.
Department of Bio-based Structures and Materials

Masters Student

Pallavi Palla (5019419)
Track: Structural Engineering
Specialization: Structural Mechanics
MSc Civil Engineering and Geo-Sciences

ACKNOWLEDGEMENT

This Master thesis is performed at Delft University of Technology during the academic year of 2020-21. The basis for this thesis stemmed from the idea of time and computationally effective estimation of dynamic properties of a complex structure subjected to seismic damage.

I could not have achieved my current level of success without a strong support group. First of all, my parents, who supported me with love and inspired me to dream bigger every single day. Lastly, my friends who helped me and kept me motivated throughout. Thank you all for your unwavering support.

Pallavi Palla
Delft University of Technology
Delft, The Netherlands.

SUMMARY

The gas production in the Groningen gas field of the Netherlands has caused a significant amount of shallow-human induced earthquakes. Among various building typologies, Groningen is home to many Dutch historical churches constructed by unreinforced masonry which has shown to be highly vulnerable to these earthquakes. From the perspective of conservation and prevention of loss of our historical and cultural heritage, the structural assessment of these churches and their monitoring is of importance.

The assessment of the seismic performance of historic churches is a challenging task because of their unique design, governed by macro element behaviour and non-linear material behaviour. An accurate and reliable earthquake resistant assessment with appropriate numerical modelling of the structure and proper assumptions of all the uncertainties is crucial. The structural monitoring cannot be applied to all historical churches. By selecting representative case studies, in-depth study regarding both numerical modelling and structural monitoring are possible. This information can then serve engineers and professionals to evaluate similar structures. The research gap lies in accurate modelling of historical churches to achieve reliable and faster results by linear dynamic modelling.

The fundamental modes, eigen-frequencies and modal shapes, geometry and material properties, boundary conditions, connections between structural elements and loading variations are studied using 3D models with shell elements of the case-study.

Although, the models described cannot closely represent the real structure. Firstly, a regular thickness has been assigned to masonry walls and piers despite their irregularities. Secondly, the material properties have been estimated from similar structures in Groningen, and may not represent the actual material characteristics of this case study. Thirdly, the cavity ties has been disregarded because they have been assumed to be corroded (no actual information was available). Finally, the concrete slab at the entrance of the church is disconnected to the foundation, which was an approximation from the drawings but could not be verified.

For the case-study prior structural retrofitting (models 1-5); Numerical Model 3 with eliminated foundation and timber flooring and a rigid base at the ground level is expected to give the best approximation of dynamic response of the church. The fundamental frequency in X direction of the case-study prior structural retrofitting can be approximated between 2.30Hz to 2.75Hz and the fundamental frequency in Y direction between 3.0Hz to 3.45Hz. The fundamental global modes in this model show maximum deformation in the timber roof of the main-structure and tip of the bell-tower in global

X and Y directions. This indicates weakness of the case-study prior structural retrofitting.

The Old Church has undergone structural retrofitting in July 2018, to prevent further seismic damage on the structure. From the survey of the case-study and the retrofitting measures, the recent findings (eg., cavity walls, installation of steel frame, steel and timber columns) are incorporated into the finite element model of the case-study and various modelling variations are presented in models 6 to 10. From comparing the results of these models post structural modifications, Numerical Model-8 (or Model-9 which has almost similar results) with degraded material properties of masonry and timber diaphragms, a shallow masonry step foundation and a rigid base at the foundation level are predicted as the closest approximation of the dynamic properties of the church. The fundamental frequency of the case-study post structural retrofitting can be predicted to lie between 1.5Hz-2.6Hz in global X direction and between 1.1Hz-1.65 Hz in global Y direction. It can be observed that the implemented measures make the church stiffer and the weakness of the structure post structural retrofitting is localised at masonry facade walls of the bell-tower, cavity wall between the bell-tower and main-structure, tip of the bell-tower, lateral walls and timber roofing of the main-structure.

This research on simulating a numerical model that closely represents the dynamic properties of the Old Church in Garrelsweer for achieving reliable, computationally effective and faster results. This can be used as a basis to compare the results of ambient vibration testing and operational modal analysis, and a relevant guide to study how the numerical models can be defined for modelling similar structures.

Keywords: Historical masonry churches, Dynamic response, Numerical modelling, Eigenvalue analysis, Fundamental frequency, Curved shell finite elements, Groningen.

ACRONYMS

URM - Un-Reinforced Masonry
EMM - Engineering Masonry Model
TCSM - Total Strain-based Cracking Masonry model
EMPF - Effective Mass Participation Factor
CEMPF - Cumulative Effective Mass Participation Factor

CONTENTS

1

INTRODUCTION

This chapter gives the general context of this thesis, states the main research question and provides an overview of the following chapters.

1.1. BACKGROUND & RESEARCH MOTIVATION

The Groningen gas field, located in the north of Netherlands is one of the world's largest gas fields (2,800 billion m³) with a significant volume of gas still present in the field today. It was discovered in 1959 and NAM has been producing Groningen natural gas since 1963. NAM supplies 75% of the natural gas required by Dutch households and businesses and 93% of all Dutch households use natural gas. Natural gas accounts for 45% of all the energy that is used in the Netherlands and the Groningen gas field supplies gas to 98 percent of the population of the Netherlands. After 55 years of extraction, the 900 km2 large Groningen field still holds about 600 billion cubic meters out of the original 2800 billion cubic meters (bcm). In principle, this would allow for a further 30 years of extracting at an average annual extraction of 20 bcm. [1]

However, in the past decades, gas production in the province of Groningen have caused a significant amount of shallow human-induced earthquakes. An induced seismicity event in the field was first recorded in 1991 with local magnitude (ML) 2.4. In the subsequent years, there have been more than 1,300 registered small-magnitude earthquakes. On August 16, 2012, an earthquake with a magnitude of 3.6 on the Richter scale occurred near Huizinge which was the largest one so far and this earthquake was felt more strongly by residents than previous seismic activity.[2]. Groningen has been turned into the spearhead of the research related to induced seismicity in recent years as it is the most intensely populated area in the world with many induced earthquakes. The induced seismicity is obviously due to increasing reservoir (porous sandstone) compaction along many faults, which seem to become more critical as gas extraction continues.
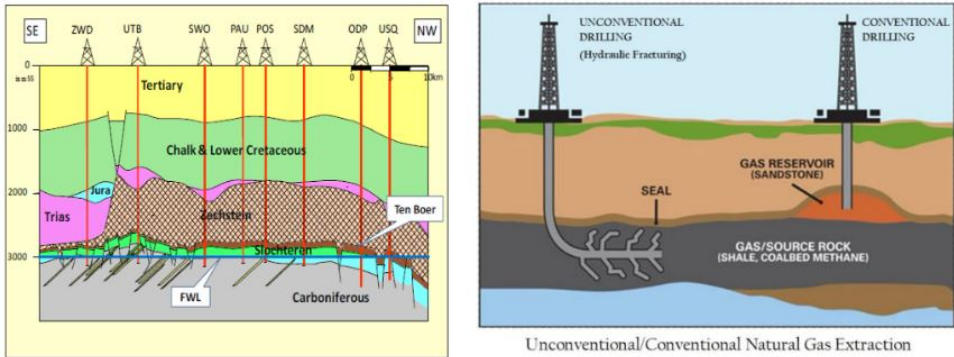
1

Figure 1.1: Geological cross section of the Groningen field ('Slochteren') from south-east (SE) to north-west (NW), in between a carboniferous source layer and a Zechstein rock-salt layer[2]

Earthquakes with magnitude $1.0 \leq M \leq 3.0$ on the Richter scale are generally considered 'light' and not problematic. In the province of Groningen (population of 600,000), however, the limited depth (3 km) of the Earthquakes, the relatively soft and wet surface soil (clay, peat, sand), local construction techniques, ground water table very close to surface and the long repetitiveness of seismic activity, all contribute to considerable damage and safety risks over time in a tectonically inactive region which never needed to be earthquake resistant. In 2015, the Dutch government expanded the application of the Meijdam norm to Groningen. This is a norm defining a risk of death for an individual from external causes such as flooding. That practically meant that the risk of dying from earthquake in Groningen should be limited to 1 in 100,000 annually. A lower level of 1 in 10,000 per year is also allowed provided that the risk will be reduced to the norm within 5 years [3].

The building stock in the Groningen province is mainly constructed by unreinforced masonry (URM) which has shown to be highly vulnerable to these earthquakes. Regardless of step-wise reductions in annual extraction: from 54 bcm in 2013 to 20 bcm in 2018, well-fitting trends over 1991–2018 reveal a steady growth of seismic activity per unit of gas extraction, hence the Dutch cabinet made a decision in March 2018 to reduce Groningen gas extraction to below 12 bcm in 2022 and to end all field operations by 2030. This would reduce the remaining number of risky earthquakes with $M \geq 2.5$ to some seven or eight, with one expected $M_{max} \simeq 4.0$. [2]

More than 2,000 registered historical monuments and heritage structures in this region consist of traditional Dutch farmhouses, churches together with surrounding premises, public and administrative buildings of importance, residential houses, towers and noble houses ("borg" structures). Most structures are supported on piles or deep foundations, which is not always the case for historical buildings either because the piles were not placed in the first place or have deteriorated over time. The earthquake safety and structural integrity during repeated induced earthquakes of small magnitude is a major concern for authorities, local communities and owners, and the motivation behind a

a

Gas extraction (bcm)   N(M ≥ 1.5)

Polynomial trend 1990-2000:
$y = -0.526x^2 + 5.08x + 27.61$; $R^2 = 0.78$

Polynomial trend 1990-2000:
$y = -0.043x^2 + 1.20x - 1.21$; $R^2 = 0.63$

1990 1991 1992 1993 1994 1995 1996 1997 1998 1999 2000

b

Gas extraction (bcm)   N(M ≥ 1.5)   N(M ≥ 2.5)

Policy change
2014

Policy change
2018

Uncertain ⇑
prognosis ⇓

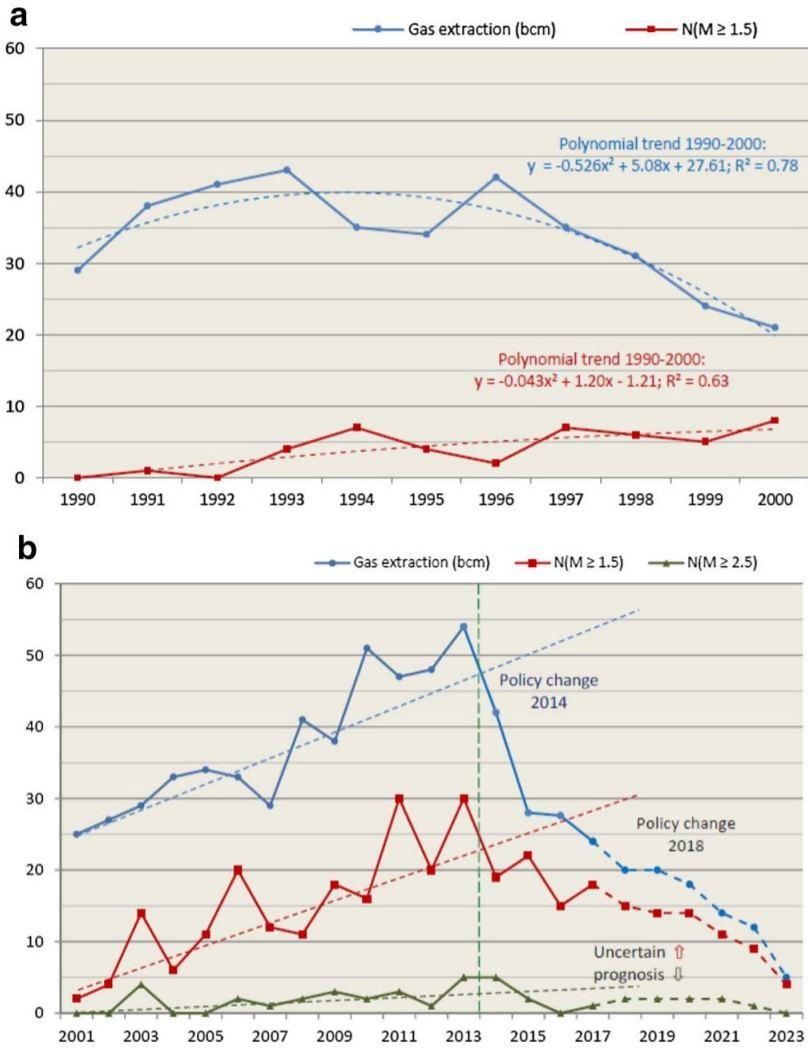2001 2003 2005 2007 2009 2011 2013 2015 2017 2019 2021 2023

Figure 1.2: a, b Annual gas extraction (bcm; upper curve) versus annual number (N) of earthquakes with $M \geq$ 1.5$and \geq$ 2.5 (Richter; lower curves). The ordinate (y) fits both annual bcm and earthquake frequency [2]

1

large research program commissioned by the licensee company extracting the gas, NAM (Nederlandse Aardolie Maatschappij). [1]

Among various building typologies, the province of Groningen is home to 11.3% of all Dutch historical churches (Fig.1.3). Up to July 2019, damage has been reported for approximately 12.9% of these churches. From the perspective of conservation and prevention of loss of our historical and cultural heritage, the assessment of churches is therefore of importance.[4]
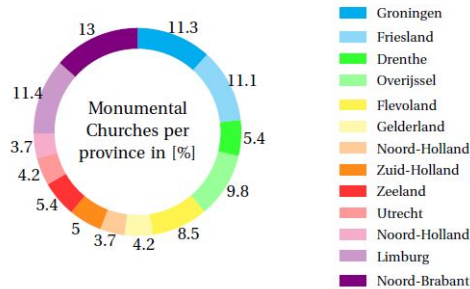
Figure 1.3: Monumental churches per province in Netherlands [4]

Historical structures constructed by unreinforced masonry respond to cyclic load reversals in a non-ductile way unless special measures are taken. As a result of the observed damage, a significant amount of the existing unreinforced masonry stock have shown to require strengthening. Due to the small magnitude and continuous occurrence of induced earthquakes, structural monitoring of these structures with slight damages become an important issue as the determination of causality of such cracks is very difficult. Given the necessity to preserve the authentic style of the monumental structures, non-destructive testing techniques are implemented. Particularly, in case of a post-earthquake diagnosis, the geometric survey and visual inspections are used in parallel with ambient vibration tests and the monitoring of vibration and temperature act as a seismic early warning system. [1]

1.2. OBJECTIVES

The assessment of the seismic performance of historic structures is a challenging task because of their unique construction of structural and non-structural elements, complex design governed by macro element behaviour. In addition, the highly nonlinear behaviour of unreinforced masonry structures (URM) and the dynamic nature of the seismic loading will add to this complexity which cannot be simplified to any standard structural scheme for which a detailed analysis methods would be available.
An accurate and reliable assessment with appropriate numerical modelling of the structure and proper assumptions of all the uncertainties is crucial. As well as, the structural monitoring cannot be applied to all historical structures (and namely churches); this

case-study constitutes a benchmark to study how the numerical models should be defined by providing useful information to engineers and professionals to model similar structures in the future.

Therefore, the research gap lies in accurate modelling of historical structures with simplified material and geometrical assumptions and being able to achieve reliable and faster results by linear dynamic modelling, leading to the main research question.

MAIN RESEARCH QUESTION
How can the dynamic properties of a historical masonry church in Groningen be accurately determined by numerical modelling?

SUB QUESTIONS
- How to simplify the geometry and material properties of load carrying and non-load carrying elements to represent the complex structure of unreinforced masonry church ?

- What is the main modal response of this case-study prior and post structural modifications in both global X and Y directions?

The scope of this thesis is limited to analyzing the dynamic behaviour of *The Old Church (Het Oude Kerkje) in Garrelsweer* in the province of Groningen, The Netherlands. The technical drawings of this church are attached in Annex A. The numerical and analytical representation of this unreinforced masonry church structure only includes the main structural elements. By modelling the main structural elements and carrying out eigenvalue analysis, the global fundamental mode of the case-study is analysed and compared with all modelling variations to predict the dynamic properties of the case-study.

Figure 1.4: Case Study: The Old Church, Garrelsweer (site visit,2021)

1

1.3. THESIS OVERVIEW

The research starts in Chapter 2, with providing the reader background on seismic behaviour of unreinforced masonry structures and detailed structural behaviour of historical masonry church structures. It covers the post earthquakes diagnosis, structural assessment methods and the theory of Eigen-value analysis to estimate the dynamic behaviour of a system.

Chapter 3, presents the structural characteristics of the case study- The Old Church (Het Oude Kerkje)in Garrelsweer. Detailed geometrical, material and shape properties assumed for modelling the structural elements and simplifications for the numerical modelling are presented. The element meshing properties of all the structural elements and analysis methods for various simulations are discussed.

Following the numerical modelling, Chapter 4 presents the eigen-value analysis- results, and the main modal deformations in each direction for all the simulated models.

Chapter 5 presents new insights acquired during the thesis work on structural properties and on a recent retrofitting of the church in 2018; related modelling modifications are presented. Modified case-study structure and the results of the eigen-value analysis of simulated models of the structurally modified case-study showing the main modal deformations and the natural frequencies of vibration are presented.

Chapter 6 discusses the results of all the modelling variations in detail by qualitative and quantitative comparison leading to predicting the numerical model representing the dynamic properties of the case-study with accuracy.

Chapter 7 concludes the research highlighting the key findings and recommendations for new additional research.

2

LITERATURE REVIEW

This chapter provides a background on seismic (dynamic) behaviour of unreinforced masonry structures and structural behaviour of unreinforced masonry historical churches. It covers the post earthquake diagnosis, structural assessment methods and the theory of Eigen-value analysis to estimate the dynamic behaviour of a system.

2.1. EIGEN-VALUE ANALYSIS
A complete full 3D finite element model can be used to quantitatively examine a structure's seismic vulnerability. The structure's geometry is derived from both existing data and in-situ surveys. A detailed 3D realistic mesh is designed on the basis of such geometrical data, with a point-by-point characterisation of each geometric component.

First, a standard eigen-frequency analysis is performed with the aim of identifying the vibration modes characterized by a high participating mass as well as the corresponding periods to compare with accelerations provided by code response spectra. Albeit approximate, because masonry exhibits a non-linear behavior even at very low levels of the external loads, such a standard approach may give a rough indication of the weaknesses of the structures corresponding to maximum deformation in the structural elements, that can be compared with more sophisticated methods of analysis.[5]

The first step in performing a dynamic analysis is determining the natural frequencies and mode shapes of the structure with damping neglected. These results characterize the basic dynamic behaviour of the structure and an indication of how a structure will respond under dynamic loading.

Eigen-value analysis or free vibration analysis is performed to understand the natural modes of vibration characteristic of the structure. Free vibration is a condition in which external force is absent.

The natural frequencies of a structure are the frequencies at which the structure naturally tends to vibrate if subjected to a disturbance and the deformed shape of the structure at a specific natural frequency of vibration is termed as its normal mode of vibration. Natural frequencies and modal shapes are a function of the structural properties and boundary conditions.

The results of dynamic analysis can be compared to the physical test results and a normal modal analysis can be used as a guide to indicate the exact placement of accelerometers or to correlate the physical test results to the analytical results of the structure.

MULTIPLE DEGREE OF FREEDOM SYSTEM WITHOUT DAMPING

The solution of the equation of motion for natural frequencies and normal modes requires a special reduced form of the equation of motion without damping and additional loading. Assuming single degree of freedom, for a structure of mass '**M**', stiffness '**K**', displacement vector 'x(t)' and external force 'F(t)', with predefined initial (at t = 0) displacement ($x(0) = x_0$) and velocity ($\dot{x}(0) = v_0$), the equation of motion in matrix form reduces to

$$[M]\{\ddot{u}\} + [K]\{u\} = 0 \tag{2.1}$$

where,
$[M]$ = mass matrix
$[K]$ = stiffness matrix

This is the equation of motion for undamped free vibration. To solve eq. 2.1 assume a harmonic solution of the form,

$$\{u\} = [\phi]\sin\omega t \tag{2.2}$$

where,
$[\phi]$ = the eigen vector or mode shape
ω = is the circular natural frequency

This harmonic form has a physical significance in addition to providing the key to the numerical solution of the problem. The harmonic shape of the solution denotes that the vibrating structure's degrees of freedom move in lockstep. During motion, the structural structure does not change its basic shape; only the amplitude varies. [6]

If differentiation of the assumed harmonic solution is performed and substituted into the equation of motion, the following is obtained:

$$-\omega^2[M]\{\phi\}\sin\omega t + [K]\{\phi\}\sin\omega t = 0 \tag{2.3}$$

which after simplifying becomes

$$\left([K] - \omega^2[M]\right)\{\phi\} = 0 \tag{2.4}$$

This equation is called the eigen equation, which is a set of homogeneous algebraic equations for the components of the eigen-vector and forms the basis for the eigen-value problem. An eigen-value problem is a specific equation form that has many applications in linear matrix algebra. The basic form of an eigen-value problem is

$$[A - \lambda I]x = 0 \tag{2.5}$$

where
A = square matrix
λ = eigenvalues
I = identity matrix
x = eigen-vector

In structural analysis, the representations of stiffness and mass in the eigen- equation result in the physical representations of natural frequencies and mode shapes. Therefore, the eigen-equation is written in terms of K, ω, and M as shown in Eq. (2.4) with $\omega^2 = \lambda$. There are two possible solution forms for Eq.2.4:

1. If $\det\left([K] - \omega^2[M]\right) \neq 0$, the only possible solution is

$$\{\phi\} = 0 \tag{2.6}$$

This is the trivial solution, which does not provide any valuable information from a physical point of view, since it represents the case of no motion. ("det" denotes the determinant of a matrix.)

2. If $\det\left([K] - \omega^2[M]\right) = 0$, then a non-trivial solution $\left(\{\phi\} \neq 0\right)$ is obtained for

$$\left([K] - \omega^2[M]\right)\{\phi\} = 0 \tag{2.7}$$

From a structural engineering point of view, the general mathematical eigenvalue problem reduces to one of solving the equation of the form

$$\det\left([K] - \omega^2[M]\right) = 0 \tag{2.8}$$

or

$$\det([K] - \lambda[M]) = 0 \tag{2.9}$$

where $\lambda = \omega^2$
The determinant is zero only at a set of discrete eigenvalues λ_i or ω_i^2. There is an eigen vector $\{\phi_i\}$. which satisfies Eq. (2.7) and corresponds to each eigenvalue. Therefore, Eq. (2.7) can be rewritten as

$$\left[K - \omega_i^2 M\right]\{\phi_i\} = 0 \quad i = 1, 2, 3\ldots \tag{2.10}$$

Each eigen-value and eigen-vector define a free vibration mode of the structure. The ith eigenvalue λ_i is related to the ith natural frequency as follows:

$$f_i = \frac{\omega_i}{2\pi} \tag{2.11}$$

where f_i = i[th] natural frequency

$$\omega_i = \sqrt{\lambda_i}$$

The number of eigenvalues and eigen-vectors is equal to the number of degrees of freedom that have mass or the number of dynamic degrees of freedom.[6]

There are a number of characteristics of natural frequencies and mode shapes that make them useful in various dynamic analyses. First, when a linear elastic structure is vibrating in free or forced vibration, its deflected shape at any given time is a linear combination of all of its normal nodes.

$$\{u\} = \sum_i \{\phi_i\} \xi_i \tag{2.12}$$

where,
$\{u\}$ = vector of physical displacements.
$\{\phi_i\}$ = i -th mode shape
ξ_i = i -th modal displacement

At a specific eigen-mode corresponding to an eigen-frequency, a structure deforms into a specific shape. Only when an actual excitation and damping qualities are known, the size of the deformation can be determined.[7]

Determining the eigen-frequencies of a structure is an important part of structural engineering. Some objectives of such an analysis are to:

- Ascertain that a periodic excitation does not result in a resonance that could generate excessive stress or noise emission;

- Determine whether a periodic stimulation creates a resonance in a piezoelectric vibrator (for example) ;

- Investigate appropriate time steps and frequencies for a subsequent dynamic response analysis;

- Provide eigen-modes for a subsequent mode superposition analysis;

- By examining the mode shape of a particular eigen-frequency, you'll be able to see how design modifications can affect it.

System with Multiple Degrees of Freedom

If there are more than a few degrees of freedom, various methods are utilized in practice. The number of eigen-values is usually equal to the number of degrees of freedom (DOFs). For example, a linear system with multiple degrees of freedom (DOFs) can be characterized by a matrix equation of the type

$$\mathbf{M}\ddot{\mathbf{u}} + \mathbf{C}\dot{\mathbf{u}} + \mathbf{K}\mathbf{u} = \mathbf{f}(t) \tag{2.13}$$
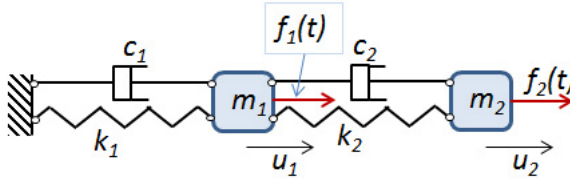
Figure 2.1: An example of a Linear Two-degrees of freedom system [6]

where $\mathbf{M}$ is the mass matrix, $\mathbf{C}$ is the damping matrix, and $\mathbf{K}$ is the stiffness matrix. The DOF's are placed in the row vector $\mathbf{u}$ and the forces in $\mathbf{f(t)}$.[Fig 2.1]
 The free vibration problem is then described by the matrix equation

$$\left(-\omega^2\mathbf{M} + i\omega\mathbf{C} + \mathbf{K}\right)\tilde{\mathbf{u}}e^{i\omega t} = \mathbf{0} \tag{2.14}$$

which forms a complex eigenvalue problem. Formally, the eigenvalues can be solved by finding

$$\det\left(-\omega^2\mathbf{M} + i\omega\mathbf{C} + \mathbf{K}\right) = \mathbf{0} \tag{2.15}$$

The number of eigen-values is equal to the rank of the mass matrix. A mode shape is associated with each eigen-value (also known as the eigen-mode). The contour of the deformation is that of the corresponding eigen-mode when the structure vibrates at a particular natural frequency. For the two-DOF system [fig. 2.1], the first eigen-mode corresponding to the lowest eigen-frequency..

Participation factors

Modal participation factors are a way of describing how much a certain mode will be excited by a rigid body acceleration in a particular direction. The participation factor Γ_{ij} , with respect to mode i and excitation direction j, is defined as

$$\Gamma_{ij} = \frac{\mathbf{u}_i^T\mathbf{M}\mathbf{d}_j}{\mathbf{u}_i^T\mathbf{M}\mathbf{u}_i} \tag{2.16}$$

Here, $\mathbf{d}_j$ is a vector that has the value 1 in all components containing DOF's moving in direction j and 0 in all other components. Note that if mass matrix scaling is used, the denominator has the value 1. [6]

Effective Modal Mass

Definition of modal mass is the inner product

$$m_i = \mathbf{u}_i^T\mathbf{M}\mathbf{u}_i \tag{2.17}$$

When mass matrix scaling is used, the modal mass for each mode is $\mathbf{m}_i = 1$. Other choices of normalization give other values, so the modal mass does not have a physical meaning.

The *effective modal mass* is a quantity related to the modal participation factor. The effective modal mass for mode i, with respect to excitation in direction j, is defined from the participation factor and the modal mass as

$$m_{\text{eff},ij} = m_i \Gamma_{ij}^2 \tag{2.18}$$

The sum of the effective modal masses in a certain direction j for all eigen-modes equals the total mass of the structure:

$$\sum_{i=1}^{N} m_{\text{eff},ij} = m_{\text{tot}} \tag{2.19}$$

The effective modal mass thus has a physical interpretation- for an acceleration in direction j, it shows how much of the total inertial force can be attributed to mode i. It can be used to estimate how many modes are needed for a good representation in a subsequent response analysis based on mode superposition.[6]

The eigen-frequencies of a continuous system (such as a generic solid, beam, or plate) are determined by geometry, material qualities, and restrictions. In a continuous system, the number of eigen-frequencies is infinite. Only a few number of modes are relevant for practical applications. Larger modes are less likely to be stimulated to a substantial degree, and their damping is frequently higher.

It is impossible to analyze all modes for structures with multiple modes and degrees of freedom. As a result, the EMPF (effective mass participation factor) is utilized. The energy contained in that mode is measured by the EMPF. It depends on the vibration's direction and magnitude, as well as the available mass vibrating in that direction. From the free vibration analysis of the model, the important modes analysed based on highest EMPF in each direction.

According to NPR 9998:2021 [8], the response of all mode shapes contributing significantly to the global response shall be taken into account. This requirement may be deemed to be satisfied if either of the following can be demonstrated:

1. The sum of the effective activated masses for the mode shapes taken into account amounts to at least 90% of the total mass to be taken into account.

2. All mode shapes with effective activated masses greater than 5% of the total mass have been taken into account.

The effective activated mass m_k, corresponding to a mode shape k, has been determined so that the base shear force F_{bk}, at the foundation, acting in the direction of application of the seismic action, can be expressed as:

$$F_{bk} = S_d(T_k) \times m_k \tag{2.20}$$

where:
F_{bk} is the base shear force at the foundation acting in the direction of application of the seismic action;

$S_d(T_k)$ is the design spectrum with mode shape k;

m_k is the effective activated mass with mode shape k.

2

When using a spatial model, the above conditions shall be verified for each relevant direction. If the requirements specified above regarding the effective activated masses cannot be satisfied (e.g. in buildings with a significant contribution from torsional mode shapes), the minimum number k of mode shapes to be taken into account in a spatial analysis shall satisfy both the two following conditions:

$$k \geq 3 \times \sqrt{n} \tag{2.21}$$

and

$$T_k \leq 0.20s \tag{2.22}$$

where:
k is the number of mode shapes which shall be taken into account;
n is the number of floors above the foundation or above the top of a rigid basement;
T_k is the vibration period of mode shape k.[8]

2.2. Post-earthquake Structural Diagnosis- Structural Health Monitoring

Effective diagnostic survey in the structural assessment of the structure plays a vital role in cultural heritage preservation. The diagnostic phase entails gathering information about the building's characteristics, material attributes, historical structure transformations and existing damage, which provides a sound basis for any further evaluation of the safety level as well as for the definition of appropriate intervention measures.

The collected information should include accurate investigation of the actual geometry, survey of the crack pattern and local visual inspections: these tasks, joined to historic research, provide a first interpretation of the structural layout and reveal the presence of masonry discontinuities (generally associated to transformations of the building and/or repair), possible vulnerabilities and ageing issues. [9]

Information for Structural Assessment

Amount and quality of the information usable for the assessment is defined in EN 1998-3 [10] into three "levels", called "Knowledge Levels" (KL), ordered by increasing completeness.
The information refers to three aspects:

1. **Geometry:** the term geometry includes structural geometry and member sizes,

2. **Details:** refers to the amount and layout of reinforcement (for RC structures) and connections in URM structures,

3. **Materials:** to the mechanical properties of the constituent materials.

The Table (2.2) reproduced from the code summarizes the definition of these levels.

Knowledge Level	Geometry	Details	Materials
KL1		Simulated design in accordance with relevant practice *and* from limited *in-situ* inspection	Default values in accordance with standards of the time of construction *and* from limited *in-situ* testing
KL2	From original outline construction drawings with sample visual survey *or* from full survey	From incomplete original detailed construction drawings with limited *in-situ* inspection *or* from extended in-situ inspection	From original design specifications with limited *in-situ* testing *or* from extended *in-situ* testing
KL3		From original detailed construction drawings with limited *in-situ* inspection *or* from comprehensive *in-situ* inspection	From original test reports with limited *in-situ* testing *or* from comprehensive *in-situ* testing

Figure 2.2: Knowledge levels in seismic assessment [11]

A thorough understanding would necessitate the availability of both the original and as-built design drawings, as well as complete documentation on material tests, all of which would be supplemented by some in-situ testing to ensure the design specifications and the current state of the materials. Original designs, on the other hand, are unlikely to be found for masonry structures dating back a century or more. [11]

Because masonry buildings were not engineered structures, missing information can be assumed with more confidence: for example, regularity in plan and elevation, distance between main walls, vertical alignment of openings, etc., so that at least their basic structural geometry can be reconstructed with minor uncertainty. [11]

Visual Inspection
The goal of the on-site assessment was to provide information on the structure's geometry as well as to identify crucial spots that need further detailed inspection. Visual examination and strati-graphic survey, on the other hand, provide valuable support to historical study by finding unrecorded alterations as well as areas where masonry is homogeneous and/or marked by discontinuity. In a seismic assessment framework, this study of masonry textures gives evidence of local damages and is especially important in detecting local vulnerabilities and possible overturning mechanisms of unconnected masonry parts. [12]

Visual inspections also suggest the positions that are more suitable for non-destructive (ND) or minor destructive (MD) tests and material sampling, necessary to evaluate the characteristics of the masonry and to explore local defects. [12]

SEISMIC SENSING

In the process of architectural heritage preservation, linking the information locally collected and the overall structural behaviour especially in complex structures evolved over time, the most effective tools to support the structural assessment are ambient vibration testing (AVT) and operational modal analysis (OMA, i.e. the identification of modal parameters from ambient vibration responses), since they are capable of collecting information on the global modal characteristics (i.e. natural frequencies, mode shapes and modal damping ratios) and might identify the presence and the position of damage. In addition, AVT is a fully ND test, especially suitable to Cultural Heritage structures since the test is performed by just measuring the response to ambient excitation (microtremors, wind, etc.).

It should be noticed that AVT could be employed in prompt surveys (e.g. post-earthquake emergency) by using either traditional accelerometers mounted on outdoor walls or innovative non-contact sensors. Furthermore, the results of AVT should represent the starting point of long-term dynamic monitoring in order to perform vibration-based damage assessment or to evaluate the effects of repair interventions.[9]

Vibration-based damage identification methods, usually defined as Global methods, can alert for the presence of damage and define its location, but they might not give sufficiently accurate information about the type and extent of the damage. Visual inspections or experimental non-destructive tests like the acoustic or ultrasonic methods, magnetic field methods, radiography, eddy-current methods and thermal field methods can be preceded by a global method that indicates that damage is present. Local methods are certainly more accurate to localize and describe the damage.[12]

Ambient Vibration Testing (AVT)

Analysis based on ambient vibrations test is a methodology used to characterize the dynamic behavior of a structure excited by low amplitude vibrations. The information obtained can be useful to calibrate and update finite element models of the building, or can be used for the health monitoring of the building. [12]

2.2.1. SEISMIC DAMAGES IN HISTORICAL STRUCTURES

Through the centuries, earthquakes have been one of the most common causes of cultural heritage damage and loss [13]. The examination of post-earthquake damage patterns is a valuable source of knowledge on recurring damage patterns. In addition to the typical damages often seen in historic structures, the effects of the seismic events revealed that, in several cases, the adopted structural models (which presumably described the historic building's structural system) were inadequate, and the retrofitting techniques had failed to produce the desired results due to lack of sufficient documentation. Thus, the necessity for new structural models for existing masonry buildings, as well as intervention for code requirements, were both highlighted. [14]

2.3. THE SEISMIC BEHAVIOUR OF EXISTING MASONRY BUILD-INGS

2

A masonry structure is a box-like structural system composed of vertical structural elements such as walls and horizontal structural elements such as floors and roofs. Vertical loads are transferred from the floors to the bearing walls, which act as horizontal flexural, and from the bearing walls to the foundation system, which act as vertical compression members. [14]

When a structure is subjected to an earthquake, the inertia force, which is proportional to the mass of the structural system, should be accounted. These action effects are influenced by a number of parameters, including the mass and stiffness of the structure, as well as their distribution, the magnitude of the imposed actions, the number of seismic motion cycles, and the properties of the foundation soil, among others. While ground motion is generally three-directional, both vertical and horizontal inertia forces will act on the structure, inducing displacements that change in magnitude and sign over time, resulting in three-dimensional vibrations of the building. [15]

Horizontal inertial forces are transmitted from the floor structures, which should serve as rigid horizontal diaphragms, to the bearing walls, producing shearing and bending effects, and from the bearing walls into the foundation system. Furthermore, distributed inertia forces are caused by the distributed mass of wall elements, resulting in out-of-plane bending of walls. [15]

According to laboratory testing and observation of damage modes of real structures, masonry walls are less resistant to activities perpendicular to their medium plane (out-of-plane actions) than to actions parallel to this plane (in-plane actions). In the first situation, the wall rigidity is substantially lower than in the second. For good load bearing behavior and to avoid inflection and overturning, all walls of a masonry building should resist actions parallel to them. In this notion, the building's behavior is viewed as a box. The walls should be connected to the floor by stiff limitations because the floor should be able to transfer seismic movements across the walls as a function of their stiffness. It is well known that satisfactory seismic behavior can only be accomplished by preventing out-of-plane collapse and fully using the in-plane strength and deformation capacity of walls. [14]

2.3.1. MORPHOLOGY OF DAMAGES AND FAILURE MECHANISMS

The damage to masonry structures can largely be evaluated based on two basic collapse modes. The "First Damage Mode," as defined by Giuffrè [16], is caused by seismic actions that are perpendicular to the wall (out-of-plane) and result in the overturning of the entire wall panel or a large section of it [Fig 2.3(a)]. The shedding of a section of the outer masonry leaves or the emergence of vertical cracks at the corners of a structure where the wall began to develop a hinge from the swaying are both signs of such damage. This is the highest building vulnerability, and it was previously prevented through

using ties to compensate for the lack of connection between the exterior and orthogonal walls. They resist the in-plane seismic action imparted by the facades and exhibit a higher resistance to such force. When the force of the movement exceeds the strength of the walls, they are stressed in their plane and crack diagonally, isolating a triangular area of the wind-brace wall and enabling it to participate in the cracking motion. While the "first mode" is always ruinous, as it implies the complete collapse of the wall and consequent collapse of all supported elements, the "second mode" does not necessarily determine the collapse, though it still implies small, medium and even large cracks of the wind-brace walls.
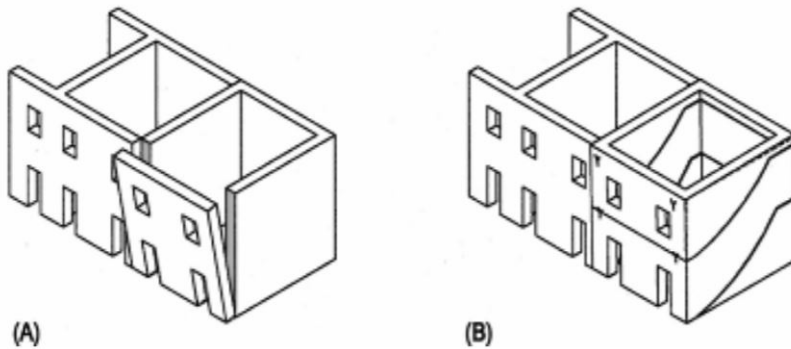
Figure 2.3: First mode (a) and second mode (b) collapse mechanisms [16]

The Second Damage Mode is induced by forces acting in the plane of the wall, as previously stated, and is typically characterized by inclined cracks associated with shear stresses that commonly result in a "X" pattern, but it seldom approaches total collapse. When a full shear crack occurs during an earthquake, however, the panel's triangular parts can become unstable, resulting in collapse. The addition of adjacent constructions or portions to historic structures, as well as residential buildings that have evolved over the years, implies a lack of strong connections between the parts, and structural integrity is one of the primary sources of weakness that leads to severe damage and collapse (Fig.2.3(b)).

In existing masonry buildings, in-plane flexible diaphragms, typically timber floors and roofs, as well as thin masonry vaults are prevalent. Even though appropriate connections between walls and floors prevent local first mode mechanisms, the global seismic response in masonry buildings with flexible floors is highly complex. Vertical structures (walls) tend to behave independently because horizontal structures have no or little coupling effect. However, in practice, analyzing the in-plane seismic response of each masonry wall as derived from the global structure with its associated loads and inertial masses could be an acceptable approach. [16]
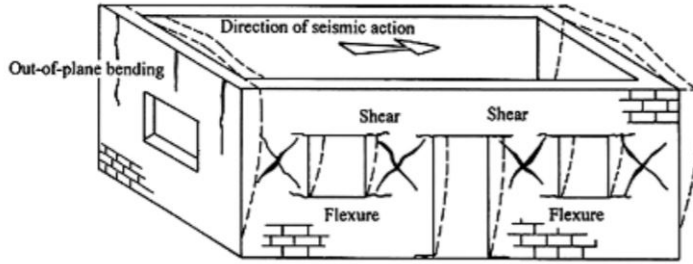
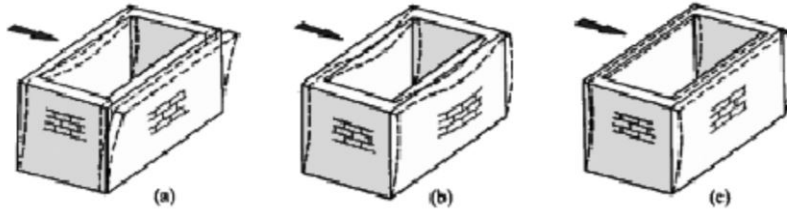Figure 2.4: Deformation of a masonry building and typical damage to structural walls [14]

Figure 2.5: Behaviour of masonry buildings: (a) structural walls not tied together, (b) building with deformable floors and tied walls, (c) building with rigid floors and tied walls (Tomazevic, 2000)[14]

IN-PLANE BEHAVIOUR

In the plane of walls bending and shear cause horizontal and diagonal cracks respectively (Fig 2.4). In-plane mechanisms cause the conventional shear damage, which does not always result in the structure collapsing. The little damage is due to the efficient strong connection between structural components and the presence of floors capable of transmitting horizontal forces to shear walls, both of which characterize the favorable "box" behavior of structures under seismic activities, as seen in Fig 2.5. Unfortunately the layout of historic buildings, their discontinuities, the changing in time, lack of maintenance etc, lead to different behaviours. [14]

Seismic damage to masonry walls, as well as laboratory testing, revealed that masonry piers subjected to in-plane loading can exhibit two distinct forms of behavior, with local cracks as shown in Figure 2.5, with which different failure modes are associated:

1. **Flexural behaviour**: It involves two different modes of failure. If the applied vertical load is low with respect to compressive strength, the horizontal load produces tensile flexural cracking at the corners, (2.6(a)), and the pier begins to behave as a nearly rigid body rotating around the toe (rocking). If no significant flexural cracking occurs, due to a sufficiently high vertical load, the pier is progressively characterized by a widespread damage pattern, with sub-vertical cracks oriented towards the more compressed corners (crushing). In both cases, the ultimate limit state is obtained by failure at the compressed corners.(2.6(a))

2. **Shear behaviour:** This may produce two different modes of failure: (a) in sliding

shear failure- the development of flexural cracking at the tense corners reduces the resisting section; failure is attained with sliding on a horizontal bed joint plane, usually located at one of the ends of the pier, (2.6(b)); (b) in diagonal cracking, when failure is attained with the formation of a diagonal crack, which usually develops at the centre of the pier and then propagates towards the corners, (2.6(c)). The crack may pass prevailing through mortar joints (assuming the shape of a 'stair-stepped' path in the case of a regular masonry pattern, or also through the blocks, (Fig 2.7).
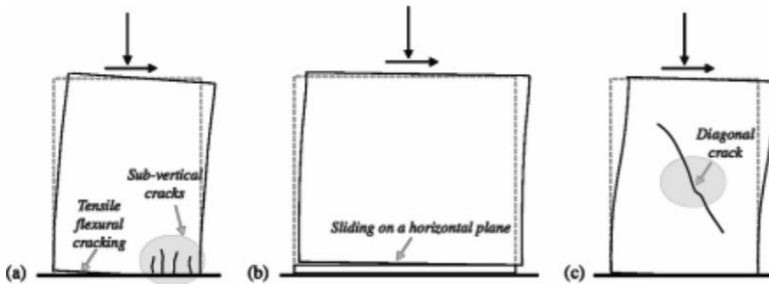
Figure 2.6: Typical failure modes of masonry piers due to horizontal loads: (a) rocking; (b) sliding shear failure; and (c) diagonal cracking [17]
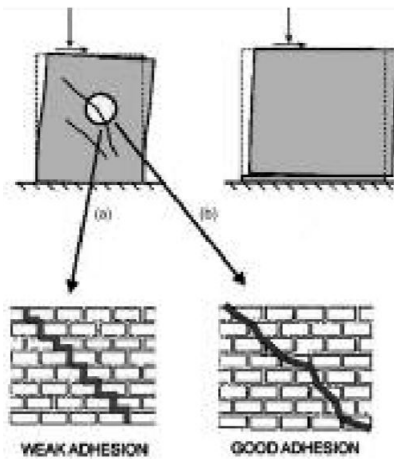
Figure 2.7: Influence of the mortar-brick adhesion in the joints [17]

The occurrence of different failure modes depends on several parameters:
(a) the geometry of the pier;
(b) the boundary conditions;
(c) the acting axial load;
(d) the mechanical characteristics of the masonry constituents (mortar, blocks and interfaces);

(e) the masonry geometrical characteristics (block aspect ratio, in-plane and cross-section masonry pattern).

Many experimental tests were performed in the past to investigate the impact of these characteristics on the failure mode of masonry piers. In general, it has been determined that rocking predominates in slender piers, while bed joint sliding occurring only in extremely squat piers. For increasing levels of vertical compression in moderately slender piers, diagonal cracking tends to win out over rocking and bed joint sliding. [14]

OUT-OF-PLANE BEHAVIOUR

Direct observation of crack patterns recorded in post-earthquake damage surveys yields to the conclusion that often the most recurrent failure mechanism surveyed is the overturning. The way in which this will develop depends on the quality and strength of the connections with other elements of the structure -internal load-bearing partitions, floors, and roof structures. If the structure was not strengthened, it is assumed that the only means of restraint to overturning exerted by other elements to a wall is governed by the friction of the contact surface, and this will give rise to different types of failures, highlighted in the examples of Fig 2.8. [14]
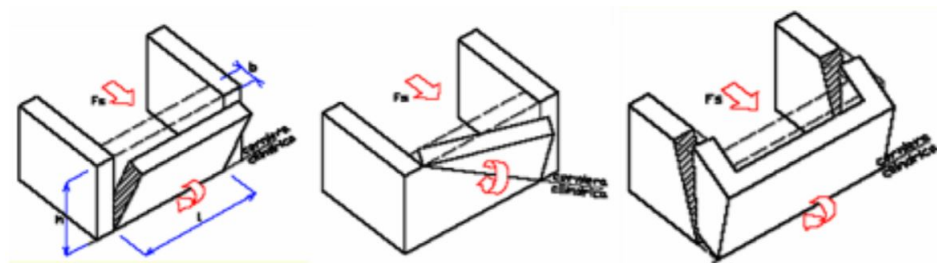

Figure 2.8: Overturning mechanisms related to the restraints effectiveness,[14]

2.3.2. NUMERICAL MODELLING OF MASONRY STRUCTURES

The accurate material mechanical characterization is fundamental for simulating the structural behavior of existing masonry structures. The mechanics of masonry is complex, varied, and highly nonlinear as it comprised of blocks usually bonded with mortar and assembled with a specific texture. The overall masonry response of this heterogeneous material is governed by mechanical properties of block, mortar, and the bond between them. [18]

Classification of numerical strategies for masonry structures is based on how masonry and/or masonry structures are conceived and modeled and each numerical approach has characteristics, which are optimal for a specific field of utilization. There are 4 types of numerical modelling strategies:

1. Block-by-block Models (BBMs): By definition, masonry is modelled by considering each block as a rigid or a deformable body, while the mechanical interaction between blocks can be modeled through various convenient formulations.

2. Continuum Models (CMs): Masonry is conceived as a continuum deformable body, without differentiation between blocks and mortar layers.

3. Macro-element Models (MMs): Panel-scale structural components (macro-elements) with phenomenological or mechanical-based responses are employed to idealize the structure. Two macro-elements- piers and spandrels) are recognised and the distinction between these macro-elements in a masonry structure is carried out on the basis of the interpretation of the structural arrangement.

4. Geometry Based Models (GBMs): A rigid body is employed to model the structure. The only input data needed in these modeling approaches is represented by the geometry of the structure. [18]

CONTINUUM MODELS

In this class of models, the mesh does not need to represent the masonry blocks and, accordingly, the mesh size could be considerably greater than the block size. Homogenization procedures are generally based on accurate modeling strategies (e.g., BBM) [19]

The use of these models was found to be favorable for the investigation of structural performance of historic monumental masonry buildings, especially for the restricted computational demand of these models and their ease in representing complex geometries. Monumental buildings usually show thick and irregular masonry which are very complex to characterize mechanically, also due to the restrictions for destructive tests on these buildings. These aspects promoted the utilization of isotropic nonlinear models in monumental masonry buildings. Numerous studies that used isotropic smeared crack, damage, and plastic-damage models have been favorably carried out on historic masonry towers, churches and temples based on 3D models [19], [18].

2.3.3. STRUCTURAL BEHAVIOUR OF HISTORICAL STRUCTURES: CHURCHES

The structural behavior of complex historic structures, especially in case of agglomerates of buildings may be particularly difficult. For this reason, the initial stage is to identify structural components (structural units), followed by damage and collapse mechanisms. These structural units are called as Macro-elements. It should be noted that these macro-elements are different from the macro-element models (MMs) in numerical modelling strategies of masonry [18], [14].

A Macro-element is a physically distinguishable building component that functions independently of the rest of the structure. They are single elements or a combination of structural components (such as walls, floors, and roofs) that are designed to work together (possible damage pattern, cracking, weak connection borders, and so on), as well as restraints (e.g. the presence of ties or ring beams), the constructive deficiencies and the characteristics of the constitutive materials. Although they follow both in-plane and

out-of-plane kinematic mechanisms, they behave as a single unit without the assistance of other structural units. [14]

In the case of churches, the seismic response owes to local damage and collapse mechanisms of the various architectonic elements, known as macro-elements (i.e., facade, nave, triumphal arch, and so on), which behaved nearly independently.[Fig. 2.9] If masonry shows good characteristics, local damage mechanisms (e.g.out-of plane over-turning, rocking) develop as loss of equilibrium of the masonry portions capable of sliding and rotating. [14]
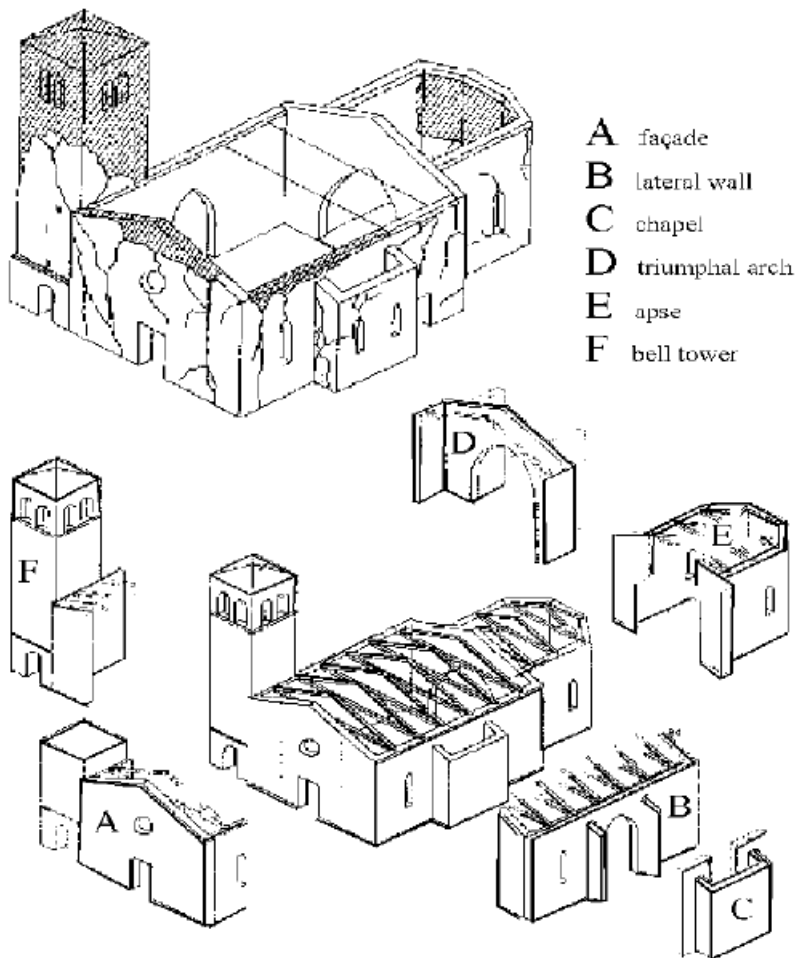
Figure 2.9: Macro-elements of a church, example [14]

2

IDENTIFICATION OF FAILURE MECHANISMS IN HISTORIC STRUCTURES

In the case of churches as discussed in section 2.3.3, the seismic response showed a recurrent behaviour according to local damage and collapse mechanisms of the different architectonic parts called macro-elements. Local damage mechanisms (out-of-plane overturning, rocking) emerge as a loss of equilibrium of masonry components capable of sliding and rotating if the masonry exhibits good characteristics. When looking at the progression of these types of failures, the initial damage phase can be quite different from the final state. Empirical evaluations known as "vulnerability indexes" for masonry buildings have been developed with specific attention to historic masonry buildings. They are based on the detection of horizontal static-equivalent force levels that can activate certain mechanisms of local failure / overturning of structural macro-elements (composed by single walls or sub assemblages, as intersecting walls, walls and floors or roof, etc.) in-plane and, more importantly, out-of-plane. The lack of systematic linkages between intersecting walls and between walls and horizontal structures in these systems may result in kinematic mechanisms related to structural portions loss of equilibrium rather than stress surpassing the materials ultimate capability. [14]

3

NUMERICAL MODELLING THE OLD CHURCH BEFORE RETROFITTING

This chapter presents the structural detailing of the present case-study - The Old Church (Het Oude Kerkje)in Garrelsweer. Detailed geometrical, material and shape properties assumed for modelling the structural elements and simplifications for the numerical modelling are presented. The element meshing properties of all the structural elements and analysis methods for various simulations are discussed.

Garrelsweer is a small village in the municipality of Loppersum in the province of Groningen (the Netherlands), on the Damsterdiep. Garrelsweer has almost 700 inhabitants.[Fig3.1] The Dutch reformed hall church was built in 1912 to a design by H. Rozema and G. Hoekzema. It is built of clay-brick masonry and Timber roofing and floor structures. All windows have colored stained glass. The architectural style is known as rationalism. Originally a bell from 1695 by C. Fremy hung in the tower. This clock was moved to the Reformed Church in Garrelsweer in 2013. The organ was built by the Rohlfing firm in 1921 (using older interior). On the north side, a consistory has been built on a rectangular plan, in the same style as the church. In the east facade is the entrance with a natural stone sidewalk (two steps). A small extension with a flat roof was built on the west facade in the 1960s. [20]

The following are specifics in interior of the church; in the bell-tower (portal): the tiled floor, the wooden spiral staircase and the two framed sliding doors (panel) under a brick segment arch; in the church, the pointed barrel vault with draw beams, the wooden platform pulpit in a niche with an entrance on both sides, the consistory benches to the left and right of the pulpit, the wooden balustrade with lectern, the wooden organ stand supported by two decorative wooden pillars and the organ case [20].

Figure 3.1: Location of Case Study: Old Kerkje, Garrelsweer, Groningen [21]

(a) Front view of the Old church,Garrelsweer
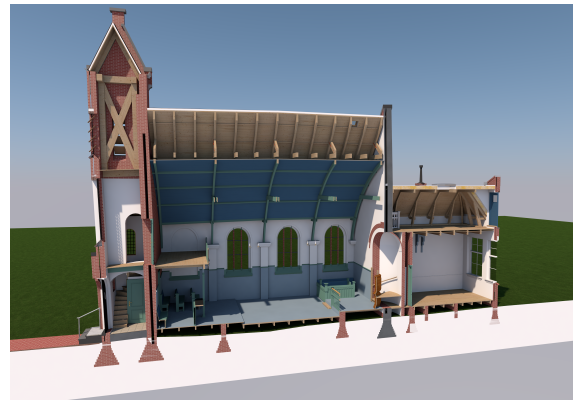
(b) Side view of the Old church,Garrelsweer

Figure 3.2: Case Study:The Old Church, Garrelsweer [20]

3.1. Characteristics of the Old Church in Garrelsweer, Groningen

In order to obtain a preliminary assessment of the dynamic behavior of the church under study, an eigen-frequency analysis is performed using a three-dimensional finite element model. For precise modelling of the structure, the structural characteristics of the church are studied by detailing the macro-elements of the structural unit, (Section 2.3.3).

From the drawings (Fig 3.3), the macro elements of the church are
Masonry:

- Main facade in x-direction along with the bell-tower (masonry);

- Lateral walls in y-directions with window openings (masonry);

- Piers supporting the cross beams of the main roof structure and curved roof structure connecting to the foundation;

- Shallow masonry step-foundation running through-out the length of the walls and through the main piers;

- Sub-structure adjacent to the main hall (Polygonal Apse) with two levels: Masonry walls, foundation.

Timber:

- Inclined roof structure with timber sheets and timber cross beams running in y-direction supported by inclined timber beams;

- Curved timber roof structure and curved timber beams supported by cross timber beams on the curved roof below the main roof structure;

- Sub-structure adjacent to the main hall (Polygonal Apse) with two levels: Timber flooring, roof;

- Timber flooring through the ground-floor and the first floor with flexible timber sheets supported on timber beams connected to the masonry walls;

- Two level stair-cases in bell-tower up-to the first floor and in between the main structure and the adjacent substructure up to the first floor level.

The arched window and door openings in the main structure and the adjacent substructure are identified and modelled carefully as these openings in the masonry wall play an important role in the analysis of dynamic behaviour of the structure.

As shown in Fig 3.3b & Fig 3.3c, due to previous seismic activity, the bell tower has moved along the y-axis towards the main- structure causing the main shear cracks along the lateral walls in y-axis through the window openings (as can be seen by the crack pattern & broken stained glass of both the windows near the bell tower). Due to these damages, there has been a retrofitting of this church which is discussed in Chapter 5.

3

(a) Front view (x axis)

(b) Right side view (y axis)
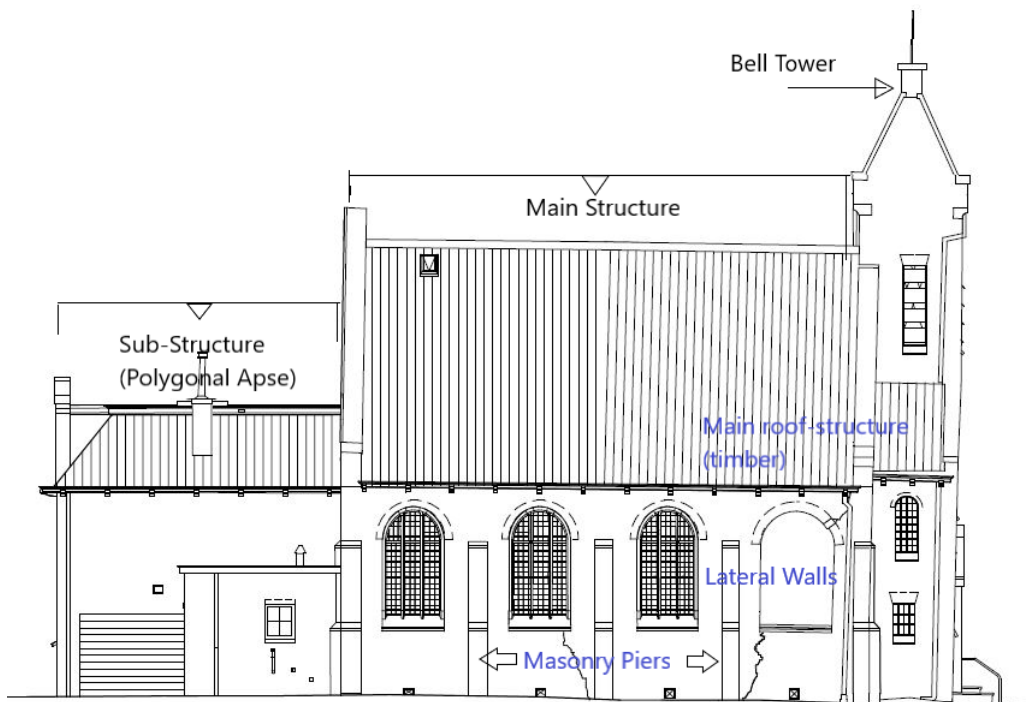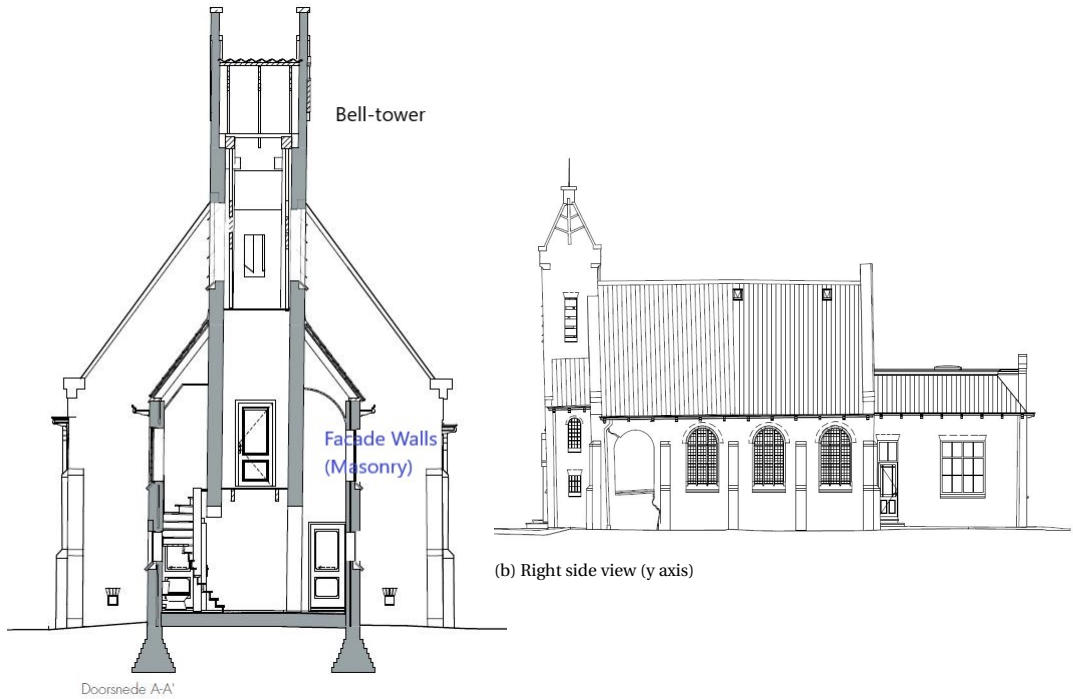
(c) Left side view (y axis)

Figure 3.3: Elevation drawings of The Old Church- Garrelsweer prior structural modifications (Source: Arcadis)

3.2. NUMERICAL MODELLING

A 3D representation of the case study as presented in section 3.1 is set-up with the aid of the commercial software package DIANA FEA 10.4 [22]. This section presents the modeling choices for the eigen-frequency analyses and elaborates on the characteristics of the numerical models. The material of all the masonry specimens in this study was replicated by clay-brick masonry typical of the period before 1950 in the Netherlands. The goal of this study is to investigate the structural characteristics of the church in dynamic loading including fundamental modes and eigen-frequencies of the whole structure to validate the results with the physical tests.

After identifying the macro-elements of the church, many simplified modelling assumptions are considered to rationalize the complex structure, material properties and connections which are discussed in detail in this section with the aim of reducing the computational time and effort.

3.2.1. MASONRY WALLS

Most of the buildings in the region are constructed of unreinforced masonry. In the case-study, it can be observed that the structural wall thickness of the church is not uniform over the length due to various factors over the time [Appendix A]. A homogenized cross-section is considered for the walls with an average thickness of 500 mm, in X-direction and 460mm, in Y-direction of the main structure and 220 mm thick walls of the adjacent substructure [Fig 3.4].

GEOMETRICAL & MESH PROPERTIES

The cross-sectional details of all the masonry walls is shown in table 3.1.
Masonry Walls are modelled with triangular and quadrilateral shell elements and the element types are described in table 3.2

| Wall element	Location	Total Wall thickness(mm)
Masonry Walls -Y axis	Main Structure -Lateral	460
Masonry Walls- Y axis	Vestibule	220
Masonry Walls- Y axis	Sub-structure (Apse)	220
Masonry Walls -X axis	Bell Tower -Facade	100
Masonry Walls- X axis	Main Structure	500
Masonry Walls- X axis	Sub-structure (Apse)	220

Table 3.1: Element Cross-sectional properties- Masonry Walls (The Old Church, Garrelsweer)

Figure 3.4: Kerk Garrelsweer(y-section) showing the cross-section of masonry walls

Element Types	CQ40S	CT30S
Degrees of Freedom	40	30
interpolation scheme	Quadratic	Quadratic
Integration scheme	Gauss and Simpson (2 x2x2)	Gauss and Simpson (2 x2x2)
Stress Components	$\sigma_{xx},\sigma_{yy},\sigma_{zz},\sigma_{xy},\sigma_{yz},\sigma_{xz}$	$\sigma_{xx},\sigma_{yy},\sigma_{zz},\sigma_{xy},\sigma_{yz},\sigma_{xz}$
Inclusion of shear deformation	Yes	Yes
Topological dimension	3D	3D
Average element size	200 mm	200 mm
Total number of elements	11752	201

Table 3.2: Classification of element types in masonry wall
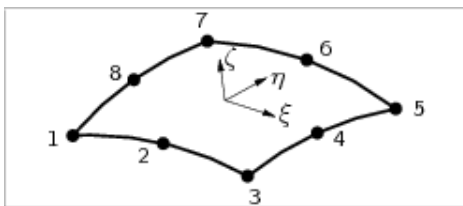
(a) CQ40S
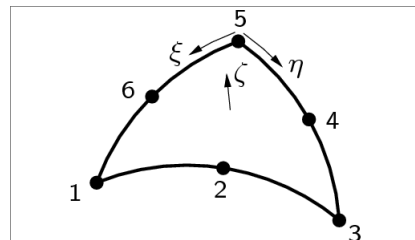
(b) CT30S

Figure 3.5: Element Models of quadrilateral & triangular Shell elements -Masonry Walls [23], [24]

Material Properties- Masonry Model

A smeared, continuum Engineering Masonry Model (EMM), recently developed by TU Delft and DIANA FEA was chosen for the elaboration of the macro (or continuum) model. This material model accounts for the orthotropy from bed and head joints, tensile softening with secant unloading, shear friction and cohesion softening with elastic unloading, and compression hardening and softening with bi-linear elastic-secant unloading.

Note that these material parameters are partially obtained from [8] and from experimental correlations on residential buildings of Groningen subjected to seismic damage [25] as shown in table 3.3.

Property	Symbol	Value	Units
Density	ρ	1708[a]	kg/m^3
Young's modulus (vertical)	E_y	3087[a]	MPa
Young's modulus (horizontal)	E_x	2157[b]	MPa
Shear modulus	G_{xy}	1354[b]	MPa
Tensile strength	f_t	0.09[a]	MPa
Fracture energy (tension)	G_t^1	7.527[c]	N/m
Compressive strength	f_c	11.35[a]	MPa
Fracture energy (Compression)	G_C	26050[a]	N/m
Friction angle	φ	0.669[a]	rad
Cohesion (no softening)	c	0.14[a]	MPa
Diagonal crack orientation	α	0.5[a]	rad

[a] From material characterisation [26], [8] ;
[b] From calibration [25];
[c] From formulation [8].

Table 3.3: Calibrated Properties of Engineering Masonry Model(EMM)-Macro Model

3.2.2. Piers

Piers are vertical load bearing structural elements which are integrated in the main walls and carry the load of roof structure. Figure 3.6a depicts the interior and exterior detail of the piers and the connection with the main load bearing walls. The connection between the main walls and piers are difficult to define based on the provided information, so are assumed to be fixed due to likely presence of interlocking between the masonry bricks. The geometry of the columns/ piers is varying along the height from 525mm to 637mm as shown in Fig 3.6. Therefore, the piers are modelled as beam elements with constant thickness equal to the average of both values (580 mm).

Beam elements are those in which the length dimension "l" is considerably higher than its thickness "d". They can simulate axial deformation Δl, shear deformation γ, curvature κ and torsion. Such an element is shown in figure 3.7.
DIANA offers three classes of beams:

3

- Class I: These elements are directly integrated along cross-sections and behave according to the classical Bernoulli beam theory. This element can be used for linear and geometrically non-linear analysis, although it is limited to stress-strain curves in terms of physical non-linearity.

- Class II: These elements are fully numerically integrated and similar to Class I, but they can also be employed for issues involving material physical non-linearity.

- Class III: Cross-sections that are fully numerically integrated and correspond to the Mindlin-Reissner theory. [27]

For the thesis, class III beam element CL18B is used. The cross-sectional properties of the piers and the element properties are discussed in Table 3.4 and Table 3.5 respectively.

(a) Kerk Garrelsweer, x-section

(b) Cross-sectional Geometry of Piers
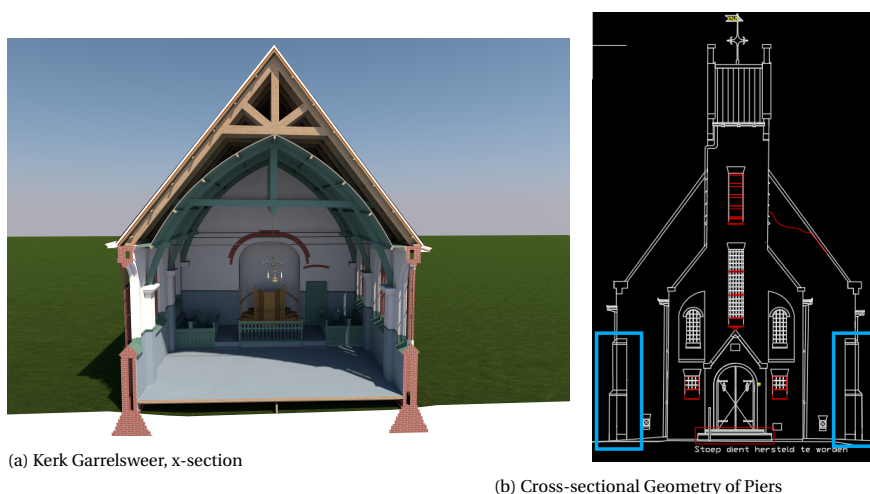
Figure 3.6: Element Models of Shells-Masonry Walls

GEOMETRICAL & MESH PROPERTIES

Element	length(mm)	thickness(mm)	Width (mm)
Piers	3600	580mm(average)	737mm

Table 3.4: Cross-sectional details of Piers

Element Types	CL18B
Degrees of Freedom	6
interpolation scheme	quadratic
Integration scheme	2 point Gauss integration
Stress Components	$\sigma_{xx}, \sigma_{xy}, \sigma_{zx}$
Inclusion of shear deformation	Yes
Topological dimension	3D
Average element size	200 mm
Total number of elements	184

Table 3.5: Classification of element types in masonry piers- CL18B
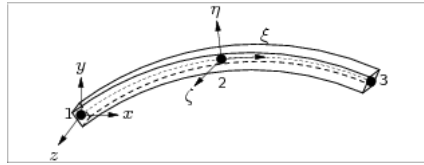
Figure 3.7: Element Model of Class III beam element- (CL18B)

MATERIAL PROPERTIES

For the masonry piers the Total Strain Based Cracking Model (TSCM) is assigned.This TSCM requires only

- Elastic properties, such as: Young's modulus and Poission's ratio.

- Material strength parameters, such as tensile, compressive and shear.

This model doesn't include the anisotropic material properties of masonry, and as it not feasible to assign the local axes since to the piers designed as 2D line elements, this material model is appropriate. Note that the values for masonry are partially obtained from the NPR 9998 and partially from experimental test correlations [25] as shown in table 3.6.

3.2.3. FOUNDATION

The foundation below the masonry walls is a shallow step foundation composed of clay-brick masonry. This foundation is approximated by considering a step function along z-axis with varying thickness starting from 500mm at the ground level up-to 630mm thickness at 1500mm below the ground level as shown in figure 3.8.

The masonry step-foundation is modelled with triangular and quadrilateral shell elements- CQ40S & CT30S (Fig 3.5) and these element properties are described in table 3.2. The material model considered for the masonry foundation is the continuum Engineering Masonry Model (EMM) and the material properties are shown in table 3.3.

Property	Parameter	Symbol	Unit	Value
Elasticity	Young's Modulus	E	MPa	4000
	Poisson's ratio	v	-	0.15
	Density	ρ	kg/m3	1708
Crack orientation	Rotating			
Cracking	Linear-crack energy based			
	Tensile strength	f_t	MPa	0.30
	Tensile fracture energy	G_t	N/mm	0.01
Crushing	Compressive strength	f_c	MPa	8.0
	Compressive fracture energy	G_c	N/mm	20

Table 3.6: Material properties masonry Piers with TSCM model
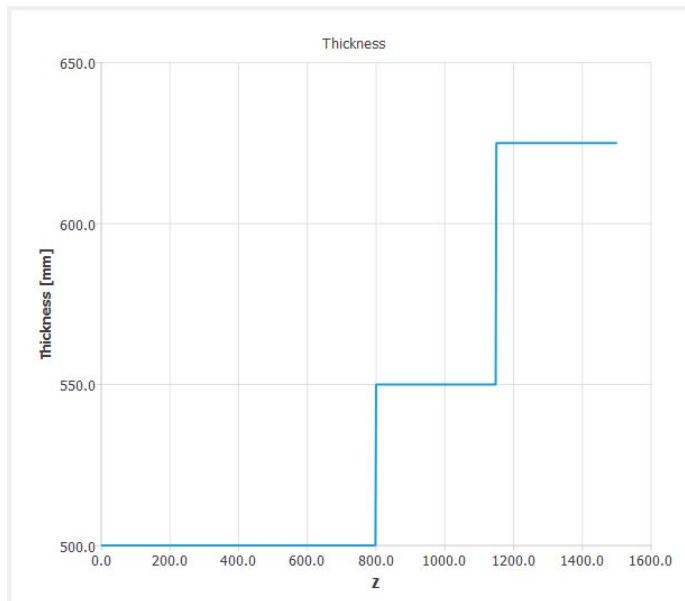
Figure 3.8: Modelling the masonry foundation with a step function

3.2.4. TIMBER JOISTS

Timber joists in the roof and the floor are modelled as class III beam elements with linear elastic isotropic material properties which is considered a good approximation as linear dynamic analysis is considered.

GEOMETRIC AND MESH PROPERTIES

The cross-sectional details of the timber joists are in table 3.7 and the model of timber joists in floor and roof structures in figure 3.9.

Element	width (h) (mm)	thickness (b) (mm)
Main roof-Inclined beams	241	110
Main roof- cross beams	241	110
Main roof-roof joists	95	95
Curved roof- curved beams	182	100
Curved roof- cross beams	182	100
Main roof- center beams(vertical)	222	222
Adjacent apse- roof beams	100	100
Floor beams - bell tower	130	75
Floor beams- Main structure	250	60
Floor beams- Adjacent apse	130	75
Floor beams- first level	130	75
Braces-bell tower(second level)	280	280

Table 3.7: Cross-sectional details of timber joists

MATERIAL PROPERTIES

The simplified material model considered for the timber joists is linear elastic isotropic model with the properties described in table 3.8.

Property	Parameter	Symbol	Unit	Value
Linear Elastic Isotropic	Young's Modulus	E	MPa	10000
	Poisson's ratio	ν		0.35
	Density	ρ	T/mm3	5 e-09

Table 3.8: Material properties of timber joists (Linear Elastic Isotropic model)

3
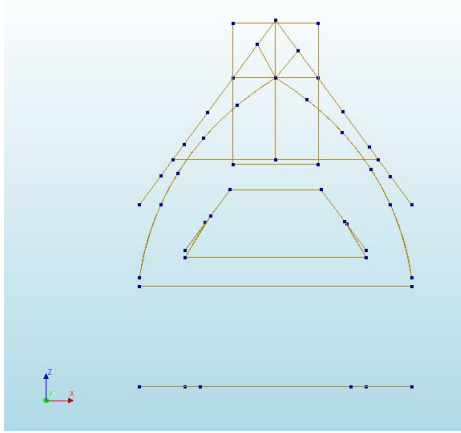
(a) x-z section (front view)
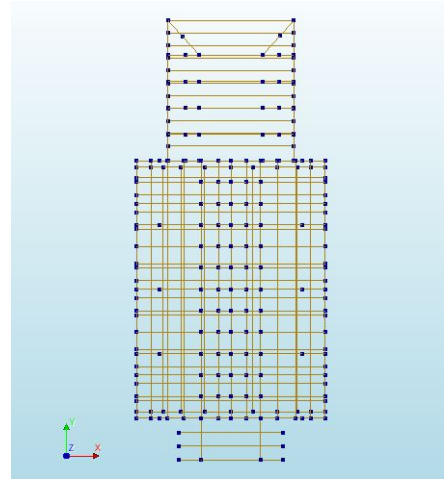
(b) x-y section (top view)
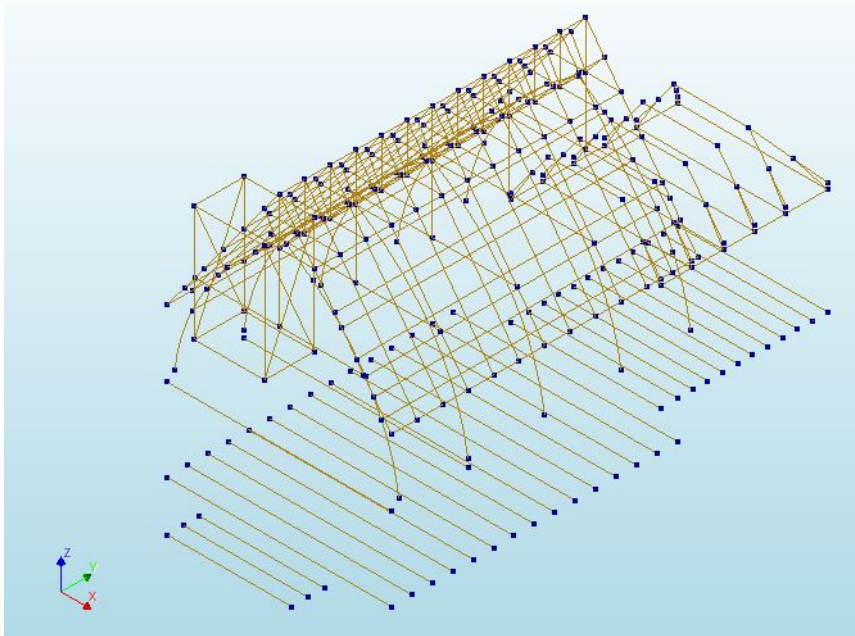
(c) isotropic view

Figure 3.9: Modelling the timber joists in the floor and roof structures (CL18B)

3.2.5. TIMBER DIAPHRAGMS- ROOF AND FLOOR

Existing or historical constructions with timber floors and roofs represent a significant part of the building stock and the architectural heritage for several countries. These diaphragms are often poorly connected to unreinforced masonry walls, making such existing buildings potentially vulnerable to earthquakes.

For the Dutch context a lack of knowledge can be observed; this is because on the one hand the area around Groningen started to be subjected to more intense earthquakes generated by gas extraction only in recent years. Therefore, the seismic assessment of existing or historical buildings was no issue until recently. On the other hand, the timber diaphragms have specific characteristics different from other floors analysed in literature. From the analytical point of view, the in-plane behaviour of the tested diaphragms was characterized by examining their flexural or shear-related response, non-linearity and orthotropy. Based on literature, two different material models are used for modelling the roof and floor timber diaphragms in this thesis discussed in detail below.

GEOMETRIC AND ELEMENT MESH PROPERTIES

The cross-sectional details of flooring, inclined roof and the curved roof structure correspond to the plans included in appendix A. The thickness of these timber diaphragms vary from 25mm-35mm for both floor and roof structures, hence a simplified assumption of 30mm thickness is made for modelling the case study and the material properties are also calculated based on this assumption.

The timber diaphragms are modelled as regular curved shells with constant thickness and the element types of the mesh are described in table 3.9.

Element Types	CQ40S	CT30S
Degrees of Freedom	40	30
interpolation scheme	Quadratic	Quadratic
Integration scheme	Gauss and Simpson (2 x2x2)	Gauss and Simpson (2 x2x2)
Stress Components	$\sigma_{xx}, \sigma_{yy}, \sigma_{zz}, \sigma_{xy}, \sigma_{yz}, \sigma_{xz}$	$\sigma_{xx}, \sigma_{yy}, \sigma_{zz}, \sigma_{xy}, \sigma_{yz}, \sigma_{xz}$
Inclusion of shear deformation	Yes	Yes
Topological dimension	3D	3D
Average element size	200 mm	200 mm

Table 3.9: Classification of element types in timber diaphragms

(a) CQ40S

(b) CT30S
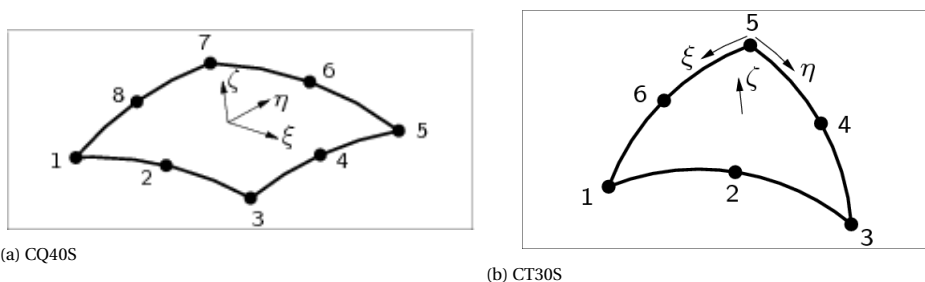
Figure 3.10: Element Models of quadrilateral and triangular shell elements - Timber diaphragms

MATERIAL MODELS- TIMBER DIAPHRAGMS

In the *first material model*, the timber diaphragms are modelled as a fictitious material with negligible mass density and as a linear elastic orthotropic material (Table 3.10). It can be seen that the mass density is of the order $10^{-20} T/mm^3$ and hence, the masses of the timber diaphragms are applied as an external load acting normally on the cross-beams as shown in figure 3.11. The dead weight calculations of the timber diaphragms is shown in appendix B.

Property	Parameter	Symbol	Unit	Value
Linear Elastic Orthotropic	Young's Modulus	E_x	N/mm^2	1.5
		E_y	N/mm^2	11
		E_z	N/mm^2	400
	Poisson's ratio	ν_{xy}		0
		ν_{yz}		0
		ν_{zx}		0
	Shear Modulus	G_{xy}	N/mm^2	1100
		G_{yz}	N/mm^2	1100
		G_{zx}	N/mm^2	500
	Density	ρ	T/mm3	10^{-20}

Table 3.10: Material properties of timber diaphragm (Linear Elastic Orthotropic model-1)
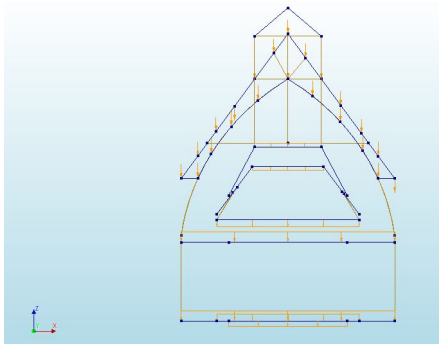
(a) x-z section (front view)
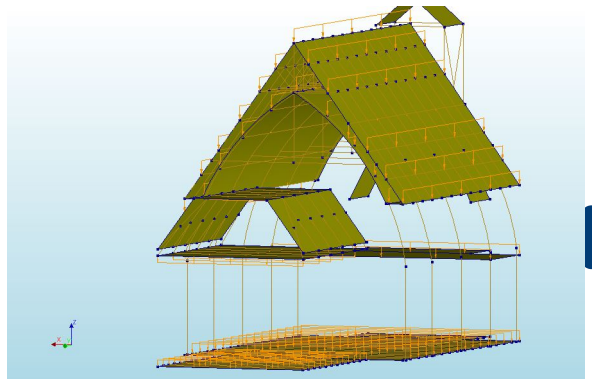
(b) Isotropic (back view)
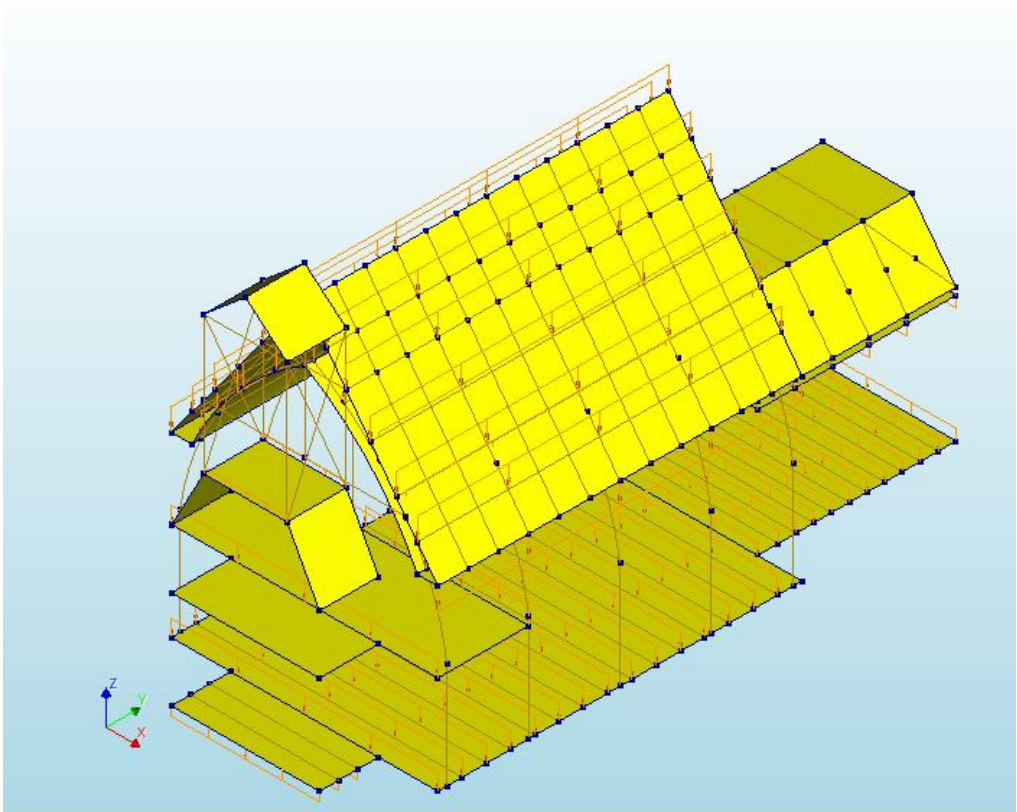
(c) Isotropic (front view)

Figure 3.11: External Additional Loading applied on the Timber cross-beams on the roof and floor structure (Material Model -1)

Furthermore, the *second material model* has emphasised on the tested and calibrated properties of timber diaphragms in the local constructions of Groningen with mainly unreinforced masonry structures and timber floors, and similar historic constructions from similar timelines.

Flexible timber diaphragms are known to deform as shear beams and they exhibit orthotropic behaviour when loaded in their plane, due to the orientation of the joists (see 3.12(a)) [28]. The in-plane behaviour of timber diaphragms with Dutch features from both experimental tests and analytical calculations as studied in detail in [29], [30]. The most widely respected recommendations for diaphragm stiffness are the data published in ASCE 41-13, which specifies a shear stiffness for straight sheathed diaphragms of 350 kN/m [31], [28].

(a) Orthogonal diaphragm response due to joist orientation.

(b) Nail joint rotation due to nail slip and nail spacing.
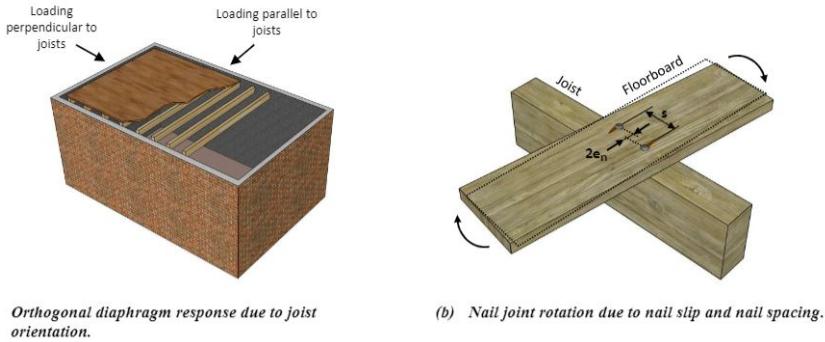
Figure 3.12: Schematics showing aspects of diaphragm response, [28]

A common way to homogenize the stiffness values of timber diaphragms is to adopt a size-independent parameter, the equivalent shear stiffness ($G_d = G.t$, with G, floor's global shear modulus and t= thickness of floor planking). This parameter can be considered reliable for diaphragms for which the in-plane behavior can be assumed as shear-related, such as the strengthened ones; for as-built floors with continuous planks and joists where the flexural response is dominant, and hence G_d is size-dependent and loading direction dependent [28].

Additionally, the material properties of an experimentally validated vintage flexible timber diaphragms which underwent seismic damage (a historical building in Whanganui (lower North Island of New Zealand) that was constructed in 1913, making the diaphragms 99 years old at the time of testing) are considered in this variation. Both diaphragm test sections were in poor condition, as shown in figure 3.13 and the figure 3.16 shows the experimentally calibrated shear stiffness values. [28]

It should be noted that even though testing, time period and the seismic loading is similar, these values correspond to the material model of the regional timber species in New-Zealand but with no experimental data or physical tests of the timber diaphragms in the case-study structure, the material properties for timber diaphragms in this second

(a) *Evidence of mass-loss due to insect infestation.*

(b) *Evidence of decay due to moisture.*

Figure 3.13: Deteriorated condition of vintage Whanganui timber diaphragm tested in-situ.[32]

Direction of loading	Joist continuity	Condition rating	Shear stiffness†, G_d (kN/m)
Parallel to joists	Continuous or discontinuous joists	Good	350
		Fair	285
		Poor	225
Perpendicular to joists††	Continuous joist, or discontinuous joist with reliable mechanical anchorage	Good	265
		Fair	215
		Poor	170
	Discontinuous joist without reliable mechanical anchorage	Good	210
		Fair	170
		Poor	135

† Values may be amplified by 20% when the diaphragm has been renailed using modern nails and nail gun
†† Values should be interpolated when there is mixed continuity of joists or to account for continuous sheathing at joist lap

Figure 3.14: Shear stiffness values for straight sheathed vintage flexible timber floor diaphragms [32]

material model [table 3.11] are assumed from [28], [30].

3

Property	Parameter	Symbol	Unit	Value
Elasticity	Young's Modulus	E_x	MPa	10000
		E_y	MPa	10000
		E_z	MPa	10000
	Poisson's ratio	v		0
	Density	ρ	T/mm3	9 e-09
	Shear Modulus	G_{xy}	N/mm2	6.66
		G_{yz}	N/mm2	625
		G_{zx}	N/mm2	625

Table 3.11: Material properties of timber diaphragm (Linear Elastic Orthotropic model-2)

From the plans of the case-study, (The Old Church in Garrelsweer, Groningen) the flooring and roof of existing timber diaphragms are 30mm thick with board widths of 100-150mm. The diaphragm response properties can be approximated as an equivalent elastic system.

In the table 3.11, the in-plane shear modulus (G_{xy}) is calculated based on equivalent shear stiffness of 200 N/mm and out of plane shear modulus (G_{yz}, G_{zx}) is calculated based on the established formula of $G = E/16$ for elastic timber systems. Due to negligible thickness compared to other dimensions of diaphragm panels and due to no slab effect in the timber floors, the Poisson's ratio is assumed to be zero ($v = 0$) in this material model-2.

3.2.6. SUPPORT CONDITIONS

The initial assumption for modelling the support conditions of the case study is considering a fixed base structure. Generally, the effects of soil- structure interaction should be considered in design when they concern massive and embedded foundations, slender structures like towers, masts and chimneys, more specifically any structure sensitive to second order effect (P-δ effects), structures founded on soft soil deposits with a wave velocity V_{S30} less than 100m/s, and piled foundations.

As a result of soil-structure interaction, the seismic response of a structure is modified with respect to the case of a fixed base structure. Soil-structure interaction generally has a beneficial effect on the performance of a structure, due to the flexibility of the ground the fundamental period of vibration is elongated, significant rocking movements may take place and the overall damping of the system is increased due to radiation damping. For the majority of structures, except those listed above, these effects tend to be beneficial because they reduce the seismic forces.

In this case-study of The Old Church none of the above mentioned design concerns are met. This structure is founded on soft soil deposits described by the strati-graphic profiles and parameters taken from the NPR9998:2020 Webtool (fig 3.15) at the location of the church with a average wave velocity of V_{S30} = 177m/s indicating deposits

of loose-to-medium cohesion-less soil (with or without soft cohesive layers), or of pre-dominantly soft-to-firm cohesive soil. (soil category D) from the table 3.1 in Eurocode 8 [11] and it is greater than $V_{s30} = 100m/s$. Hence, the second order effects can be neglected and the conservative assumption to use a 'fixed-base' structural model of the foundation is expected to continue to serve its function for the model under consideration [NPR9998:2021] [8].
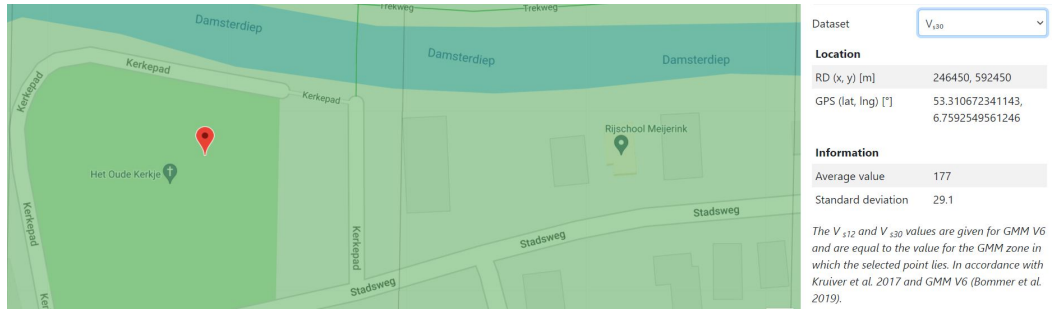

Figure 3.15: average shear wave velocity at case study, NPR9998:2020 webtool [8]

The foundation is modelled as a fixed base at the ground level by restraining all the translations and rotations at the boundary. For simplifying the modelling further, a tying is modelled connecting all the edges to a single vertex at the foundation by an equal connection of translations and rotations as shown in figure 3.16.
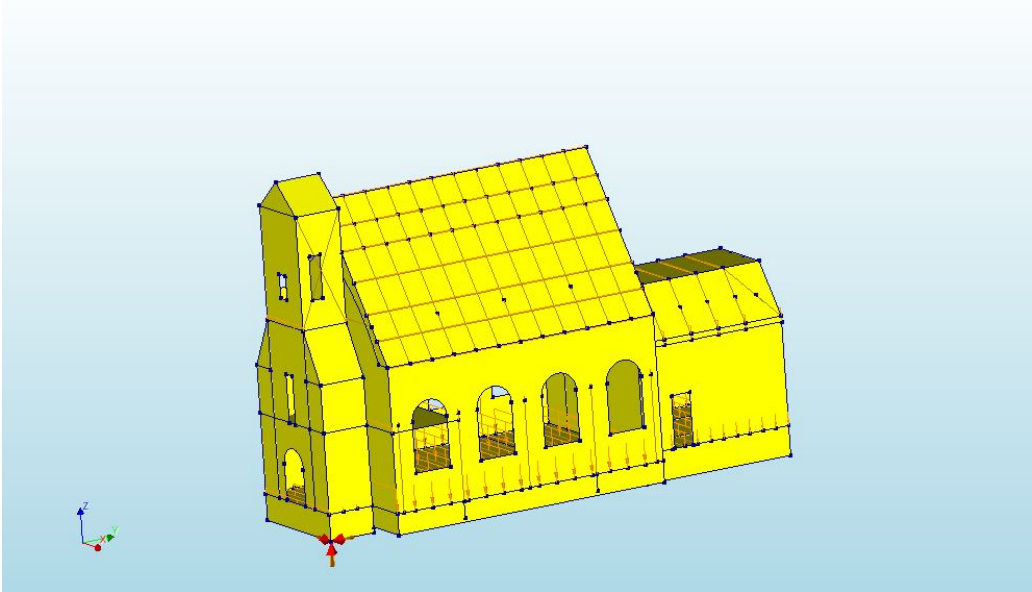
Figure 3.16: Modelling the fixed base support using tyings

3.2.7. LOADING CONSIDERATIONS

Two load combinations are considered in modelling the case study

1. Gravity/ Self-weight: Global load computed for all the structural elements based on their mass density. It should be noted that when material model-1 is considered for timber diaphragms the corresponding mass of the timber floor and roof structure is assigned in addition to the global load (Annex: B).

2. Additional characteristic loads according to Eurocode 8, discussed in detail below.

CHARACTERISTIC-LOADS

Along-side the self weight of the structure, additional dead load and imposed loads are considered on the roof and floor structures according to Eurocode 8 [11]. In order to apply these loads, the category of usage of the church is defined as C2: Areas with fixed seats (eg. churches), where

- Imposed loads on floors, stairs and balconies in the building is $q_k = 4.0 kN/m^2$ (table 6.2, Eurocode 1 1991-1-1)

- Roof load: Roofs not accessible except for normal maintenance and repair.(category H) has a recommended value of $q_k = 0.4 kN/m^2$ (Table 6.10 Eurocode 1 1991-1-1) [33]

- Dead load on the floors is $q_k = 2kN/m^2$

These characteristic loads are applied as a line load (kN/m) in the normal direction over the cross beams of the roof and floor as shown in Fig 3.17.
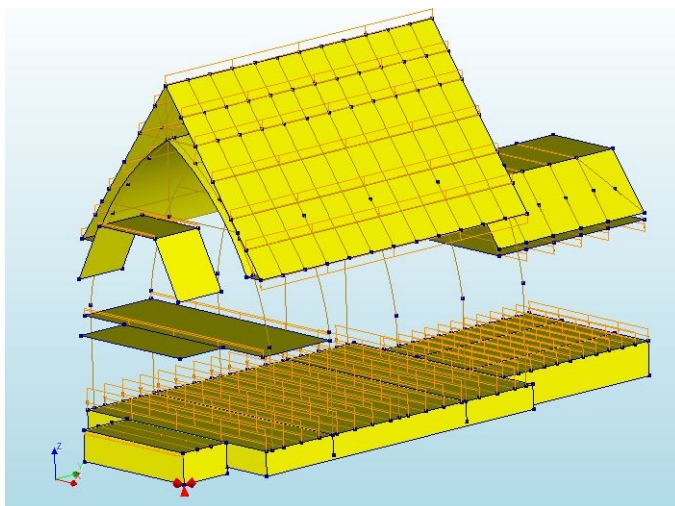
Figure 3.17: Characteristic loads applied on floor and roof structure

3.3. DISCRETIZATION

As discussed in previous sections, regular curved shell elements and class-III beam elements are adopted to capture the in- and out-of-plane behaviour of the structural components of the case study. These higher order finite elements are based on Mindlin-Reissner theory for which transverse shear deformation is included. Non-linear behaviour is included for the masonry only and lastly, the orientation of the local axes of the masonry elements is treated with extra care due to the orthotropic material behaviour. Figure 3.18 depicts the meshing, local axis orientation, loading and support conditions of the reference model.The average element size considered for all structural elements is 200mm.
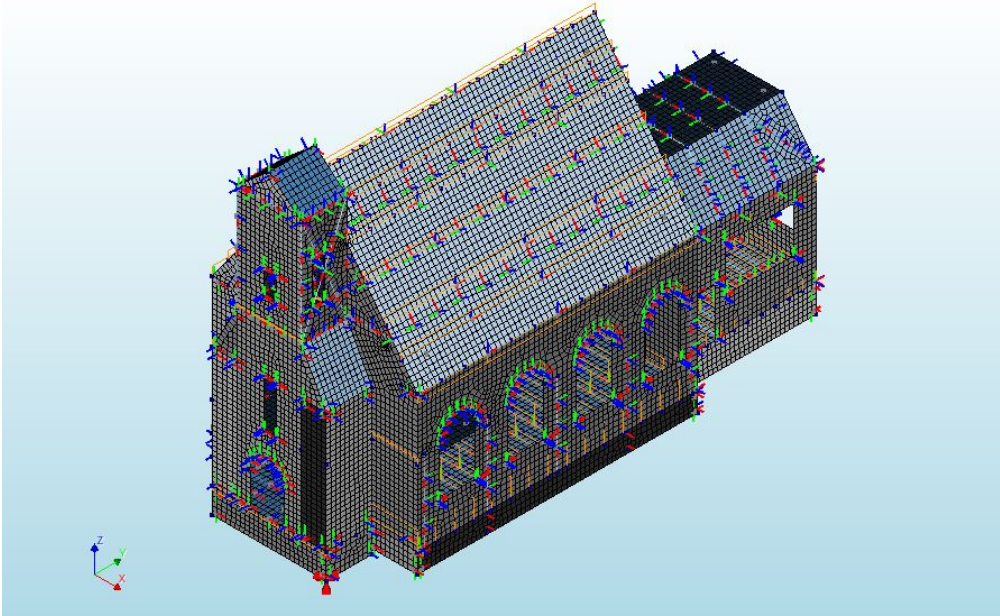
Figure 3.18: Finite element meshing of the reference model depicting local axis, loading and support conditions (average element size of 200mm)

3.4. CHARACTERISTICS OF EIGEN FREQUENCY

As discussed in section 2.1, the first step in performing a dynamic analysis is determining the natural frequencies and mode shapes of the structure with damping neglected-free vibration analysis. These results characterize the basic dynamic behaviour of the structure and indicate how a structure will respond under dynamic loading.

Considering the equation of motion of an undamped single degree of freedom (SDOF) system

$$m\ddot{u} + ku = f(t) \tag{3.1}$$

If, however, no external force is acting on the mass, nonzero solutions may still exist. It can be immediately verified that

$$u = A\sin\omega_0 t + B\cos\omega_0 t \tag{3.2}$$

fulfills the homogeneous equation of motion if

$$\omega_0 = \sqrt{\frac{k}{m}} \tag{3.3}$$

Here, ω_0 is the natural angular frequency, having the unit rad/s. It is related to the natural frequency (unit: Hz) by $\omega_0 = 2\pi f_0$. We can interpret the solution above as: Once the

process has started, a free vibration can exist at exactly this frequency without any external excitation. In real life, there is always some damping, so ultimately the vibrations would fade away. [34]

The expression for the eigen-frequency above exhibits very general behavior in terms of how stiffness and mass influence eigen-frequencies:

$$\omega_0 \propto \sqrt{\frac{\text{stiffness}}{\text{inertia}}} \tag{3.4}$$

So, we can predict that as the stiffness of the system decreases or the mass of the system increases in the particular direction considered, the eigen-frequencies decrease.

Effective mass participation in Eigen-modes

The Effective Mass Participation Factor (EMPF) represents the percentage of the system mass that participates in a particular mode. It provides a measure of the energy contained within each resonant mode. A mode with a large effective mass participation factor (EMPF) is usually a significant contributor to the dynamic response of a system. The EMPF for each mode and each direction is a reflection of how the center of gravity of the structure gets excited by that mode. [27]

The Cumulative Effective Mass Participation Factor (CEMPF) is a measure of how the EMPF builds up as additional modes are included in the analysis. In general, the number of modes considered must contribute to a CEMPF of at least 80% of the system mass in the direction of excitation. Hence, by evaluating the Effective Mass Participation of global modes in each direction, the dynamic response of the structure can be predicted. [27]

The Old Church in Garrelsweer (case-study) is numerically modelled with variations in geometrical, material and shape properties of the structural elements as discussed in this chapter and from the free vibration analysis of the model, the important modes based on highest EMPF in each direction are recorded and presented in the next chapters.

4

NUMERICAL RESULTS

Following the numerical modelling, this chapter presents the eigen-value analysis, results and the main modal deformations in each direction for all the simulated models with a detailed description of the modelling simplifications and variations assumed for each model.

4.1. MODEL-1

As a starting point in the first model, the geometrical details, loading and support conditions are as discussed in chapter-3. The material models and further assumptions considered are shown in table 4.1.

Finite Element Model-1		
Structural elements	*Material Model*	*Further assumptions, reference*
Masonry Walls	Continuum EMM	Table 3.3
Masonry Foundation	Continuum EMM	Table 3.3
Masonry Piers	TSCM	Table 3.6
Timber Joists	Linear Elastic Isotropic Model	Table 3.8
Timber Diaphragms	Linear Elastic Orthotropic Model -1 (fictitious material)	Additional Timber diaphragm Loading, Table 3.10

Table 4.1: Material Models and specific assumptions for Model-1

Eigen-value analysis is conducted to find the global eigen-modes of the structure. The important properties of the eigen-modes are the natural period, shape and the modal mass participation. The modal mass participation provides a method for judging the significance of each eigen-mode. The modal shape indicates the direction in which the structure is most likely going to deform due to a dynamic loading. First 350 eigen-values are evaluated, with eigen-frequencies ranging from 0.2Hz to 4.36Hz (C.1) to obtain cumulative mass percentage of 39.043% in X-direction and 74.25% in Y direction respectively. The global eigen-modes in the first 350 eigen-modes with modal mass participation ≥ 5% are shown in table 4.2.

Mode Number	Frequency (Hz)	Time Period (s)	Effective Mass & Direction	Effective Mass Percentage (%)
25	0.7428	1.3462	0.3167 E+03	9.349
197	2.7516	0.3634	0.37137 E+03 (Y)	10.96

Table 4.2: Modal Mass participation of global modes in global X and global Y direction for the first 350 Eigen values (Model 1)

Governing Eigen modes in Global X direction

From the eigen-value analysis, the global eigen modes in X direction with a modal mass participation ≥ 5% are recorded. It can be seen that only one eigen mode -25 shows a maximum mass participation of 9.349% within the first 350 eigen-modes evaluated and the cumulative modal mass participation in global X direction is limited to 39%. As the cumulative modal mass participation factor is less than 80%, the NPR 9998 states that higher modes are likely to be significant for the structural dynamic response of the church.
Out of all considered global modes in X-direction, Mode 25 (Eigen-frequency of 0.7428 Hz & time period of 1.3462s) is recognised as a significant mode with effective modal mass participation percentage of 9.349% [Fig 4.1].

Governing Eigen Modes- Global Y direction

The global eigen-modes in Y direction with a modal mass participation ≥ 5% in the first 350 eigen-modes are presented in Table 4.2. The cumulative modal mass participation is 74.25%, lesser than 80%, so higher modes are likely to be significant for the dynamic behaviour of the structure in Y direction. One of the governing global eigen-mode in the global Y-direction is Mode 197 (natural frequency of 2.7516Hz and Time period of 0.3634s) with highest modal mass participation of 10.96% [Fig 4.2].
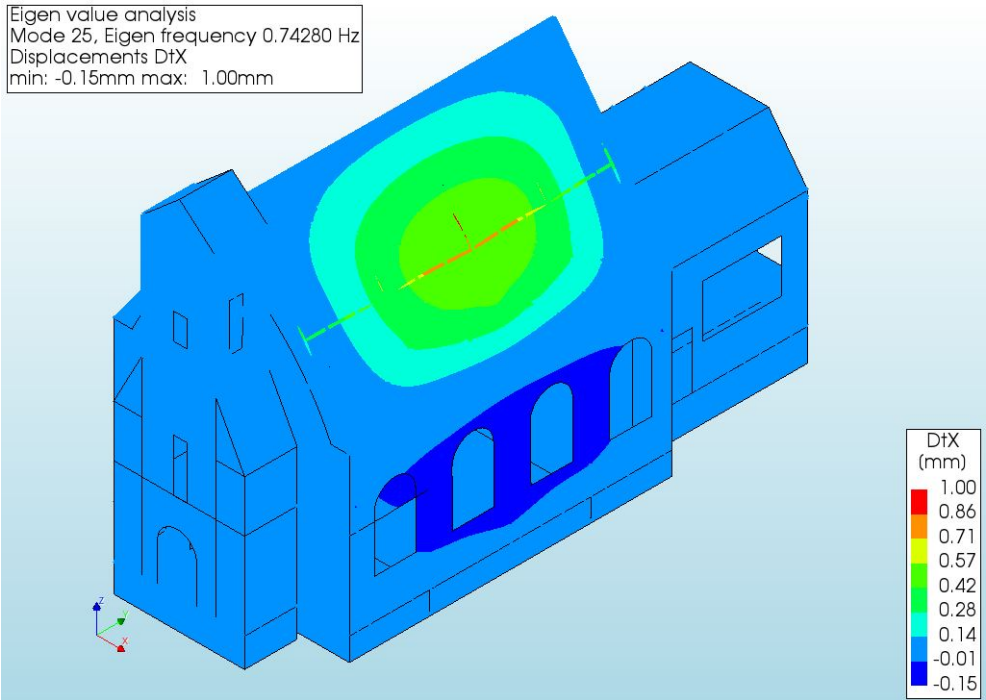
(a) Isotropic view- Mode 25
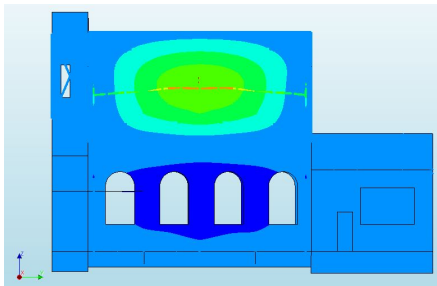
(b) Side View- Mode 25
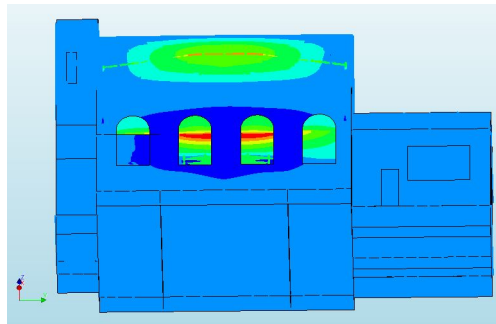
(c) Side View- Mode 25

Figure 4.1: Global Mode 25(X)- indicating modal deformation (out-of plane) of roof and wall systems [scale factor-0.05]

Eigen value analysis
Mode 197, Eigen frequency 2.7516 Hz
Displacements DtXYZ
min: 0.00mm max: 1.00mm

DtXYZ
(mm)
1.00
0.88
0.75
0.63
0.50
0.38
0.25
0.13
0.00
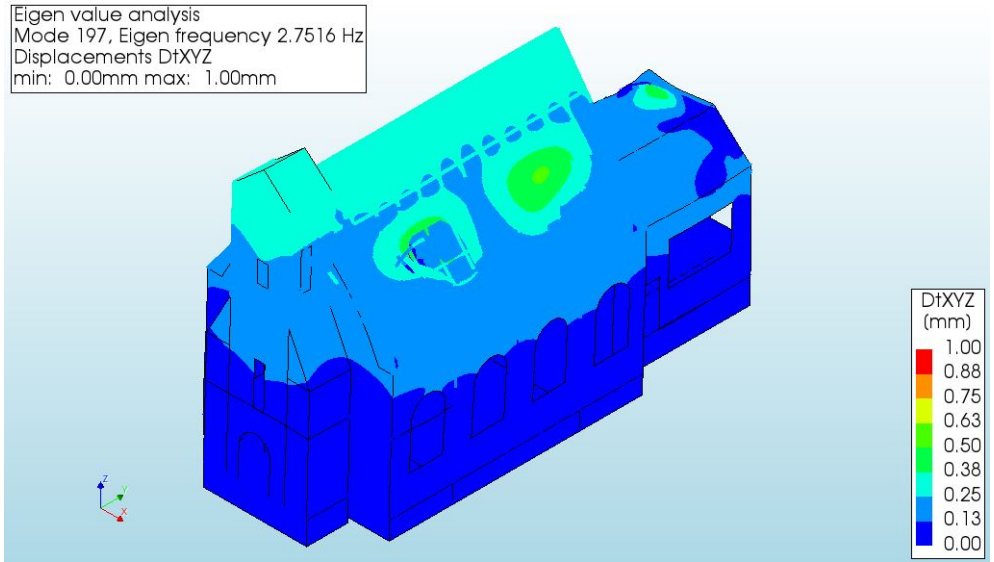
(a) Isotropic view- Mode 197
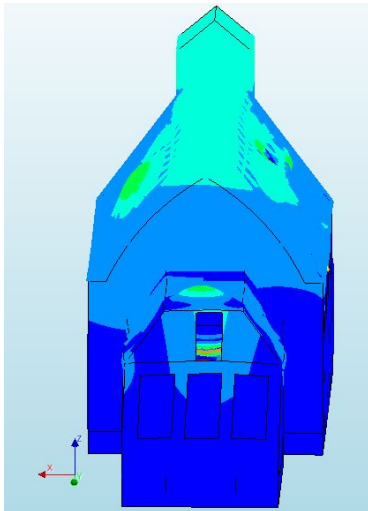
(b) Back view- Mode 197
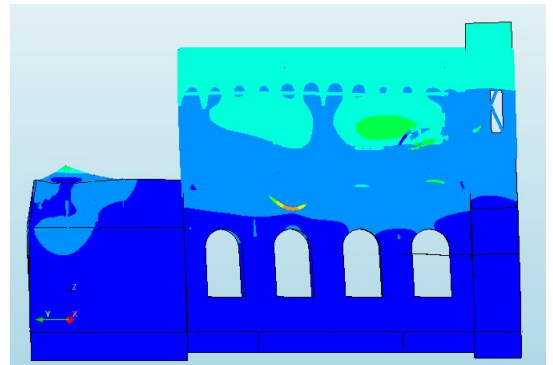
(c) Side view- Mode 197

Figure 4.2: Global Mode 197- indicating modal deformation (translation) of roof, floor and wall systems [scale factor-0.05]

OVERALL BEHAVIOUR OF FIRST MODEL (FINITE ELEMENT MODEL-1)

The response of all natural modes of vibration contributing significantly to the global response of the structure are taken into account and when using a spatial model. The above conditions should be verified for each relevant direction according to [8]. From table 4.2, it can be noted that the time period of the main global modes in X and Y are within the same range of 0.35- 1.35 seconds.
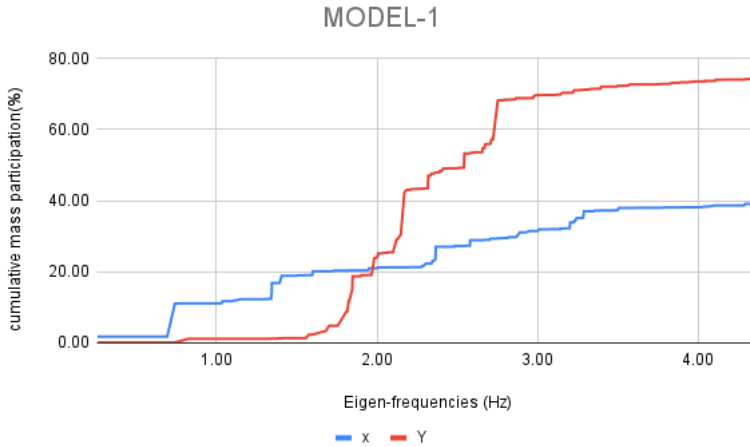
Figure 4.3: Eigen-frequencies and cumulative mass participation in X and Y direction- Model 1

The cumulative mass participation of the global modes in model-1 is very low in X direction [Fig 4.3], it can be seen that at the eigen-frequency of around 0.7Hz there is a jump in mass participation due to a localized mode of the roof-structure and there is a gradual increase in the modal mass participation up to 40% in the X direction. In Y direction, jumps in the mass participation can be observed around the eigen-frequencies of 1.8 Hz, 2.3Hz and 2.75Hz each corresponding to the out-of plane deformation of timber joists in the roof or the first-floor of the sub-structure. Due to the presence of many localised modes in the timber flooring, it should be noted that 350 eigen-modes are analyzed to reach the cumulative mass participation of 40% and 70% which makes the model very inefficient.

The main hindrance of this model is presence of many localized modes in the ground floor which cannot be captured with the sensors and the major modal deformation in both global X,Y direction in the timber joists with external normal loading from the timber diaphragms [fig. 4.4]. In practical applications, considering 350 eigen-values will be very inefficient due to increased computational time and memory requirement. In-order to overcome these, the first model is modified as discussed in the next section.
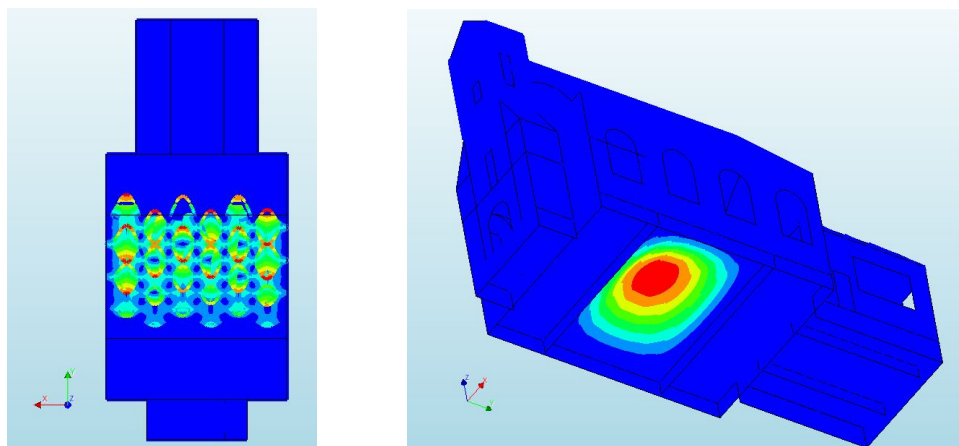
Figure 4.4: Localised modes in the ground floor of Model-1

4.2. MODEL-2 (*Reference Model*)

In Model-1, major modal deformation has occurred on the timber joists instead of a global deformation due to considering the fictitious timber diaphragms, thus in this Model-2 the timber material model is modified as shown in table 4.3 considering the equivalent shear stiffness model from [30],[28].

Finite Element Model-2

Structural elements	Material Model	Further assumptions, reference
Masonry Walls	Continuum EMM	Table 3.3
Masonry Foundation	Continuum EMM	Table 3.3
Masonry Piers	TSCM	Table 3.6
Timber Joists	Linear Elastic Isotropic Model	Table 3.8
Timber Diaphragms	Linear Elastic Orthotropic Model -2	Table 3.11

Table 4.3: Material models and specific assumptions for Model-2

Eigen-value analysis is carried out for the first 350 eigen-modes of the structure with eigen-frequencies ranging from 0.467 Hz to 16.53 Hz (C.2). The cumulative modal mass participation for this model is 80.79% in global X and 80.28% in global Y direction for the considered 350 eigen modes. Hence, as per [8], the significant eigen modes depicting the dynamic behaviour of the case-study lie within the first 350 eigen-modes in both global X and Y directions. All modes with effective activated mass-participation percentage ≥ 5% are recorded in table 4.4 with the corresponding eigen-frequencies and time periods.

Mode Number	Frequency (Hz)	Time Period (s)	Effective Mass & Direction	Effective Mass Percentage (%)
40	2.7065	0.3695	0.9287 E+02 (X)	4.927
108	6.434	0.1554	0.3279 E+03 (X)	17.40
115	6.8437	0.1461	0.9836 E+02 (X)	5.218
116	6.8796	0.1453	0.23593 E+03 (X)	12.52
348	16.408	0.0609	0.19127 E+03 (X)	10.148
49	3.173	0.3152	0.18344 E+03 (Y)	9.732
52	3.2248	0.3101	0.10105 E+03 (Y)	5.361
203	9.7326	0.1027	0.9287 E+02 (Y)	4.927
205	10.192	0.0981	0.7000 E+03 (Y)	37.142
226	10.851	0.0921	0.1433 E+03 (Y)	7.602

Table 4.4: Modal Mass participation of global Modes in global X and global Y direction for the first 350 eigenvalues (Model 2)

GOVERNING EIGEN MODES IN GLOBAL X DIRECTION

The first governing global mode with maximum mass participation percentage of 5% is mode 40 with an eigen-frequency of 2.7065 Hz and time period of 0.369s [Fig 4.5]. However, global mode 108 (eigen frequency-6.434Hz), has the highest mass participation percentage of 17.40% in global X direction.

GOVERNING EIGEN MODES- GLOBAL Y DIRECTION

Similar to global X direction, the cumulative modal mass participation percentage has increased to 80.28% in global Y direction. The first global governing mode with maximum modal mass participation of 9.73% is mode 49 with eigen-frequency 3.173Hz and time period 0.3152s. [Fig 4.6] However, global mode 205(eigen frequency-10.192Hz) has the highest mass participation percentage of 37.142% in global Y direction.

4

Eigen value analysis
Mode 40, Eigen frequency 2.7065 Hz
Displacements DtXYZ
min: 0.00mm max: 1.07mm

DtXYZ
(mm)
1.07
0.94
0.80
0.67
0.54
0.40
0.27
0.13
0.00
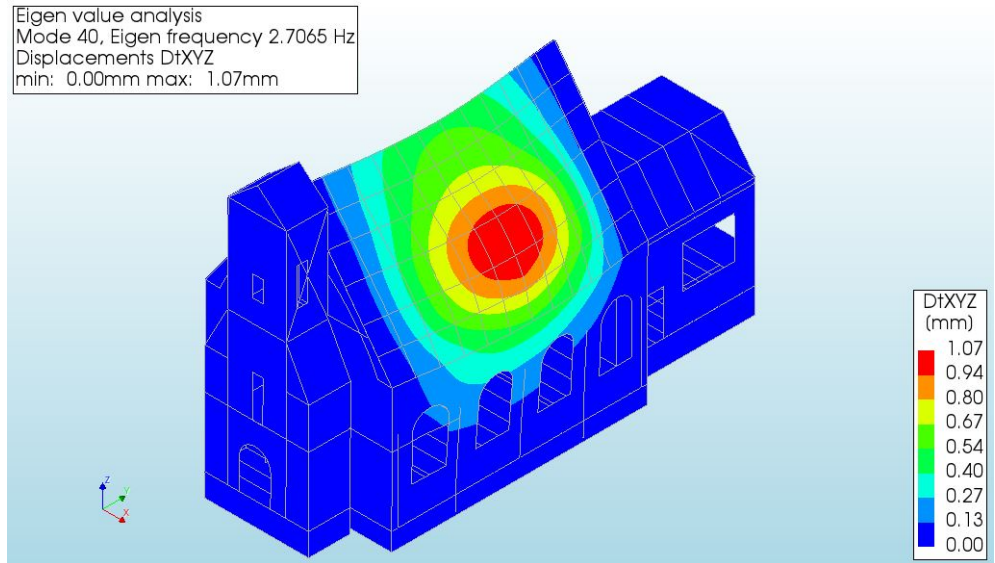
(a) Isotropic view- Mode 40
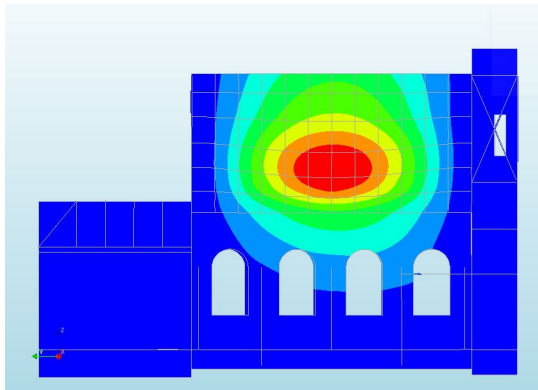
(b) Side View- Mode 40
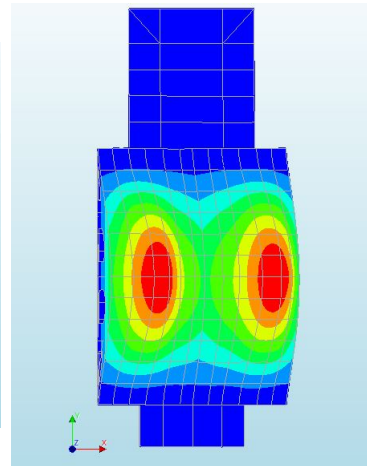
(c) Top View- Mode 40

Figure 4.5: Global mode 40 - indicating modal deformation (out-of plane) of roof and wall systems [scale factor-0.05]
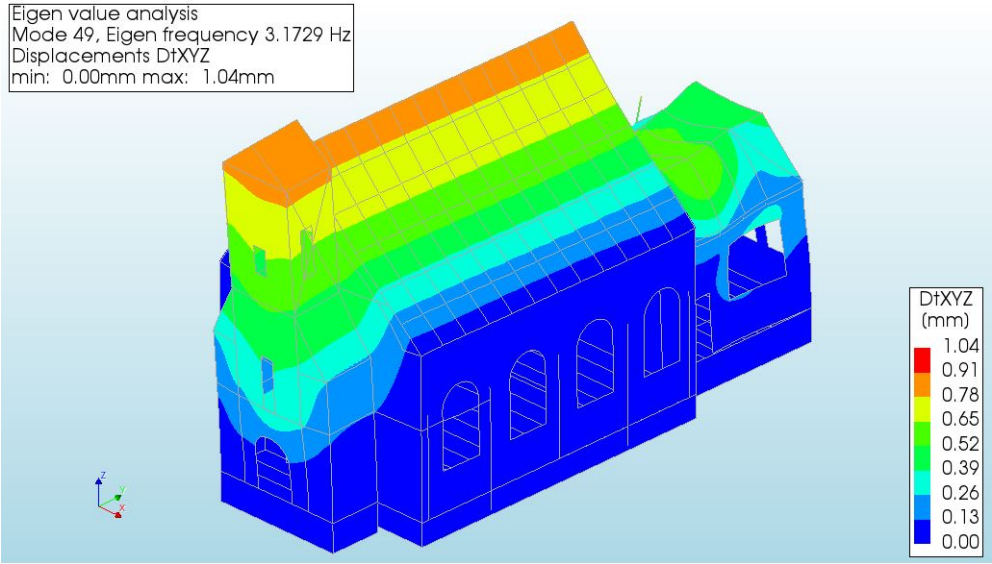
(a) Isotropic view- Mode 49
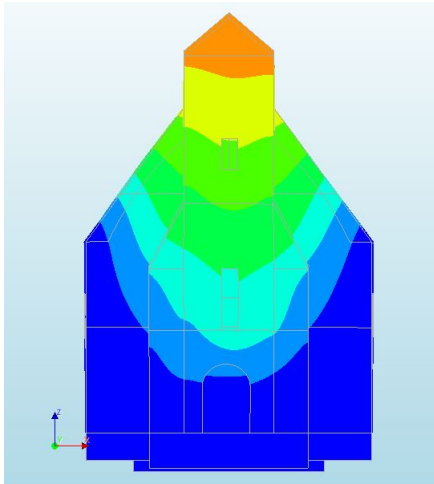
(b) Front View- Mode 49
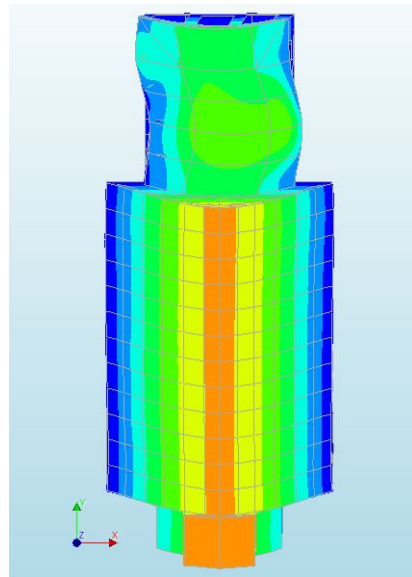
(c) Top View- Mode 49

Figure 4.6: Global mode 49- indicating modal deformation (translation) of roof and wall systems [scale factor- 0.05]

OVERALL BEHAVIOUR OF MODEL-2

The response of all modes of vibration contributing significantly to the global response are taken into account. It can be seen that the cumulative mass participation is same

in both global X and Y directions (80%) and the fundamental eigen-frequencies depict a global mode deformation with maximum effective mass participation. In X direction, there is a distinctive jump at 2.7Hz and 6.5Hz while in Y direction, the distinctive jumps are around 3.2Hz and 10.2Hz indicating the clear modes of vibration [fig 4.7]. The fundamental modes of vibration were found within the first 50 eigen-modes making the model more efficient for computation.
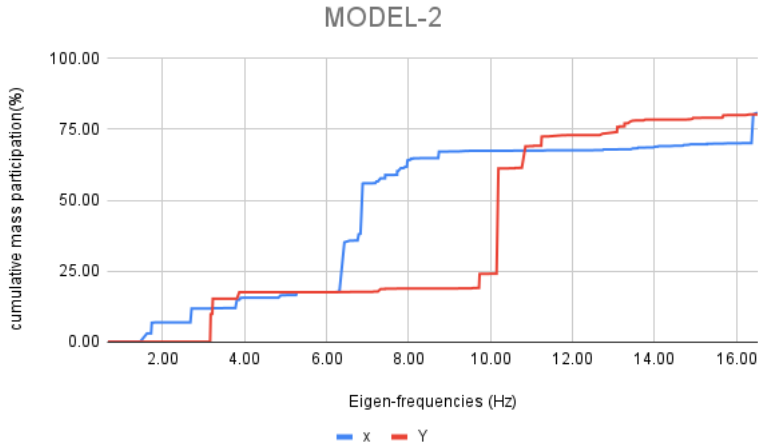
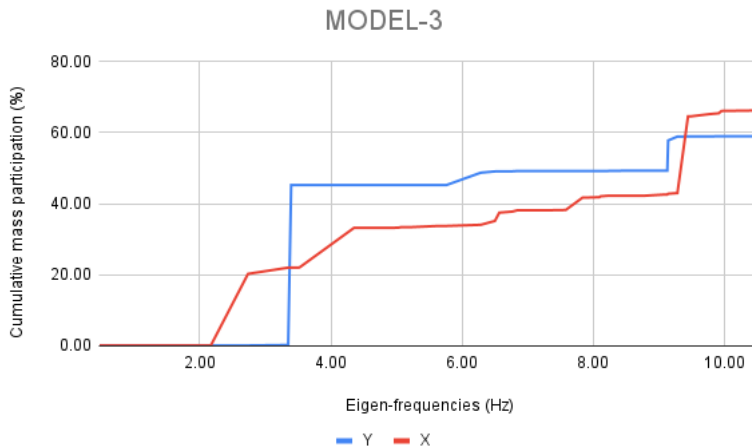Figure 4.7: Eigen-frequencies and cumulative mass participation in X and Y direction- Model 2

With the increase in the effective mass participation and clear indication of global modes, this model can be regarded as the *"Reference Model"* from here on and further simulations are compared with the reference model as a base.

4.3. MODEL-3

A simplified assumption of a rigid base at ground level is made in this Model-3 in order to reduce the local modes on the floor, also the sensors for ambient vibration testing cannot be placed on the timber floors. Modelling the foundation and flooring is eliminated and rigid boundary conditions are applied on the edge of masonry walls by restricting the rotations and translations (T1,T2,T3,R1,R2,R3 are fixed) as shown in figure 4.8. The material models and further assumptions of Model-3 are similar to the reference model [table 4.3].

First 200 eigen-modes ranging from 0.467Hz to 27.96Hz (C.3) are evaluated and the cumulative mass participation percentage is 83.89 % in global X and 81.192% in global Y direction respectively. All the global eigen-modes with a mass participation ≥ 5% are shown in table 4.5 as the total mass participation percentage is below 90%. [8]
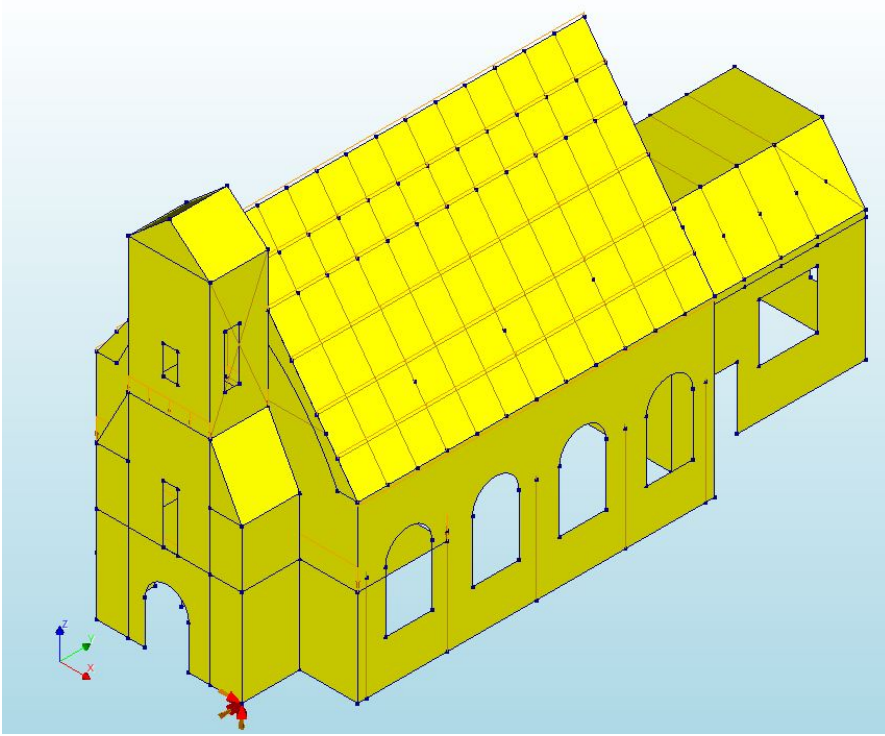
Figure 4.8: Finite element model-3 with fixed base

Mode Number	Frequency (Hz)	Time Period (s)	Effective Mass & Direction	Effective Mass Percentage (%)
4	2.7377	0.3653	0.69537E+02 (X)	20.187
8	4.3521	0.2297	0.38500E+02 (X)	11.177
24	7.8363	0.1276	0.12092 E+02 (X)	3.5103
36	9.4412	0.1059	0.74450 E+02 (X)	21.613
6	3.3950	0.2945	0.215535 E+03 (Y)	45.098
16	6.2828	0.1592	0.11929 E+02 (Y)	3.463
34	9.1390	0.1094	0.29293 E+02 (Y)	8.5041
48	11.621	0.0860	0.15071 E+02 (Y)	4.3754
53	12.348	0.0809	0.11655E+02 (Y)	3.3837

Table 4.5: Modal mass participation of global modes of the first 200 eigen-modes in global X and global Y direction (Model 3)

Governing Eigen Modes in Global X direction

The cumulative modal mass participation is 83.89% in global X direction for the first 200 eigen-modes, hence the dynamic properties of the case-study in X direction lie within the first 200 eigen-modes. The governing first global mode is Mode 4 (Eigen Frequency of 3.59Hz and time period of 0.3653s) with a maximum mass participation of 20.187% in global X direction [Fig 4.10].

Governing Eigen Modes in Global Y direction

The cumulative modal mass participation is 81.19% for the first 200 eigen-modes hence the significant dynamic properties of the structure in the Y direction lie with-in the first 200 eigen-modes. The governing first global mode is Mode 6 (Eigen frequency of 3.3950Hz and time period of 0.2945s) with the maximum modal mass participation of 45.098% in global Y direction. [fig 4.11]

Overall Behaviour of Model-3

In comparison to the reference model (model-2), the cumulative mass participation percentage of 80% is achieved within the first 200 eigen-modes in both global X and Y direction. In X axis, at eigen-frequencies around 2.5Hz and 9.5Hz and in Y axis around 3.5Hz and 9Hz there is a distinctive jump. [Fig 4.9] The first global modal deformation shape in global X and global Y direction is similar to the reference model but the activated mass participation percentage of these modes is increased to 20.2% and 45% in each direction respectively and these main modes are obtained within the first 10 eigen-values. But it was also noted that the period of vibration roughly doubles in both directions.

Figure 4.9: Eigen-frequencies and cumulative mass participation in X and Y direction- Model 3
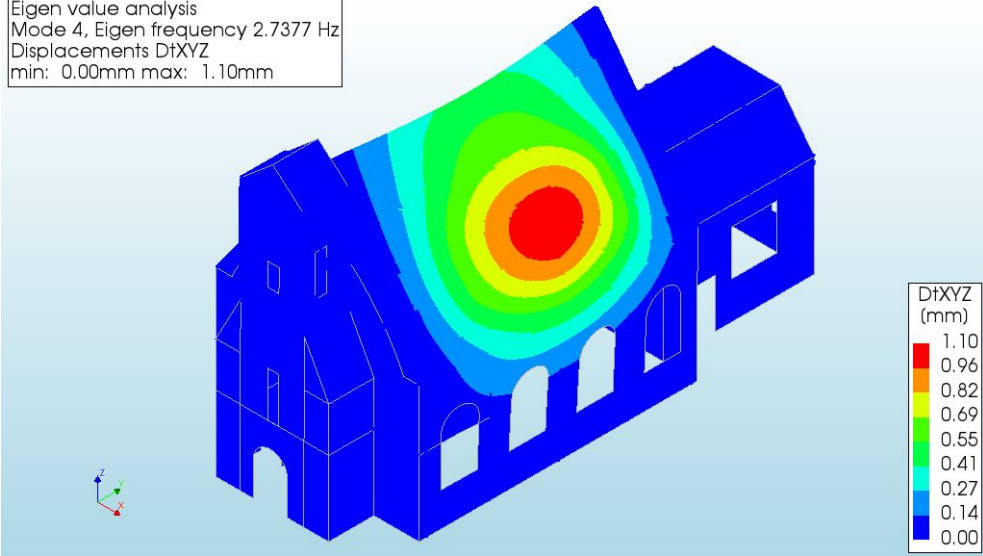
(a) Isotropic view- Mode 4
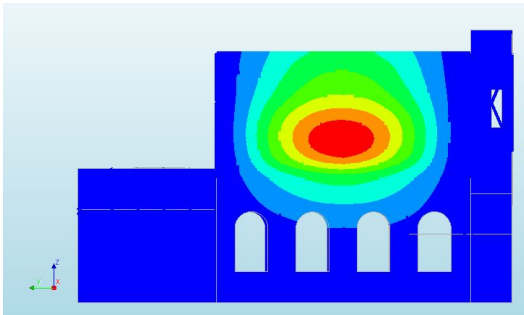
(b) Side View- Mode 4
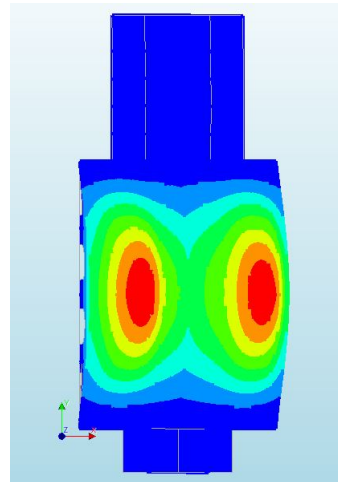
(c) Top View- Mode 4

Figure 4.10: Global mode 4 - indicating modal deformation (out-of plane) of roof and wall systems [scale factor-0.05]

Eigen value analysis
Mode 6, Eigen frequency 3.3950 Hz
Displacements DtXYZ
min: 0.00mm max: 1.01mm

DtXYZ
(mm)
1.01
0.88
0.76
0.63
0.50
0.38
0.25
0.13
0.00
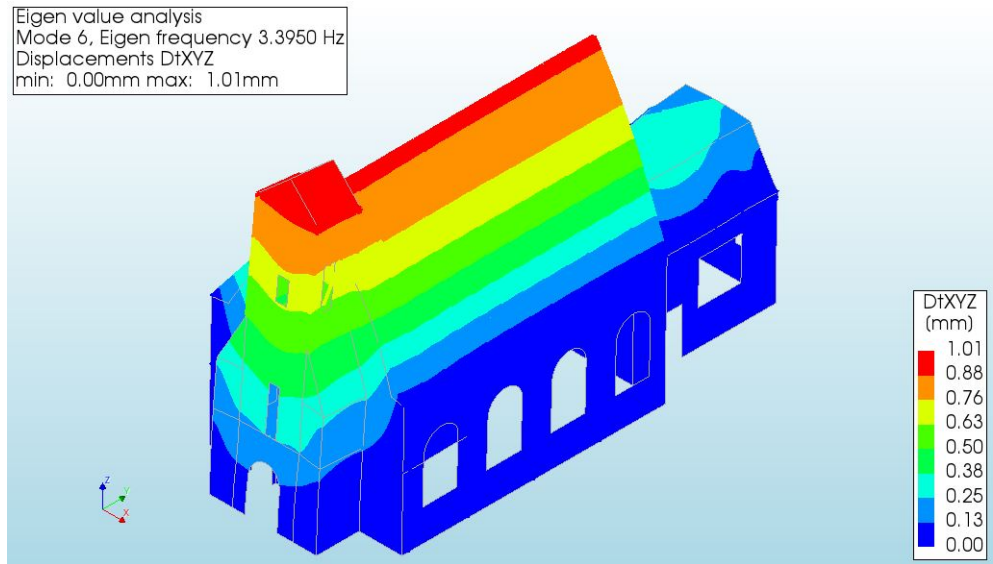
(a) Isotropic view- Mode 6
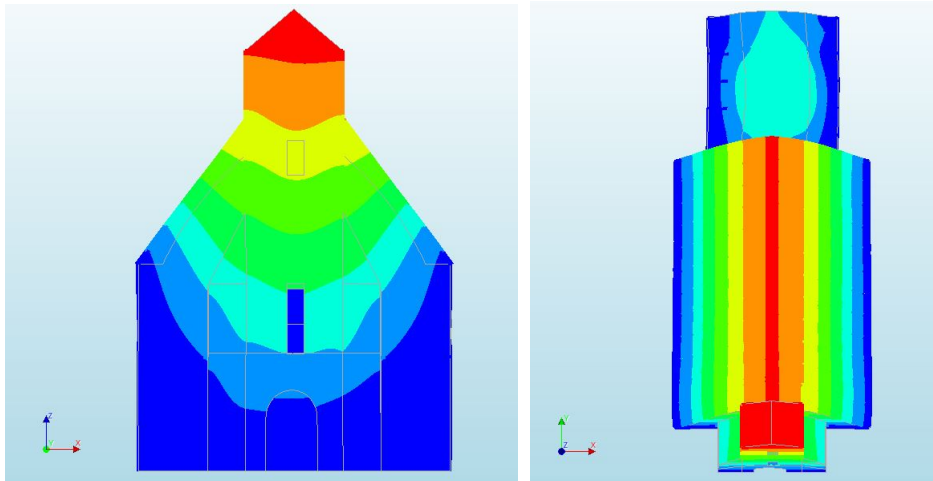
(b) Front View- Mode 6

(c) Top View- Mode 6

Figure 4.11: Global mode 6- indicating modal deformation (translation) of roof and wall systems [scale factor- 0.05]

4.4. MODEL-4

In this model simulation, additional to the assumptions of model-3 instead of assuming a fixed base, the rotations are released at every edge of the masonry-wall (R1,R2,R3) as shown in Fig 4.12 to approximate the flexible foundation.
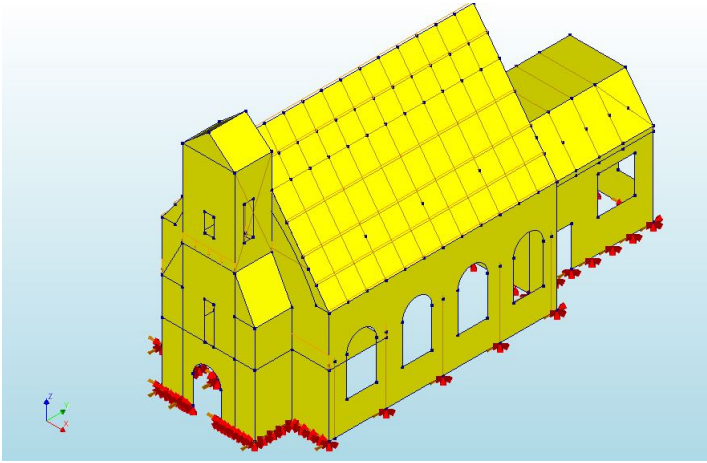
Figure 4.12: Finite element model 4 with released rotations at the masonry wall edges

The first 200 eigen-modes are evaluated ranging from 0.4696Hz to 27.154Hz (C.4) with cumulative mass participation percentage of 87.216% in global X direction and 82.064% in global Y direction. All the global modes with mass participation percentage ≥ 5% in global X and Y direction are shown in table 4.6.

Mode Number	Frequency (Hz)	Time Period (s)	Effective Mass & Direction	Effective Mass Percentage (%)
4	2.3422	0.4269	0.98954 E+02 (X)	28.845
5	3.3074	0.3023	0.14482 E+02 (X)	4.2217
16	5.9598	0.1677	0.15271 E+02 (X)	4.4515
38	9.1963	0.1087	0.42057 E+02 (X)	12.260
42	9.9580	0.1004	0.18374 E+02 (X)	5.3560
7	3.4516	0.2897	0.15982 E+03 (Y)	46.5880
17	6.1647	0.1622	0.12636 E+02 (Y)	3.6835
32	8.5313	0.1172	0.11277 E+02 (Y)	3.2872
52	11.799	0.0847	0.50139 E+02 (Y)	14.616

Table 4.6: Modal mass participation of global modes of the first 200 eigen-modes in global X and global Y direction (Model 4)

GOVERNING EIGEN MODES IN GLOBAL X DIRECTION

The cumulative modal mass participation is 87.216% in global X direction for the first 200 eigen-modes. The governing first global mode is Mode 4 (eigen frequency of 2.3422 Hz and time period of 0.4269 s) with a maximum mass participation of 28.845% in global X direction [Fig 4.14].

GOVERNING EIGEN MODES IN GLOBAL Y DIRECTION

The cumulative modal mass participation is 82.064% for the first 200 eigen-modes. The governing first global mode is Mode 7 (eigen frequency of 3.4516 Hz and time period of 0.2897s) with the maximum modal mass participation of 46.588 % in global Y direction. [fig 4.15]

OVERALL BEHAVIOUR OF MODEL-4

Compared to model 3, the principal mode in X direction has a longer period while a small difference in Y direction. This is due to release of the degrees of freedom has more influence in the opposite direction (and hence in the X direction, where the walls are shorter). Two distinctive jumps at 2.3Hz and 9.2Hz in X direction & at 3.5Hz and 12Hz in Y direction indicating the natural modes of vibration of the system. The first global modal deformation shape in global X and global Y direction is similar to the reference model but the activated mass participation percentage of these modes is increased to 28.845% and 46.588% in each direction respectively and these main modes are obtained within the first 10 eigen-values as seen in the graph 4.13.
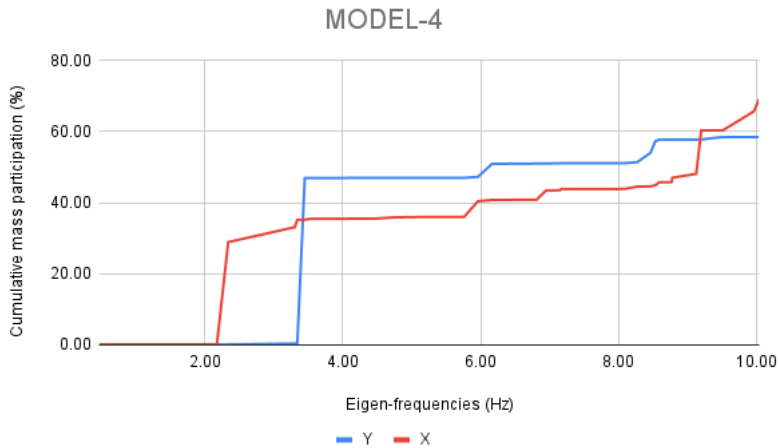
Figure 4.13: Eigen-frequencies and cumulative mass participation in X and Y direction- Model 4
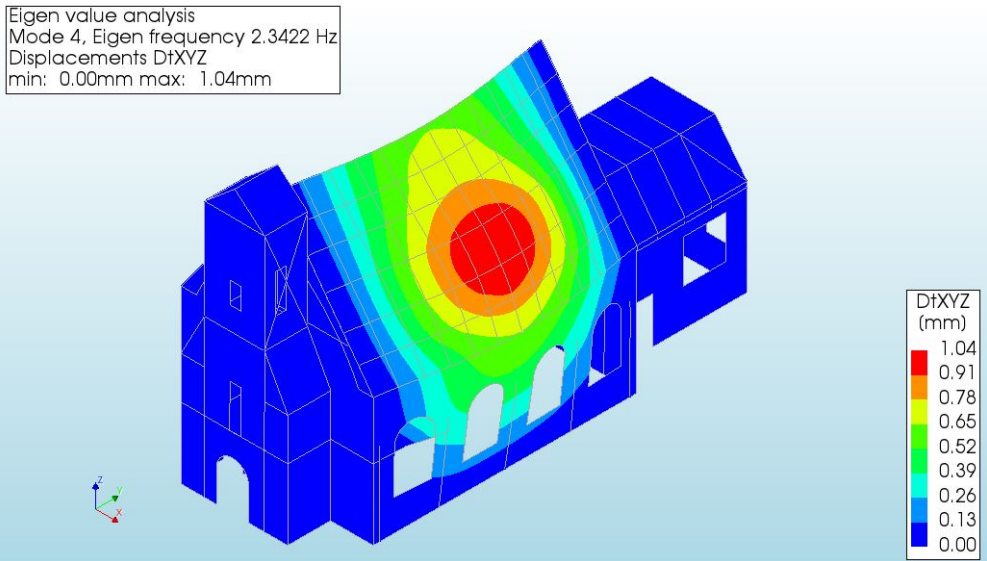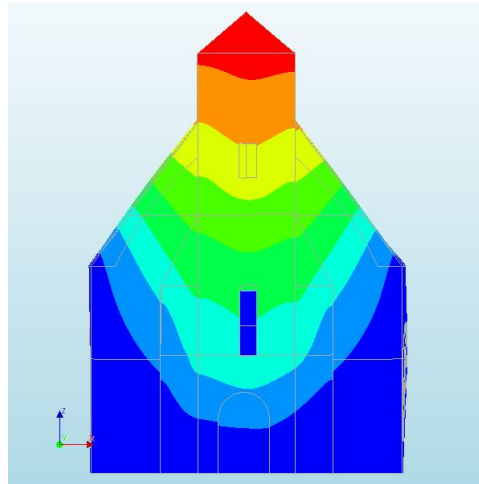
(a) Isotropic view- Mode 4
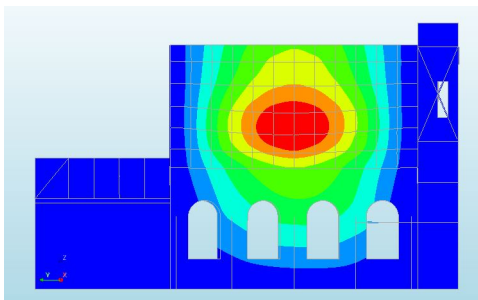
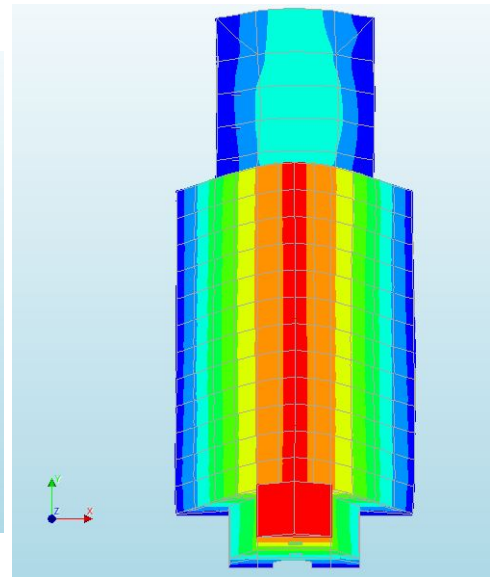(b) Side View- Mode 4
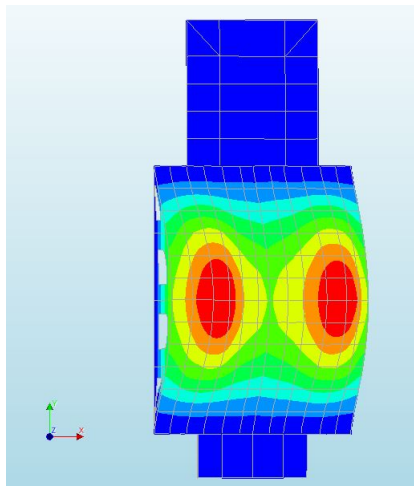
(c) Top View- Mode 4

Figure 4.14: Global mode 4(X) - indicating modal deformation (out-of plane) of roof and wall systems [scale factor-0.05]

Eigen value analysis
Mode 7, Eigen frequency 3.4516 Hz
Displacements DtXYZ
min: 0.00mm max: 1.01mm

DtXYZ
(mm)
1.01
0.88
0.76
0.63
0.50
0.38
0.25
0.13
0.00
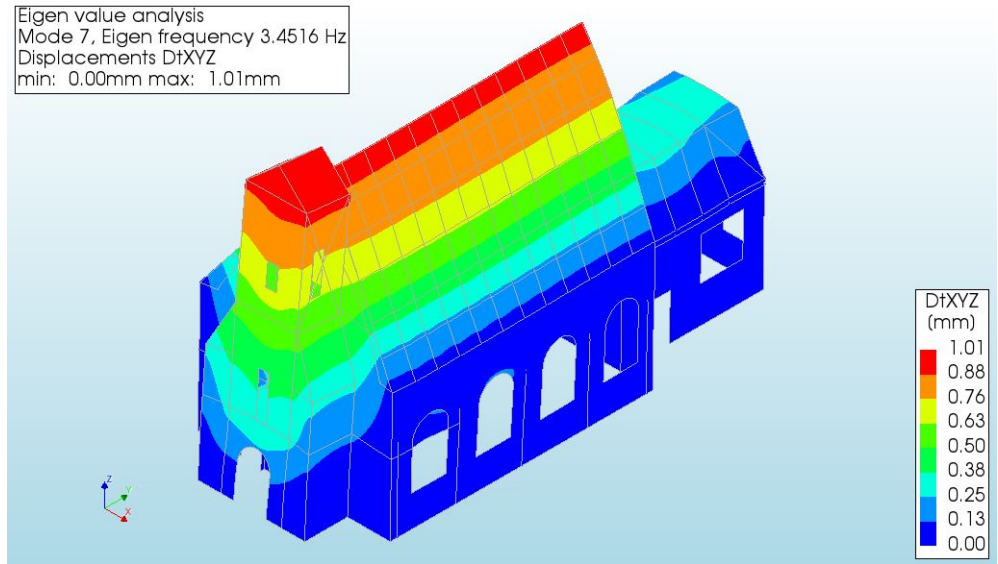
(a) Isotropic view- Mode 7

(b) Front View- Mode 7

(c) Top View- Mode 7

Figure 4.15: Global mode 7(Y)- indicating modal deformation (translation) of roof and wall systems [scale factor-0.05]

4.5. MODEL-5

From the first four simulations of the case study the main limitation of localized modes due to flexible timber diaphragms can be observed. As the sensors cannot be placed on these timber diaphragms, to limit these local modes in this fifth model, timber diaphragms are not modelled and instead the load of the roof diaphragms and timber joists is applied as a normal line load over the masonry walls. The fixed base with restricted translations and rotations similar to Model-3 [Fig 4.8] is assumed as well as the material models similar to the reference model[table 4.3]. The load calculations of normal line loads is attached in appendix: B.
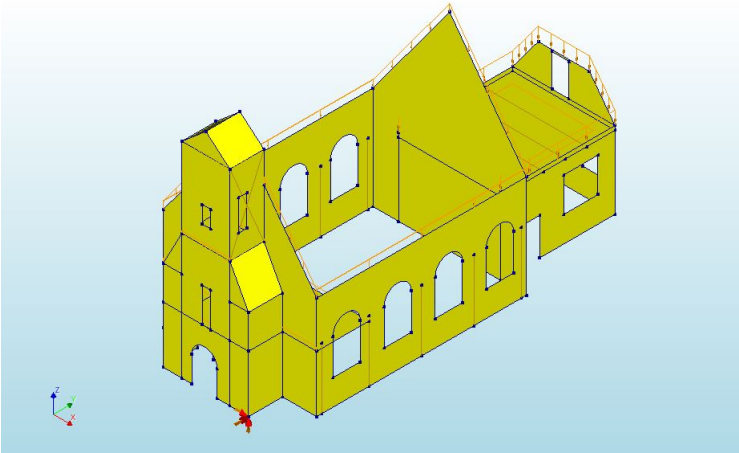
Figure 4.16: Model 5- without roof structure, applied as a line load on masonry walls

By eliminating all the timber diaphragms in modelling [Fig 4.16], the eigenvalue analysis of Model-5, first 200 modes is evaluated with cumulative modal mass participation of 92.26% in global X direction and 91.675% in global Y direction and the eigenfrequencies ranging from 0.428 Hz to 27.755Hz. The global modes with modal mass participation ≥ 5% are shown in table 4.7 and it should be noted that the cumulative modal mass of 90% is reached within the first 130 eigen-modes in both global X and Y directions, hence the dynamic behaviour of the case-study lies within first 100 eigen-modes.[8]

Mode Number	Frequency (Hz)	Time Period (s)	Effective Mass & Direction	Effective Mass Percentage (%)
3	0.8523	1.173	0.16235 E+03 (X)	23.371
9	1.5692	0.6373	0.11661 E+03 (X)	16.768
27	4.9204	0.2032	0.34544 E+02 (X)	4.972
39	7.0577	0.1416	0.43322 E+02 (X)	6.236
40	7.1420	0.1400	0.40372 E+02 (X)	5.812
47	8.2902	0.1206	0.74420 E+02 (X)	10.713
1	0.4288	2.3320	0.48683 E+02 (Y)	7.008
5	0.9367	1.0675	0.44599 E+02 (Y)	6.420
17	3.0335	0.3296	0.12678 E+03 (Y)	18.250
31	5.8021	0.1723	0.95707 E+02 (Y)	13.777
32	6.0685	0.1647	0.11868 E+03 (Y)	17.084

Table 4.7: Modal mass participation of global modes of the first 200 eigen-modes in global X and global Y direction (Model 5)

4

GOVERNING EIGEN MODES IN GLOBAL X DIRECTION
The cumulative modal mass participation is 92.26% in global X direction for the first 200 eigen-modes. The governing first global mode is Mode 3 (eigen frequency of 0.85233 Hz and time period of 1.173s) with a maximum mass participation of 23.37% in global X direction [Fig 4.18].

GOVERNING EIGEN MODES IN GLOBAL Y DIRECTION
The cumulative modal mass participation is 91.675% for the first 200 eigen-modes. The governing global mode is mode 17 (eigen frequency of 3.0335 Hz and time period of 0.329s) with the maximum modal mass participation of 18.25 % in global Y direction. [Fig 4.19]

OVERALL BEHAVIOUR OF MODEL-5
In comparison to the reference model, it should be noted that the local modes of the floor and roof have been eliminated and the cumulative mass participation percentage of 92% is achieved within the first 200 eigen-modes in both global X and Y directions. However, the removal of the timber diaphragms does not allow to identify a single predominant global mode, as for the previous models (since the participated mass of the main mode decreases drastically). Two distinctive jumps in the modal mass participation can be observed in Y direction at 3Hz and 6Hz and 3 distinctive jumps in X direction at 0.8Hz, 1.5Hz and 8.3Hz indicating the natural frequencies of vibration of the structure.

It is observed that due to the additional line load on the lateral masonry walls of the main structure, there was a maximum modal deformation at the point of loading in the masonry walls in global X direction. But in global Y direction, the major deformation is concentrated in the bell-tower similar to the reference model.
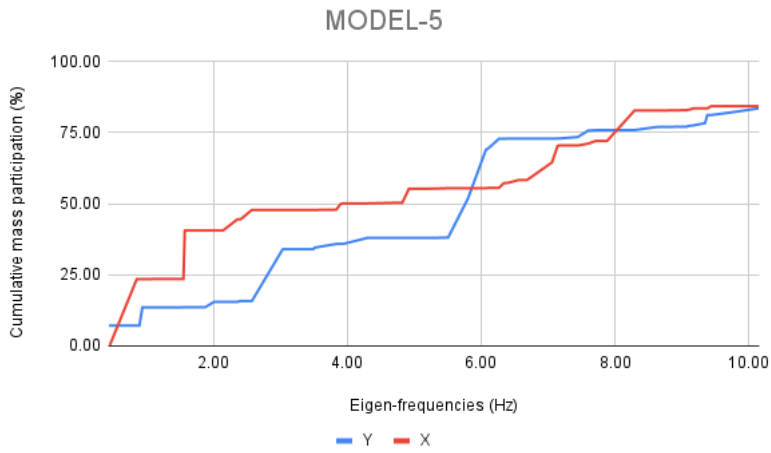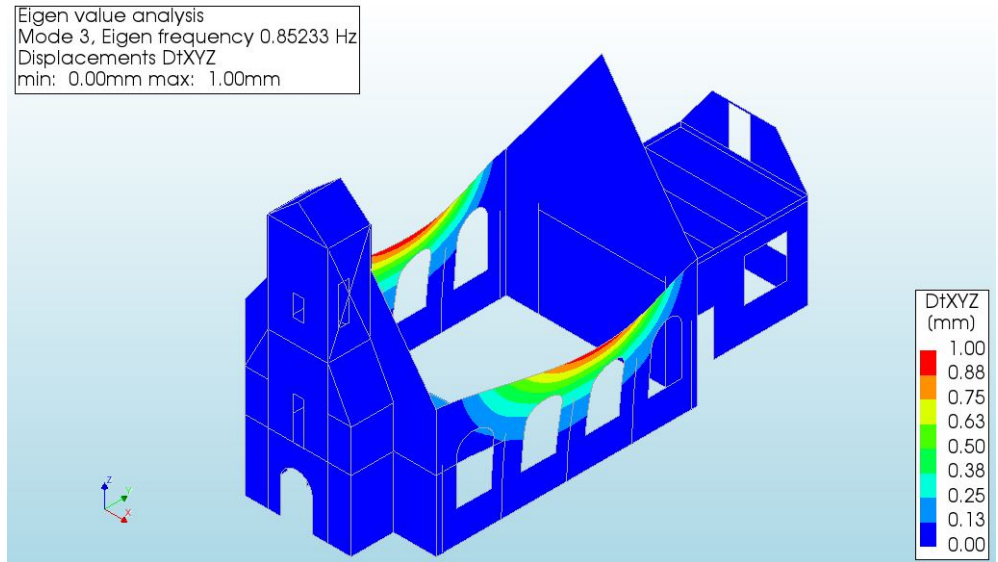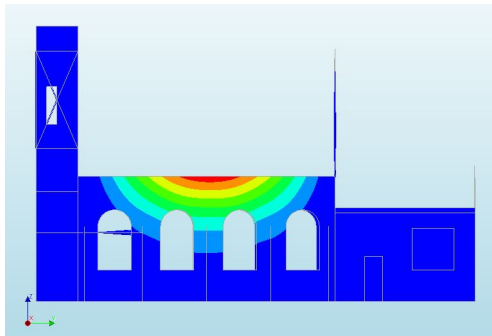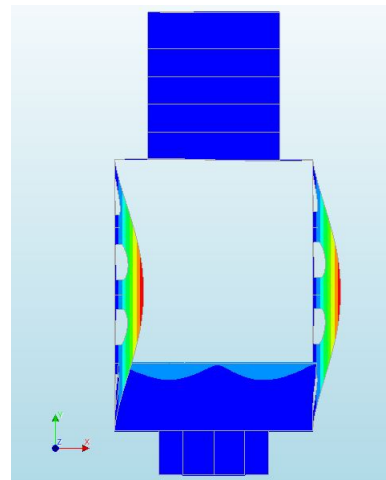
Figure 4.17: Eigen-frequencies and cumulative mass participation in X and Y direction- Model 5

4

Eigen value analysis
Mode 3, Eigen frequency 0.85233 Hz
Displacements DtXYZ
min: 0.00mm max: 1.00mm

DtXYZ
(mm)
1.00
0.88
0.75
0.63
0.50
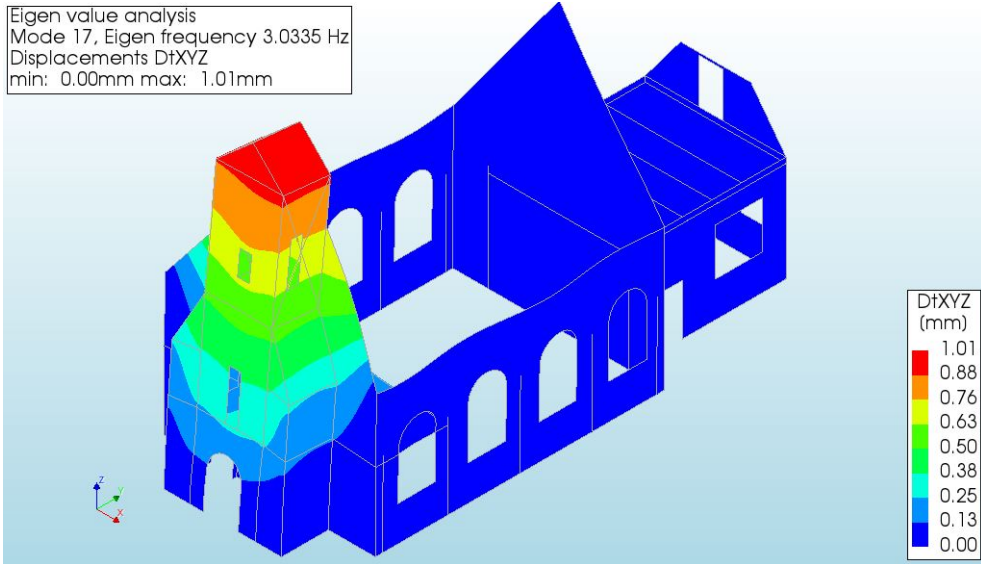0.38
0.25
0.13
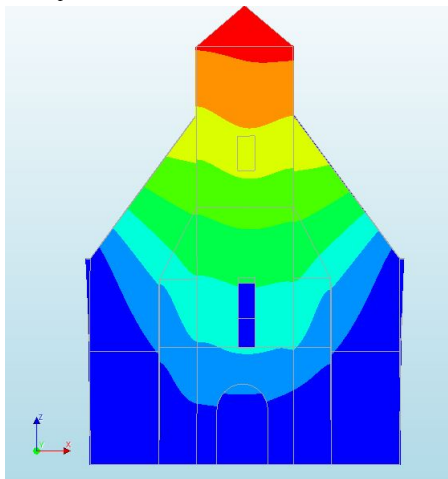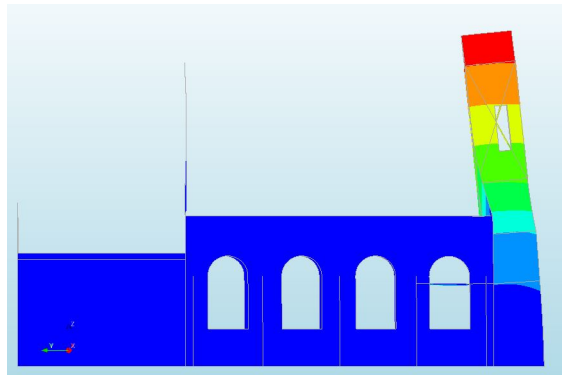0.00

(a) Isotropic view- Mode 3

(b) Side View- Mode 3

(c) Top View- Mode 3

Figure 4.18: Global mode 3(X) - indicating modal deformation (out-of plane) of roof and wall systems [scale factor-0.05]

Eigen value analysis
Mode 17, Eigen frequency 3.0335 Hz
Displacements DtXYZ
min: 0.00mm max: 1.01mm

DtXYZ
(mm)
1.01
0.88
0.76
0.63
0.50
0.38
0.25
0.13
0.00

(a) Isotropic view- Mode 17

(b) Front View- Mode 17

(c) side View- Mode 17

Figure 4.19: Global mode 17(Y)- indicating modal deformation (translation) of roof and wall systems [scale factor-0.05]

5

MODEL MODIFICATIONS INCLUDING STRUCTURAL RETROFITTING

In this chapter, the recent structural findings and the retrofitting measures taken on the case-study in 2018 are discussed in detail leading to the modified modelling assumptions. It also presents the literature behind the material models considered as well as geometrical, material and shape properties of the modified case-study structure. This chapter also presents the results of the eigen-value analysis of simulated models of the structurally modified case-study showing the main modal deformations and the natural frequencies of vibration.

5.1. RECENT FINDINGS AND STRUCTURAL MODIFICATIONS

In July 2018, this structure has undergone structural modifications (retrofitting of the church) to prevent further damage of the structure [fig 5.1]. During the survey prior to retrofitting, certain characteristics of the case-study (eg. cavity walls) are described in detail. The detailed drawings are attached in Annex A.

The main structural findings and modifications are:

- Firstly, in the preliminary survey, it was found that the main masonry wall structure of the church is constructed as a cavity wall with a cavity of 115 mm. This is to prevent the water seepage inside the church as indicated in Fig A.5.

- Secondly, based on the studies of historical monuments in the area [35], it is reasonable to assume that the elastic modulus of the masonry should be decreased to a value of 1GPa.

- Due to the presence of cavity wall, the bell-tower is disconnected from the main roof structure as shown in Fig A.4.
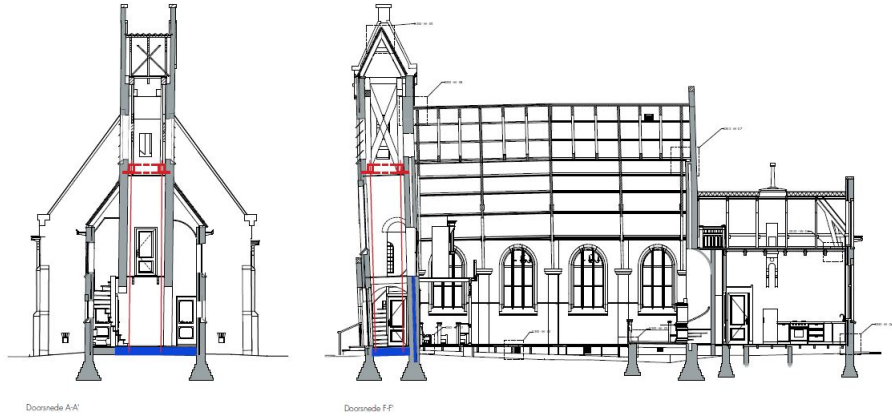
Figure 5.1: Kerk Garrelsweer after structural modifications

- A steel frame was installed in the bell-tower of the church up to the first floor level to prevent further sway of the bell-tower towards the main roof-structure. (fig. A.2, fig. A.3) with the cross-sectional details of the framework shown in figure A.6.

- In-order to support the steel frame, a concrete slab of approximately 100mm thickness is laid below the entrance of the church at the ground level of bell-tower as indicated in figure A.8.

- 4 Additional columns are installed supporting the first floor of the main-structure in the church.

- Two linear damping devices (LD-740 series in PVC buls) are installed at the roof-structure to decrease the impact of dynamic effects of the bell-tower on the roof-structure. These shock absorbers are connected to the roof structure at the horizontal timber joists and the cavity wall between the main structure and the bell-tower as shown in fig. A.4 and fig. A.7. The specifications of these damping devices is discussed in detail later in this chapter.

5.2. Modified Modelling Assumptions
Based on the recent findings and the retrofitting measures, the following modelling assumptions are made to represent the case study in present state.

5.2.1. Masonry Cavity Walls
The cross-sectional details of the outer wall, cavity and inner wall is given in table 5.1.
A cavity wall is a type of wall that has a hollow center. They can be described as consisting of two "skins" separated by a hollow space (cavity). The skins typically are masonry, such as brick or cinder block. Masonry is an absorbent material that can slowly draw rainwater or even humidity into the wall. One function of the cavity is to drain water

Wall elements	Location	inner(mm)	cavity (mm)	outer[t](mm)	Total thickness(mm)
Masonry Walls -Y axis	Main Structure -Lateral	220	115	125	460
Masonry Walls- Y axis	Vestibule	220	-	-	220
Masonry Walls- Y axis	Sub-structure (Apse)	220	-	-	220
Masonry Walls -X axis	Bell Tower -Facade	100	-	-	100
Masonry Walls- X axis	Main Structure	220	115	125	460
Masonry Walls- X axis	Sub-structure (Apse)	220	-	-	220

Table 5.1: Element Cross-sectional properties- masonry walls (The Old Church, Garrelsweer)

through weep holes at the base of the wall system or above windows. The weep holes allow wind to create an air stream through the cavity that exports evaporated water from the cavity to the outside. [36]
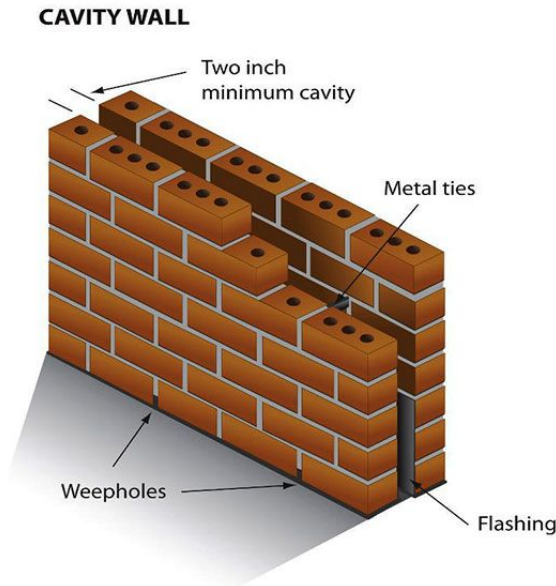
Figure 5.2: cavity wall with metal ties- double-wythe masonry wall [36]

It is composed of two masonry walls separated by an air space [fig 5.2]. The outer wall is made of brick and faces the outside of the building structure. The inner wall may be constructed of masonry units such as concrete block, structural clay, brick or reinforced concrete. These two walls are fastened together with metal ties or bonding blocks. The ties strengthen the cavity wall. In the early 1900s, the ties used are iron anchors which are prone to rusting and expansion.

Geometrical Assumptions

In this case study of The Old Church in Garrelsweer, there has been no information regarding the iron ties and no specific retrofitting measures have been taken for these cavity walls. Hence, it is safe to assume that these main cavity walls are disconnected to each other due to degraded ties over time.

- The first assumption of the main masonry walls in y-axis is due to disconnected cavity wall construction, the inner wall is considered as the main load bearing wall so modified elemental thickness of the inner-wall is modelled.

- For modelling the cavity wall between the bell tower and the main church which is of significance, a disconnect connection is modelled between the bell tower wall and the main church wall.

From the assumptions, the simplified cross-sectional details of the masonry walls are shown in table 5.1. These masonry walls are modelled with regular curved shell elements - (CQ40S, CT30S) with element properties given in table 5.2.

Element	Location	Element thickness(mm)
Masonry Walls -Y axis	Main Structure -Lateral	220
Masonry Walls- Y axis	Sub-structure (Apse)	220
Masonry Walls- X axis	Main structure- Facades	220
Masonry Walls -X axis	Bell Tower & Facades	100
Masonry Walls- X axis	Sub-structure (Apse)	220

Table 5.2: Modified element cross-sectional properties- masonry walls (The Old Church, Garrelsweer)

Material Properties of Historical Masonry structures

The material properties of the masonry walls in the first five models are calibrated from the reported value for the residential unreinforced masonry houses in the region of Groningen [37]. As this case study is an emblematic historical unreinforced masonry building of the region that has suffered damage, for the accurate assessment of dynamic response, material properties of the masonry walls in current condition can be of importance.

The material properties of another historical structure in the same region "Fraeylemaborg in Slochteren" constructed during similar time frame can be considered as a better fit to model the case-study. The Fraeylemaborg structure is composed of thick clay brick walls and wooden floors. Their compressive strength was 0.25 MPa in average (standard deviation 0.052 MPa) [35], a value considerably lower than those obtained from recent experimental studies on clay bricks currently used in the construction in Groningen [37]. The modulus of elasticity of the URM walls was derived as E = 1 GPa [35]. The difference between this value and the value of 4.7 GPa estimated after tests on Groningen resembling wall specimens [37] is justifiable considering that materials used some centuries ago are expected to have considerably lower properties than similar modern materials. [35]. The modified masonry material properties of the case-study are shown in table 5.3

and table 5.4. Here on, they are referred to as EMM (Material Model 2) and TSCM (Material Model 2) respectively.

Property	Symbol	Value	Units
Density	ρ	1805	kg/m^3
Young's modulus (perpendicular to bed joints)	E_y	1000[a]	MPa
Young's modulus (parallel to bed joints)	E_x	1000[a]	MPa
Shear modulus	G_{xy}	400	MPa
Tensile strength	f_t	0.14	MPa
Fracture energy (tension)	G_t^1	0.01025	N/mm
Compressive strength	f_c	0.25[a]	MPa
Fracture energy (Compression)	G_C	26050	N/m
Friction angle	φ	0.669	rad
Cohesion (no softening)	c	0.14	MPa
Diagonal crack orientation	α	0.5	rad

[a] from experimental tests [35]

Table 5.3: Engineering Masonry Model(EMM)-Material Model 2

Property	Parameter	Symbol	Unit	Value
Elasticity	Young's Modulus	E	MPa	1000
	Poisson's ratio	ν		0.15
	Density	ρ	kg/m3	1805
Crack orientation	Rotating			
Cracking	Linear-crack energy based			
	Tensile strength	f_t	MPa	0.14
	Tensile fracture energy	G_t	N/mm	0.01025
Crushing	Compressive strength	f_c	MPa	0.25
	Compressive fracture energy	G_c	N/mm	20

Table 5.4: Total Strain-based Cracking Masonry (TSCM)model- Material Model 2

5.2.2. MATERIAL MODEL OF TIMBER DIAPHRAGMS

As the tested or calibrated material properties of timber diaphragms of the case study in the present state are not available, in the first five Finite element models the timber diaphragm properties are calibrated by comparing the properties between the tested timber diaphragms from residential buildings in seismically damaged Groningen and a similar historical structure in New-Zealand (section 3.2.5). In-order to account for significance of further degradation in the material properties of timber diaphragm on the eigen-value analysis, the material properties are modified further.

For the present case-study structure with loading perpendicular to the joists and

assuming discontinuous joists without reliable mechanical anchorage, the equivalent shear stiffness is assumed to be $G_t = 140 kN/m$ instead of initially assumed $G_t = 200 kN/m$ for considering the poor condition. The modified material properties of timber-diaphragms are shown table 5.5 and here after referred to as linear orthotropic material model-3.

Property	Parameter	Symbol	Unit	Value
Elasticity	Young's Modulus	E_x	MPa	10000
		E_y	MPa	10000
		E_z	MPa	10000
	Poisson's ratio	v		0
	Density	ρ	T/mm3	9 e-09
	Shear Modulus	G_{xy}	N/mm2	4.66
		G_{yz}	N/mm2	625
		G_{zx}	N/mm2	625

Table 5.5: Timber diaphragm properties- Material model 3

5

5.2.3. LINEAR DAMPING DEVICES
From the previous recorded damage due to seismic activity, it was observed that the bell-tower and the main-church structure are not fully connected due to the presence of a cavity-wall. Due to this disconnection, the dynamic movement of the bell-tower towards the main structure may lead to severe damage of the lateral masonry walls of the main structure and to limit this damage, linear damping devices are installed at the roof level and the cavity wall of the bell-tower. [fig A.7]. The specifications of the damping devices are given in fig. 5.3

The damping devices are modelled as a translational spring-dashpot systems (SP2TR) connecting the horizontal timber girders in the roof-structure and the cavity wall connecting the main-church structure and the bell-tower as shown in fig. 5.5. The element properties of these spring dash-pot elements is shown in table 5.6 [fig. 5.4]. The material properties of LD740 series spring-dashpot systems taken from the fig. 5.3 are shown in table 5.7

Element type	SP2TR
Number of nodes	2
Basic variables	translation, elongation, axial force.
Topological dimension	2D

Table 5.6: Classification of element types in spring/dash-pots- SP2TR
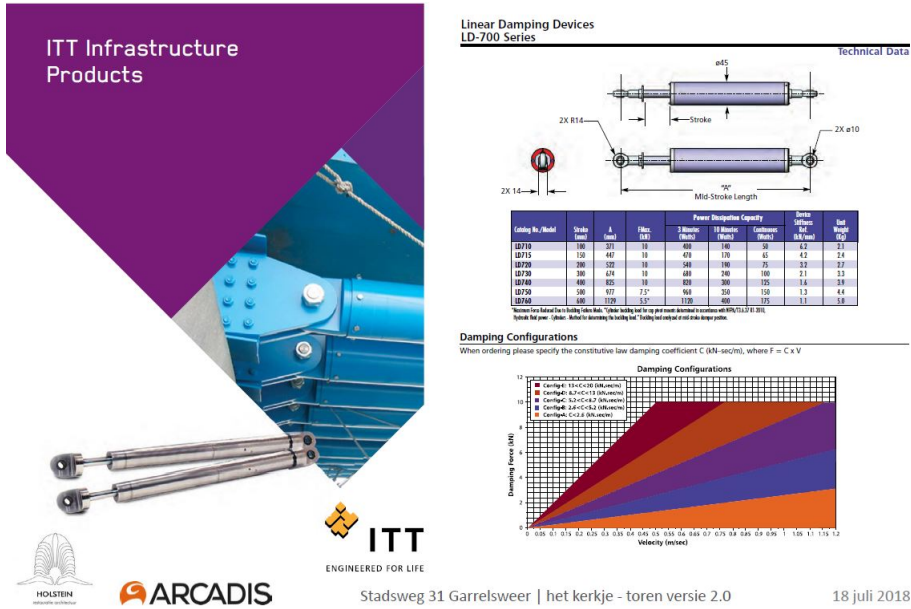
Figure 5.3: Specifications of linear damping devices adopted [38]
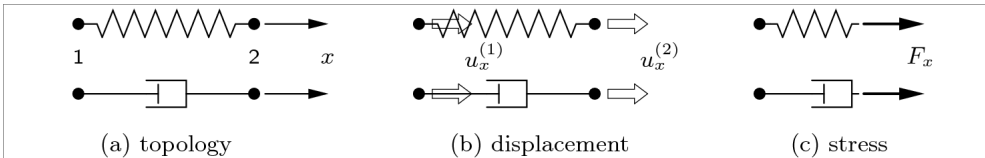
Figure 5.4: Element type- SPT2R [39]

Property	Units	Value
translational spring dashpot		
spring stiffness	N/mm	1600
spring behaviour	-	Linear elastic
constant damping coefficient	Ns/mm	15000

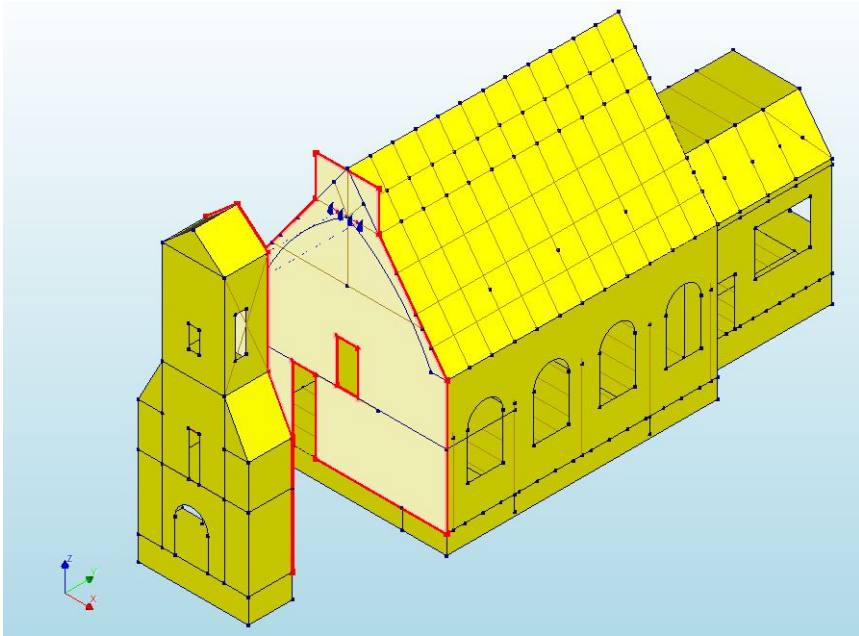Table 5.7: Material properties of Linear Damping devices (LD740series)

Figure 5.5: Modelling dampers as translational linear elastic spring/dashpot systems

5.2.4. STEEL FRAME IN BELL-TOWER

The second modification to the case-study is the installation of a steel-framework in the bell-tower up to the first-floor level [Fig. A.3, Fig. A.6]. For modelling this modification it is assumed that the steel-frame is directly connected to the masonry facade in the bell-tower and the outer-leaf of the cavity wall between the main structure and the bell-tower. The square hollow cross-sectional details and material properties of standard S235 steel (Eurocode 3 1993-1-1) are shown in table 5.8 and table 5.9 respectively. The horizontal and vertical elements in the steel frame are modelled with Class III beam elements (CL18B) with the element properties in table 3.5.

Steel-frame	Length (b)	breadth (h)	thickness
cross-section (horizontal members)	90 mm	90 mm	6 mm
cross-section (vertical members)	90 mm	90 mm	6 mm

Table 5.8: Cross-sectional details of the steel frame in the bell-tower

5.2.5. CONCRETE FLOOR IN BELL-TOWER

The third modification is replacing the flexible timber flooring with a concrete slab (C35) at the ground floor level of the bell-tower(vestibule). The steel-frame in the bell-tower is fixed at the concrete slab level. From figure A.8 it is assumed that the concrete slab is connected to the masonry walls (fixed) of the bell-tower. The material properties of

Property	Units	Value
Steel grade	(EN10025-2)	S235
Young's Modulus	N/mm^2	210000
Poisson's ratio	-	0.3
Density	T/mm^3	7.83e-09
Thermal expansion coefficient	/K	1.2e-05

Table 5.9: Material properties of steel framework (S235)

C35 standard concrete (Eurocode 2 EN1992-1-1) are shown in table 5.10 and the slab is modelled with regular curved shell elements (CQ40S, CT30S) with element properties in table 3.2.

Property	Symbol	Units	Value
Concrete Grade		(EN1992-1-1)	C35/45
Young's Modulus	E_{cm}	N/mm^2	34077.1
Poisson's ratio	ν	-	0.2
Density		T/mm^3	2.4e-09
Mean uni-axial tensile strength	f_{ctm}	N/mm^2	3.20996
mean compressive strength	f_{cm}	N/mm^2	43
Thermal expansion coefficient	α_t	-	1e-05

Table 5.10: Material properties of concrete slab C35/45

5.2.6. ADDITIONAL COLUMNS

The fourth modification of the case-study, is the installation of 4 additional columns supporting the first floor of the main structure [Fig 5.6]. It should be noted that the 2 center columns are made of timber while the 2 corner columns are made of S235 steel [FigA.5] and these steel columns are not connected to the masonry walls and the masonry piers. This modification reduces the impact of first floor load to the masonry walls by directly transferring the load to the foundation. The cross-sectional details of these columns are shown in table 5.11. The timber columns are modelled as linear elastic isotropic material model (Table 3.8) and the steel columns are modelled as standard S235 material properties (Table 5.9). Both the steel and timber columns are modelled with 2D class III beam elements (CL18B) with element properties as table 3.5.

columns	Length (b)	breadth (h)	thickness
cross-section (timber)	90 mm	90 mm	-
cross-section (S235)	70 mm	70 mm	4 mm

Table 5.11: Cross-sectional details of the columns supporting the first floor of the main structure

Figure 5.6: Installation of 4 new columns supporting the first floor in the main-structure (site visit,2021)

5.3. MODEL-6

Following these structural modifications discussed in the previous section, the reference model (model-2) of the case-study is modelled with

1. Modified geometric properties of masonry walls (section 5.2.1)[table 5.2] and disconnecting the outer-wall and inner-wall of the bell-tower.

2. Installation of steel frame connected to the masonry walls of the bell-tower [section 5.2.4]

3. Modified rigid concrete slab (thickness of 100mm) at the ground level of bell-tower [section 5.2.5]

4. Installation of additional columns at the first floor of main structure [section 5.2.6]

The model-6 with these modifications is shown in fig. 5.7. The eigen-value analysis show the first 200 eigen-modes of the structure with eigen-frequencies ranging from 0.496 Hz to 8.1798 Hz (fig C.6). The cumulative mass participation percentage for the first 200 eigen-modes is ≥ 90% (97.192% in global X direction and 95.132% in global Y direction). The main global modes with modal mass participation ≥ 5% are presented in table 5.13.

GOVERNING EIGEN MODES IN GLOBAL X DIRECTION
After evaluating first 200 eigen-modes of model-6 with cumulative mass participation of 97.192%, one significant global mode can be identified - Mode 44 with modal mass

Finite Element Model-6		
Structural elements	*Material Model*	*Further assumptions, reference*
Masonry walls	Continuum EMM-1	Table 3.3
Masonry foundation	Continuum EMM-1	Table 3.3
Masonry piers	TSCM-1	Table 3.6
Timber joists	Linear Elastic Isotropic Model-1	Table 3.8
Timber diaphragms	Linear Elastic Orthotropic Model-2	Table 3.11
Steel frame	EN10025-2 (S235)	Table 5.9
Steel columns	EN10025-2 (S235)	Table 5.9
Timber columns	Linear Elastic Isotropic Model-1	Table 3.8
Concrete slab	C35/45 (EN1992-1-1)	Table 5.10

Table 5.12: Material models and specific assumptions for Model-6
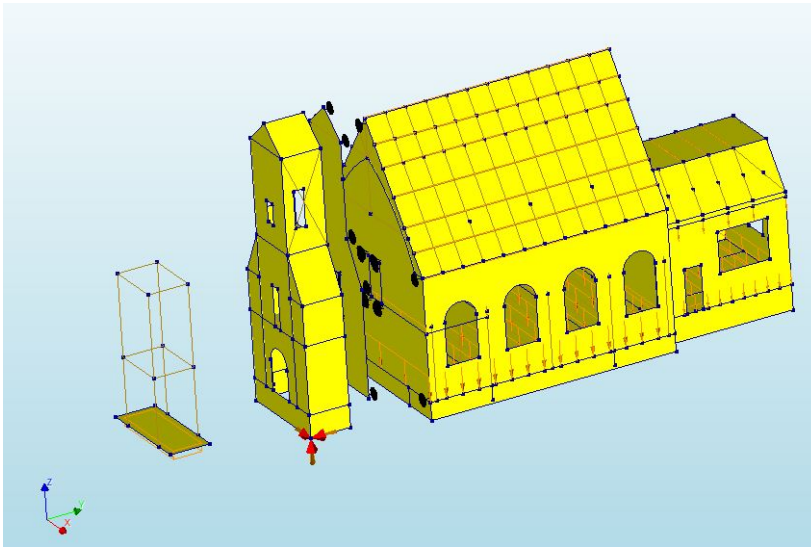
Figure 5.7: Finite element model-6 with the structural modifications (represented by virtual transformation)

Mode Number	Frequency (Hz)	Time Period (s)	Effective Mass & Direction	Effective Mass Percentage (%)
43	2.5888	0.3862	0.16984 E+04 (X)	6.450
44	2.6076	0.3834	0.21983 E+05 (X)	83.483
19	1.6536	0.6047	0.19988 E+05 (Y)	75.906
21	1.6838	0.5938	0.21764 E+04 (Y)	8.265
36	2.4666	0.4054	0.14354 E+04 (Y)	5.451

Table 5.13: Modal mass participation of global modes of the first 200 eigen-modes in global X and global Y direction (Model 6)

participation of 83.483% in global X direction. It should be noted that the modal deformation is comparable to the reference model (Model-2) as shown in figure 5.9.

GOVERNING EIGEN MODES IN GLOBAL Y DIRECTION

After evaluating first 200 eigen-modes of model-6 with cumulative mass participation of 95.132%, 3 significant global modes with maximum mass participation could be identified. Mode 19 (eigen frequency- 1.6536Hz) has a maximum modal mass participation of 75.90% in global Y direction [fig 5.10].

OVERALL BEHAVIOUR OF MODEL-6

With these structural modifications in the case-study, it can be observed that the single significant modes with maximum modal mass participation could be identified in the X direction and Y direction. The cumulative mass participation in both X and Y directions is greater than 90% within the first 50 eigen-modes and one distinctive jump at eigen-frequency 2.6076Hz in X direction and 2.4666Hz in Y direction can be found corresponding to the natural frequencies of the structure [fig 5.8].
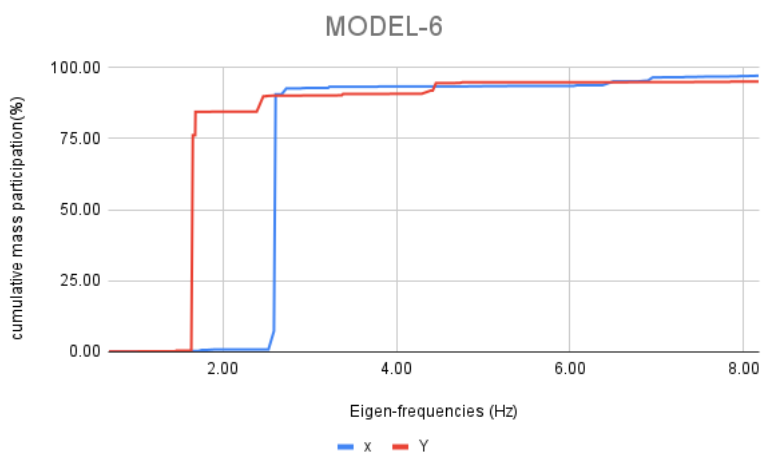
Figure 5.8: Eigen-frequencies and cumulative mass participation in X and Y direction- Model 6

In general, much higher mass participation for the main mode is found indicating a single principal mode. The modal shape in Mode-44 in global X direction indicates significant deformation in the main roof-structure comparable to the reference model (Model-2) and from the modal shape of Mode-19 in global Y direction indicates maximum deformation at the masonry cavity wall between the bell-tower and roof structure. Also, the modal deformation in Mode -36 in global Y direction is similar to the reference model with maximum deformation at the roof and bell tower.

Eigen value analysis
Mode 44, Eigen frequency 2.6076 Hz
Displacements DtXYZ
min: 0.00mm max: 1.07mm

DtXYZ
(mm)
1.07
0.94
0.80
0.67
0.54
0.40
0.27
0.13
0.00
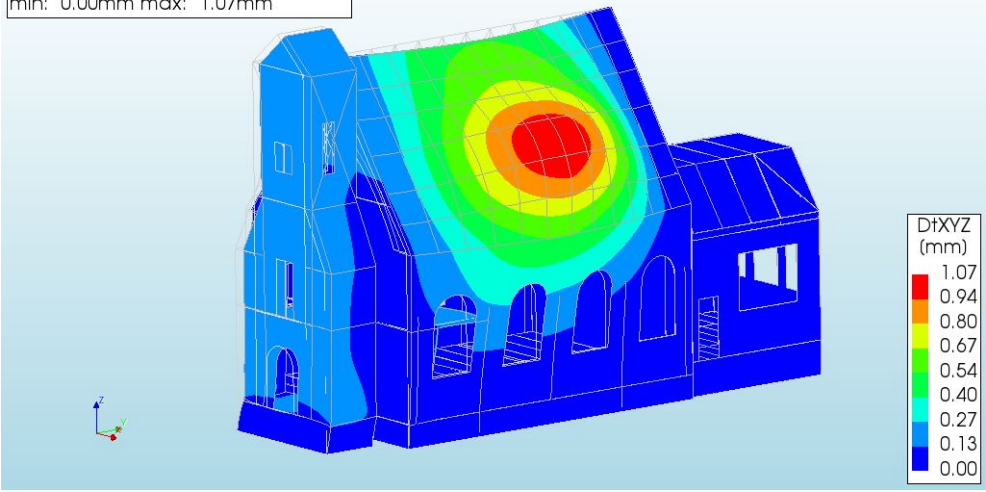
(a) Isotropic view- Mode 44
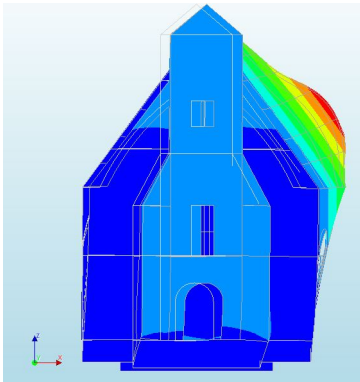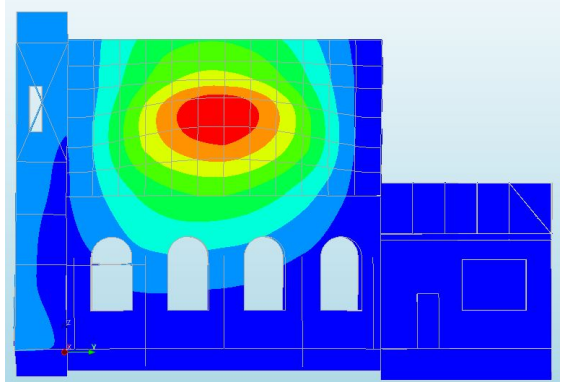
(b) Front View- Mode 44

(c) Side View- Mode 44

Figure 5.9: Global Mode 44 - indicating Modal deformation (out-of plane) of roof and wall systems [scale factor-0.05]

Eigen value analysis
Mode 19, Eigen frequency 1.6536 Hz
Displacements DtY
min: -0.24mm max: 0.00mm

DtY
(mm)
0.00
-0.03
-0.06
-0.09
-0.12
-0.15
-0.18
-0.21
-0.24
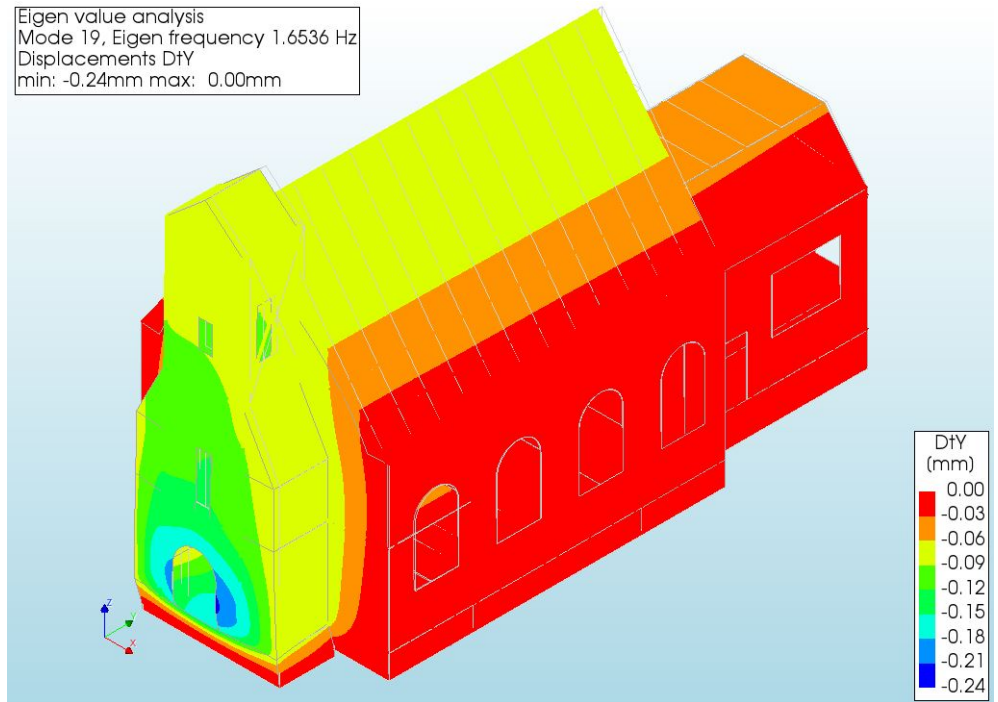
(a) Isotropic view- Mode 19
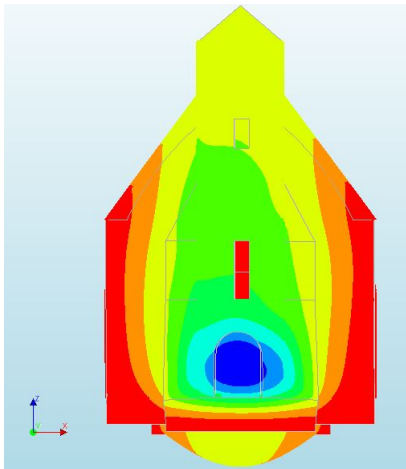
(b) Front view- Mode 19
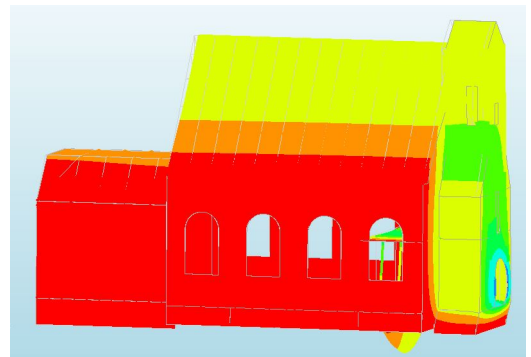
(c) Side view- Mode 19

Figure 5.10: Global Mode 19 (Y)- indicating modal deformation of the bell-tower and floor systems [scale factor-0.05]

5.4. Model-7

In-order to compare the difference in the dynamic properties due to installation of linear damping devices, the model-6 has been modified with addition of two translation linear elastic spring/dash-pod systems (linear damping devices) at the roof level between the horizontal timber joists and the cavity wall connecting the bell-tower [Fig A.6]. The properties of the linear damping devices installed is discussed in section 5.2.3, the modelling and material properties are shown in figure 5.5 and table 5.14 respectively.

Finite Element Model-7

Structural elements	Material Model	Further assumptions, reference
Masonry walls	Continuum EMM-1	Table 3.3
Masonry foundation	Continuum EMM-1	Table 3.3
Masonry piers	TSCM-1	Table 3.6
Timber joists	Linear Elastic Isotropic Model-1	Table 3.8
Timber diaphragms	Linear Elastic Orthotropic Model-2	Table 3.11
Steel frame	EN10025-2 (S235)	Table 5.9
Steel columns	EN10025-2 (S235)	Table 5.9
Timber columns	Linear Elastic Isotropic Model-1	Table 3.8
Concrete slab	C35/45 (EN1992-1-1)	Table 5.9
Damping Devices	*Linear elastic*	*Table 5.7*

Table 5.14: Material Models and specific assumptions for Model-7

The eigen-value analysis of first 200 eigen-modes shows the eigen-frequencies ranging from 0.49604Hz to 8.1798Hz (C.7). The cumulative mass participation percentage for the first 200 eigen-modes is ≥ 90% (97.192% in global X direction and 95.132% in global Y direction). The main global modes with modal mass participation ≥ 5% are presented in table 5.15.

Mode Number	Frequency (Hz)	Time Period (s)	Effective Mass & Direction	Effective Mass Percentage (%)
43	2.5888	0.3862	0.16984 E+04 (X)	6.450
44	2.6076	0.3834	0.21983 E+05 (X)	83.483
19	1.6536	0.6047	0.19988 E+05 (Y)	75.906
21	1.6838	0.5938	0.21764 E+04 (Y)	8.265
36	2.4666	0.4054	0.14354 E+04 (Y)	5.451

Table 5.15: Modal mass participation of global modes of the first 200 eigen-modes in global X and global Y direction (Model 7)

GOVERNING EIGEN MODES IN GLOBAL X DIRECTION
After evaluating first 200 eigen-modes of Model-7 with cumulative mass participation of 97.192%, one significant global mode can be identified - Mode 44 with modal mass participation of 83.483% in global X direction as shown in figure 5.11.

GOVERNING EIGEN MODES IN GLOBAL Y DIRECTION
After evaluating first 200 eigen-modes of Model-7 with cumulative mass participation of 95.132%, 3 significant global modes with maximum mass participation ≥ 5% could be

identified. Mode 19 (eigen frequency- 1.6536Hz) has a maximum modal mass participation of 75.90% in global Y direction [fig 5.12].
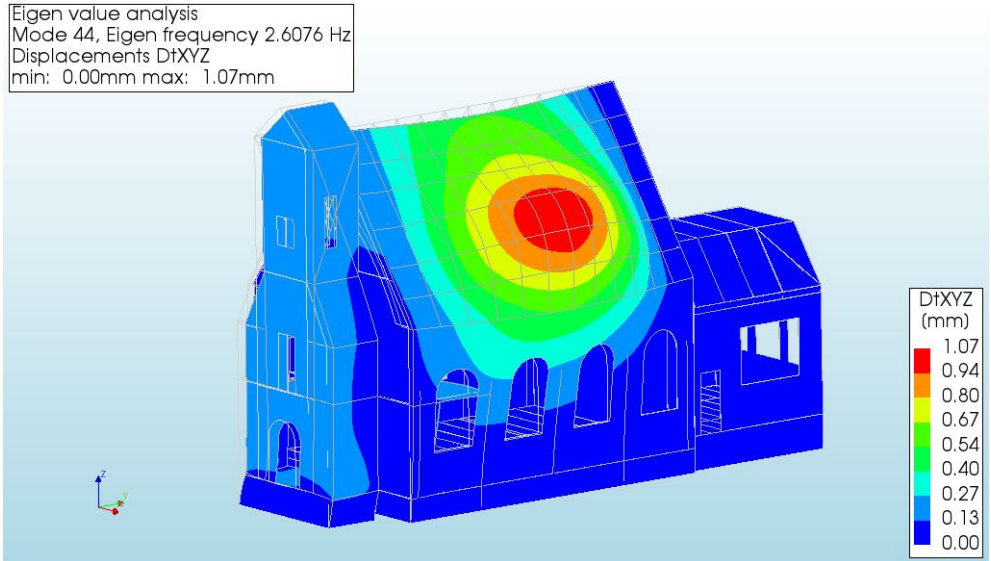
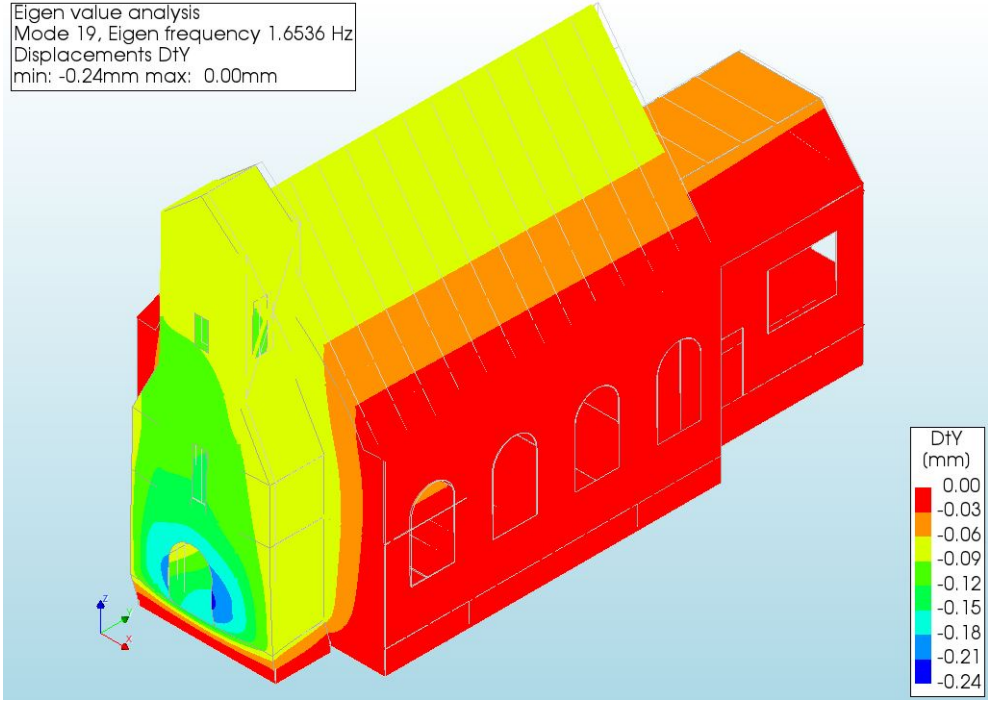(a) Isotropic view- Mode 44
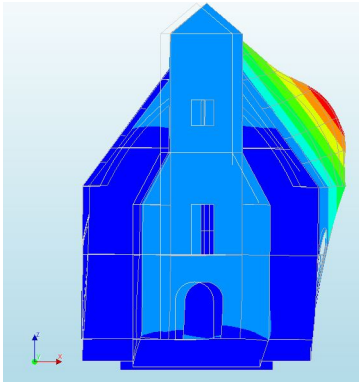
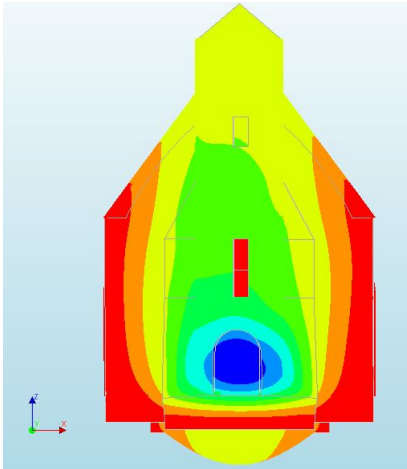(b) Front View- Mode 44
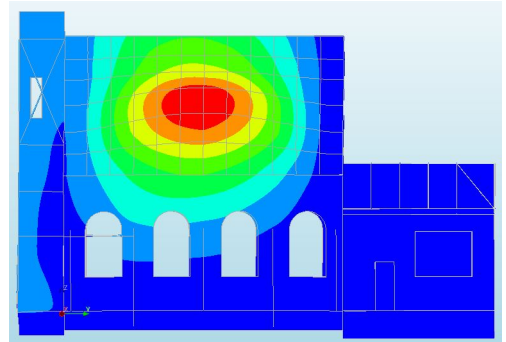
(c) Side View- Mode 44

Figure 5.11: Global Mode 44 - indicating modal deformation (out-of plane) of roof and wall systems [scale factor-0.05]
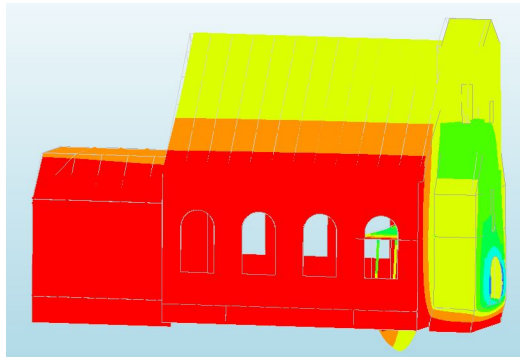
(a) Isotropic view- Mode 19

(b) Front View- Mode 19

(c) bottom View- Mode 19

Figure 5.12: Global Mode 19(Y)- indicating local modal deformation of floor systems [scale factor-0.05]

OVERALL BEHAVIOUR OF MODEL-7

The overall behaviour of the Model-7 is same as the previous modelling variation (Model-6). Similar to Model-6, it can be seen that in global X direction, Mode-44 indicates maximum modal deformation at timber diaphragm of the main-roof structure (out-of-plane deformation) similar to the reference model and in global Y direction Mode-19 indicates maximum modal deformation at the masonry cavity wall in the bell-tower while Mode-36 indicates maximum deformation at the roof level of the bell-tower and roof-structure similar to the reference model.
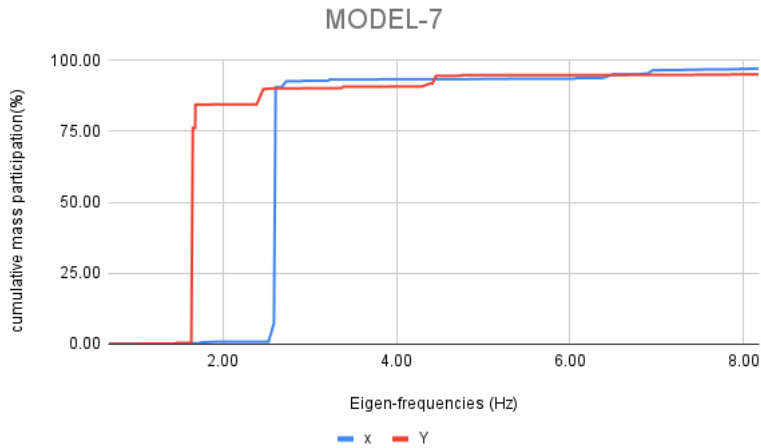
Figure 5.13: Eigen-frequencies and cumulative mass participation in X and Y direction- Model 7

5.5. MODEL-8

After modelling the geometrical retrofitting modifications, in this model the material properties of masonry-walls, piers and foundation are varied based on section 5.2.1. The material properties considered for this Model-8 are shown in detail in the table 5.16.

Finite Element Model-8

Structural elements	Material Model	Further assumptions, reference
Masonry walls	Continuum EMM-2	Table 5.3
Masonry foundation	Continuum EMM-2	Table 5.3
Masonry piers	TSCM-2	Table 5.4
Timber joists	Linear Elastic Isotropic Model-1	Table 3.8
Timber diaphragms	Linear Elastic Orthotropic Model-2	Table 3.11
Steel frame	EN10025-2 (S235)	Table 5.9
Steel columns	EN10025-2 (S235)	Table 5.9
Timber columns	Linear Elastic Isotropic Model-1	Table 3.8
Concrete slab	C35/45 (EN1992-1-1)	Table 5.9
Damping devices	Linear elastic	Table 5.7

Table 5.16: Material models and specific assumptions for Model-8

The eigen value analysis of first 200 eigen modes with eigen frequencies varying from 0.4823Hz to 7.707Hz (C.8) with a cumulative mass participation percentage of 98.202% in global X direction and 97.806% in global Y direction. The significant modes with maximum mass participation percentage ≥ 5% are shown in table 5.17.

Mode Number	Frequency (Hz)	Time Period (s)	Effective Mass & Direction	Effective Mass Percentage (%)
19	1.5488	0.6456	0.23244 E+05 (X)	88.329
10	1.1125	0.8988	0.23916 E+05 (Y)	90.881

Table 5.17: Modal mass participation of global modes in the first 200 eigen-modes in global X and global Y direction (Model 8)

GOVERNING EIGEN MODES IN GLOBAL X DIRECTION

After evaluating first 200 eigen-modes of Model-8, one significant global mode can be identified - Mode 19 with modal mass participation of 88.329% in global X direction [Fig 5.14].

GOVERNING EIGEN MODES IN GLOBAL Y DIRECTION

After evaluating first 200 eigen-modes of Model-8, one significant global mode can be identified - Mode 10 with maximum modal mass participation of 90.747% in global Y direction [fig 5.15].
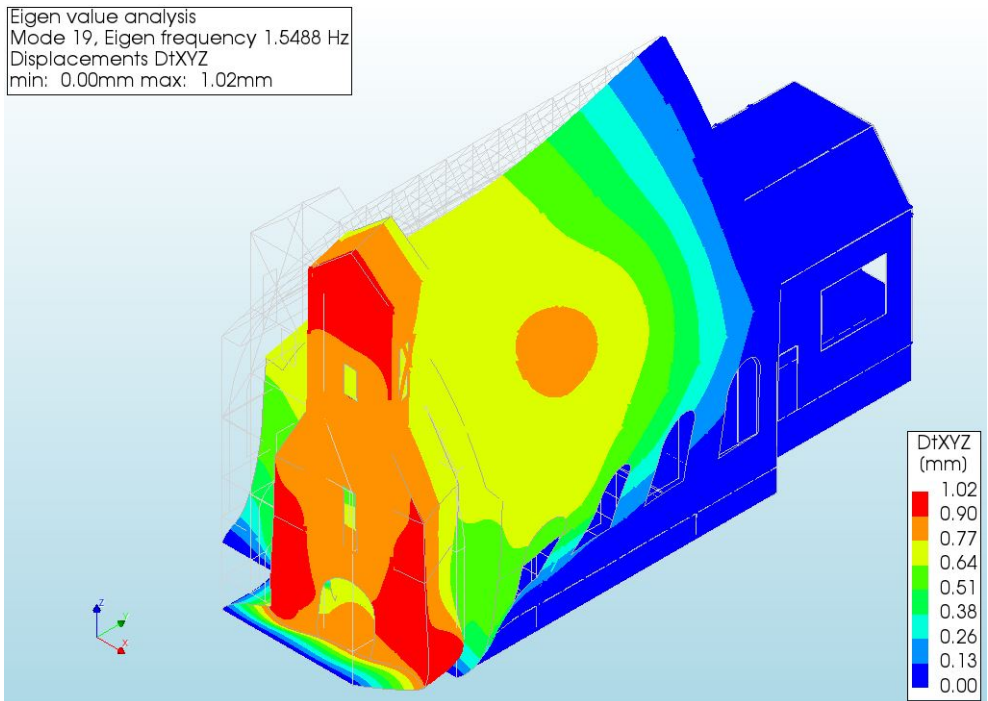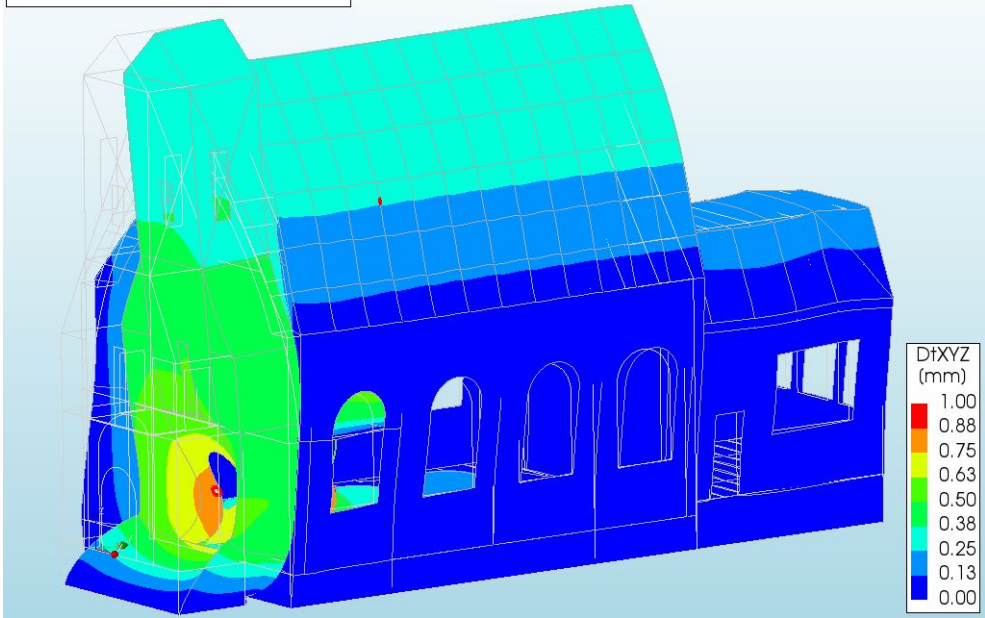
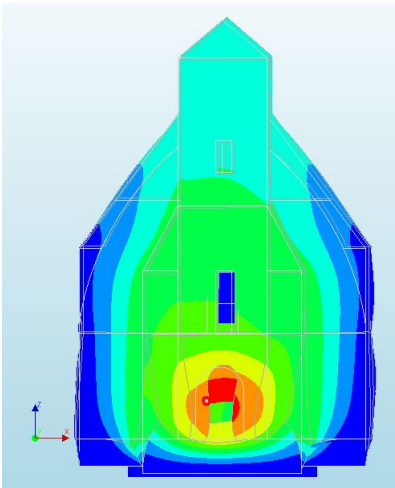(a) Isotropic view- Mode 19
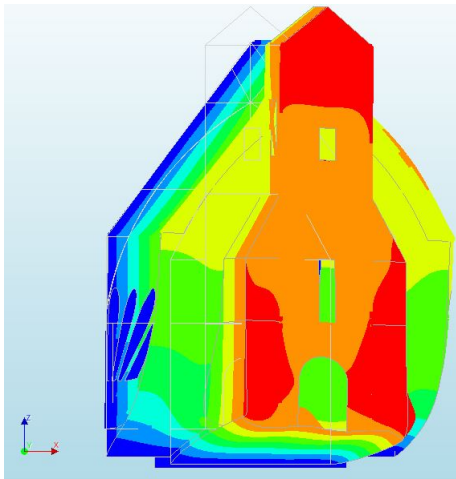
(b) Front View- Mode 19
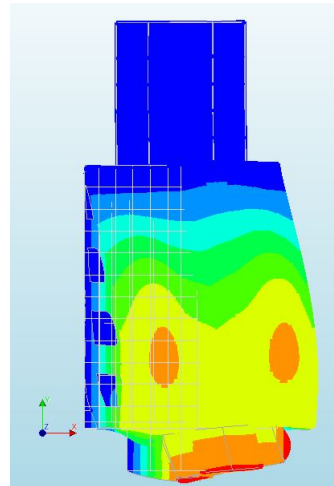
(c) Top View- Mode 19

Figure 5.14: Global Mode 19 - indicating modal deformation of roof and wall systems of bell-tower with major deformation in masonry walls. [scale factor-0.05]
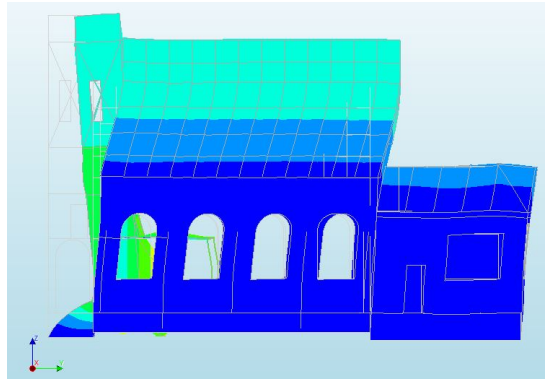
Eigen value analysis
Mode 10, Eigen frequency 1.1125 Hz
Displacements DtXYZ
min: 0.00mm max: 1.00mm

DtXYZ
(mm)
1.00
0.88
0.75
0.63
0.50
0.38
0.25
0.13
0.00

(a) Isotropic view- Mode 10

(c) side View- Mode 10

(b) Front View- Mode 10

Figure 5.15: Global Mode 10 - indicating modal deformation of roof and wall systems with major deformation in the cavity masonry wall. [scale factor-0.05]

OVERALL BEHAVIOUR OF MODEL-8

Due to significant decrease in the stiffness values of the masonry (Young's modulus and compressive strength), there is a significant decrease in the eigen-frequencies. The modal deformations in the global X direction indicates major damage in the masonry-wall (facade) of the bell-tower and modal deformation in the global Y direction indicates significant damage in the cavity wall of the bell-tower. This localised modal deformation in the masonry can be due to strike decrease in the Young's modulus in masonry elements.
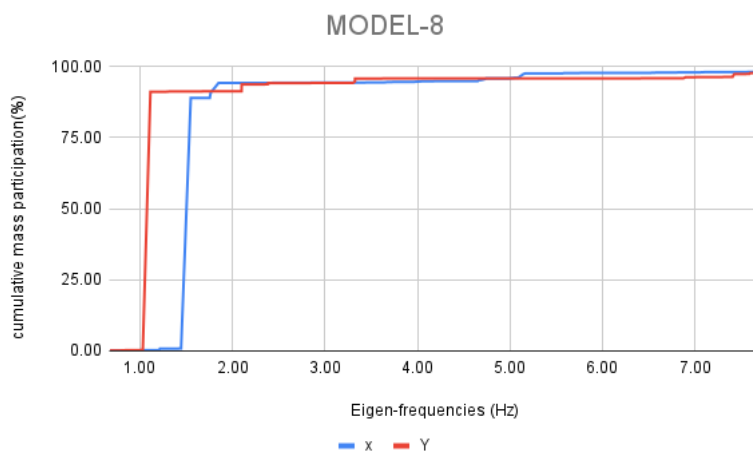
Figure 5.16: Eigen-frequencies and cumulative mass participation in X and Y direction- Model 8

One distinctive jump in the eigen-frequency and cumulative mass participation graph at the fundamental frequency of the structure in both X axis(1.5488Hz) and Y axis(1.1125Hz) is very clear [fig. 5.16].

5.6. MODEL-9

In this model, along with the masonry material variations of Model-8, the timber diaphragm material model is also modified to compare the difference in the results of eigen-value analysis. The material models considered are shown in table 5.18.

Finite Element Model-9

Structural elements	Material Model	Further assumptions, reference
Masonry walls	Continuum EMM-2	Table 5.3
Masonry foundation	Continuum EMM-2	Table 5.3
Masonry piers	TSCM-2	Table 5.4
Timber joists	Linear Elastic Isotropic Model-1	Table 3.8
Timber diaphragms	Linear Elastic Orthotropic Model-3	Table 5.5
Steel frame	EN10025-2 (S235)	Table 5.9
Steel columns	EN10025-2 (S235)	Table 5.9
Timber columns	Linear Elastic Isotropic Model-1	Table 3.8
Concrete slab	C35/45 (EN1992-1-1)	Table 5.9
Damping devices	Linear elastic	Table 5.7

Table 5.18: Material models and specific assumptions for Model-9

The eigen value analysis of first 200 eigen modes with eigen frequencies vary from 0.48232Hz to 7.670Hz (C.9) with a cumulative mass participation percentage of 98.202% in global X direction and 97.806% in global Y direction. The significant modes with maximum mass participation percentage ≥ 5% are shown in table 5.19.

Mode Number	Frequency (Hz)	Time Period (s)	Effective Mass & Direction	Effective Mass Percentage (%)
19	1.5483	0.6458	0.23253 E+05 (X)	88.363
10	1.1111	0.9000	0.23915 E+05 (Y)	90.879

Table 5.19: Modal mass participation of global modes in the first 200 eigen-modes in global X and global Y direction (Model 9)

GOVERNING EIGEN MODES IN GLOBAL X DIRECTION

After evaluating first 200 eigen-modes of Model-9, one significant global mode can be identified - Mode 19 with modal mass participation of 88.363% in global X direction [Fig 5.18].

GOVERNING EIGEN MODES IN GLOBAL Y DIRECTION

After evaluating first 200 eigen-modes of Model-9, one significant global mode can be identified- Mode 10 with maximum modal mass participation of 90.879% in global Y direction [fig 5.19].

OVERALL BEHAVIOUR OF MODEL-9

The modal deformations of this model indicate major damage in the masonry-wall of the bell-tower as well as the roof systems in both global modes. There is a very slight difference in the eigen-frequencies of model-8 and model-9 due to change in the shear
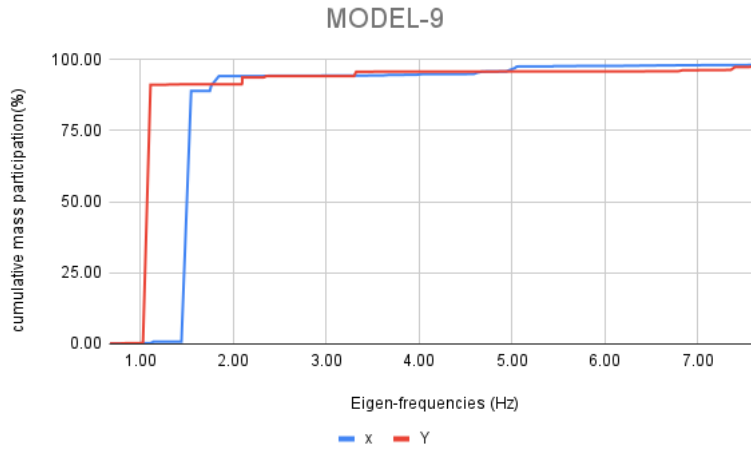
Figure 5.17: Eigen-frequencies and cumulative mass participation in X and Y direction- Model 9
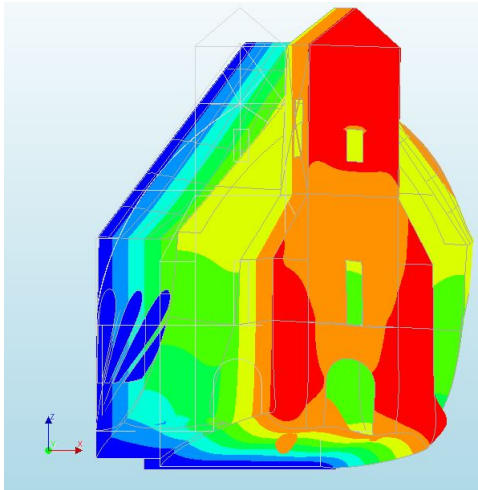
stiffness value of timber diaphragms.

The significant jump at the fundamental modes of vibration in both X (1.5483Hz) and Y(1.1114Hz) direction similar to the Model-8 is observed and the mass participation (%) is around 90% in both the fundamental modes. The fundamental eigen-modes of the structure are evaluated within the first 50 eigen-modes.
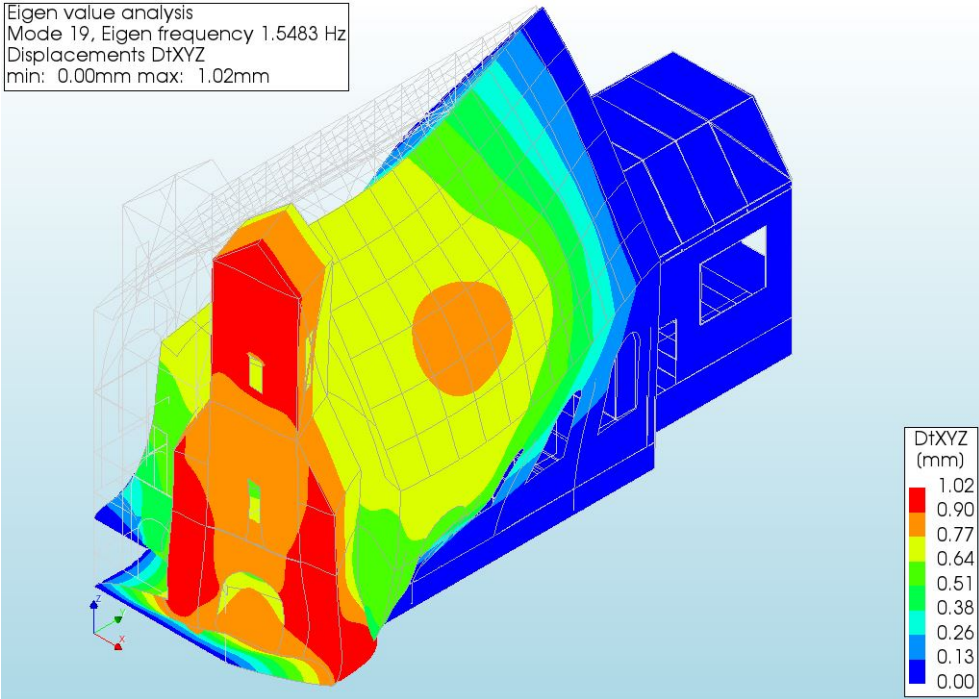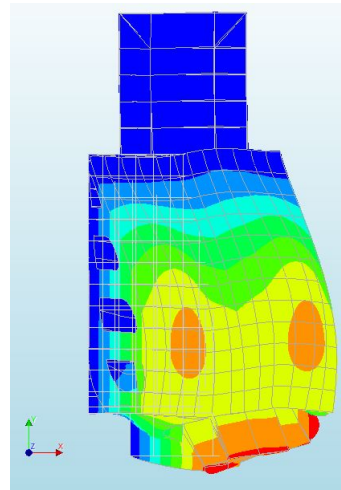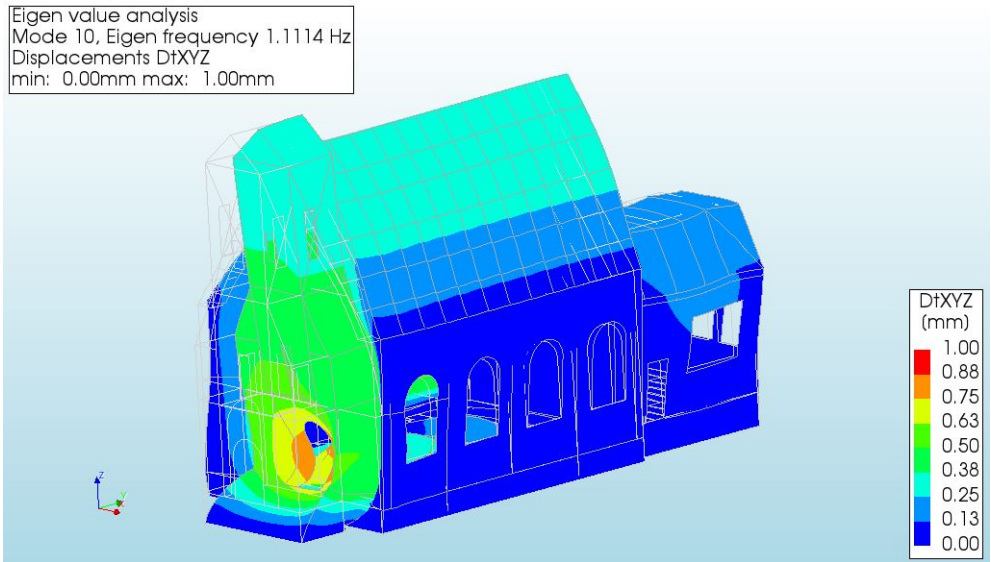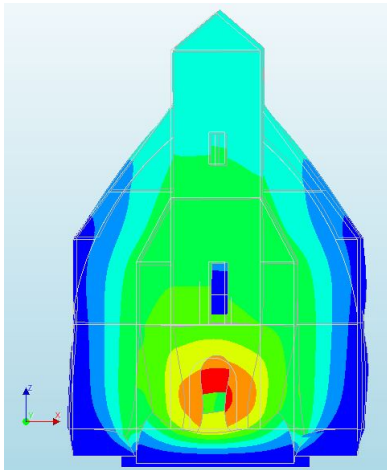
(a) Isotropic view- Mode 19

(b) Front view- Mode 19

(c) Top View- Mode 19

Figure 5.18: Global Mode 19(X)- indicating modal deformation (out-of-plane) of roof and wall systems [scale factor-0.05]

(a) Isotropic view- Mode 10

(b) Front View- Mode 10
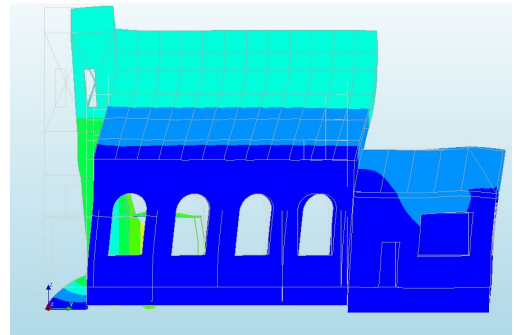
(c) Side View- Mode 10

Figure 5.19: Global Mode 10 - indicating modal deformation of roof and wall systems [scale factor-0.05]

5.7. MODEL-10

In this model, along with the geometrical and material modifications (model-9), a fixed base at ground level is assumed to compare the effect of local modes of the flexible foundation model on the eigen-value analysis. As the concrete slab at the bell-tower has a thickness of 100mm, it is safe to assume that the foundation is rigid and the boundary conditions of the steel-frame is fixed as well. The model-10 is shown in figure 5.20.

With these modifications, eigen-value analysis of first 200 eigen-modes derive eigen-frequencies varying from 0.623 Hz to 20.121 Hz (C.10) and a cumulative mass participation of 90.914% in global X direction and 88.967% in global Y direction. The global modes with significant mass participation are shown in Table 5.20.
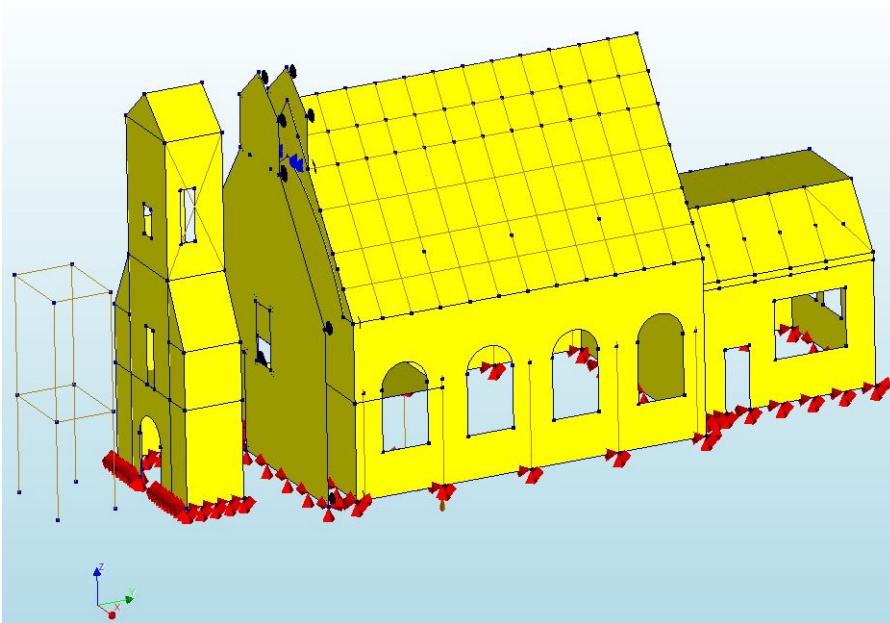
Figure 5.20: Finite Element Model-10 with structural modifications and fixed base with released rotations (virtually transformed representation)

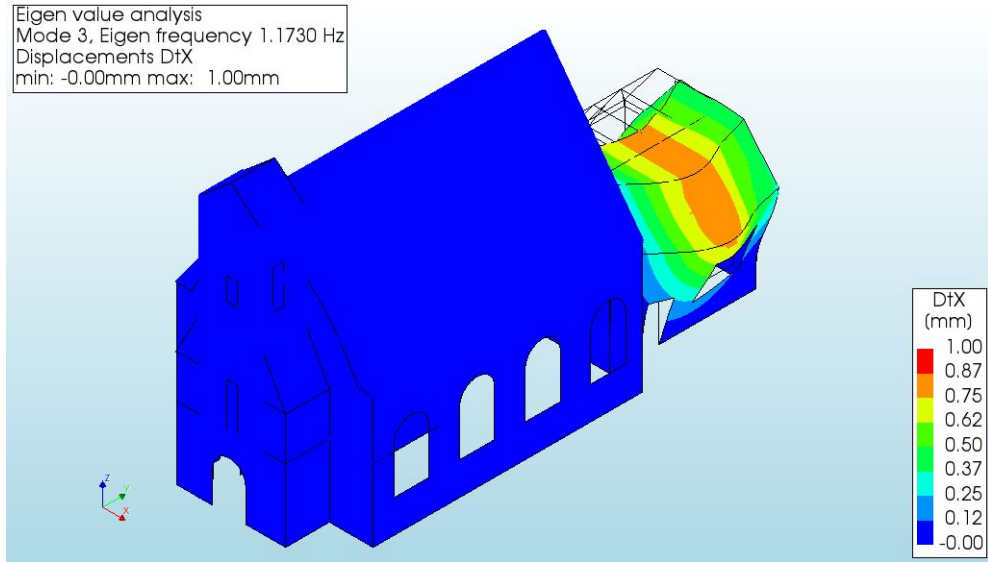| Mode Number	Frequency (Hz)	Time Period (s)	Effective Mass & Direction	Effective Mass Percentage (%)
3	1.1730	0.8525	0.12908 E+03 (X)	28.155
11	2.1867	0.4573	0.94208 E+02 (X)	20.548
40	6.0916	0.1641	0.23595 E+02 (X)	5.146
13	2.4687	0.4288	0.24509 E+03 (Y)	53.458
15	2.8625	0.3493	0.64410 E+02 (Y)	14.049
49	7.2836	0.1373	0.59613 E+02 (Y)	13.002

Table 5.20: Modal mass participation of global modes of the first 200 eigen-modes in global X and global Y direction (Model 10)

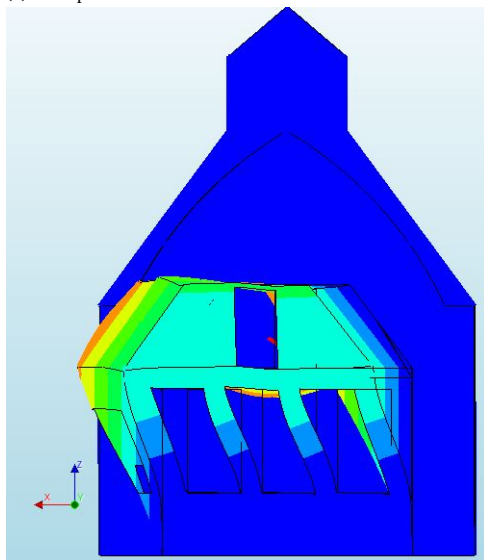GOVERNING EIGEN MODES IN GLOBAL X DIRECTION

After evaluating first 200 eigen-modes of Model-10, global mode 3 is a significant mode with maximum mass participation in X direction with maximum deformation localised in the substructure [fig 5.21]. Mode-11 with a mass participation of 20.548% has a modal deformation in the masonry walls of the main structure similar to previous models. [Fig 5.23a]
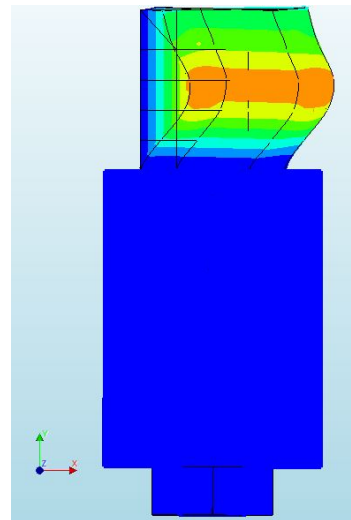
GOVERNING EIGEN MODES IN GLOBAL Y DIRECTION

After evaluating first 200 eigen-modes of Model-10, global mode 13 has the maximum mass participation of 53.458% with major deformation localized in the masonry walls of the sub-structure [fig 5.22], while mode-15 with mass participation of 14.049% has a modal deformation localised in the roof of bell-tower and main-structure similar to previous models. [Fig 5.23b]

5

Eigen value analysis
Mode 3, Eigen frequency 1.1730 Hz
Displacements DtX
min: -0.00mm max: 1.00mm

DtX
(mm)
1.00
0.87
0.75
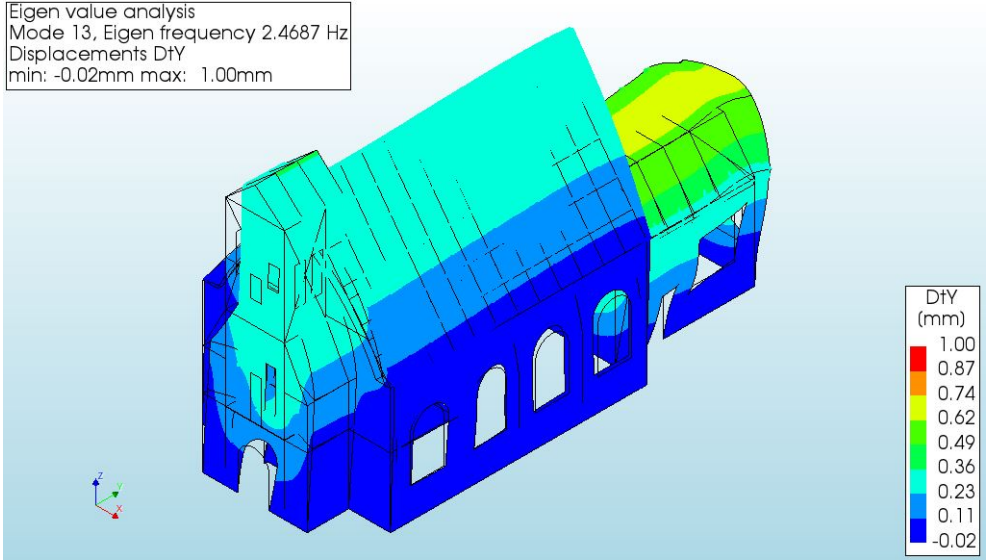0.62
0.50
0.37
0.25
0.12
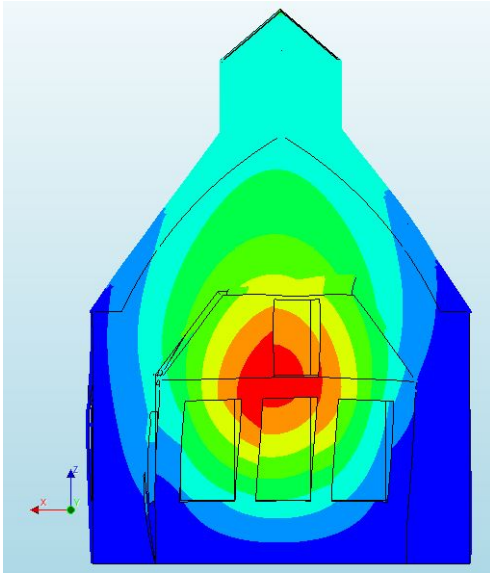-0.00

(a) Isotropic view- Mode 3

(b) Back view- Mode 3

(c) Top view- Mode 3

Figure 5.21: Global Mode 3(X) - indicating out of plane modal deformation [scale factor-0.05]
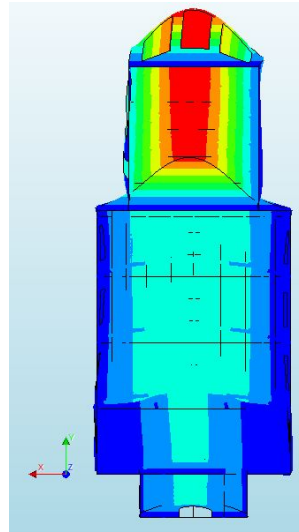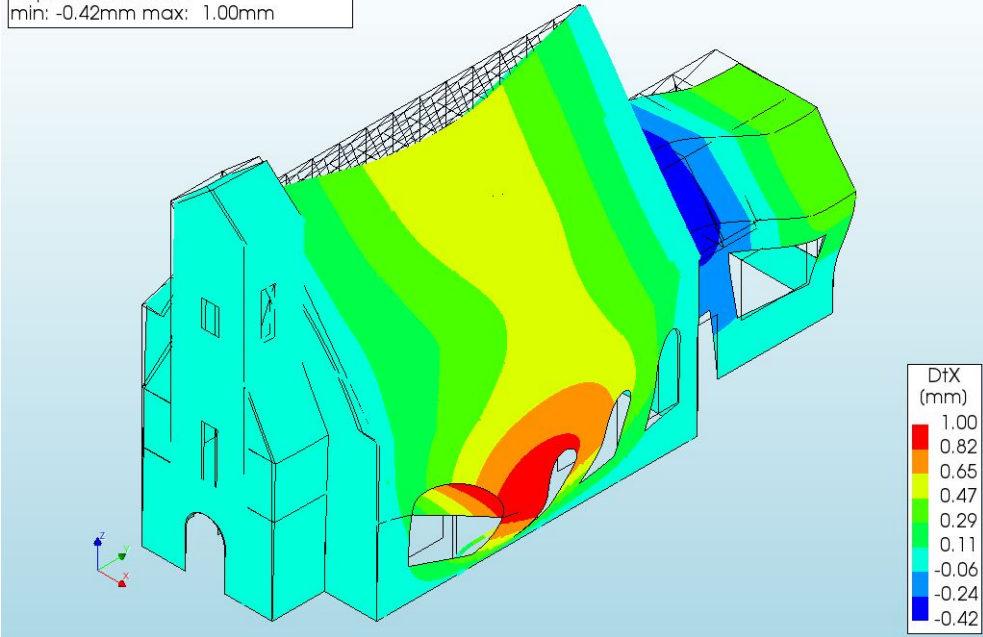
(a) Isotropic view- Mode 13

(b) Back view- Mode 13

(c) Bottom view- Mode 13

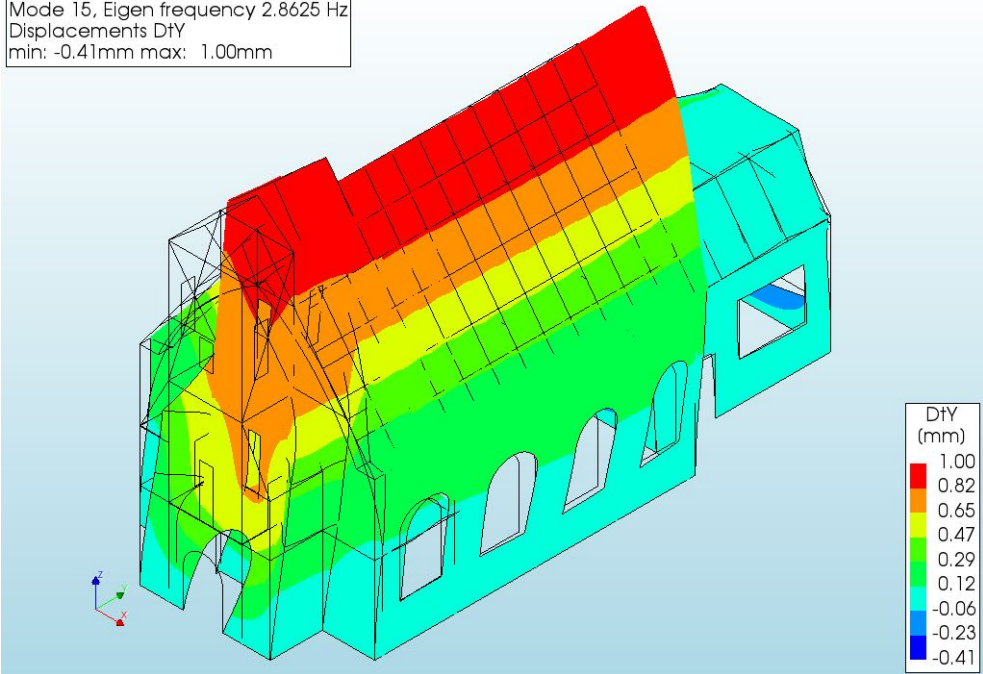Figure 5.22: Global Mode 13- indicating modal deformation (translation) of roof and wall systems [scale factor-0.05]

(a) Global mode-11 indicating main deformation of roof and masonry wall systems of the sub-structure.

(b) Global Mode-15 indicating main deformation in the masonry of sub-structure.

Figure 5.23: Modal deformations of global modes in X and Y direction [scale factor-0.05]

OVERALL BEHAVIOUR OF MODEL-10

After the geometric and material modifications in modelling the case-study, by assuming a fixed base at ground level, the behavior of the structure changes dramatically. The main modal deformation in global X direction - Mode 3 indicates major deformation in the sub-structure while Mode 13 in global Y direction indicates major deformation in the masonry walls of the sub-structure too. It is interesting to note that, the modal deformation in Modes 11 (X), 15(Y) is comparable to the reference model.

The eigen-frequency and cumulative mass participation graph shown 2 distinctive jumps in the X direction (1.17Hz and 2.18Hz) and 3 distinctive jumps in the Y direction (2.45Hz, 2.85Hz and 7.28Hz) [fig. 5.24]. The cumulative mass participation has reached 90% at the end of 200 eigen-frequencies and the fundamental modes of vibration lie within the first 50 eigen modes.
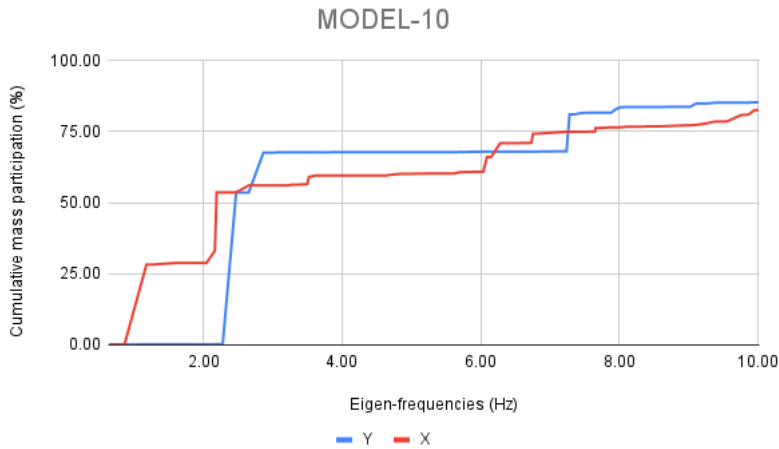

Figure 5.24: Eigen-frequencies and cumulative mass participation in X and Y direction- Model 10

6

DISCUSSION

The main research objective of this thesis is to accurately predict the dynamic properties of this historical Dutch church subjected to seismic damage by numerical modelling. The first sub-question of this thesis was determining the simplified geometric and material properties of the load carrying and non-load carrying elements to precisely represent the complex structure of the case-study. Ten different modelling variations of the case-study prior and post structural modifications are analyzed in Chapters 3, 4 and 5 with the main modelling characteristic of each model summarised below:

6.1. MAIN MODELLING CHARACTERISTICS

The summary of main modelling characteristics of all Models 1-10 are presented below. Table 6.1 presents the Finite element types of all the structural elements in the case-study, table 6.2 summarises the material models for Models 1-10 and table 6.3 depicts the additional modelling simplifications/ assumptions for each model.

Structural element	Element type	Reference
Masonry wall	Regular curved shells : CQ40S, CT30S	Table 3.2
Masonry piers	Class III beam elements: CL18B	Table 3.5
Masonry foundation	Regular curved shells: CQ40S, CT30S	Table 3.2, step function (Fig. 3.8)
Timber joists, columns	Class III beam elements : CL18B	Table 3.5
Timber diaphragms	Regular curved shells: CQ40S, CT30S	Table 3.2
Steel frame, columns	Class III beam elements : CL18B	Table 3.5
Linear damping devices	Elastic spring dash-pots: SP2TR	Table 5.6

Table 6.1: Summary of finite elements types of all structural elements in the case-study

Main Modelling Characteristics		
Structural elements	*Material model*	*Reference*
MODEL-1		
Masonry walls, foundation	Continuum EMM-1,	Table 3.3
Masonry piers	TSCM-1	Table 3.6
Timber joists	Linear Elastic Isotropic Model-1	Table 3.8
Timber diaphragms	Linear Elastic Orthotropic Model -1	Table 3.10
MODEL-2		
Masonry walls, foundation	Continuum EMM-1	Table3.3
Masonry piers	TSCM-1	Table 3.6
Timber joists	Linear Elastic Isotropic Model-1	Table 3.8
Timber diaphragms	Linear Elastic Orthotropic Model -2	Table 3.11
MODELS-3,4,5		
Masonry walls	Continuum EMM-1	Table3.3
Masonry piers	TSCM-1	Table 3.6
Timber joists	Linear Elastic Isotropic Model-1	Table 3.8
Timber diaphragms	Linear Elastic Orthotropic Model -2	Table 3.11
MODEL-6		
Masonry walls, foundation	Continuum EMM-1	Table 3.3
Masonry piers	TSCM-1	Table 3.6
Timber joists, columns	Linear Elastic Isotropic Model-1	Table 3.8
Timber diaphragms	Linear Elastic Orthotropic Model-2	Table 3.11
Steel frame, columns	EN10025-2 (S235)	Table 5.9
Concrete slab	C35/45 (EN1992-1-1)	Table 5.10
MODEL-7		
Masonry walls, foundation	Continuum EMM-1	Table 3.3
Masonry piers	TSCM-1	Table 3.6
Timber joists, columns	Linear Elastic Isotropic Model-1	Table 3.8
Timber diaphragms	Linear Elastic Orthotropic Model-2	Table 3.11
Steel frame, columns	EN10025-2 (S235)	Table 5.9
Concrete slab	C35/45 (EN1992-1-1)	Table 5.10
Damping devices	Linear elastic spring dash-pots	Table 5.7
MODEL-8		
Masonry walls,foundation	Continuum EMM-2	Table 5.3
Masonry piers	TSCM-2	Table 5.4
Timber joists, columns	Linear Elastic Isotropic Model-1	Table 3.8
Timber diaphragms	Linear Elastic Orthotropic Model-2	Table 3.11
Steel frame, columns	EN10025-2 (S235)	Table 5.9
Concrete slab	C35/45 (EN1992-1-1)	Table 5.10
Damping devices	Linear elastic spring dash-pots	Table 5.7

Structural elements	Material model	Reference
MODEL-9		
Masonry walls,foundation	Continuum EMM-2	Table 5.3
Masonry piers	TSCM-2	Table 5.4
Timber joists, columns	Linear Elastic Isotropic Model-1	Table 3.8
Timber diaphragms	Linear Elastic Orthotropic Model-3	Table 5.5
Steel frame, columns	EN10025-2 (S235)	Table 5.9
Concrete slab	C35/45 (EN1992-1-1)	Table 5.10
Damping devices	Linear elastic spring dash-pots	Table 5.7
MODEL-10		
Masonry walls,	Continuum EMM-2	Table 5.3
Masonry piers	TSCM-2	Table 5.4
Timber joists, columns	Linear Elastic Isotropic Model-1	Table 3.8
Timber diaphragms	Linear Elastic Orthotropic Model-3	Table 5.5
Steel frame, columns	EN10025-2 (S235)	Table 5.9
Concrete slab	C35/45 (EN1992-1-1)	Table 5.10
Damping devices	Linear elastic spring dash-pots	Table 5.7

Table 6.2: Material models of all structural elements in Models 1-10

6

Models	Additional modelling characteristics
Models prior retrofitting: case-study (as built)	
Model-1	Modeled all structural elements Self weight of timber diaphragms: Additional line load on cross-beams Fixed base at masonry foundation level
Model-2	Modeled all structural elements Fixed base at masonry foundation level
Model-3	Eliminated masonry foundation and timber floor-system at ground level; Fixed base at ground level.
Model-4	Eliminated masonry foundation and timber floor-system at ground level; Fixed base at ground level with released rotations in specific global x, y directions.
Model-5	Eliminated masonry foundation, timber floor-system at ground level and roof-systems; Fixed base at ground level.
Models post retrofitting: case-study (present state)	
Model-6	Modeled all structural elements; Disconnecting the masonry wall at bell-tower and main-structure; Installation of steel frame, timber and steel columns; Fixed base at masonry foundation level.
Model-7	Modeled linear damping devices between the bell-tower and roof structure.
Model-8	Modification of masonry properties (considering degradation of masonry)
Model -9	Modification of timber diaphragm and masonry properties. (considering degradation of masonry and timber diaphragms)
Model-10	Elimination of masonry foundation and ground floor. Fixed base at ground level.

Table 6.3: Additional modelling characteristics of Models 1-10.

6.2. INTERPRETING THE RESULTS OF MODELLING VARIATIONS

The second sub-question is determining the main modal response of the case-study structure prior and post structural retrofitting in both global x and y directions:

In order to achieve this objective, as discussed in section 3.4, the results of eigen-value analysis of all modelling variations (Model 1-10) are analyzed based on

• How the eigen-frequencies are influenced by stiffness and mass of the structure? As, the stiffness of the system decreases or the mass of the system increases in the particular direction considered, the eigen-frequencies decrease. (according to equation 6.1)

$$\omega_0 \propto \sqrt{\frac{\text{stiffness}}{\text{inertia}}} \tag{6.1}$$

• How the effective mass participation of a particular mode in the considered direction, contributes to the dynamic response of the case-study structure? The effective mass participation of the considered eigen-frequencies (fundamental mode of vibration) in both directions are compared for all Models 1-10, to predict the dynamic response of the case-study.

Chapters 4 and 5 presents the eigen-frequencies, modal mass participation, natural time period of vibration and main modal deformation in both global x and y directions for all modeling variations. Table 6.4 summarises the results of all 10 models.

Models	Main Global Modes -X	Main Global Modes-Y
Model 1		
Mode Number	146	197
Eigen Frequency (Hz)	2.3662	2.7516
Time period (s)	0.4226	0.3634
Mass participation	3.636	10.96
Model 2		
Mode Number	40	49
Eigen Frequency (Hz)	2.7065	3.173
Time period (s)	0.3695	0.3152
Mass participation	4.927	9.732
Model -3		
Mode Number	4	6
Eigen Frequency (Hz)	2.7377	3.3950
Time period (s)	0.3653	0.2945
Mass participation	20.187	45.098
Model-4		
Mode Number	4	7
Eigen Frequency (Hz)	2.3422	3.4516
Time period (s)	0.4269	0.2897
Mass participation	28.845	46.588
Model-5		
Mode Number	3	17
Eigen Frequency (Hz)	0.8523	3.0335
Time period (s)	1.173	0.3296
Mass participation	23.371	18.250
Model 6		
Mode Number	44	36
Eigen Frequency (Hz)	2.6076	2.4666
Time period (s)	0.3834	0.4054
Mass participation	83.483	5.451
Model-7		
Mode Number	44	36
Eigen Frequency (Hz)	2.6076	2.4660
Time period (s)	0.3827	0.4055
Mass participation	84.493	5.439
Model-8		
Mode Number	19	10
Eigen Frequency (Hz)	1.5488	1.1125
Time period (s)	0.6456	0.8988
Mass participation	88.329	90.881
Model-9		
Mode Number	19	10
Eigen Frequency (Hz)	1.5483	1.1114
Time period (s)	0.6458	0.89997
Mass participation	88.363	90.879
Model-10		
Mode Number	3	13
Eigen Frequency (Hz)	1.1730	2.4687
Time period (s)	0.8525	0.4050
Mass participation	28.155	53.458

6

6.2.1. MODELS BEFORE THE STRUCTURAL RETROFITTING

It can be observed from table 6.4, the values of the fundamental frequencies and the normalized modal shapes in the X and the Y directions obtained from the eigen-value analysis for the first 5 models, shows lower eigen-frequencies in X directions compared to the eigen-frequencies in the Y-direction. The slight difference between the fundamental frequencies evidences higher constraints in the X direction given by the lateral masonry walls of the church adjacent to the tower.

MODELLING VARIATION-1

The cumulative mass participation of the global modes in model -1 is very low in X direction (40%) and also the Y direction (75%) and the graph 4.3 indicates insignificant/minor jumps at the fundamental eigen-frequencies considered in both directions which can be due to many localised modes in the model.

The Model-1 has lower natural frequency in X direction (2.3662HZ) compared to the Y direction(2.7516Hz) showing higher constraints in the X direction. The modal shape for Mode-146 (maximum mass participation in Global X direction) indicates maximum deformation in the roof at the timber joists (Cross-beams) which is due to the additional load equal to the weight of the timber diaphragms acting on the timber-joists. Similarly in the Y direction, the modal deformation of Mode-197 indicates maximum deformation at the timber joists at the first floor level of the sub-structure which is due to the additional load.

The natural-frequencies of the model are lower than the other models, due to insufficient stiffness consideration of timber diaphragms and it can be concluded that the damage is confined to the timber joists with additional loading (local), hence the material model considered for the timber diaphragms may not be ideal and this model doesn't represent the case-study accurately.

MODELLING VARIATION-2

In model-2, the cumulative mass participation is the same in both X and Y direction and there is a clear distinction between the first and second natural modes of vibration as indicated in graph 4.7. The fundamental modes of vibration were found within the first 50 eigen-modes making the model more efficient for computation.

In model-2, first global modes- Mode 40 (X)and Mode 49 (Y) shows global deformation of the entire structure. The natural frequencies of this model are lower in X-direction compared to Y-direction similar to model-1 and both the eigen-frequencies are greater than the model-1 indicating increased stiffness of the model in both directions, probably due to large number of local modes. This model also indicates major deformation in the roof of the main-structure (timber diaphragm) as well as the tip of the bell-tower, roughly indicating the weakness of the structure at these locations. The modal response of this Model-2 can be predicted as the probable dynamic response of the Old Church, thus it is considered as the "reference model."

Modelling Variation-3

In this model, instead of a flexible foundation a rigid base at ground-level is assumed leading to an increased stiffness of the structure which can be observed with a slight increase in the natural frequencies of the structure, although minimal.

The cumulative mass participation is same in both X and Y direction and the natural modes of vibration can be distinctively recognised from the graph 4.9 in both directions. It can be seen that the fundamental modes of vibration are within the first 10 eigen-modes making the computation as well as modeling easier than the reference model and the difference between the eigen-frequencies obtained is also minimal.

In model-3, first global modes Mode 4(X) and Mode 6(Y) have the modal deformation similar to the reference-model indicating roof and the bell-tower as the weakness of the structure. Hence, for achieving the goal of predicting the dynamic behaviour of the case-study, it can be show that the assumption of a fixed base is beneficial for the rough estimation of the modal shape as well as the natural frequencies of the structure.

Modelling Variation-4

In this variation, instead of considering a fixed base, the rotations are released to approximate the flexible foundation design. The cumulative mass participation is slightly higher in the X direction compared to the Y direction at the end of 200 eigen-modes, due to released degrees of freedom has more influence in the opposite direction (and hence in the X direction, where the walls are shorter). The fundamental modal frequencies are found within 10 eigen-modes as well making the computation easier [graph 4.13].

In model-4, the fundamental frequency in X decreases to 2.3422Hz compared to Model-3 (2.7377Hz) due to significant decrease in stiffness in X direction, while there is a slight increase in the fundamental frequency in Y from 3.3950Hz(Model-3) to 3.4516Hz indicating a minimal increase in stiffness in this direction. Although, the cumulative mass participation has increased in this model, it may not represent the flexible masonry foundation of the case-study accurately.

Modelling Variation-5

In this variation, timber diaphragm is not modelled entirely leading to the major modal deformations in the masonry-walls. The cumulative mass participation percentage is same in both X and Y directions at the end of 200 eigen-modes. [fig.4.17]

In model-5, the fundamental frequency in X decreases to 0.8523Hz and the major deformation is observed at the top of the masonry-wall which is due to the additional line loading directly placed on the masonry-walls. In the Y direction, the eigen-frequency of 3.033Hz has a significant decrease in comparison to the reference model due to a significant decrease in the stiffness of the structure as the roof-structure is not modelled, the masonry-walls act like cantilever structures. Although, the global eigen-frequencies are obtained within 50 eigen-modes, this model is not the best fit to represent the case-study as the eigen-modes are not comparable to the reference model.

6.2.2. Modelling after structural retrofitting

The main structural retrofitting measures of the case-study included addition of a steel-frame supporting the bell-tower, timber and steel columns supporting the first floor of

the main structure, concreting the base of the bell-tower and installation of linear damping devices. In the models 6-10, these variations are compared with the reference model to evaluate the influence of these modifications on the modal shape of the structure.

MODELLING VARIATION-6

Along with the structural modifications of the structure, the cavity-wall between the bell-tower and the main-structure is modelled with a disconnect connection. This connection is checked by the presence of two separate nodes on both the walls (Node Multiplicity =2) as shown in Fig 6.1.

In Model-6, there is a slight difference between the fundamental frequencies with higher
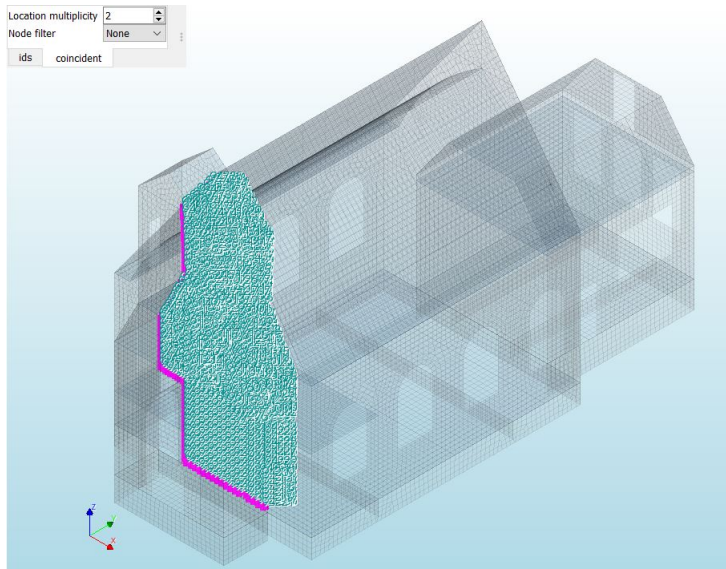
Figure 6.1: Modelling the cavity-wall with a disconnect connection

frequency in X direction compared to Y direction [fig.5.8]. Although, the difference is small, it can be predicted that due to the installation of the Steel-frame and additional columns, the constraint effect in the Y direction has increased leading to the decrease of eigen-frequency in the Y direction. The eigen-frequency in the X direction (2.6076Hz) has reduced slightly compared to the reference model(2.7065Hz) due to the additional mass of the steel-frame and column elements [Fig 5.7].

The analysis of this model depicts the changes accurately. It should also be noted that even with a disconnection between the bell-tower and the main-structure [Fig 6.1], the deformation of the bell-tower and roof structure is continuous. The critical elements are the timber diaphragm in the roof structure in X direction and the cavity wall between the bell-tower and the main-structure in Y direction indicating the weakness of the case-study.

MODELLING VARIATION-7

In this modelling variation, the effect of modelling linear dampers at the bell-tower and the roof structure is compared.

Comparing the eigen-frequencies and the mass participation percentages [fig 5.13], it can be clearly seen that there is no significant change in the results and the modal-shape with respect to Model-6. As eigen-value analysis assumes no damping in the system, modelling the linear dampers doesn't modify the behaviour of the structure or the results.

MODELLING VARIATION-8

In this Model-8, the degradation in the masonry material properties due to existing seismic damage, water-seepage and other factors is considered to compare the effect of the masonry material properties on the eigen-value analysis.

From figure 5.16, it can be observed that the mass participation at the fundamental mode in both x and y direction is very high (90%) making these global fundamental modes significant. The global modes corresponding to the fundamental frequency are found within the first 50 eigen-modes.

In comparison to the reference model and the Model-6 after structural modifications, a clear decrease in the eigen-frequencies can be found in both X and Y direction due to a significant decrease in the stiffness of the system. But similar to Model-6, the eigen-frequency in X direction is greater than the y direction due to additional constraints in the Y direction.

The modal deformation in X direction (Mode-19) is concentrated at the facade-wall of the bell-tower in the masonry, similarly the modal deformation in Y direction(Mode-10) is also concentrated in the masonry cavity wall between the bell-tower and the main-structure.

Hence, it can be concluded that the material properties of masonry heavily effects the fundamental frequency of the structure and the weakness of the structure is concentrated at the masonry walls and the bell-tower.

MODELLING VARIATION-9

In this Model-9 the material properties of timber diaphragms (the effective shear stiffness) is modified to account for the degradation over time. The effect of material properties of timber on the eigen-value analysis is compared.

In comparison to Model-8, there is a slight decrease in the eigen-values in both directions which is insignificant [fig. 5.17] but can be concluded that, decrease in the stiffness properties of Timber diaphragms leading to a very slight decrease in stiffness of the structure. The major deformation is still concentrated in the masonry of the bell-tower (X direction) and the cavity-wall between the bell-tower and the main-structure.

Hence, for this particular case-study it can be concluded that the material properties of masonry affect the modal analysis more than the timber diaphragm properties and the variation of the effective shear stiffness of the timber diaphragm is not significant.

MODELLING VARIATION-10

In this last modelling variation, a fixed base at ground-level is modelled instead of a flexible foundation to simplify the modelling and comparing the variation in the eigen-value analysis.

In comparison with the previous models, despite the additional constraints in Y direction due to retrofitting, the eigen frequency in the X axis (2.1867Hz) is lesser than 2.8625Hz in the Y direction which is due to increased constraints in the X direction due to a fixed base. [fig 5.24] It can also be observed that, despite the modified material properties, modelling a fixed base has increased the stiffness of the whole structure increasing the eigen-frequencies in both X and Y directions compared to model 8,9 but they are smaller than the eigen-frequencies of the reference model due to degraded material properties. The modal shape of global Mode-3(X) shows major deformation concentrated in the sub-structure and the global Mode-13(Y) shows major deformation concentrated at the masonry walls of the sub-structure and the roof of the main-structure. Hence, it can be noted that modelling a fixed base shows a significant difference in the fundamental modes of vibration as well as modal deformation. Model-10 which is a further simplification of Model-8, returns clear results with no unexpected and local deformations but the fundamental mode shows maximum deformation in the sub-structure unlike Model-8 which requires further research.

6.3. DYNAMIC RESPONSE OF THE CASE-STUDY

From section 6.2, the eigen-frequencies and effective mass participation of each mode are analyzed by interpreting the variation of stiffness, constraints and effects of structural modifications on the case-study structure. From these models, the results are compared to roughly predict the fundamental frequency of the case-study and critical elements of the structure.

DYNAMIC RESPONSE OF THE CASE-STUDY IN GLOBAL-X DIRECTION

For all the modelling variations in X direction; from figure 6.2, it can be seen that the cumulative mass participation of at least 80% is not achieved for Model 1. While models 2-5 does have a cumulative mass participation of 80%, from figure 6.2 the indication of fundamental frequency of the structure prior structural modifications (models 2-5) is not quite significant.

From figure 6.3, the fundamental frequency in X direction of the case-study prior structural retrofitting lies approximately between *2.30Hz to 2.75Hz* and the maximum deformation in the timber roof of the main-structure indicates it to be the critical element in the case-study. Considering, the case-study post structural modifications; Models 6,7 indicate very slight decrease in the stiffness of the structure in X direction, yet the fundamental frequency of the case-study still lies within 2.30Hz- 2.75Hz and the timber diaphragm in the roof-system of the main-structure still remains the critical element of weakness in the structure.
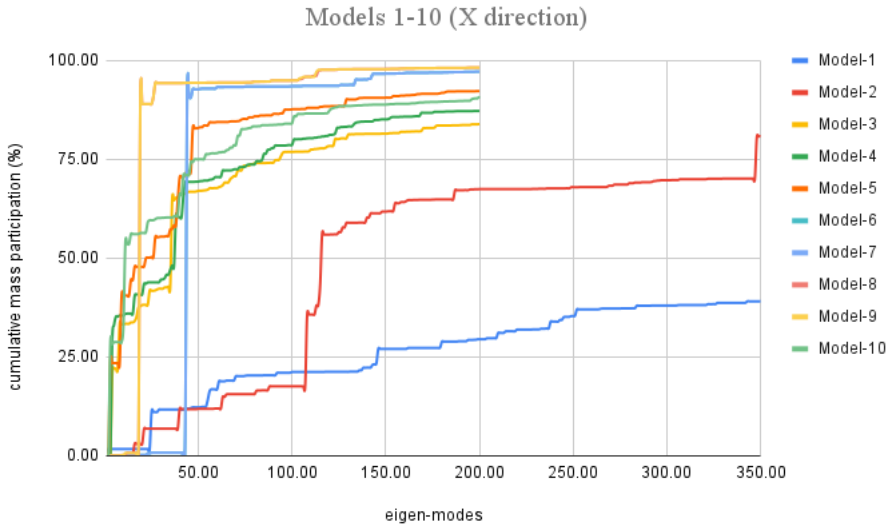
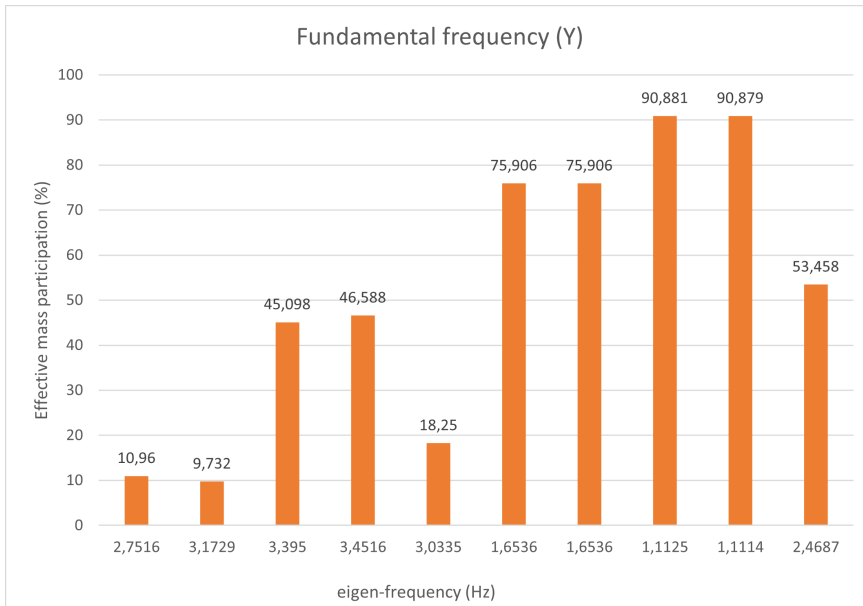Figure 6.2: Cumulative mass participation with respect to the eigen modes in the X direction (Models 1-10)
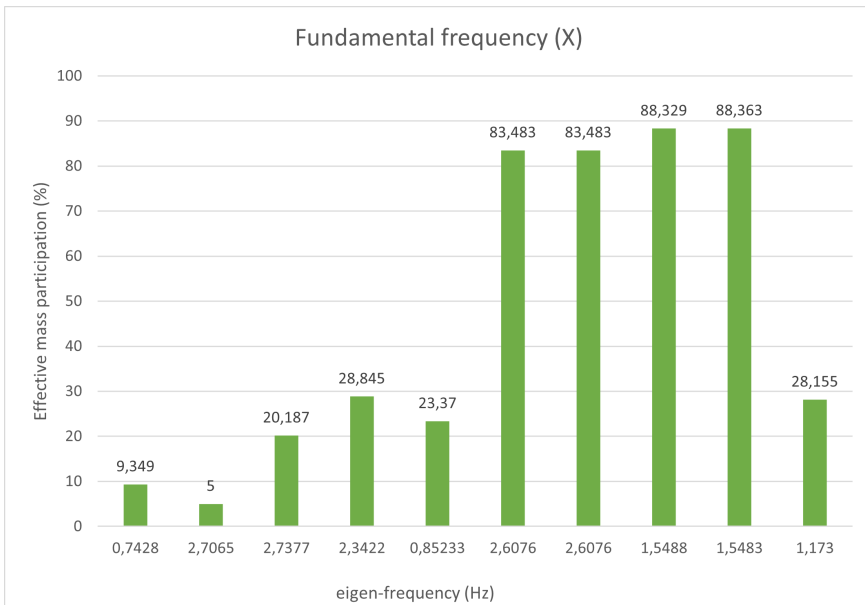
Figure 6.3: Plot between the fundamental eigen-frequency (Hz) and corresponding effective mass participation (%) in global X direction.

When the degraded material properties of masonry and timber are considered (Models 8-10), the stiffness of the whole structure has reduced by a significant amount and the *fundamental frequency of the case-study in present state in X direction can be approximated to 1.55Hz- 2.6Hz* [fig. 6.3]. It should also be noted that, Model-8 presents the approximation of degraded masonry material properties of Model-6 hence, the upper-limit of fundamental frequency.

The critical-elements in the case-study subjected to maximum deformation are the masonry walls of the bell-tower as well as the timber diaphragm in the roof of the main-structure.

Thus, Mode-19 in Model-8 (maximum EMPF) can be predicted to represent the dynamic response of the case-study in the present state in global X direction.

DYNAMIC RESPONSE IN GLOBAL-Y DIRECTION

Similar to the X direction, the cumulative mass participation of Model-1 is not 80% hence it isn't considered further. From figure 6.4, all the models indicate a distinctive jump showing fundamental frequency within the first 50 eigen-modes.

For the case-study prior to structural modifications (as-built), *the fundamental fre-*
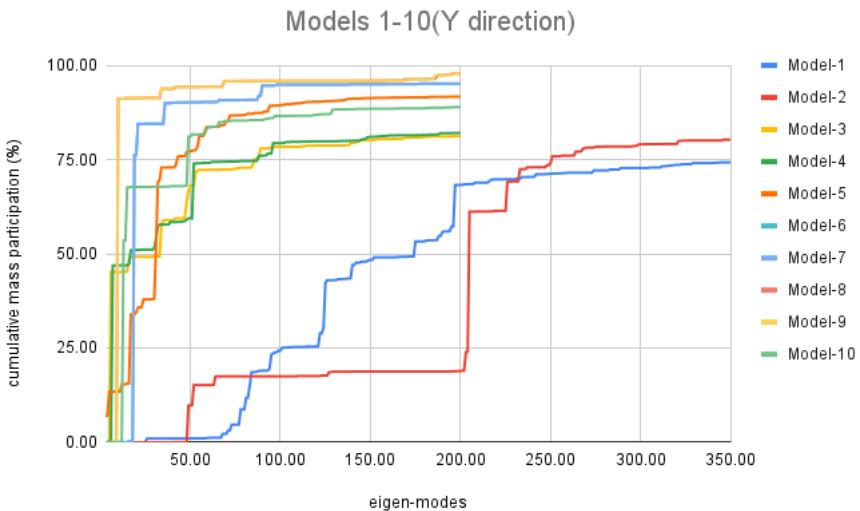
Figure 6.4: Cumulative mass participation with respect to the eigen modes in the Y direction (models 1-10)

quency in Y direction approximately lies between 3.0Hz to 3.45Hz (fig 6.5) with maximum deformation at the tip of the bell-tower as well as the roof-structure indicating the critical elements of weakness in the structure.

In the case-study post structural retrofitting, there is a large drop in stiffness of the whole structure in Y direction leading to a significant decrease in the fundamental frequency as indicated in Models 6,7. Although, by considering degraded masonry and

Figure 6.5: Plot between the fundamental eigen-frequency (Hz) and corresponding effective mass participation (%) in global X direction.

timber diaphragm properties to represent the present state of the case-study, *the fundamental frequency of the structure in Y direction can be approximated from 1.1Hz to 1.65 Hz.* It should also be noted that, Model-8 presents the approximation of degraded masonry material properties of Model-6 hence, the upper-limit of fundamental frequency. The critical elements in the case-study (present state) are the cavity wall between the main-structure and bell-tower, main facade wall of bell tower as well as the tip of the roof in main-structure, indicating the weakness in the church.

Thus, Mode-10 of Model-8 (maximum EMPF) can be predicted as the precise approximation of dynamic response of the case-study post structural retrofitting in global Y direction.

6.4. LIMITATIONS
The following aspects are disregarded in the analysis and assessment of the church Structure:

- The non-homogeneous thickness of the masonry walls and piers is not represented in these models.

- Due to limited research on historical structures in this region, the material properties considered in this thesis are derived from the residential buildings in Groningen and a historical "borg" structure from the similar timeline. Thus, there is a limitation in the accuracy of the material model of masonry-walls of the case-study

structure.

- Due to lack of information about the metal ties between the masonry cavity walls, they are disregarded and the cavity walls are modelled as disconnected walls assuming complete degradation of the ties.

- The concrete slab at the entrance of the church is assumed to be connected to the masonry walls of the structure and not as a fixed foundation due to lack of specific details.

With limited research and no physical test results available to support the main modal response of the case-study by numerical modelling, this thesis report can be considered as a base to compare the physical test results and further investigate to which extent these analyses methods can provide insight in the global behaviour of the Old Church in Garrelsweer.

6

7

CONCLUSIONS

The main research question of this thesis aimed to accurately predict the numerical model that represents the dynamic properties of the historical unreinforced masonry church. Based on a quantitative and qualitative analogy of modelling variations and comparing the results of analysis, these main conclusions can be drawn:

7.1. CONCLUSIONS

Prior to considering the structural retrofitting of the case-study, Numerical Model-3 with a fixed base at ground-level can be considered as a computationally effective approximation representing the approximate dynamic response of the case-study prior structural retrofitting. The following are the main conclusions drawn on numerical modelling of the case-study:

- *The masonry walls can be modelled as a 2D regular curved shell elements (CQ40S, CT30S) with a constant thickness obtained by averaging all values along the length.*

- *As the difference between the thickness of masonry walls and piers is comparable, the masonry piers can be modelled as 2D Class III beam elements (CL18B) with a constant thickness obtained by averaging all the values.*

- *The masonry step foundation can be modeled with a step function in Z direction.*

- *The masonry walls and foundation are modeled with a continuum Engineering Masonry Model (EMM), while the masonry piers are modeled with a Total Strain based Cracking Model (TSCM).*

- *The timber joists are modeled with 2D class III beam elements (CL18B) with an linear elastic isotropic material model while the timber diaphragms are modeled with a 2D regular curved shell elements (CQ40S, CT30S) with a linear elastic orthotropic material model.*

- *Considering a fixed base at ground-level instead of modelling the flexible founda-tion and timber flooring can be beneficial in-order to investigate faster and deter-mine the clear modal response of the structure effectively but with lesser accuracy.*

- *As the structural weakness of the case-study prior structural retrofitting lies in the timber-roof structure, modelling only masonry part of the structure may not achieve reliable results. Hence, it can be concluded that modelling the timber-roof is impor-tant to determine the dynamic response of the structure.*

Post structural modifications in the case-study, the eigen value analysis indicated that the structural modifications and material properties of masonry have a significant influ-ence on the global dynamic response of the church. The main conclusions on numerical modeling of the case-study post structural retrofitting are:

- *It can be concluded that, in analyses assuming no damping (free-vibration analy-ses), modelling the linear damping devices is of no significance. Hence, the mod-elling can be simplified.*

- *The material properties of the masonry structures in the case-study have major in-fluence on the global dynamic response of the structure. Hence, modelling the ma-sonry material properties accurately is of importance.*

- *It can be concluded that the variation of effective shear stiffness of timber diaphragms have almost negligible influence on the eigen-value analysis of this case-study.*

- *The steel-frame in the bell tower and the additional columns have influenced the global response of the structure. It can be observed that the natural modes of vi-bration are closer in both global X and Y directions and the slight difference in the fundamental-frequencies evidences increase in stiffness in Y-direction.*

- *Considering a fixed base at ground-level in the case-study post structural modifi-cations, shows a drastic change in the eigen-frequencies and modal deformation of the structure in comparison to previous models.*

In conclusion, answering the main research question:
How can the dynamic properties of a historical masonry church in Groningen be accu-rately determined by numerical modelling?

In order to simulate the structure as it is now, Numerical Model-8 (or Model-9 which has almost similar results) can be predicted as the closest approximation of the dynamic properties in the case-study.

- *The fundamental frequency of the case-study post structural retrofitting can be pre-dicted to lie between 1.5Hz-2.6Hz in global X direction and between 1.1Hz-1.65Hz in global Y direction.*

- *The critical elements in the case-study roughly indicating the weakness of the structure are: the masonry facade walls of the bell-tower, cavity wall between the bell-tower and main-structure, tip of the bell-tower, lateral walls and timber roofing of the main-structure.*

7.2. FURTHER RECOMMENDATIONS

For further studies it is recommended:

- *To collect samples from the real structure or more detailed information by observations in order to eliminate assumptions regarding the boundary and interface connections and material properties.*

- *To compare the predicted modal response of the church structure to the physical ambient vibration tests to validate the results obtained.*

- *Comparing the modal deformation in the sub-structure of Model-10 with the physical test results to understand the modal response of the case-study.*

- *To study the orthotropy of multi-leaf walls on component level as for historical structures in particular so the physical model is reflected better. Layered curved shell elements can be used with appropriate material properties for the layers to study the effect of orthotropic cavity walls for a three-dimensional case.*

- *Eigen-value analysis gives a rough indication of the weakness in the structure that can be compared with more sophisticated method of analysis like a cyclic nonlinear analysis for the study of the church structure in order to observe the degradation and propagation of the damage.*

- *To use the Nonlinear Pushover Analysis (NLPO) method in combination with the Modal Response Spectrum Analysis (MRS) method or the Nonlinear Time History Analysis (NLTH) method. The methods provide a solution for considering multi-modes simultaneously and a detailed insight of damage progression in the structure due to dynamic loading.*

7

BIBLIOGRAPHY

[1] İhsan Engin Bal et al. "Monitoring of a Historical Masonry Structure in Case of Induced Seismicity". In: *International Journal of Architectural Heritage* 15.1 (Jan. 2021), pp. 187–204. ISSN: 1558-3058. DOI: 10.1080/15583058.2020.1719230. URL: https://www.tandfonline.com/doi/full/10.1080/15583058.2020.1719230.

[2] Charles Vlek. "Rise and reduction of induced earthquakes in the Groningen gas field, 1991-2018: statistical trends, social impacts, and policy change". In: *Environmental Earth Sciences* 78 (2019), p. 59. DOI: 10.1007/s12665-019-8051-4. URL: https://doi.org/10.1007/s12665-019-8051-4.

[3] *Liability and damage claim issues in induced earthquakes: case of Groningen — Hanze University of Applied Sciences.* URL: https://research.hanze.nl/en/publications/liability-and-damage-claim-issues-in-induced-earthquakes-case-of-.

[4] *Erfgoedmonitor databank - Listed buildings in the Netherlands 1965-2018.* URL: https://erfgoed.databank.nl/jive.

[5] Angelo D'Ambrisi, Valentina Mariani, and Marco Mezzi. "Seismic assessment of a historical masonry tower with nonlinear static and dynamic analyses tuned on ambient vibration tests". In: *Engineering Structures* 36 (Mar. 2012), pp. 210–219. ISSN: 01410296. DOI: 10.1016/j.engstruct.2011.12.009.

[6] *Eigenfrequency Analysis.* URL: https://www.comsol.nl/multiphysics/eigenfrequency-analysis.

[7] Marco Valente and Gabriele Milani. "Seismic assessment of historical masonry towers by means of simplified approaches and standard FEM". In: *Construction and Building Materials* 108 (Apr. 2016), pp. 74–104. ISSN: 09500618. DOI: 10.1016/j.conbuildmat.2016.01.025.

[8] *NPR 9998:2018+C1:2020 en.* URL: https://www.nen.nl/en/npr-9998-2018-c1-2020-en-256373.

[9] Antonella Saisi and Carmelo Gentile. "Post-earthquake diagnostic investigation of a historic masonry tower". In: *Journal of Cultural Heritage* 16.4 (July 2015), pp. 602–609. ISSN: 12962074. DOI: 10.1016/j.culher.2014.09.002.

[10] "EN 1998-3: Eurocode 8: Design of structures for earthquake resistance – Part 3: Assessment and retrofitting of buildings". In: (2005).

[11] P Bisch et al. "Eurocode 8: Seismic Design of Buildings Worked examples Support to the implementation, harmonization and further development of the Eurocodes". In: (). DOI: 10.2788/91658. URL: http://www.jrc.ec.europa.eu/.

[12] L. F. Ramos et al. "Monitoring historical masonry structures with operational modal analysis: Two case studies". In: *Mechanical Systems and Signal Processing* 24.5 (July 2010), pp. 1291–1305. ISSN: 08883270. DOI: 10.1016/j.ymssp.2010.01.011.

[13] Thierry Camelbeeck et al. "The impact of the earthquake activity in Western Europe from the historical and architectural heritage records". In: *Intraplate Earthquakes* (Jan. 2012), pp. 198–230. DOI: 10.1017/CB09781139628921.009.

[14] *Deliverable 3.1 Inventory of earthquake-induced failure mechanisms related to construction types, structural elements, and materials.* Tech. rep.

[15] Luigia Binda et al. "Investigations On Historic Centers In Seismic Areas: Guidelines For The Diagnosis". In: *AIPC* 1020.PART 1 (2008), pp. 795–802. ISSN: 0094-243X. DOI: 10.1063/1.2963916. URL: https://ui.adsabs.harvard.edu/abs/2008AIPC.1020..795B/abstract.

[16] Antonino Giuffre, Tommaso Pagnoni, and Cesare Tocci. "IN-PLANE SEISMIC BEHAVIOR OF HISTORICAL MASONR Y W ALLS". In: ().

[17] Chiara Calderini, Serena Cattari, and Sergio Lagomarsino. "In-plane strength of unreinforced masonry piers". In: *Earthquake Engineering & Structural Dynamics* 38.2 (Feb. 2009), pp. 243–267. ISSN: 1096-9845. DOI: 10.1002/EQE.860. URL: https://onlinelibrary.wiley.com/doi/full/10.1002/eqe.860%20https://onlinelibrary.wiley.com/doi/abs/10.1002/eqe.860%20https://onlinelibrary.wiley.com/doi/10.1002/eqe.860.

[18] D. Addessi et al. "Modeling Approaches for Masonry Structures". In: *The Open Civil Engineering Journal* 8.1 (Nov. 2014), pp. 288–300. DOI: 10.2174/1874149501408010288.

[19] Jessica Toti, Vincenzo Gattulli, and Elio Sacco. "Nonlocal damage propagation in the dynamics of masonry elements". In: *Computers & Structures* 152 (May 2015), pp. 215–227. ISSN: 0045-7949. DOI: 10.1016/J.COMPSTRUC.2015.01.011.

[20] URL. *History | The Old Church*. URL: https://www.hetoudekerkje.nl/historie/.

[21] *Old Kerkje - Google Maps*. URL: https://www.google.com/maps/place/Old+Kerkje/@53.3106066,6.7569307,17z/data=!3m1!4b1!4m5!3m4!1s0x47c9d6f3a7fa7c6b:0x866032ba937a5041!8m2!3d53.3106066!4d6.7591194.

[22] *Library of Articles | DIANA FEA*. URL: https://dianafea.com/index.php/article-library.

[23] *10.8.4 CQ40S - quadrilateral, 8 nodes*. URL: https://dianafea.com/manuals/d944/ElmLib/node288.html.

[24] *10.8.3 CT30S - triangle, 6 nodes*. URL: https://dianafea.com/manuals/d944/ElmLib/node287.html.

[25] Jan G. Rots et al. "Multi-Scale Approach towards Groningen Masonry and Induced Seismicity". In: *Key Engineering Materials* 747 (2017), pp. 653–661. ISSN: 1662-9795. DOI: 10.4028/WWW.SCIENTIFIC.NET/KEM.747.653. URL: https://www.scientific.net/KEM.747.653.

7

[26] Paul A ; Korswagen et al. "Crack initiation and propagation in unreinforced masonry specimens subjected to repeated in-plane loading during light damage". In: (). DOI: 10.1007/s10518-018-00553-5. URL: https://doi.org/10.1007/s10518-018-00553-5.

[27] Adarsha Kadaba Srinivasan. *Seismic assessment of a de-tached masonry building using non-linear analyses*. Tech. rep.

[28] Ivan Giongo et al. "Detailed seismic assessment and improvement procedure for vintage flexible timber diaphragms". In: *Bulletin of the New Zealand Society for Earthquake Engineering* 47.2 (2014), pp. 97–118. ISSN: 11749857. DOI: 10.5459/bnzsee.47.2.97-118.

[29] Michele Mirra, Geert Ravenshorst, and Jan Willem van de Kuilen. "Experimental and analytical evaluation of the in-plane behaviour of as-built and strengthened traditional wooden floors". In: *Engineering Structures* 211 (May 2020), p. 110432. ISSN: 18737323. DOI: 10.1016/j.engstruct.2020.110432.

[30] Michele Mirra et al. "An analytical model describing the in-plane behaviour of timber diaphragms strengthened with plywood panels". In: *Engineering Structures* 235 (May 2021), p. 112128. ISSN: 18737323. DOI: 10.1016/j.engstruct.2021.112128.

[31] null null null. "Seismic Evaluation and Retrofit of Existing Buildings". In: *Seismic Evaluation and Retrofit of Existing Buildings* (May 2014). DOI: 10.1061/9780784412855. URL: https://ascelibrary.org/doi/10.1061/9780784412855.

[32] Ivan Giongo et al. "Detailed seismic assessment and improvement procedure for vintage flexible timber diaphragms". In: *Bulletin of the New Zealand Society for Earthquake Engineering* 47.2 (2014), pp. 97–118. DOI: 10.5459/BNZSEE.47.2.97-118.

[33] Eurocode 1. *EN 1991-1-1: Eurocode 1: Actions on structures - Part 1-1: General actions - Densities, self-weight, imposed loads for buildings*. Tech. rep. 1991.

[34] *Eigenfrequencies - an overview | ScienceDirect Topics*. URL: https://www.sciencedirect.com/topics/engineering/eigenfrequencies.

[35] Dimitris Dais et al. "Monitoring, Assessment and Diagnosis of Fraeylemaborg in Groningen, Netherlands". In: *RILEM Bookseries* 18 (2019), pp. 2188–2196. ISSN: 22110852. DOI: 10.1007/978-3-319-99441-3{_}235. URL: https://doi.org/10.1007/978-3-319-99441-3_235.

[36] "CAVITY WALLS Design Guide for Taller Cavity Walls". In: ().

[37] F. Messali et al. "Large-scale testing program for the seismic characterization of Dutch masonry walls." In: *16th World Conference on Earthquake : Santiago, Chile* (2017). URL: https://repository.tudelft.nl/islandora/object/uuid%3A7f4baaa0-b1d4-49ad-b41c-584f324c102e.

[38] "Infrastructure Products". In: (). URL: www.enidine.com..

[39] *14.1.4 SP2TR - translation, 2 nodes*. URL: https://dianafea.com/manuals/d101/ElmLib/node409.html.

7

LIST OF FIGURES

7

7

LIST OF TABLES

7

A

ANNEX A: TECHNICAL DRAWINGS OF CASE-STUDY

This chapter includes the detailed drawings of The case study: Het Oude Kerkje, Garrelsweer before & after Structural Modifications as a part of the retrofitting measures taken in July,2018.
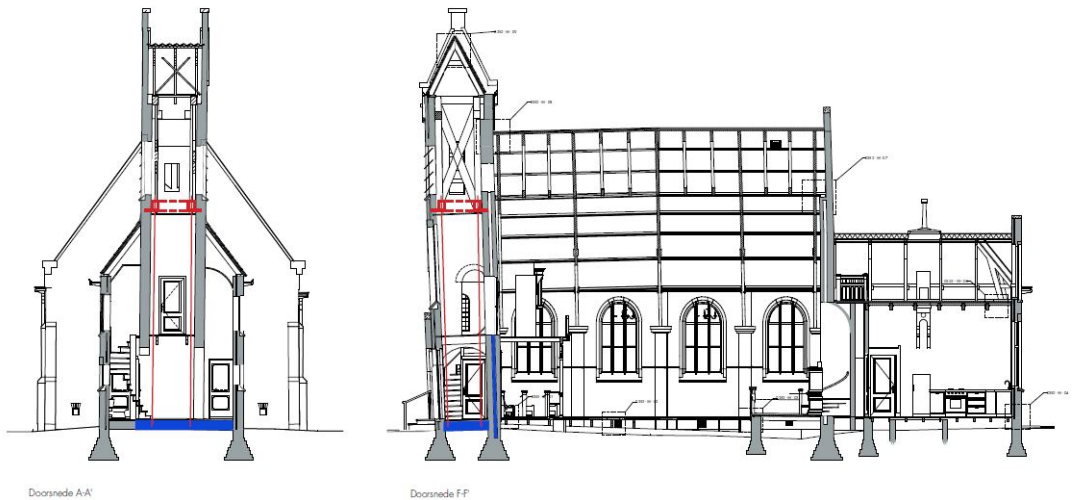
Figure A.1: Structural Modifications of the Case Study: The Old Church

A steel frame is installed at the bell tower upto the first level to control the sway of the tower.Two Linear damping devices (LD-740 series) were installed in between the

bell-tower and the connecting roof structure. Concrete slab is laid at the ground level of the tower/entrance while installing the steel frame. These modifications are clearly indicated in the below figures.
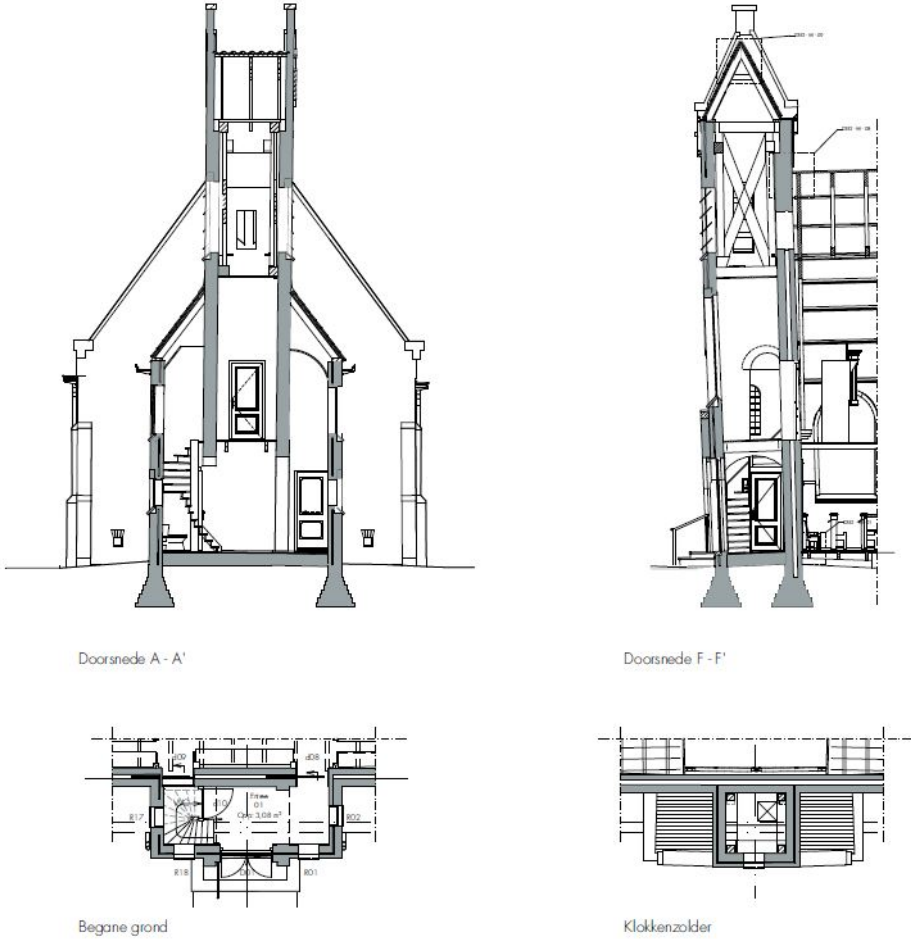
Figure A.2: Main Facade and Bell tower before structural modifications(Front View,side view, Top view- ground level, Top view-first level/clock loft respectively clockwise)

Doorsnede A - A'

Schuifdeur van richting veranderen

Doorsnede F - F'

Stalen kolommen in de hoeken van de toren.
Bevestigen aan het metselwerk H.o.H. 500 mm
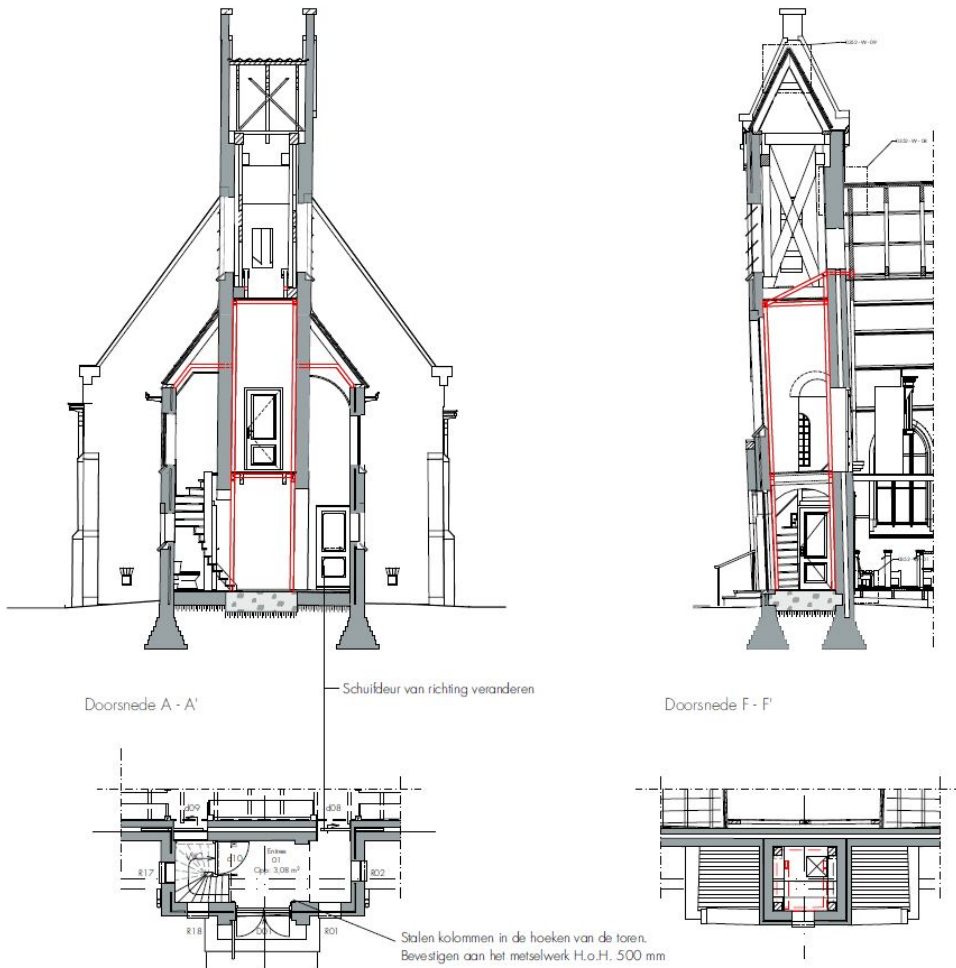
Figure A.3: Main Facade and Bell tower after structural modifications- Installation of steel framework (Front View,side view, Top view- ground level, Top view-first level/clock loft respectively clockwise)
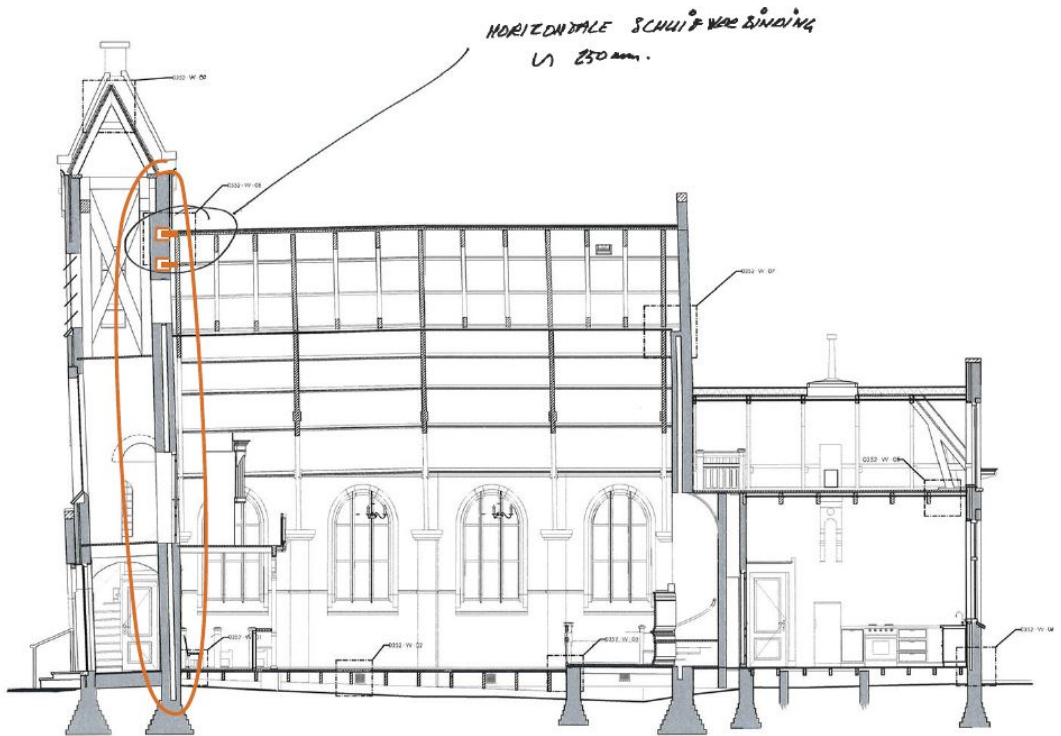
Figure A.4: Disconnected tower due to cavity wall(indicated by orange)

ARCADIS

Ontwerp versterkingen
9918_PK_31 Stadsweg 31 te Garrelsweer
11-07-2018

evenwijdig aan spant randbalk verankeren aan
spouwmuur d.m.v. boorankers M10, h.o.h. 500 mm

bestaande oplegging
behouden

kolom ∅ 70~70~4 (S235)

(bestaande) kolom ∅ 90 (hout)

(bestaande) kolom ∅ 90 (hout)

kolom ∅ 70~70~4 (S235)

bestaande oplegging
behouden

1e Verdiepingsvloer
(schaal 1:50)

UNP240

∅ 90-90-7

∅ 90-50-6

∅ 90-90-6

Figure A.5: Floor Plan of the case study - indicating the cavity walls in both facade and lateral walls, placement of new Timber columns & steel frame
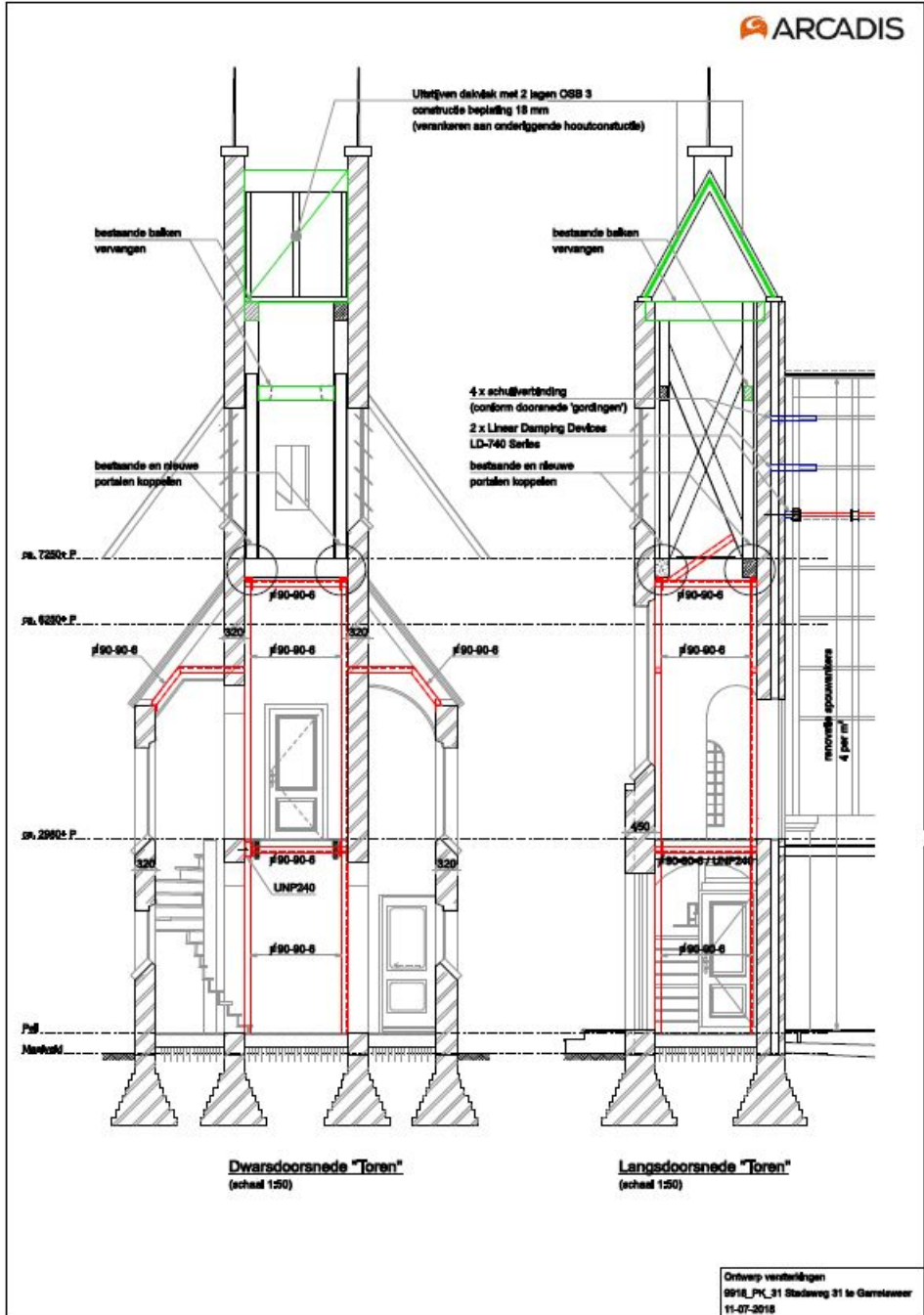
Figure A.6: Cross-sectional details of steel frame in Bell-tower
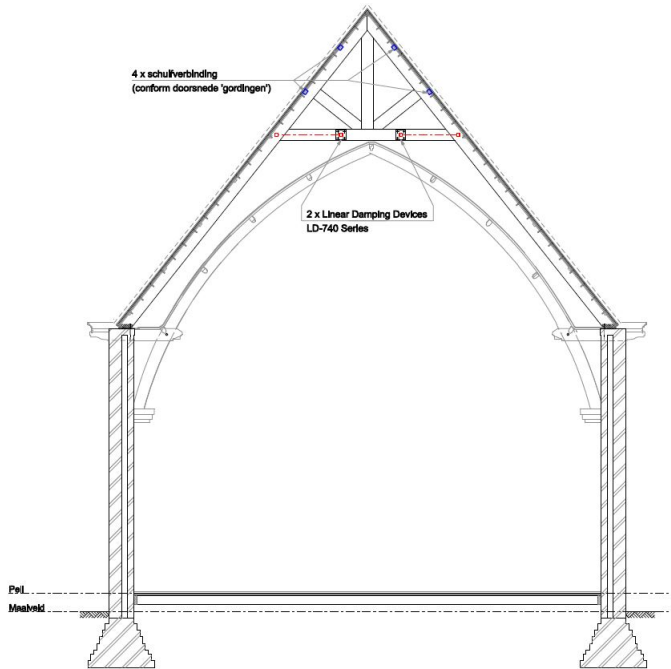
(a) Structural modifications of main Roof-structure
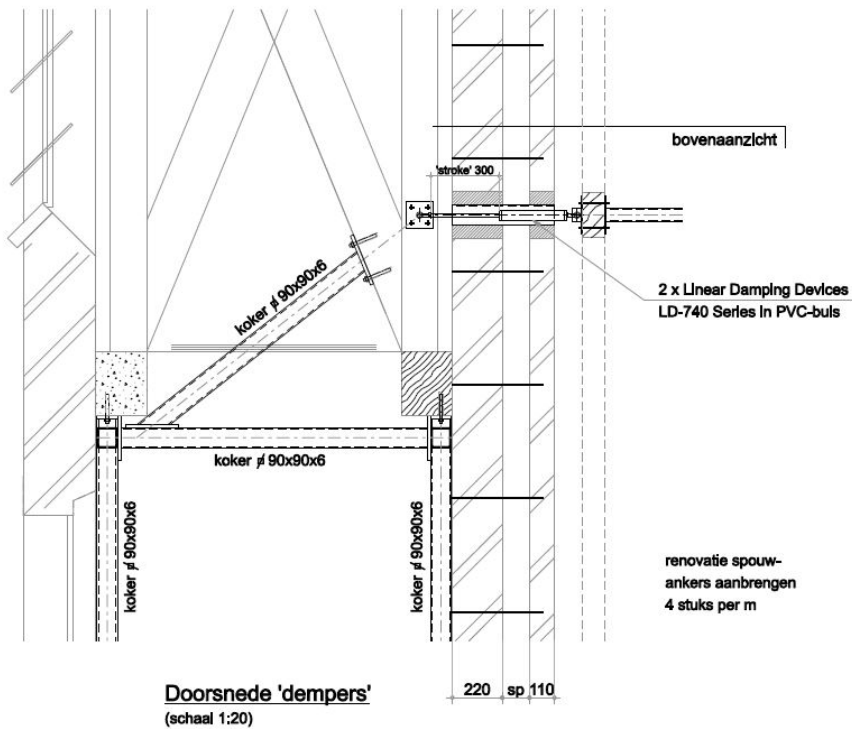
(b) Placement of Linear Damping Devices

Figure A.7: Case Study:The Old Church- Linear Damping devices
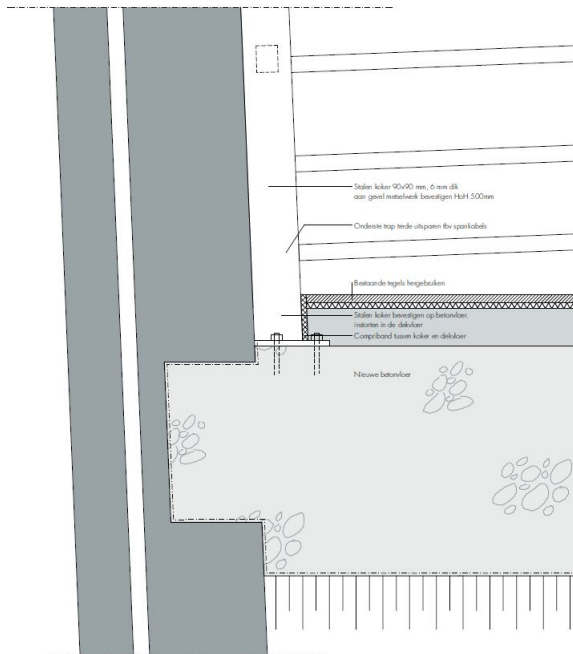
Figure A.8: Layer of New Concrete slab below the ground level of bell-tower (approximate thickness =100mm)
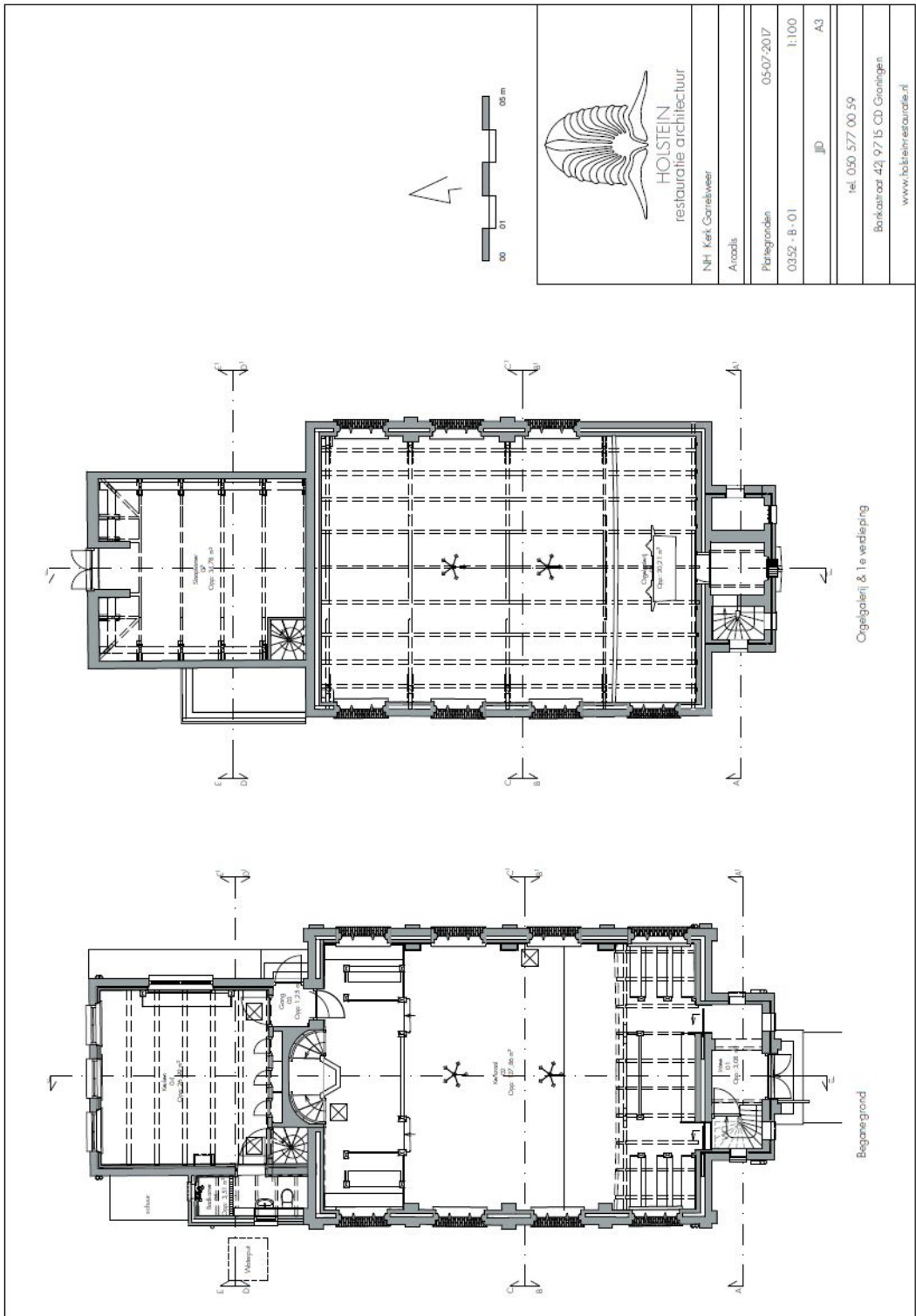
Figure A.9: Floor Plan of the case study indicating the timber joists in the roof

A
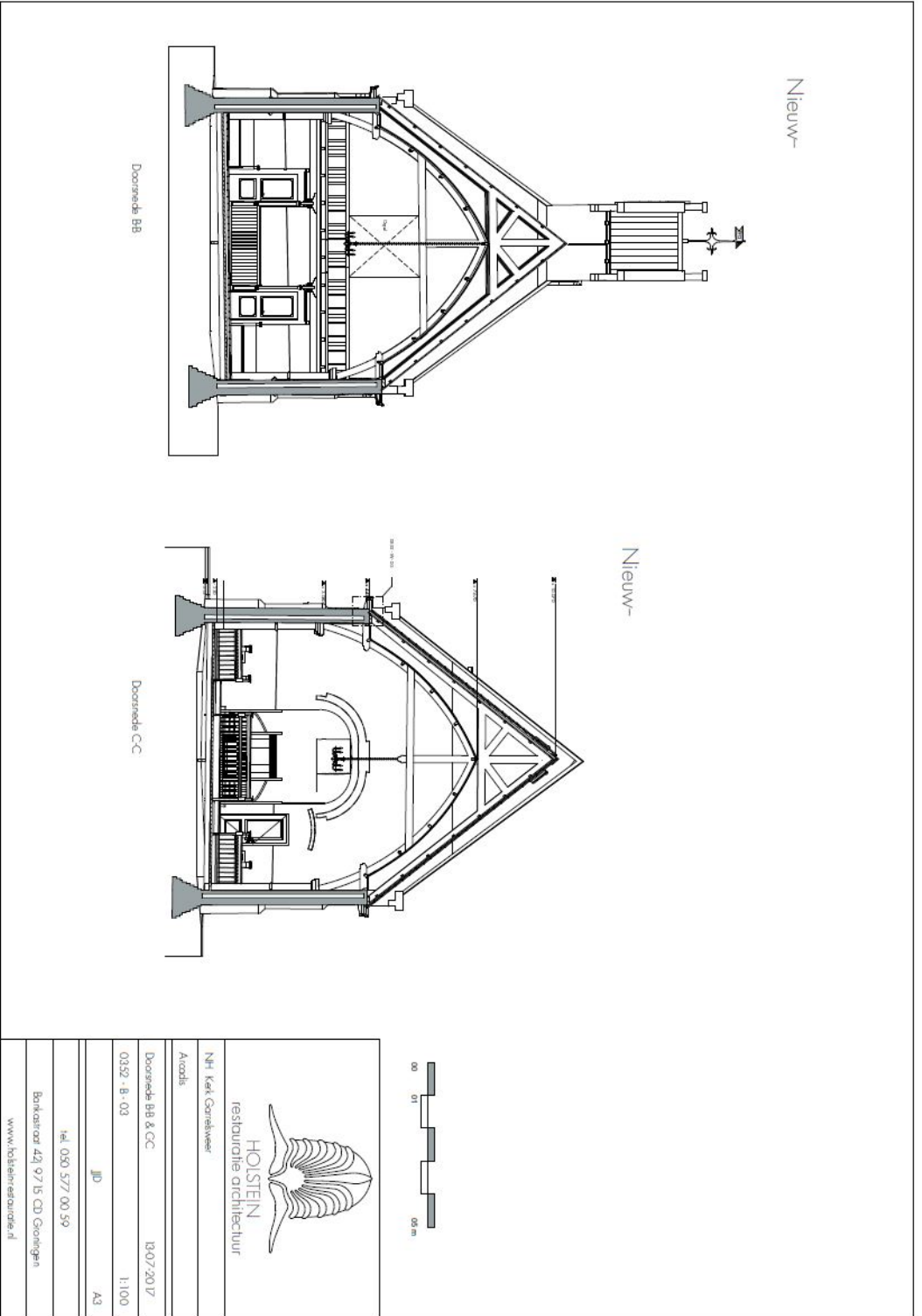
Figure A.10: Elevation of Case Study- Z section

Oud-

Oud-
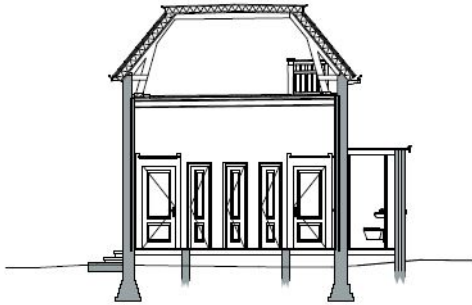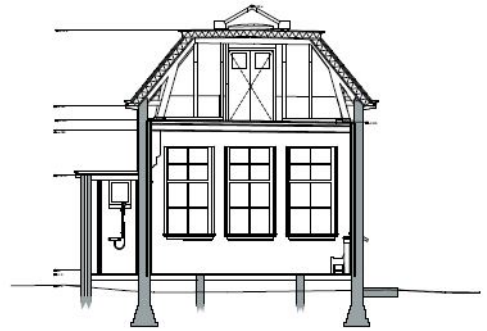
Doorsnede D-D

Doorsnede E-E

Figure A.11: Elevation of Sub-Structure -Z section
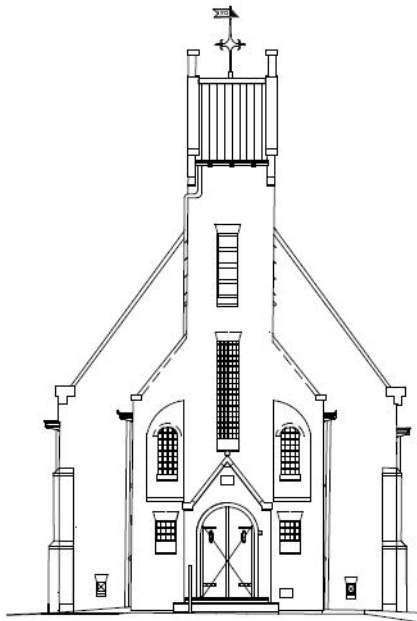
Zuidgevel
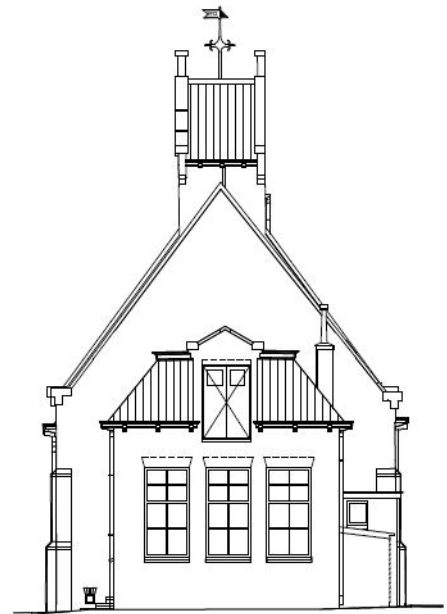
Noordgevel

Figure A.12: Elevation of the case-study (front and back view)

B

ANNEX-B: DEAD LOAD CALCULATIONS

This Annex presents the Dead Load calculations in all the Modelling variations

B.1. CHARACTERISTIC LOAD CALCULATIONS

All the Modelling Variations 1-10 have additional characteristic load acting on the roof and floor systems according to the Eurocode 8.

FLOOR-SYSTEMS:

According to Table 6.2, Eurocode 1 1991-1-1 the characteristic loads on the floor systems in addition to the self weight of the Timber diaphragms and the timber joists are

Imposed Loads on floors $q_k = 4.0 kN/m^2$

Dead Load on the floors $q_k = 2kN/m^2$

Total Additional Loading on floor systems $Q_k = 6kN/m^2$

Example of load calculation - Floor 1 in Fig B.1

Area of Cross-section of Floor 1= 12300 mm x 9000 mm

thickness of timber diaphragm =30 mm

Total Characteristic load $Q_k = 6000 N/m^2$

Total Load acting Normally (-Z) on the Timber Joists:

$$W_1 = 6000 x 12.3 x 9 = 664.2 kN$$

$$Load\,acting\,per\,unit\,length\,of\,the\,floor\,[w_1] = 54 N/mm$$
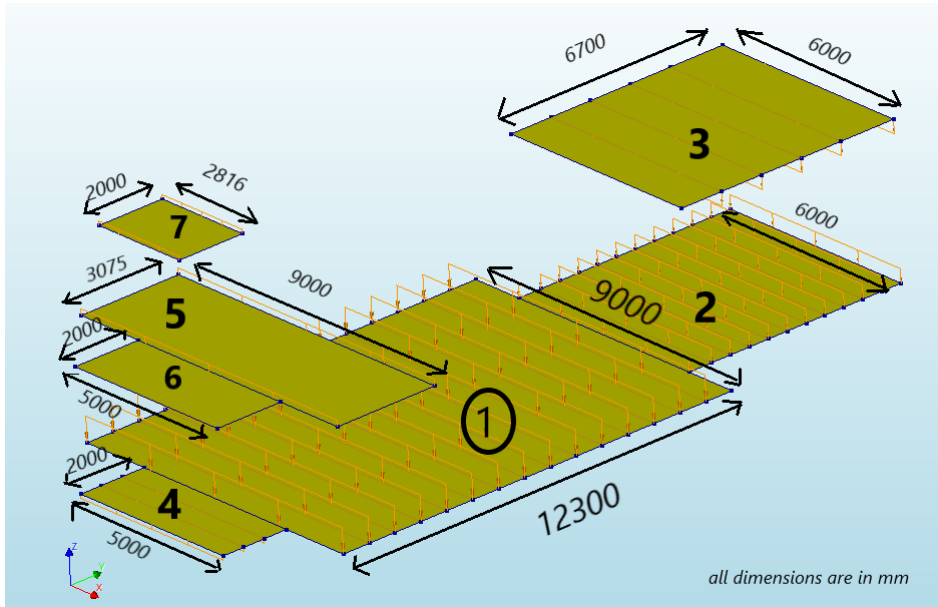
Figure B.1: Loading on Floor Systems

Similarly for all the floor systems 1-7, the additional characteristic load acting per unit length (N/mm) normally (-Z) on the timber joists is:
Characteristic Load/ unit length of Floor 2[w_2] =36 N/mm
Characteristic Load/ unit length of Floor 3[w_3] =36 N/mm
Characteristic Load/ unit length of Floor 4[w_4] =30 N/mm
Characteristic Load/ unit length of Floor 5[w_5] =54 N/mm
Characteristic Load/ unit length of Floor 6[w_6] =30 N/mm
Characteristic Load/ unit length of Floor 7[w_7] =16.896 N/mm

CHARACTERISTIC LOADING ON STAIRS:
From the Technical drawings of the Case-study A, there are 2 flights of stairs - one in the bell-tower and one in the substructure. It is assumed that the additional characteristic loading of the stairs acts on the floor systems, divided equally between floors where the stairs are located.
Hence the additional loading of Stairs in the bell-tower is divided equally between floors 4, 6. The additional loading of stairs in the substructure is divided equally between floors 2, 3.
Additional Imposed Load on the stairs $q_k = 4kN/m^2$
Characteristic load of the stairs acting on Floors 4, 6 =20 N/mm
Characteristic load of the stairs acting on Floors 2,3= 24 N/mm

ROOF-SYSTEMS:

The Characteristic load on the roofs not accessible except for normal maintenance and repair (category H) from the Table 6.10 (Eurocode 1 1991-1-1) has a recommended value of $q_k = 0.4 kN/m^2$
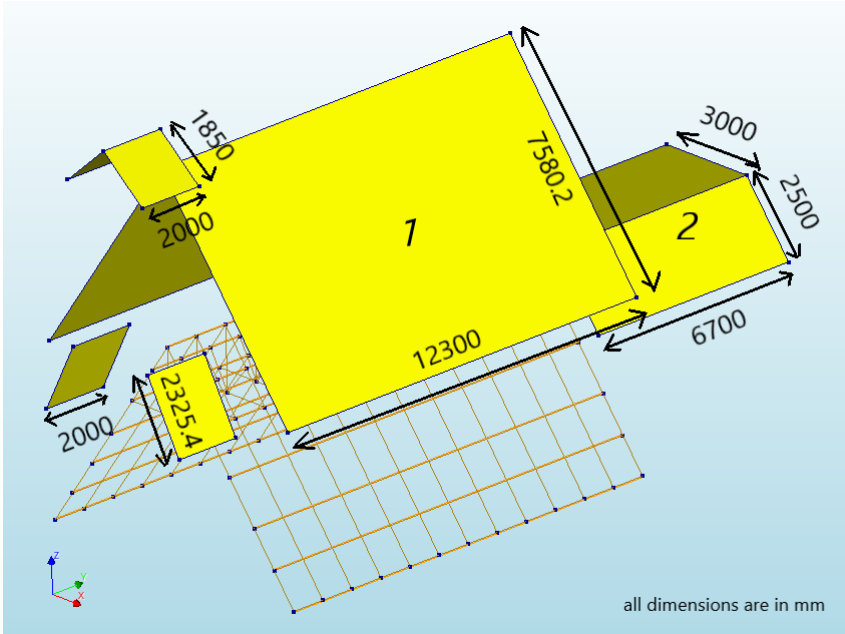
Figure B.2: Cross-sectional details of roof systems [case study]

Example of load calculation on Main Roof (1) in Fig B.2

Total additional loading on Roof 1 =0.4x12.3x7.5802 =37.29kN

Additional roof loading acting /unit length normally (-Z) on the cross beams of roof 1= 4.92N/mm.

Similarly, the additional roof loading on the cross-beams on roof 2= 3.2N/mm.

B.2. DEAD LOAD CALCULATIONS OF TIMBER DIAPHRAGMS

For Modelling Variation 1 (Model-1), as fictitious timber diaphragms are assumed, the self weight of these timber diaphragms are calculated and these loads are externally added acting normally on the timber joists.

From Fig B.1, the example calculation of self weight of floor -1 is shown below.

Density of timber diaphragms = 900 kg/m^3 =9000x 9.806 N/m^3
thickness of floor diaphragms (t)=30mm.

B

Total Weight of Floor-1 [W_1] :293.091kN

Additional loading on timber joists [w_1]= 293091.53/12300 =23.83N/mm.
Similarly,
w_2= 15.885 N/mm.
w_3= 15.885N/mm.
w_4=13.238N/mm.
w_5=23.83N/mm.
w_6=13.238N/mm.
w_7=8.141N/mm.

Similar to the Floor systems, from Fig B.2, the self weight of timber diaphragms of roof-systems can be calculated.
Self-weight acting on the cross-beams of Roof-1 = 32.56N/mm
Self weight acting on the cross-beams of Curved Roof= 35 N/mm(approximate)
Self weight acting on the cross-beams of Roof-2= 8.869 N/mm

B.3. DEAD LOAD CALCULATION OF ROOF-SYSTEMS

For Model-5,[fig 4.16] the roof is eliminated completely, hence the self weight of the Timber diaphragm roof + timber joists is externally loaded as a line load(N/mm) on the Masonry-walls of the main and the sub-structure of the case-study.
For Calculating the Self weight of Roof-systems:

Density of Timber = 9000 x 9.806 N/mm^3
Thickness of timber diaphragms = 30mm.

In additional to Self weight of timber diaphragms calculated in the previous section, the self weight of timber-joists is calculated
From Fig B.3,
Cross-section of Timber Joists 1= 241 mm x 110 mm
Cross-section of Timber Joists 2 = 241 mm x 110 mm
Cross-section of Timber Joists 3 = 95 mm x 95 mm
Cross-section of Timber Joists 4 = 95 mm x 95 mm
Cross-section of Timber Joists 5 = 100 mm x 100 mm

From Fig B.4,
Cross-section of Timber Joists 1 = 182 mm x 100 mm
Cross-section of Timber Joists 2 = 95 mm x 95 mm
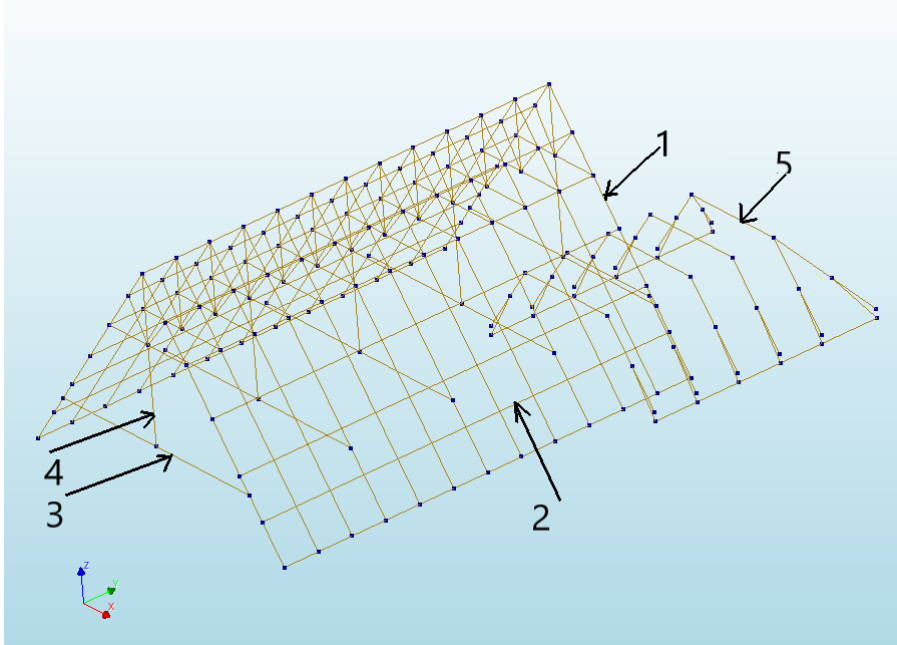
Figure B.3: Cross-sections of Timber joists in Roof-structure
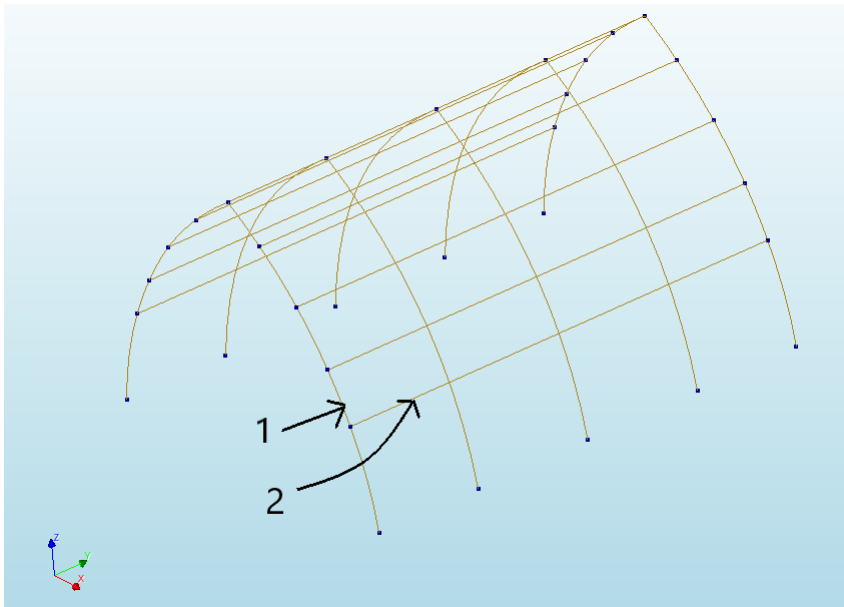
Figure B.4: Cross-section of Timber joists in Curved Roof

Considering the self-weight of both the Timber Diaphragm and Timber Joists of the roof structure, the weight of main-roof 1, Curved roof and substructure roof -2 [Fig B.2] is divided equally between the lateral masonry-walls. The line load acting normally on the center of Masonry walls is:

Line load acting on Main masonry walls (Roof 1)= 36 N/mm
Line load acting on Main masonry walls (Curved Roof)= 38 N/mm
Line load acting on Sub-structure masonry walls (Roof 2)= 67 N/mm

C

ANNEX C: EIGEN VALUE ANALYSIS-RESULTS

This chapter includes the detailed eigen-frequencies of all the modelling variations

FINITE ELEMENT MODEL-1

```
RHS-VECTORS INITIALIZED: ML=     3 ND=  490728 SF.RHSIDE
EXTER. LOAD INITIALIZED: ML=     3 ND=  490728 SF.EXTLOD
CONST.DISP. INITIALIZED: ML=     3 ND=  490728 SF.DISCON
ELEMENTLOAD TO RHS-VECT: NV=     3 SF.RHSIDE
ELEMENTLOAD TO EXT.LOAD: NV=     3 SF.EXTLOD
ELEM. STIFFNESS STORED.
CONSIST. EL.MASS STORED.
DYNAMIC STRUCTURAL MASS  TM=   0.339E+04
RHS-VECTORS INITIALIZED: ML=     3 ND=  490728 SF.RHSIDE
EXTER. LOAD INITIALIZED: ML=     3 ND=  490728 SF.EXTLOD
CONST.DISP. INITIALIZED: ML=     3 ND=  490728 SF.DISCON
ELEMENTLOAD TO RHS-VECT: NV=     3 SF.RHSIDE
ELEMENTLOAD TO EXT.LOAD: NV=     3 SF.EXTLOD
TOTAL MASS OF FE-MODEL FOR LOAD-CASE(  2): 0.36102D+03
WEIGHT LOAD R.H.S.     : NV=     3 SF.RHSIDE
WEIGHT LOAD EXTERNAL   : NV=     3 SF.EXTLOD
 SPARSE: DIM=484503 NNZ(MAT)=18784196
 SOLVE: REDUCTION RES= 0.00E+00 (INIT. RES= 0.00E+00) NI=    1
 SOLVE: REDUCTION RES= 0.18E-09 (INIT. RES= 0.32E+05) NI=    1
 SOLVE: REDUCTION RES= 0.18E-09 (INIT. RES= 0.32E+05) NI=    1
STRESS STIFFNESS STORED
 SPARSE: DIM=484503 NNZ(MAT)=18784196
EIG-VEC, FILLED->TYINGS: ND=490728 NV=   350 NT=  6222

   350 EIGENVALUES FOUND AFTER    2 ITERATIONS
```

C

```
EIGEN-FREQUENCIES:
0.23516E+00(  1)  0.24104E+00(  2)  0.25804E+00(  3)  0.38130E+00(  4)
0.38501E+00(  5)  0.38573E+00(  6)  0.38611E+00(  7)  0.39300E+00(  8)
0.39723E+00(  9)  0.39924E+00( 10)  0.40061E+00( 11)  0.40759E+00( 12)
0.40945E+00( 13)  0.41089E+00( 14)  0.41259E+00( 15)  0.42830E+00( 16)
0.46795E+00( 17)  0.48736E+00( 18)  0.50460E+00( 19)  0.50607E+00( 20)
0.52073E+00( 21)  0.59118E+00( 22)  0.59292E+00( 23)  0.69487E+00( 24)
0.74280E+00( 25)  0.82543E+00( 26)  0.96125E+00( 27)  0.10317E+01( 28)
0.10388E+01( 29)  0.10415E+01( 30)  0.10475E+01( 31)  0.10483E+01( 32)
0.10488E+01( 33)  0.10573E+01( 34)  0.10631E+01( 35)  0.10647E+01( 36)
0.10663E+01( 37)  0.10745E+01( 38)  0.10775E+01( 39)  0.10784E+01( 40)
0.10807E+01( 41)  0.10941E+01( 42)  0.11163E+01( 43)  0.11193E+01( 44)
0.11257E+01( 45)  0.11339E+01( 46)  0.11565E+01( 47)  0.12062E+01( 48)
0.12168E+01( 49)  0.12781E+01( 50)  0.13136E+01( 51)  0.13196E+01( 52)
0.13296E+01( 53)  0.13410E+01( 54)  0.13453E+01( 55)  0.13456E+01( 56)
0.13459E+01( 57)  0.13614E+01( 58)  0.13939E+01( 59)  0.13941E+01( 60)
0.14069E+01( 61)  0.14275E+01( 62)  0.14458E+01( 63)  0.14928E+01( 64)
0.15166E+01( 65)  0.15496E+01( 66)  0.15582E+01( 67)  0.15763E+01( 68)
0.15971E+01( 69)  0.16018E+01( 70)  0.16672E+01( 71)  0.16801E+01( 72)
0.17023E+01( 73)  0.17210E+01( 74)  0.17274E+01( 75)  0.17406E+01( 76)
0.17550E+01( 77)  0.18099E+01( 78)  0.18117E+01( 79)  0.18156E+01( 80)
0.18239E+01( 81)  0.18281E+01( 82)  0.18458E+01( 83)  0.18485E+01( 84)
0.18804E+01( 85)  0.18921E+01( 86)  0.19008E+01( 87)  0.19018E+01( 88)
0.19117E+01( 89)  0.19437E+01( 90)  0.19451E+01( 91)  0.19507E+01( 92)
0.19653E+01( 93)  0.19687E+01( 94)  0.19811E+01( 95)  0.19824E+01( 96)
0.19863E+01( 97)  0.19964E+01( 98)  0.20035E+01( 99)  0.20052E+01(100)
0.20063E+01(101)  0.20221E+01(102)  0.20262E+01(103)  0.20333E+01(104)
0.20338E+01(105)  0.20364E+01(106)  0.20434E+01(107)  0.20520E+01(108)
0.20528E+01(109)  0.20532E+01(110)  0.20547E+01(111)  0.20634E+01(112)
0.20669E+01(113)  0.20676E+01(114)  0.20681E+01(115)  0.20692E+01(116)
0.20703E+01(117)  0.20767E+01(118)  0.20819E+01(119)  0.20836E+01(120)
0.20994E+01(121)  0.21208E+01(122)  0.21244E+01(123)  0.21483E+01(124)
0.21706E+01(125)  0.21840E+01(126)  0.21916E+01(127)  0.21949E+01(128)
0.21982E+01(129)  0.21989E+01(130)  0.22079E+01(131)  0.22148E+01(132)
0.22404E+01(133)  0.22405E+01(134)  0.22769E+01(135)  0.22815E+01(136)
0.22887E+01(137)  0.23032E+01(138)  0.23163E+01(139)  0.23191E+01(140)
0.23327E+01(141)  0.23398E+01(142)  0.23450E+01(143)  0.23566E+01(144)
0.23634E+01(145)  0.23662E+01(146)  0.23700E+01(147)  0.23890E+01(148)
0.23916E+01(149)  0.23982E+01(150)  0.24016E+01(151)  0.24120E+01(152)
0.24154E+01(153)  0.24189E+01(154)  0.24227E+01(155)  0.24334E+01(156)
0.24339E+01(157)  0.24436E+01(158)  0.24481E+01(159)  0.24643E+01(160)
0.24811E+01(161)  0.24837E+01(162)  0.24849E+01(163)  0.24933E+01(164)
0.24972E+01(165)  0.25049E+01(166)  0.25113E+01(167)  0.25160E+01(168)
0.25223E+01(169)  0.25243E+01(170)  0.25243E+01(171)  0.25259E+01(172)
0.25292E+01(173)  0.25407E+01(174)  0.25440E+01(175)  0.25457E+01(176)
0.25521E+01(177)  0.25523E+01(178)  0.25788E+01(179)  0.25796E+01(180)

0.25864E+01(181)  0.26028E+01(182)  0.26042E+01(183)  0.26255E+01(184)
0.26354E+01(185)  0.26541E+01(186)  0.26549E+01(187)  0.26574E+01(188)
0.26682E+01(189)  0.26725E+01(190)  0.26866E+01(191)  0.26915E+01(192)
0.26996E+01(193)  0.27060E+01(194)  0.27118E+01(195)  0.27217E+01(196)
0.27516E+01(197)  0.27537E+01(198)  0.27667E+01(199)  0.27761E+01(200)
0.27880E+01(201)  0.27893E+01(202)  0.28106E+01(203)  0.28183E+01(204)
0.28309E+01(205)  0.28466E+01(206)  0.28590E+01(207)  0.28654E+01(208)
0.28671E+01(209)  0.28893E+01(210)  0.28981E+01(211)  0.29015E+01(212)
0.29260E+01(213)  0.29514E+01(214)  0.29701E+01(215)  0.29714E+01(216)
0.29872E+01(217)  0.29897E+01(218)  0.30017E+01(219)  0.30058E+01(220)
0.30153E+01(221)  0.30224E+01(222)  0.30291E+01(223)  0.30358E+01(224)
0.30431E+01(225)  0.30511E+01(226)  0.30644E+01(227)  0.30709E+01(228)
0.30814E+01(229)  0.31125E+01(230)  0.31219E+01(231)  0.31407E+01(232)
0.31415E+01(233)  0.31522E+01(234)  0.31527E+01(235)  0.31644E+01(236)
0.31990E+01(237)  0.32024E+01(238)  0.32099E+01(239)  0.32145E+01(240)
0.32179E+01(241)  0.32252E+01(242)  0.32297E+01(243)  0.32341E+01(244)
0.32411E+01(245)  0.32432E+01(246)  0.32472E+01(247)  0.32797E+01(248)
0.32822E+01(249)  0.32832E+01(250)  0.32835E+01(251)  0.32881E+01(252)
0.33144E+01(253)  0.33179E+01(254)  0.33244E+01(255)  0.33257E+01(256)
0.33264E+01(257)  0.33276E+01(258)  0.33281E+01(259)  0.33342E+01(260)
0.33391E+01(261)  0.33464E+01(262)  0.33478E+01(263)  0.33498E+01(264)
0.33517E+01(265)  0.33603E+01(266)  0.33640E+01(267)  0.33645E+01(268)
0.33673E+01(269)  0.33764E+01(270)  0.33808E+01(271)  0.33853E+01(272)
0.33909E+01(273)  0.33952E+01(274)  0.33991E+01(275)  0.34068E+01(276)
0.34215E+01(277)  0.34285E+01(278)  0.34669E+01(279)  0.34795E+01(280)
0.34802E+01(281)  0.34928E+01(282)  0.34971E+01(283)  0.35047E+01(284)
0.35231E+01(285)  0.35364E+01(286)  0.35578E+01(287)  0.35604E+01(288)
0.35716E+01(289)  0.35724E+01(290)  0.35950E+01(291)  0.36046E+01(292)
0.36171E+01(293)  0.36365E+01(294)  0.36372E+01(295)  0.36377E+01(296)
0.36631E+01(297)  0.36748E+01(298)  0.37000E+01(299)  0.37100E+01(300)
0.37153E+01(301)  0.37233E+01(302)  0.37313E+01(303)  0.37324E+01(304)
0.37689E+01(305)  0.37938E+01(306)  0.37954E+01(307)  0.37977E+01(308)
0.37980E+01(309)  0.38061E+01(310)  0.38157E+01(311)  0.38442E+01(312)
0.38714E+01(313)  0.38817E+01(314)  0.38917E+01(315)  0.39395E+01(316)
0.39428E+01(317)  0.39596E+01(318)  0.39717E+01(319)  0.39867E+01(320)
0.40117E+01(321)  0.40396E+01(322)  0.40401E+01(323)  0.40499E+01(324)
0.40592E+01(325)  0.40649E+01(326)  0.41021E+01(327)  0.41054E+01(328)
0.41071E+01(329)  0.41518E+01(330)  0.41615E+01(331)  0.41708E+01(332)
0.41716E+01(333)  0.41890E+01(334)  0.42066E+01(335)  0.42178E+01(336)
0.42312E+01(337)  0.42353E+01(338)  0.42507E+01(339)  0.42694E+01(340)
0.42856E+01(341)  0.42858E+01(342)  0.42902E+01(343)  0.42964E+01(344)
0.43031E+01(345)  0.43160E+01(346)  0.43218E+01(347)  0.43258E+01(348)
0.43566E+01(349)  0.43657E+01(350)
```

Figure C.1: Eigen Frequencies of Model-1

FINITE ELEMENT MODEL-2

```
RHS-VECTORS INITIALIZED: ML=      3 ND=  491233 SF.RHSIDE
EXTER. LOAD INITIALIZED: ML=      3 ND=  491233 SF.EXTLOD
CONST.DISP. INITIALIZED: ML=      3 ND=  491233 SF.DISCON
ELEMENTLOAD TO RHS-VECT: NV=      3 SF.RHSIDE
ELEMENTLOAD TO EXT.LOAD: NV=      3 SF.EXTLOD
ELEM. STIFFNESS STORED.
CONSIST. EL.MASS STORED.
DYNAMIC STRUCTURAL MASS  TM=   0.188E+04
RHS-VECTORS INITIALIZED: ML=      3 ND=  491233 SF.RHSIDE
EXTER. LOAD INITIALIZED: ML=      3 ND=  491233 SF.EXTLOD
CONST.DISP. INITIALIZED: ML=      3 ND=  491233 SF.DISCON
ELEMENTLOAD TO RHS-VECT: NV=      3 SF.RHSIDE
ELEMENTLOAD TO EXT.LOAD: NV=      3 SF.EXTLOD
TOTAL MASS OF FE-MODEL FOR LOAD-CASE(  2): 0.33889D+03
WEIGHT LOAD R.H.S.      : NV=      3 SF.RHSIDE
WEIGHT LOAD EXTERNAL    : NV=      3 SF.EXTLOD
 SPARSE: DIM=485005 NNZ(MAT)=18788006
 SOLVE: REDUCTION RES= 0.00E+00 (INIT. RES= 0.00E+00) NI=    1
 SOLVE: REDUCTION RES= 0.13E-09 (INIT. RES= 0.30E+05) NI=    1
 SOLVE: REDUCTION RES= 0.13E-09 (INIT. RES= 0.30E+05) NI=    1
STRESS STIFFNESS STORED
 SPARSE: DIM=485005 NNZ(MAT)=18788006
EIG-VEC, FILLED->TYINGS: ND=491233 NV=   350 NT=  6222

    350 EIGENVALUES FOUND AFTER    2 ITERATIONS
```

C

```
EIGEN-FREQUENCIES:
0.46695E+00(  1)  0.49605E+00(  2)  0.65167E+00(  3)  0.68017E+00(  4)
0.80248E+00(  5)  0.80271E+00(  6)  0.87409E+00(  7)  0.10077E+01(  8)
0.11449E+01(  9)  0.12517E+01( 10)  0.12801E+01( 11)  0.13900E+01( 12)
0.14514E+01( 13)  0.14530E+01( 14)  0.14546E+01( 15)  0.16202E+01( 16)
0.16355E+01( 17)  0.16803E+01( 18)  0.16806E+01( 19)  0.17181E+01( 20)
0.17352E+01( 21)  0.18124E+01( 22)  0.19517E+01( 23)  0.19754E+01( 24)
0.20442E+01( 25)  0.21188E+01( 26)  0.21234E+01( 27)  0.21729E+01( 28)
0.23060E+01( 29)  0.23568E+01( 30)  0.23877E+01( 31)  0.23895E+01( 32)
0.24903E+01( 33)  0.24991E+01( 34)  0.24998E+01( 35)  0.25232E+01( 36)
0.25251E+01( 37)  0.26637E+01( 38)  0.26771E+01( 39)  0.27065E+01( 40)
0.27565E+01( 41)  0.27595E+01( 42)  0.28989E+01( 43)  0.29767E+01( 44)
0.29824E+01( 45)  0.30066E+01( 46)  0.30750E+01( 47)  0.31581E+01( 48)
0.31729E+01( 49)  0.31997E+01( 50)  0.32117E+01( 51)  0.32248E+01( 52)
0.33253E+01( 53)  0.33713E+01( 54)  0.34258E+01( 55)  0.34286E+01( 56)
0.34402E+01( 57)  0.34469E+01( 58)  0.35184E+01( 59)  0.35701E+01( 60)
0.36175E+01( 61)  0.37756E+01( 62)  0.38129E+01( 63)  0.38707E+01( 64)
0.38993E+01( 65)  0.39551E+01( 66)  0.39724E+01( 67)  0.39763E+01( 68)
0.40823E+01( 69)  0.42142E+01( 70)  0.42449E+01( 71)  0.42874E+01( 72)
0.42918E+01( 73)  0.44173E+01( 74)  0.45552E+01( 75)  0.45889E+01( 76)
0.45919E+01( 77)  0.45939E+01( 78)  0.47266E+01( 79)  0.48258E+01( 80)
0.48790E+01( 81)  0.50548E+01( 82)  0.50899E+01( 83)  0.51382E+01( 84)
0.52036E+01( 85)  0.52104E+01( 86)  0.52560E+01( 87)  0.52776E+01( 88)
0.53540E+01( 89)  0.54046E+01( 90)  0.54448E+01( 91)  0.57233E+01( 92)
0.57236E+01( 93)  0.57716E+01( 94)  0.57802E+01( 95)  0.57910E+01( 96)
0.57913E+01( 97)  0.58723E+01( 98)  0.59858E+01( 99)  0.60112E+01(100)
0.60129E+01(101)  0.60450E+01(102)  0.61019E+01(103)  0.61928E+01(104)
0.62193E+01(105)  0.62202E+01(106)  0.63131E+01(107)  0.64339E+01(108)
0.65616E+01(109)  0.65747E+01(110)  0.65773E+01(111)  0.67554E+01(112)
0.67832E+01(113)  0.68263E+01(114)  0.68437E+01(115)  0.68796E+01(116)
0.68919E+01(117)  0.70116E+01(118)  0.70520E+01(119)  0.70590E+01(120)
0.70609E+01(121)  0.71279E+01(122)  0.71522E+01(123)  0.71893E+01(124)
0.72154E+01(125)  0.72499E+01(126)  0.73167E+01(127)  0.74258E+01(128)
0.74305E+01(129)  0.75493E+01(130)  0.75892E+01(131)  0.76279E+01(132)
0.76383E+01(133)  0.76574E+01(134)  0.76620E+01(135)  0.76880E+01(136)
0.77002E+01(137)  0.77161E+01(138)  0.77197E+01(139)  0.77226E+01(140)
0.77468E+01(141)  0.78107E+01(142)  0.78145E+01(143)  0.78222E+01(144)
0.78505E+01(145)  0.78566E+01(146)  0.78754E+01(147)  0.79108E+01(148)
0.79223E+01(149)  0.79335E+01(150)  0.79396E+01(151)  0.79515E+01(152)
0.79536E+01(153)  0.79589E+01(154)  0.79718E+01(155)  0.79768E+01(156)
0.79786E+01(157)  0.79838E+01(158)  0.80146E+01(159)  0.80294E+01(160)
0.80582E+01(161)  0.80598E+01(162)  0.80820E+01(163)  0.80954E+01(164)
0.81067E+01(165)  0.81139E+01(166)  0.81185E+01(167)  0.81203E+01(168)
0.81330E+01(169)  0.81724E+01(170)  0.81936E+01(171)  0.82199E+01(172)
0.82256E+01(173)  0.82318E+01(174)  0.82516E+01(175)  0.82524E+01(176)
0.82934E+01(177)  0.83463E+01(178)  0.84490E+01(179)  0.84892E+01(180)
0.85149E+01(181)  0.85706E+01(182)  0.85741E+01(183)  0.86740E+01(184)
0.87172E+01(185)  0.87236E+01(186)  0.87419E+01(187)  0.89546E+01(188)
0.89626E+01(189)  0.89673E+01(190)  0.90794E+01(191)  0.91213E+01(192)
0.91319E+01(193)  0.91910E+01(194)  0.93626E+01(195)  0.93965E+01(196)
0.94660E+01(197)  0.94806E+01(198)  0.95375E+01(199)  0.95723E+01(200)
0.97145E+01(201)  0.97181E+01(202)  0.97326E+01(203)  0.10147E+02(204)
0.10192E+02(205)  0.10320E+02(206)  0.10367E+02(207)  0.10371E+02(208)
0.10375E+02(209)  0.10376E+02(210)  0.10429E+02(211)  0.10451E+02(212)
0.10492E+02(213)  0.10500E+02(214)  0.10501E+02(215)  0.10550E+02(216)
0.10555E+02(217)  0.10594E+02(218)  0.10603E+02(219)  0.10606E+02(220)
0.10608E+02(221)  0.10706E+02(222)  0.10709E+02(223)  0.10748E+02(224)
0.10763E+02(225)  0.10851E+02(226)  0.11040E+02(227)  0.11044E+02(228)
0.11051E+02(229)  0.11149E+02(230)  0.11231E+02(231)  0.11236E+02(232)
0.11247E+02(233)  0.11268E+02(234)  0.11302E+02(235)  0.11387E+02(236)
0.11770E+02(237)  0.11780E+02(238)  0.11914E+02(239)  0.12037E+02(240)
0.12069E+02(241)  0.12251E+02(242)  0.12299E+02(243)  0.12325E+02(244)
0.12352E+02(245)  0.12470E+02(246)  0.12663E+02(247)  0.12738E+02(248)
0.12757E+02(249)  0.13084E+02(250)  0.13093E+02(251)  0.13106E+02(252)
0.13108E+02(253)  0.13110E+02(254)  0.13138E+02(255)  0.13149E+02(256)
0.13151E+02(257)  0.13195E+02(258)  0.13200E+02(259)  0.13200E+02(260)
0.13237E+02(261)  0.13247E+02(262)  0.13267E+02(263)  0.13270E+02(264)
0.13278E+02(265)  0.13279E+02(266)  0.13348E+02(267)  0.13424E+02(268)
0.13472E+02(269)  0.13559E+02(270)  0.13585E+02(271)  0.13603E+02(272)
0.13733E+02(273)  0.13734E+02(274)  0.13771E+02(275)  0.13820E+02(276)
0.13850E+02(277)  0.13945E+02(278)  0.13954E+02(279)  0.14034E+02(280)
0.14066E+02(281)  0.14087E+02(282)  0.14103E+02(283)  0.14284E+02(284)
0.14326E+02(285)  0.14400E+02(286)  0.14493E+02(287)  0.14519E+02(288)
0.14524E+02(289)  0.14592E+02(290)  0.14612E+02(291)  0.14698E+02(292)
0.14712E+02(293)  0.14783E+02(294)  0.14840E+02(295)  0.14843E+02(296)
0.14876E+02(297)  0.14928E+02(298)  0.14942E+02(299)  0.14943E+02(300)
0.15008E+02(301)  0.15100E+02(302)  0.15165E+02(303)  0.15228E+02(304)
0.15252E+02(305)  0.15283E+02(306)  0.15285E+02(307)  0.15356E+02(308)
0.15386E+02(309)  0.15422E+02(310)  0.15425E+02(311)  0.15432E+02(312)
0.15438E+02(313)  0.15455E+02(314)  0.15481E+02(315)  0.15484E+02(316)
0.15524E+02(317)  0.15582E+02(318)  0.15583E+02(319)  0.15657E+02(320)
0.15677E+02(321)  0.15711E+02(322)  0.15745E+02(323)  0.15794E+02(324)
0.15830E+02(325)  0.15839E+02(326)  0.15913E+02(327)  0.15930E+02(328)
0.16007E+02(329)  0.16038E+02(330)  0.16059E+02(331)  0.16092E+02(332)
0.16105E+02(333)  0.16109E+02(334)  0.16111E+02(335)  0.16119E+02(336)
0.16129E+02(337)  0.16139E+02(338)  0.16167E+02(339)  0.16168E+02(340)
0.16170E+02(341)  0.16193E+02(342)  0.16213E+02(343)  0.16223E+02(344)
0.16223E+02(345)  0.16318E+02(346)  0.16366E+02(347)  0.16408E+02(348)
0.16487E+02(349)  0.16529E+02(350)
```

Figure C.2: Eigen Frequencies of Model-2

FINITE ELEMENT MODEL-3

```
RHS-VECTORS INITIALIZED: ML=      3 ND=  390876 SF.RHSIDE
EXTER. LOAD INITIALIZED: ML=      3 ND=  390876 SF.EXTLOD
CONST.DISP. INITIALIZED: ML=      3 ND=  390876 SF.DISCON
ELEMENTLOAD TO RHS-VECT: NV=      3 SF.RHSIDE
ELEMENTLOAD TO EXT.LOAD: NV=      3 SF.EXTLOD
ELEM. STIFFNESS STORED.
CONSIST. EL.MASS STORED.
DYNAMIC STRUCTURAL MASS   TM=     344.
RHS-VECTORS INITIALIZED: ML=      3 ND=  390876 SF.RHSIDE
EXTER. LOAD INITIALIZED: ML=      3 ND=  390876 SF.EXTLOD
CONST.DISP. INITIALIZED: ML=      3 ND=  390876 SF.DISCON
ELEMENTLOAD TO RHS-VECT: NV=      3 SF.RHSIDE
ELEMENTLOAD TO EXT.LOAD: NV=      3 SF.EXTLOD
TOTAL MASS OF FE-MODEL FOR LOAD-CASE(  2): 0.25003D+03
WEIGHT LOAD R.H.S.      : NV=      3 SF.RHSIDE
WEIGHT LOAD EXTERNAL    : NV=      3 SF.EXTLOD
 SPARSE: DIM=386820 NNZ(MAT)=14906762
 SOLVE: REDUCTION RES= 0.00E+00 (INIT. RES= 0.00E+00) NI=    1
 SOLVE: REDUCTION RES= 0.18E-09 (INIT. RES= 0.25E+05) NI=    1
 SOLVE: REDUCTION RES= 0.18E-09 (INIT. RES= 0.25E+05) NI=    1
STRESS STIFFNESS STORED
 SPARSE: DIM=386820 NNZ(MAT)=14906762
EIG-VEC, FILLED->TYINGS: ND=390876 NV=   200 NT=  4050

    200 EIGENVALUES FOUND AFTER    2 ITERATIONS
```

C

```
EIGEN-FREQUENCIES:
0.46721E+00(  1)    0.11425E+01(  2)    0.21713E+01(  3)    0.27377E+01(  4)
0.33495E+01(  5)    0.33950E+01(  6)    0.35210E+01(  7)    0.43521E+01(  8)
0.49103E+01(  9)    0.50271E+01( 10)    0.50649E+01( 11)    0.50974E+01( 12)
0.52028E+01( 13)    0.56408E+01( 14)    0.57636E+01( 15)    0.62828E+01( 16)
0.64989E+01( 17)    0.65659E+01( 18)    0.67670E+01( 19)    0.68380E+01( 20)
0.71925E+01( 21)    0.73292E+01( 22)    0.75781E+01( 23)    0.78363E+01( 24)
0.79083E+01( 25)    0.79130E+01( 26)    0.80900E+01( 27)    0.81094E+01( 28)
0.82228E+01( 29)    0.85123E+01( 30)    0.87779E+01( 31)    0.90721E+01( 32)
0.91257E+01( 33)    0.91390E+01( 34)    0.92798E+01( 35)    0.94412E+01( 36)
0.94798E+01( 37)    0.97659E+01( 38)    0.99098E+01( 39)    0.99519E+01( 40)
0.10526E+02( 41)    0.10592E+02( 42)    0.10975E+02( 43)    0.10977E+02( 44)
0.11209E+02( 45)    0.11386E+02( 46)    0.11532E+02( 47)    0.11621E+02( 48)
0.11826E+02( 49)    0.11942E+02( 50)    0.12070E+02( 51)    0.12225E+02( 52)
0.12348E+02( 53)    0.12412E+02( 54)    0.12542E+02( 55)    0.12977E+02( 56)
0.13136E+02( 57)    0.13275E+02( 58)    0.13565E+02( 59)    0.13689E+02( 60)
0.13750E+02( 61)    0.13814E+02( 62)    0.13873E+02( 63)    0.14083E+02( 64)
0.14206E+02( 65)    0.14396E+02( 66)    0.14533E+02( 67)    0.14599E+02( 68)
0.14802E+02( 69)    0.14867E+02( 70)    0.14891E+02( 71)    0.14901E+02( 72)
0.14961E+02( 73)    0.15087E+02( 74)    0.15280E+02( 75)    0.15308E+02( 76)
0.15351E+02( 77)    0.15415E+02( 78)    0.15447E+02( 79)    0.15559E+02( 80)
0.15593E+02( 81)    0.15864E+02( 82)    0.16056E+02( 83)    0.16146E+02( 84)
0.16296E+02( 85)    0.16348E+02( 86)    0.16551E+02( 87)    0.16580E+02( 88)
0.16652E+02( 89)    0.16739E+02( 90)    0.16792E+02( 91)    0.17300E+02( 92)
0.17339E+02( 93)    0.17370E+02( 94)    0.17418E+02( 95)    0.17558E+02( 96)
0.17965E+02( 97)    0.17986E+02( 98)    0.18065E+02( 99)    0.18100E+02(100)
0.18185E+02(101)    0.18286E+02(102)    0.18308E+02(103)    0.18493E+02(104)
0.18544E+02(105)    0.18567E+02(106)    0.18630E+02(107)    0.18753E+02(108)
0.18866E+02(109)    0.19008E+02(110)    0.19138E+02(111)    0.19342E+02(112)
0.19372E+02(113)    0.19473E+02(114)    0.19508E+02(115)    0.19754E+02(116)
0.19883E+02(117)    0.19919E+02(118)    0.19987E+02(119)    0.20020E+02(120)
0.20252E+02(121)    0.20269E+02(122)    0.20318E+02(123)    0.20500E+02(124)
0.20715E+02(125)    0.20815E+02(126)    0.21086E+02(127)    0.21128E+02(128)
0.21154E+02(129)    0.21241E+02(130)    0.21332E+02(131)    0.21459E+02(132)
0.21524E+02(133)    0.21761E+02(134)    0.21770E+02(135)    0.21871E+02(136)
0.21899E+02(137)    0.21956E+02(138)    0.22362E+02(139)    0.22450E+02(140)
0.22498E+02(141)    0.22575E+02(142)    0.22592E+02(143)    0.22725E+02(144)
0.22773E+02(145)    0.22986E+02(146)    0.23020E+02(147)    0.23176E+02(148)
0.23283E+02(149)    0.23351E+02(150)    0.23444E+02(151)    0.23623E+02(152)
0.23808E+02(153)    0.24258E+02(154)    0.24355E+02(155)    0.24454E+02(156)
0.24469E+02(157)    0.24797E+02(158)    0.25017E+02(159)    0.25026E+02(160)

0.25195E+02(161)    0.25249E+02(162)    0.25312E+02(163)    0.25630E+02(164)
0.25677E+02(165)    0.25707E+02(166)    0.25739E+02(167)    0.25753E+02(168)
0.25963E+02(169)    0.26011E+02(170)    0.26137E+02(171)    0.26172E+02(172)
0.26221E+02(173)    0.26292E+02(174)    0.26337E+02(175)    0.26426E+02(176)
0.26524E+02(177)    0.26579E+02(178)    0.26679E+02(179)    0.26748E+02(180)
0.26760E+02(181)    0.26781E+02(182)    0.26794E+02(183)    0.26806E+02(184)
0.26900E+02(185)    0.26973E+02(186)    0.27004E+02(187)    0.27144E+02(188)
0.27192E+02(189)    0.27245E+02(190)    0.27339E+02(191)    0.27447E+02(192)
0.27573E+02(193)    0.27635E+02(194)    0.27744E+02(195)    0.27785E+02(196)
0.27834E+02(197)    0.27871E+02(198)    0.27917E+02(199)    0.27959E+02(200)
```

Figure C.3: Eigen Frequencies of Model-3

FINITE ELEMENT MODEL-4

```
RHS-VECTORS INITIALIZED: ML=      3 ND=  393499 SF.RHSIDE
EXTER. LOAD INITIALIZED: ML=      3 ND=  393499 SF.EXTLOD
CONST.DISP. INITIALIZED: ML=      3 ND=  393499 SF.DISCON
ELEMENTLOAD TO RHS-VECT: NV=      3 SF.RHSIDE
ELEMENTLOAD TO EXT.LOAD: NV=      3 SF.EXTLOD
ELEM. STIFFNESS STORED.
CONSIST. EL.MASS STORED.
DYNAMIC STRUCTURAL MASS   TM=     343.
RHS-VECTORS INITIALIZED: ML=      3 ND=  393499 SF.RHSIDE
EXTER. LOAD INITIALIZED: ML=      3 ND=  393499 SF.EXTLOD
CONST.DISP. INITIALIZED: ML=      3 ND=  393499 SF.DISCON
ELEMENTLOAD TO RHS-VECT: NV=      3 SF.RHSIDE
ELEMENTLOAD TO EXT.LOAD: NV=      3 SF.EXTLOD
TOTAL MASS OF FE-MODEL FOR LOAD-CASE(  2): 0.24862D+03
WEIGHT LOAD R.H.S.      : NV=      3 SF.RHSIDE
WEIGHT LOAD EXTERNAL    : NV=      3 SF.EXTLOD
 SPARSE: DIM=390105 NNZ(MAT)=15034042
 SOLVE: REDUCTION RES= 0.00E+00 (INIT. RES= 0.00E+00) NI=     1
 SOLVE: REDUCTION RES= 0.16E-09 (INIT. RES= 0.25E+05) NI=     1
 SOLVE: REDUCTION RES= 0.16E-09 (INIT. RES= 0.25E+05) NI=     1
STRESS STIFFNESS STORED
 SPARSE: DIM=390105 NNZ(MAT)=15034042

    200 EIGENVALUES FOUND AFTER    2 ITERATIONS
```

```
EIGEN-FREQUENCIES:
0.46466E+00(  1)    0.11412E+01(  2)    0.21690E+01(  3)    0.24964E+01(  4)
0.33523E+01(  5)    0.34933E+01(  6)    0.35189E+01(  7)    0.43742E+01(  8)
0.45367E+01(  9)    0.50262E+01( 10)    0.51019E+01( 11)    0.51249E+01( 12)
0.52027E+01( 13)    0.56817E+01( 14)    0.57595E+01( 15)    0.62910E+01( 16)
0.64918E+01( 17)    0.65604E+01( 18)    0.67620E+01( 19)    0.68268E+01( 20)
0.69812E+01( 21)    0.71899E+01( 22)    0.75416E+01( 23)    0.77118E+01( 24)
0.78838E+01( 25)    0.79129E+01( 26)    0.79857E+01( 27)    0.80883E+01( 28)
0.80924E+01( 29)    0.83436E+01( 30)    0.87737E+01( 31)    0.89212E+01( 32)
0.90507E+01( 33)    0.90771E+01( 34)    0.91235E+01( 35)    0.93822E+01( 36)
0.94783E+01( 37)    0.97136E+01( 38)    0.98472E+01( 39)    0.99799E+01( 40)
0.10018E+02( 41)    0.10527E+02( 42)    0.10596E+02( 43)    0.10693E+02( 44)
0.10873E+02( 45)    0.11048E+02( 46)    0.11061E+02( 47)    0.11108E+02( 48)
0.11715E+02( 49)    0.11754E+02( 50)    0.11953E+02( 51)    0.12069E+02( 52)
0.12128E+02( 53)    0.12248E+02( 54)    0.12410E+02( 55)    0.12767E+02( 56)
0.12993E+02( 57)    0.13049E+02( 58)    0.13271E+02( 59)    0.13274E+02( 60)
0.13555E+02( 61)    0.13735E+02( 62)    0.13752E+02( 63)    0.13797E+02( 64)
0.13955E+02( 65)    0.14017E+02( 66)    0.14080E+02( 67)    0.14195E+02( 68)
0.14322E+02( 69)    0.14368E+02( 70)    0.14530E+02( 71)    0.14541E+02( 72)
0.14665E+02( 73)    0.14761E+02( 74)    0.14826E+02( 75)    0.14943E+02( 76)
0.15115E+02( 77)    0.15235E+02( 78)    0.15258E+02( 79)    0.15298E+02( 80)
0.15423E+02( 81)    0.15520E+02( 82)    0.15725E+02( 83)    0.15916E+02( 84)
0.16174E+02( 85)    0.16389E+02( 86)    0.16431E+02( 87)    0.16535E+02( 88)
0.16635E+02( 89)    0.16661E+02( 90)    0.16746E+02( 91)    0.16756E+02( 92)
0.17307E+02( 93)    0.17359E+02( 94)    0.17371E+02( 95)    0.17407E+02( 96)
0.17441E+02( 97)    0.17621E+02( 98)    0.17997E+02( 99)    0.18037E+02(100)
0.18047E+02(101)    0.18071E+02(102)    0.18101E+02(103)    0.18237E+02(104)
0.18464E+02(105)    0.18485E+02(106)    0.18512E+02(107)    0.18530E+02(108)
0.18581E+02(109)    0.18801E+02(110)    0.19011E+02(111)    0.19147E+02(112)
0.19196E+02(113)    0.19331E+02(114)    0.19374E+02(115)    0.19483E+02(116)
0.19608E+02(117)    0.19691E+02(118)    0.19826E+02(119)    0.19921E+02(120)
0.19940E+02(121)    0.20007E+02(122)    0.20115E+02(123)    0.20158E+02(124)
0.20218E+02(125)    0.20422E+02(126)    0.20632E+02(127)    0.20887E+02(128)
0.20983E+02(129)    0.21149E+02(130)    0.21183E+02(131)    0.21270E+02(132)
0.21298E+02(133)    0.21375E+02(134)    0.21522E+02(135)    0.21567E+02(136)
0.21680E+02(137)    0.21749E+02(138)    0.21898E+02(139)    0.21949E+02(140)
0.22106E+02(141)    0.22362E+02(142)    0.22403E+02(143)    0.22567E+02(144)
0.22661E+02(145)    0.22693E+02(146)    0.22848E+02(147)    0.22917E+02(148)
0.22986E+02(149)    0.23097E+02(150)    0.23269E+02(151)    0.23320E+02(152)
0.23661E+02(153)    0.23747E+02(154)    0.23828E+02(155)    0.24049E+02(156)
0.24119E+02(157)    0.24192E+02(158)    0.24342E+02(159)    0.24381E+02(160)
0.24498E+02(161)    0.25191E+02(162)    0.25259E+02(163)    0.25335E+02(164)
0.25388E+02(165)    0.25503E+02(166)    0.25578E+02(167)    0.25615E+02(168)
0.25762E+02(169)    0.25829E+02(170)    0.25932E+02(171)    0.25991E+02(172)
0.26019E+02(173)    0.26181E+02(174)    0.26234E+02(175)    0.26268E+02(176)
0.26288E+02(177)    0.26364E+02(178)    0.26438E+02(179)    0.26556E+02(180)
0.26628E+02(181)    0.26640E+02(182)    0.26741E+02(183)    0.26755E+02(184)
0.26777E+02(185)    0.26790E+02(186)    0.26799E+02(187)    0.26832E+02(188)
0.26976E+02(189)    0.27005E+02(190)    0.27027E+02(191)    0.27057E+02(192)
0.27156E+02(193)    0.27397E+02(194)    0.27485E+02(195)    0.27519E+02(196)
0.27531E+02(197)    0.27606E+02(198)    0.27715E+02(199)    0.27833E+02(200)
```

Figure C.4: Eigen Frequencies of Model-4

FINITE ELEMENT MODEL-5

```
RHS-VECTORS INITIALIZED: ML=      3 ND=  216524 SF.RHSIDE
EXTER. LOAD INITIALIZED: ML=      3 ND=  216524 SF.EXTLOD
CONST.DISP. INITIALIZED: ML=      3 ND=  216524 SF.DISCON
ELEMENTLOAD TO RHS-VECT: NV=      3 SF.RHSIDE
ELEMENTLOAD TO EXT.LOAD: NV=      3 SF.EXTLOD
ELEM. STIFFNESS STORED.
CONSIST. EL.MASS STORED.
DYNAMIC STRUCTURAL MASS   TM=     695.
RHS-VECTORS INITIALIZED: ML=      3 ND=  216524 SF.RHSIDE
EXTER. LOAD INITIALIZED: ML=      3 ND=  216524 SF.EXTLOD
CONST.DISP. INITIALIZED: ML=      3 ND=  216524 SF.DISCON
ELEMENTLOAD TO RHS-VECT: NV=      3 SF.RHSIDE
ELEMENTLOAD TO EXT.LOAD: NV=      3 SF.EXTLOD
TOTAL MASS OF FE-MODEL FOR LOAD-CASE(  2): 0.22812D+03
WEIGHT LOAD R.H.S.      : NV=      3 SF.RHSIDE
WEIGHT LOAD EXTERNAL    : NV=      3 SF.EXTLOD
 SPARSE: DIM=212468 NNZ(MAT)=8203217
 SOLVE: REDUCTION RES= 0.00E+00 (INIT. RES= 0.00E+00) NI=     1
 SOLVE: REDUCTION RES= 0.76E-10 (INIT. RES= 0.25E+05) NI=     1
 SOLVE: REDUCTION RES= 0.76E-10 (INIT. RES= 0.25E+05) NI=     1
STRESS STIFFNESS STORED
 SPARSE: DIM=212468 NNZ(MAT)=8203217
EIG-VEC, FILLED->TYINGS: ND=216524 NV=   200 NT=  4050

    200 EIGENVALUES FOUND AFTER    2 ITERATIONS
```

C

C

```
EIGEN-FREQUENCIES:
0.42811E+00(  1)    0.44809E+00(  2)    0.85233E+00(  3)    0.89178E+00(  4)
0.93670E+00(  5)    0.11155E+01(  6)    0.14532E+01(  7)    0.15500E+01(  8)
0.15692E+01(  9)    0.15712E+01( 10)    0.18746E+01( 11)    0.20076E+01( 12)
0.21406E+01( 13)    0.23556E+01( 14)    0.24041E+01( 15)    0.25731E+01( 16)
0.30335E+01( 17)    0.34759E+01( 18)    0.34913E+01( 19)    0.35128E+01( 20)
0.38337E+01( 21)    0.39001E+01( 22)    0.39437E+01( 23)    0.42988E+01( 24)
0.46719E+01( 25)    0.48192E+01( 26)    0.49204E+01( 27)    0.51697E+01( 28)
0.53550E+01( 29)    0.55059E+01( 30)    0.58021E+01( 31)    0.60685E+01( 32)
0.61151E+01( 33)    0.62653E+01( 34)    0.63392E+01( 35)    0.64054E+01( 36)
0.65536E+01( 37)    0.66834E+01( 38)    0.70577E+01( 39)    0.71420E+01( 40)
0.71603E+01( 41)    0.74444E+01( 42)    0.75977E+01( 43)    0.77097E+01( 44)
0.77724E+01( 45)    0.78805E+01( 46)    0.82902E+01( 47)    0.86194E+01( 48)
0.86972E+01( 49)    0.90705E+01( 50)    0.91034E+01( 51)    0.91136E+01( 52)
0.91650E+01( 53)    0.93437E+01( 54)    0.93801E+01( 55)    0.94388E+01( 56)
0.94464E+01( 57)    0.98342E+01( 58)    0.10154E+02( 59)    0.10253E+02( 60)
0.10259E+02( 61)    0.10278E+02( 62)    0.10907E+02( 63)    0.11030E+02( 64)
0.11031E+02( 65)    0.11047E+02( 66)    0.11436E+02( 67)    0.11476E+02( 68)
0.11586E+02( 69)    0.11652E+02( 70)    0.12032E+02( 71)    0.12057E+02( 72)
0.12152E+02( 73)    0.12646E+02( 74)    0.12721E+02( 75)    0.12730E+02( 76)
0.12904E+02( 77)    0.12914E+02( 78)    0.13141E+02( 79)    0.13215E+02( 80)
0.13417E+02( 81)    0.13545E+02( 82)    0.13659E+02( 83)    0.13712E+02( 84)
0.13842E+02( 85)    0.14049E+02( 86)    0.14272E+02( 87)    0.14397E+02( 88)
0.14427E+02( 89)    0.14482E+02( 90)    0.14710E+02( 91)    0.14807E+02( 92)
0.14901E+02( 93)    0.15094E+02( 94)    0.15219E+02( 95)    0.15326E+02( 96)
0.15540E+02( 97)    0.15593E+02( 98)    0.15689E+02( 99)    0.15825E+02(100)
0.16100E+02(101)    0.16167E+02(102)    0.16198E+02(103)    0.16369E+02(104)
0.16405E+02(105)    0.16573E+02(106)    0.16625E+02(107)    0.16652E+02(108)
0.17014E+02(109)    0.17213E+02(110)    0.17270E+02(111)    0.17277E+02(112)
0.17336E+02(113)    0.17547E+02(114)    0.17641E+02(115)    0.17750E+02(116)
0.17864E+02(117)    0.17906E+02(118)    0.17996E+02(119)    0.18068E+02(120)
0.18111E+02(121)    0.18162E+02(122)    0.18478E+02(123)    0.18770E+02(124)
0.18875E+02(125)    0.18917E+02(126)    0.18935E+02(127)    0.19092E+02(128)
0.19245E+02(129)    0.19501E+02(130)    0.19851E+02(131)    0.19907E+02(132)
0.19918E+02(133)    0.19970E+02(134)    0.20062E+02(135)    0.20116E+02(136)
0.20179E+02(137)    0.20216E+02(138)    0.20385E+02(139)    0.20907E+02(140)
0.20967E+02(141)    0.21082E+02(142)    0.21330E+02(143)    0.21478E+02(144)
0.21519E+02(145)    0.21592E+02(146)    0.21660E+02(147)    0.21715E+02(148)
0.21753E+02(149)    0.21814E+02(150)    0.21895E+02(151)    0.21944E+02(152)
0.22518E+02(153)    0.22640E+02(154)    0.22878E+02(155)    0.22985E+02(156)
0.23304E+02(157)    0.23418E+02(158)    0.23469E+02(159)    0.23493E+02(160)
0.23561E+02(161)    0.23865E+02(162)    0.23940E+02(163)    0.24082E+02(164)
0.24156E+02(165)    0.24249E+02(166)    0.24376E+02(167)    0.24435E+02(168)
0.24546E+02(169)    0.24886E+02(170)    0.25003E+02(171)    0.25195E+02(172)
0.25223E+02(173)    0.25255E+02(174)    0.25445E+02(175)    0.25481E+02(176)
0.25502E+02(177)    0.25532E+02(178)    0.25673E+02(179)    0.25753E+02(180)
0.25790E+02(181)    0.25880E+02(182)    0.25939E+02(183)    0.25963E+02(184)
0.25985E+02(185)    0.26160E+02(186)    0.26364E+02(187)    0.26549E+02(188)
0.26605E+02(189)    0.26737E+02(190)    0.26868E+02(191)    0.27123E+02(192)
0.27236E+02(193)    0.27268E+02(194)    0.27376E+02(195)    0.27415E+02(196)
0.27518E+02(197)    0.27573E+02(198)    0.27716E+02(199)    0.27755E+02(200)
```

Figure C.5: Eigen Frequencies of Model-5

FINITE ELEMENT MODEL-6

```
RHS-VECTORS INITIALIZED: ML=      3 ND=  503493 SF.RHSIDE
EXTER. LOAD INITIALIZED: ML=      3 ND=  503493 SF.EXTLOD
CONST.DISP. INITIALIZED: ML=      3 ND=  503493 SF.DISCON
ELEMENTLOAD TO RHS-VECT: NV=      3 SF.RHSIDE
ELEMENTLOAD TO EXT.LOAD: NV=      3 SF.EXTLOD
ELEM. STIFFNESS STORED.
CONSIST. EL.MASS STORED.
DYNAMIC STRUCTURAL MASS  TM=   0.263E+05
RHS-VECTORS INITIALIZED: ML=      3 ND=  503493 SF.RHSIDE
EXTER. LOAD INITIALIZED: ML=      3 ND=  503493 SF.EXTLOD
CONST.DISP. INITIALIZED: ML=      3 ND=  503493 SF.DISCON
ELEMENTLOAD TO RHS-VECT: NV=      3 SF.RHSIDE
ELEMENTLOAD TO EXT.LOAD: NV=      3 SF.EXTLOD
TOTAL MASS OF FE-MODEL FOR LOAD-CASE(  2): 0.34643D+03
WEIGHT LOAD R.H.S.     : NV=      3 SF.RHSIDE
WEIGHT LOAD EXTERNAL   : NV=      3 SF.EXTLOD
 SPARSE: DIM=497265 NNZ(MAT)=19311554
 SOLVE: REDUCTION RES= 0.00E+00 (INIT. RES= 0.00E+00) NI=     1
 SOLVE: REDUCTION RES= 0.12E-09 (INIT. RES= 0.30E+05) NI=     1
 SOLVE: REDUCTION RES= 0.12E-09 (INIT. RES= 0.30E+05) NI=     1
STRESS STIFFNESS STORED
 SPARSE: DIM=497265 NNZ(MAT)=19311554
EIG-VEC, FILLED->TYINGS: ND=503493 NV=   200 NT=  6222

    200 EIGENVALUES FOUND AFTER    2 ITERATIONS
```

```
EIGEN-FREQUENCIES:
0.49604E+00(  1)    0.65165E+00(  2)    0.68017E+00(  3)    0.80270E+00(  4)
0.80296E+00(  5)    0.87407E+00(  6)    0.95496E+00(  7)    0.10077E+01(  8)
0.11480E+01(  9)    0.12517E+01( 10)    0.12801E+01( 11)    0.13899E+01( 12)
0.14514E+01( 13)    0.14530E+01( 14)    0.14546E+01( 15)    0.14635E+01( 16)
0.16355E+01( 17)    0.16356E+01( 18)    0.16536E+01( 19)    0.16803E+01( 20)
0.16838E+01( 21)    0.17182E+01( 22)    0.17550E+01( 23)    0.18131E+01( 24)
0.19093E+01( 25)    0.19517E+01( 26)    0.19754E+01( 27)    0.20186E+01( 28)
0.20442E+01( 29)    0.21187E+01( 30)    0.21231E+01( 31)    0.23061E+01( 32)
0.23568E+01( 33)    0.23877E+01( 34)    0.23895E+01( 35)    0.24660E+01( 36)
0.24903E+01( 37)    0.24985E+01( 38)    0.24991E+01( 39)    0.25016E+01( 40)
0.25232E+01( 41)    0.25252E+01( 42)    0.25881E+01( 43)    0.26076E+01( 44)
0.26637E+01( 45)    0.26771E+01( 46)    0.27312E+01( 47)    0.27565E+01( 48)
0.27580E+01( 49)    0.28989E+01( 50)    0.29192E+01( 51)    0.29617E+01( 52)
0.29767E+01( 53)    0.29822E+01( 54)    0.30066E+01( 55)    0.30750E+01( 56)
0.31581E+01( 57)    0.32028E+01( 58)    0.32118E+01( 59)    0.32261E+01( 60)
0.32536E+01( 61)    0.33176E+01( 62)    0.33249E+01( 63)    0.33666E+01( 64)
0.33713E+01( 65)    0.33840E+01( 66)    0.34259E+01( 67)    0.34277E+01( 68)
0.34403E+01( 69)    0.34471E+01( 70)    0.35702E+01( 71)    0.37434E+01( 72)
0.37436E+01( 73)    0.37757E+01( 74)    0.37991E+01( 75)    0.38943E+01( 76)
0.39091E+01( 77)    0.39444E+01( 78)    0.39550E+01( 79)    0.39725E+01( 80)
0.39761E+01( 81)    0.40513E+01( 82)    0.40823E+01( 83)    0.42143E+01( 84)
0.42449E+01( 85)    0.42875E+01( 86)    0.42916E+01( 87)    0.43934E+01( 88)
0.44174E+01( 89)    0.44555E+01( 90)    0.45553E+01( 91)    0.45920E+01( 92)
0.45935E+01( 93)    0.45972E+01( 94)    0.46068E+01( 95)    0.46813E+01( 96)
0.47267E+01( 97)    0.47594E+01( 98)    0.49494E+01( 99)    0.49687E+01(100)
0.50201E+01(101)    0.50778E+01(102)    0.50943E+01(103)    0.52029E+01(104)
0.52561E+01(105)    0.52934E+01(106)    0.53420E+01(107)    0.54044E+01(108)
0.54047E+01(109)    0.54207E+01(110)    0.54452E+01(111)    0.54895E+01(112)
0.57234E+01(113)    0.57236E+01(114)    0.57786E+01(115)    0.57802E+01(116)
0.57911E+01(117)    0.57913E+01(118)    0.58724E+01(119)    0.59375E+01(120)
0.59858E+01(121)    0.60113E+01(122)    0.60128E+01(123)    0.60269E+01(124)
0.60451E+01(125)    0.60795E+01(126)    0.61020E+01(127)    0.61929E+01(128)
0.62194E+01(129)    0.62200E+01(130)    0.63019E+01(131)    0.63207E+01(132)
0.63763E+01(133)    0.64968E+01(134)    0.65753E+01(135)    0.65775E+01(136)
0.66281E+01(137)    0.66350E+01(138)    0.67274E+01(139)    0.67852E+01(140)
0.68606E+01(141)    0.68987E+01(142)    0.69488E+01(143)    0.69671E+01(144)
0.70116E+01(145)    0.70520E+01(146)    0.70598E+01(147)    0.70618E+01(148)
0.70641E+01(149)    0.71064E+01(150)    0.71279E+01(151)    0.71925E+01(152)
0.72499E+01(153)    0.72821E+01(154)    0.73086E+01(155)    0.73139E+01(156)
0.74000E+01(157)    0.74259E+01(158)    0.74342E+01(159)    0.74725E+01(160)
0.75718E+01(161)    0.75892E+01(162)    0.76280E+01(163)    0.76296E+01(164)
0.76575E+01(165)    0.76613E+01(166)    0.76982E+01(167)    0.77003E+01(168)
0.77161E+01(169)    0.77173E+01(170)    0.77199E+01(171)    0.77642E+01(172)
0.78073E+01(173)    0.78146E+01(174)    0.78258E+01(175)    0.78435E+01(176)
0.78520E+01(177)    0.78546E+01(178)    0.78606E+01(179)    0.79076E+01(180)
0.79136E+01(181)    0.79249E+01(182)    0.79337E+01(183)    0.79351E+01(184)
0.79543E+01(185)    0.79632E+01(186)    0.79639E+01(187)    0.79787E+01(188)
0.80191E+01(189)    0.80365E+01(190)    0.80587E+01(191)    0.80665E+01(192)
0.80820E+01(193)    0.80887E+01(194)    0.81025E+01(195)    0.81331E+01(196)
0.81364E+01(197)    0.81449E+01(198)    0.81672E+01(199)    0.81798E+01(200)
```

Figure C.6: Eigen Frequencies of Model-6

FINITE ELEMENT MODEL-7

```
RHS-VECTORS INITIALIZED: ML=      3 ND=  503403 SF.RHSIDE
EXTER. LOAD INITIALIZED: ML=      3 ND=  503403 SF.EXTLOD
CONST.DISP. INITIALIZED: ML=      3 ND=  503403 SF.DISCON
ELEMENTLOAD TO RHS-VECT: NV=      3 SF.RHSIDE
ELEMENTLOAD TO EXT.LOAD: NV=      3 SF.EXTLOD
ELEM. STIFFNESS STORED.
CONSIST. EL.MASS STORED.
DYNAMIC STRUCTURAL MASS  TM=   0.263E+05
RHS-VECTORS INITIALIZED: ML=      3 ND=  503403 SF.RHSIDE
EXTER. LOAD INITIALIZED: ML=      3 ND=  503403 SF.EXTLOD
CONST.DISP. INITIALIZED: ML=      3 ND=  503403 SF.DISCON
ELEMENTLOAD TO RHS-VECT: NV=      3 SF.RHSIDE
ELEMENTLOAD TO EXT.LOAD: NV=      3 SF.EXTLOD
TOTAL MASS OF FE-MODEL FOR LOAD-CASE(  2): 0.34643D+03
WEIGHT LOAD R.H.S.      : NV=      3 SF.RHSIDE
WEIGHT LOAD EXTERNAL    : NV=      3 SF.EXTLOD
 SPARSE: DIM=497175 NNZ(MAT)=19307959
 SOLVE: REDUCTION RES= 0.00E+00 (INIT. RES= 0.00E+00) NI=    1
 SOLVE: REDUCTION RES= 0.11E-09 (INIT. RES= 0.30E+05) NI=    1
 SOLVE: REDUCTION RES= 0.11E-09 (INIT. RES= 0.30E+05) NI=    1
STRESS STIFFNESS STORED
 SPARSE: DIM=497175 NNZ(MAT)=19307959
EIG-VEC, FILLED->TYINGS: ND=503403 NV=   200 NT=  6222

    200 EIGENVALUES FOUND AFTER    2 ITERATIONS
```

C

```
EIGEN-FREQUENCIES:
0.49604E+00(  1)    0.65165E+00(  2)    0.68017E+00(  3)    0.80273E+00(  4)
0.80296E+00(  5)    0.87407E+00(  6)    0.95496E+00(  7)    0.10077E+01(  8)
0.11480E+01(  9)    0.12517E+01( 10)    0.12801E+01( 11)    0.13899E+01( 12)
0.14514E+01( 13)    0.14530E+01( 14)    0.14546E+01( 15)    0.14635E+01( 16)
0.16355E+01( 17)    0.16356E+01( 18)    0.16536E+01( 19)    0.16803E+01( 20)
0.16838E+01( 21)    0.17182E+01( 22)    0.17550E+01( 23)    0.18131E+01( 24)
0.19093E+01( 25)    0.19517E+01( 26)    0.19754E+01( 27)    0.20186E+01( 28)
0.20442E+01( 29)    0.21188E+01( 30)    0.21231E+01( 31)    0.23061E+01( 32)
0.23568E+01( 33)    0.23877E+01( 34)    0.23895E+01( 35)    0.24660E+01( 36)
0.24903E+01( 37)    0.24985E+01( 38)    0.24991E+01( 39)    0.25016E+01( 40)
0.25232E+01( 41)    0.25252E+01( 42)    0.25881E+01( 43)    0.26076E+01( 44)
0.26637E+01( 45)    0.26771E+01( 46)    0.27312E+01( 47)    0.27566E+01( 48)
0.27580E+01( 49)    0.28989E+01( 50)    0.29192E+01( 51)    0.29617E+01( 52)
0.29768E+01( 53)    0.29822E+01( 54)    0.30066E+01( 55)    0.30750E+01( 56)
0.31581E+01( 57)    0.32028E+01( 58)    0.32118E+01( 59)    0.32261E+01( 60)
0.32536E+01( 61)    0.33176E+01( 62)    0.33249E+01( 63)    0.33666E+01( 64)
0.33713E+01( 65)    0.33840E+01( 66)    0.34259E+01( 67)    0.34277E+01( 68)
0.34403E+01( 69)    0.34471E+01( 70)    0.35702E+01( 71)    0.37434E+01( 72)
0.37436E+01( 73)    0.37757E+01( 74)    0.37991E+01( 75)    0.38943E+01( 76)
0.39091E+01( 77)    0.39444E+01( 78)    0.39550E+01( 79)    0.39725E+01( 80)
0.39761E+01( 81)    0.40513E+01( 82)    0.40823E+01( 83)    0.42143E+01( 84)
0.42449E+01( 85)    0.42875E+01( 86)    0.42916E+01( 87)    0.43934E+01( 88)
0.44174E+01( 89)    0.44555E+01( 90)    0.45553E+01( 91)    0.45920E+01( 92)
0.45935E+01( 93)    0.45972E+01( 94)    0.46068E+01( 95)    0.46813E+01( 96)
0.47267E+01( 97)    0.47594E+01( 98)    0.49494E+01( 99)    0.49687E+01(100)
0.50201E+01(101)    0.50778E+01(102)    0.50943E+01(103)    0.52029E+01(104)
0.52561E+01(105)    0.52934E+01(106)    0.53420E+01(107)    0.54044E+01(108)
0.54047E+01(109)    0.54207E+01(110)    0.54452E+01(111)    0.54895E+01(112)
0.57234E+01(113)    0.57236E+01(114)    0.57786E+01(115)    0.57802E+01(116)
0.57910E+01(117)    0.57913E+01(118)    0.58724E+01(119)    0.59375E+01(120)
0.59858E+01(121)    0.60113E+01(122)    0.60128E+01(123)    0.60269E+01(124)
0.60451E+01(125)    0.60795E+01(126)    0.61020E+01(127)    0.61929E+01(128)
0.62194E+01(129)    0.62200E+01(130)    0.63019E+01(131)    0.63207E+01(132)
0.63763E+01(133)    0.64968E+01(134)    0.65753E+01(135)    0.65775E+01(136)
0.66281E+01(137)    0.66350E+01(138)    0.67274E+01(139)    0.67852E+01(140)
0.68607E+01(141)    0.68988E+01(142)    0.69489E+01(143)    0.69672E+01(144)
0.70116E+01(145)    0.70520E+01(146)    0.70598E+01(147)    0.70618E+01(148)
0.70641E+01(149)    0.71064E+01(150)    0.71279E+01(151)    0.71925E+01(152)
0.72499E+01(153)    0.72821E+01(154)    0.73086E+01(155)    0.73139E+01(156)
0.74000E+01(157)    0.74259E+01(158)    0.74342E+01(159)    0.74725E+01(160)

0.75718E+01(161)    0.75892E+01(162)    0.76280E+01(163)    0.76296E+01(164)
0.76575E+01(165)    0.76613E+01(166)    0.76982E+01(167)    0.77003E+01(168)
0.77161E+01(169)    0.77174E+01(170)    0.77199E+01(171)    0.77642E+01(172)
0.78073E+01(173)    0.78146E+01(174)    0.78258E+01(175)    0.78435E+01(176)
0.78520E+01(177)    0.78546E+01(178)    0.78606E+01(179)    0.79076E+01(180)
0.79136E+01(181)    0.79249E+01(182)    0.79337E+01(183)    0.79351E+01(184)
0.79543E+01(185)    0.79632E+01(186)    0.79639E+01(187)    0.79787E+01(188)
0.80191E+01(189)    0.80365E+01(190)    0.80587E+01(191)    0.80665E+01(192)
0.80820E+01(193)    0.80887E+01(194)    0.81025E+01(195)    0.81331E+01(196)
0.81365E+01(197)    0.81449E+01(198)    0.81673E+01(199)    0.81798E+01(200)
```

Figure C.7: Eigen Frequencies of Model-7

FINITE ELEMENT MODEL-8

```
RHS-VECTORS INITIALIZED: ML=      3 ND=  503403 SF.RHSIDE
EXTER. LOAD INITIALIZED: ML=      3 ND=  503403 SF.EXTLOD
CONST.DISP. INITIALIZED: ML=      3 ND=  503403 SF.DISCON
ELEMENTLOAD TO RHS-VECT: NV=      3 SF.RHSIDE
ELEMENTLOAD TO EXT.LOAD: NV=      3 SF.EXTLOD
ELEM. STIFFNESS STORED.
CONSIST. EL.MASS STORED.
DYNAMIC STRUCTURAL MASS   TM=   0.263E+05
RHS-VECTORS INITIALIZED: ML=      3 ND=  503403 SF.RHSIDE
EXTER. LOAD INITIALIZED: ML=      3 ND=  503403 SF.EXTLOD
CONST.DISP. INITIALIZED: ML=      3 ND=  503403 SF.DISCON
ELEMENTLOAD TO RHS-VECT: NV=      3 SF.RHSIDE
ELEMENTLOAD TO EXT.LOAD: NV=      3 SF.EXTLOD
TOTAL MASS OF FE-MODEL FOR LOAD-CASE(  2): 0.32995D+03
WEIGHT LOAD R.H.S.     : NV=      3 SF.RHSIDE
WEIGHT LOAD EXTERNAL   : NV=      3 SF.EXTLOD
 SPARSE: DIM=497175 NNZ(MAT)=19307959
 SOLVE: REDUCTION RES= 0.00E+00 (INIT. RES= 0.00E+00) NI=     1
 SOLVE: REDUCTION RES= 0.14E-09 (INIT. RES= 0.29E+05) NI=     1
 SOLVE: REDUCTION RES= 0.14E-09 (INIT. RES= 0.29E+05) NI=     1
STRESS STIFFNESS STORED
 SPARSE: DIM=497175 NNZ(MAT)=19307959
EIG-VEC, FILLED->TYINGS: ND=503403 NV=    200 NT=  6222
```

```
EIGEN-FREQUENCIES:
0.48231E+00(  1)    0.62245E+00(  2)    0.66851E+00(  3)    0.79258E+00(  4)
0.79297E+00(  5)    0.84637E+00(  6)    0.85700E+00(  7)    0.99841E+00(  8)
0.10301E+01(  9)    0.11125E+01( 10)    0.12073E+01( 11)    0.12159E+01( 12)
0.12693E+01( 13)    0.13306E+01( 14)    0.13506E+01( 15)    0.14160E+01( 16)
0.14176E+01( 17)    0.14440E+01( 18)    0.15488E+01( 19)    0.15884E+01( 20)
0.16027E+01( 21)    0.16730E+01( 22)    0.16744E+01( 23)    0.17115E+01( 24)
0.17540E+01( 25)    0.17641E+01( 26)    0.18490E+01( 27)    0.19462E+01( 28)
0.19483E+01( 29)    0.20041E+01( 30)    0.20166E+01( 31)    0.20928E+01( 32)
0.20981E+01( 33)    0.20994E+01( 34)    0.22621E+01( 35)    0.22758E+01( 36)
0.23132E+01( 37)    0.23213E+01( 38)    0.23331E+01( 39)    0.23347E+01( 40)
0.23837E+01( 41)    0.23849E+01( 42)    0.24245E+01( 43)    0.24344E+01( 44)
0.24566E+01( 45)    0.24583E+01( 46)    0.24959E+01( 47)    0.24962E+01( 48)
0.25917E+01( 49)    0.26022E+01( 50)    0.26593E+01( 51)    0.27378E+01( 52)
0.27397E+01( 53)    0.28425E+01( 54)    0.28469E+01( 55)    0.28559E+01( 56)
0.29206E+01( 57)    0.29266E+01( 58)    0.29445E+01( 59)    0.29701E+01( 60)
0.30119E+01( 61)    0.30140E+01( 62)    0.30380E+01( 63)    0.31071E+01( 64)
0.31530E+01( 65)    0.32185E+01( 66)    0.33009E+01( 67)    0.33242E+01( 68)
0.33255E+01( 69)    0.33621E+01( 70)    0.33783E+01( 71)    0.33809E+01( 72)
0.33850E+01( 73)    0.34563E+01( 74)    0.34986E+01( 75)    0.35361E+01( 76)
0.36088E+01( 77)    0.36273E+01( 78)    0.36850E+01( 79)    0.37227E+01( 80)
0.37234E+01( 81)    0.37251E+01( 82)    0.37362E+01( 83)    0.38150E+01( 84)
0.38413E+01( 85)    0.38435E+01( 86)    0.39337E+01( 87)    0.39693E+01( 88)
0.40611E+01( 89)    0.41456E+01( 90)    0.41687E+01( 91)    0.41767E+01( 92)
0.41800E+01( 93)    0.41865E+01( 94)    0.41908E+01( 95)    0.42018E+01( 96)
0.42663E+01( 97)    0.43241E+01( 98)    0.44667E+01( 99)    0.44947E+01(100)
0.45010E+01(101)    0.45034E+01(102)    0.46530E+01(103)    0.46667E+01(104)
0.46862E+01(105)    0.47227E+01(106)    0.47411E+01(107)    0.49066E+01(108)
0.49378E+01(109)    0.49778E+01(110)    0.50439E+01(111)    0.50517E+01(112)
0.50903E+01(113)    0.51451E+01(114)    0.51538E+01(115)    0.51670E+01(116)
0.52198E+01(117)    0.52211E+01(118)    0.52790E+01(119)    0.53221E+01(120)
0.53390E+01(121)    0.54367E+01(122)    0.54431E+01(123)    0.55707E+01(124)
0.55846E+01(125)    0.56315E+01(126)    0.56422E+01(127)    0.56432E+01(128)
0.56854E+01(129)    0.56908E+01(130)    0.56930E+01(131)    0.57210E+01(132)
0.57992E+01(133)    0.58463E+01(134)    0.58675E+01(135)    0.58720E+01(136)
0.58727E+01(137)    0.58980E+01(138)    0.59423E+01(139)    0.59670E+01(140)
0.59927E+01(141)    0.60149E+01(142)    0.60199E+01(143)    0.60608E+01(144)
0.60868E+01(145)    0.60878E+01(146)    0.61199E+01(147)    0.61243E+01(148)
0.61825E+01(149)    0.62202E+01(150)    0.62720E+01(151)    0.63559E+01(152)
0.63880E+01(153)    0.64075E+01(154)    0.64950E+01(155)    0.65196E+01(156)
0.65607E+01(157)    0.65851E+01(158)    0.66699E+01(159)    0.66875E+01(160)

0.67147E+01(161)    0.67209E+01(162)    0.67482E+01(163)    0.67926E+01(164)
0.67966E+01(165)    0.68428E+01(166)    0.68752E+01(167)    0.68815E+01(168)
0.68983E+01(169)    0.69544E+01(170)    0.69781E+01(171)    0.70058E+01(172)
0.70086E+01(173)    0.70217E+01(174)    0.70644E+01(175)    0.70889E+01(176)
0.71047E+01(177)    0.71917E+01(178)    0.72572E+01(179)    0.72757E+01(180)
0.72813E+01(181)    0.73062E+01(182)    0.73264E+01(183)    0.73330E+01(184)
0.74077E+01(185)    0.74085E+01(186)    0.74226E+01(187)    0.74262E+01(188)
0.74343E+01(189)    0.74739E+01(190)    0.75320E+01(191)    0.75485E+01(192)
0.75547E+01(193)    0.75901E+01(194)    0.75979E+01(195)    0.76143E+01(196)
0.76212E+01(197)    0.76487E+01(198)    0.76704E+01(199)    0.77070E+01(200)
```

Figure C.8: Eigen Frequencies of Model-8

FINITE ELEMENT MODEL-9

```
RHS-VECTORS INITIALIZED: ML=      3 ND=  503403 SF.RHSIDE
EXTER. LOAD INITIALIZED: ML=      3 ND=  503403 SF.EXTLOD
CONST.DISP. INITIALIZED: ML=      3 ND=  503403 SF.DISCON
ELEMENTLOAD TO RHS-VECT: NV=      3 SF.RHSIDE
ELEMENTLOAD TO EXT.LOAD: NV=      3 SF.EXTLOD
ELEM. STIFFNESS STORED.
CONSIST. EL.MASS STORED.
DYNAMIC STRUCTURAL MASS  TM=   0.263E+05
RHS-VECTORS INITIALIZED: ML=      3 ND=  503403 SF.RHSIDE
EXTER. LOAD INITIALIZED: ML=      3 ND=  503403 SF.EXTLOD
CONST.DISP. INITIALIZED: ML=      3 ND=  503403 SF.DISCON
ELEMENTLOAD TO RHS-VECT: NV=      3 SF.RHSIDE
ELEMENTLOAD TO EXT.LOAD: NV=      3 SF.EXTLOD
TOTAL MASS OF FE-MODEL FOR LOAD-CASE(  2): 0.32995D+03
WEIGHT LOAD R.H.S.     : NV=      3 SF.RHSIDE
WEIGHT LOAD EXTERNAL   : NV=      3 SF.EXTLOD
 SPARSE: DIM=497175 NNZ(MAT)=19307959
 SOLVE: REDUCTION RES= 0.00E+00 (INIT. RES= 0.00E+00) NI=    1
 SOLVE: REDUCTION RES= 0.15E-09 (INIT. RES= 0.29E+05) NI=    1
 SOLVE: REDUCTION RES= 0.15E-09 (INIT. RES= 0.29E+05) NI=    1
STRESS STIFFNESS STORED
 SPARSE: DIM=497175 NNZ(MAT)=19307959
EIG-VEC, FILLED->TYINGS: ND=503403 NV=   200 NT=  6222
```

```
EIGEN-FREQUENCIES:
0.48232E+00(  1)    0.62229E+00(  2)    0.66851E+00(  3)    0.79257E+00(  4)
0.79292E+00(  5)    0.84636E+00(  6)    0.85687E+00(  7)    0.99840E+00(  8)
0.10301E+01(  9)    0.11114E+01( 10)    0.11431E+01( 11)    0.12073E+01( 12)
0.12692E+01( 13)    0.13306E+01( 14)    0.13505E+01( 15)    0.14159E+01( 16)
0.14174E+01( 17)    0.14440E+01( 18)    0.15483E+01( 19)    0.15858E+01( 20)
0.16026E+01( 21)    0.16730E+01( 22)    0.16743E+01( 23)    0.17114E+01( 24)
0.17496E+01( 25)    0.17641E+01( 26)    0.18478E+01( 27)    0.19462E+01( 28)
0.19482E+01( 29)    0.20031E+01( 30)    0.20169E+01( 31)    0.20927E+01( 32)
0.20979E+01( 33)    0.20981E+01( 34)    0.21181E+01( 35)    0.22745E+01( 36)
0.23127E+01( 37)    0.23213E+01( 38)    0.23314E+01( 39)    0.23344E+01( 40)
0.23548E+01( 41)    0.23833E+01( 42)    0.23840E+01( 43)    0.24245E+01( 44)
0.24566E+01( 45)    0.24582E+01( 46)    0.24959E+01( 47)    0.24961E+01( 48)
0.25880E+01( 49)    0.26021E+01( 50)    0.26592E+01( 51)    0.27377E+01( 52)
0.27392E+01( 53)    0.27884E+01( 54)    0.28119E+01( 55)    0.28425E+01( 56)
0.29206E+01( 57)    0.29264E+01( 58)    0.29445E+01( 59)    0.29700E+01( 60)
0.30117E+01( 61)    0.30140E+01( 62)    0.30305E+01( 63)    0.31070E+01( 64)
0.31529E+01( 65)    0.32178E+01( 66)    0.32428E+01( 67)    0.33010E+01( 68)
0.33223E+01( 69)    0.33247E+01( 70)    0.33621E+01( 71)    0.33782E+01( 72)
0.33807E+01( 73)    0.33849E+01( 74)    0.34894E+01( 75)    0.35014E+01( 76)
0.35359E+01( 77)    0.35822E+01( 78)    0.36117E+01( 79)    0.36769E+01( 80)
0.37226E+01( 81)    0.37233E+01( 82)    0.37250E+01( 83)    0.38122E+01( 84)
0.38392E+01( 85)    0.38416E+01( 86)    0.39326E+01( 87)    0.39681E+01( 88)
0.40313E+01( 89)    0.41446E+01( 90)    0.41642E+01( 91)    0.41685E+01( 92)
0.41763E+01( 93)    0.41856E+01( 94)    0.41900E+01( 95)    0.42011E+01( 96)
0.42657E+01( 97)    0.43237E+01( 98)    0.44663E+01( 99)    0.44934E+01(100)
0.45003E+01(101)    0.45028E+01(102)    0.45913E+01(103)    0.46295E+01(104)
0.46465E+01(105)    0.46748E+01(106)    0.46860E+01(107)    0.47276E+01(108)
0.48137E+01(109)    0.49057E+01(110)    0.49395E+01(111)    0.49443E+01(112)
0.50342E+01(113)    0.50514E+01(114)    0.50668E+01(115)    0.50844E+01(116)
0.51839E+01(117)    0.52195E+01(118)    0.52209E+01(119)    0.52717E+01(120)
0.53103E+01(121)    0.53260E+01(122)    0.54421E+01(123)    0.54465E+01(124)
0.55704E+01(125)    0.56312E+01(126)    0.56414E+01(127)    0.56419E+01(128)
0.56431E+01(129)    0.56866E+01(130)    0.56906E+01(131)    0.56918E+01(132)
0.57262E+01(133)    0.57808E+01(134)    0.58448E+01(135)    0.58592E+01(136)
0.58718E+01(137)    0.58871E+01(138)    0.58974E+01(139)    0.59327E+01(140)
0.59599E+01(141)    0.59668E+01(142)    0.59859E+01(143)    0.60146E+01(144)
0.60606E+01(145)    0.60673E+01(146)    0.60863E+01(147)    0.60873E+01(148)
0.60878E+01(149)    0.61076E+01(150)    0.61243E+01(151)    0.61515E+01(152)
0.63420E+01(153)    0.63563E+01(154)    0.63727E+01(155)    0.63937E+01(156)
0.64939E+01(157)    0.64963E+01(158)    0.65195E+01(159)    0.65596E+01(160)

0.66134E+01(161)    0.66261E+01(162)    0.66682E+01(163)    0.66821E+01(164)
0.67110E+01(165)    0.67196E+01(166)    0.67481E+01(167)    0.67879E+01(168)
0.67918E+01(169)    0.67961E+01(170)    0.68316E+01(171)    0.68752E+01(172)
0.69602E+01(173)    0.69893E+01(174)    0.70055E+01(175)    0.70064E+01(176)
0.70210E+01(177)    0.70577E+01(178)    0.71914E+01(179)    0.72502E+01(180)
0.72812E+01(181)    0.73004E+01(182)    0.73262E+01(183)    0.73292E+01(184)
0.73543E+01(185)    0.73986E+01(186)    0.74076E+01(187)    0.74079E+01(188)
0.74253E+01(189)    0.74335E+01(190)    0.74736E+01(191)    0.75317E+01(192)
0.75396E+01(193)    0.75531E+01(194)    0.75642E+01(195)    0.75932E+01(196)
0.76124E+01(197)    0.76204E+01(198)    0.76471E+01(199)    0.76701E+01(200)
```

Figure C.9: Eigen Frequencies of Model-9

FINITE ELEMENT MODEL-10

```
RHS-VECTORS INITIALIZED: ML=     3 ND=  406388 SF.RHSIDE
EXTER. LOAD INITIALIZED: ML=     3 ND=  406388 SF.EXTLOD
CONST.DISP. INITIALIZED: ML=     3 ND=  406388 SF.DISCON
ELEMENTLOAD TO RHS-VECT: NV=     3 SF.RHSIDE
ELEMENTLOAD TO EXT.LOAD: NV=     3 SF.EXTLOD
ELEM. STIFFNESS STORED.
CONSIST. EL.MASS STORED.
DYNAMIC STRUCTURAL MASS   TM=     458.
RHS-VECTORS INITIALIZED: ML=     3 ND=  406388 SF.RHSIDE
EXTER. LOAD INITIALIZED: ML=     3 ND=  406388 SF.EXTLOD
CONST.DISP. INITIALIZED: ML=     3 ND=  406388 SF.DISCON
ELEMENTLOAD TO RHS-VECT: NV=     3 SF.RHSIDE
ELEMENTLOAD TO EXT.LOAD: NV=     3 SF.EXTLOD
TOTAL MASS OF FE-MODEL FOR LOAD-CASE(  2): 0.24808D+03
WEIGHT LOAD R.H.S.      : NV=     3 SF.RHSIDE
WEIGHT LOAD EXTERNAL    : NV=     3 SF.EXTLOD
 SPARSE: DIM=404201 NNZ(MAT)=15622961
 SOLVE: REDUCTION RES= 0.00E+00 (INIT. RES= 0.00E+00) NI=    1
 SOLVE: REDUCTION RES= 0.19E-09 (INIT. RES= 0.24E+05) NI=    1
 SOLVE: REDUCTION RES= 0.19E-09 (INIT. RES= 0.24E+05) NI=    1
STRESS STIFFNESS STORED
 SPARSE: DIM=404201 NNZ(MAT)=15622961

   200 EIGENVALUES FOUND AFTER    2 ITERATIONS
```

C

```
EIGEN-FREQUENCIES:
0.62345E+00(  1)    0.85694E+00(  2)    0.11730E+01(  3)    0.12691E+01(  4)
0.15945E+01(  5)    0.17112E+01(  6)    0.17508E+01(  7)    0.20034E+01(  8)
0.20409E+01(  9)    0.21620E+01( 10)    0.21867E+01( 11)    0.22746E+01( 12)
0.24687E+01( 13)    0.26504E+01( 14)    0.28625E+01( 15)    0.30394E+01( 16)
0.30482E+01( 17)    0.32194E+01( 18)    0.32778E+01( 19)    0.33451E+01( 20)
0.33632E+01( 21)    0.34966E+01( 22)    0.35194E+01( 23)    0.36202E+01( 24)
0.37676E+01( 25)    0.46424E+01( 26)    0.47086E+01( 27)    0.48278E+01( 28)
0.49611E+01( 29)    0.49815E+01( 30)    0.50431E+01( 31)    0.51883E+01( 32)
0.52739E+01( 33)    0.53142E+01( 34)    0.53597E+01( 35)    0.56169E+01( 36)
0.56675E+01( 37)    0.56932E+01( 38)    0.60373E+01( 39)    0.60916E+01( 40)
0.61520E+01( 41)    0.62821E+01( 42)    0.64087E+01( 43)    0.66986E+01( 44)
0.67306E+01( 45)    0.67559E+01( 46)    0.67959E+01( 47)    0.72399E+01( 48)
0.72836E+01( 49)    0.73595E+01( 50)    0.74685E+01( 51)    0.75523E+01( 52)
0.76506E+01( 53)    0.76581E+01( 54)    0.76705E+01( 55)    0.77660E+01( 56)
0.78645E+01( 57)    0.78848E+01( 58)    0.79521E+01( 59)    0.80276E+01( 60)
0.81066E+01( 61)    0.83574E+01( 62)    0.84064E+01( 63)    0.85682E+01( 64)
0.90260E+01( 65)    0.91151E+01( 66)    0.92567E+01( 67)    0.92648E+01( 68)
0.93862E+01( 69)    0.95573E+01( 70)    0.97625E+01( 71)    0.98702E+01( 72)
0.99495E+01( 73)    0.10022E+02( 74)    0.10096E+02( 75)    0.10166E+02( 76)
0.10238E+02( 77)    0.10349E+02( 78)    0.10426E+02( 79)    0.10465E+02( 80)
0.10502E+02( 81)    0.10793E+02( 82)    0.10856E+02( 83)    0.10899E+02( 84)
0.10992E+02( 85)    0.11041E+02( 86)    0.11166E+02( 87)    0.11228E+02( 88)
0.11361E+02( 89)    0.11656E+02( 90)    0.11778E+02( 91)    0.11828E+02( 92)
0.11886E+02( 93)    0.11951E+02( 94)    0.12011E+02( 95)    0.12024E+02( 96)
0.12055E+02( 97)    0.12215E+02( 98)    0.12451E+02( 99)    0.12455E+02(100)
0.12511E+02(101)    0.12639E+02(102)    0.13077E+02(103)    0.13086E+02(104)
0.13147E+02(105)    0.13289E+02(106)    0.13330E+02(107)    0.13409E+02(108)
0.13505E+02(109)    0.13562E+02(110)    0.13646E+02(111)    0.13680E+02(112)
0.13702E+02(113)    0.13735E+02(114)    0.13745E+02(115)    0.13756E+02(116)
0.13783E+02(117)    0.13834E+02(118)    0.14017E+02(119)    0.14108E+02(120)
0.14147E+02(121)    0.14212E+02(122)    0.14267E+02(123)    0.14337E+02(124)
0.14434E+02(125)    0.14584E+02(126)    0.14649E+02(127)    0.14732E+02(128)
0.14854E+02(129)    0.14941E+02(130)    0.15024E+02(131)    0.15116E+02(132)
0.15197E+02(133)    0.15338E+02(134)    0.15344E+02(135)    0.15382E+02(136)
0.15412E+02(137)    0.15474E+02(138)    0.15654E+02(139)    0.15719E+02(140)
0.15729E+02(141)    0.15888E+02(142)    0.15998E+02(143)    0.16101E+02(144)
0.16263E+02(145)    0.16320E+02(146)    0.16324E+02(147)    0.16348E+02(148)
0.16452E+02(149)    0.16497E+02(150)    0.16634E+02(151)    0.16715E+02(152)
0.16741E+02(153)    0.16894E+02(154)    0.16982E+02(155)    0.17035E+02(156)
0.17090E+02(157)    0.17284E+02(158)    0.17371E+02(159)    0.17404E+02(160)

0.17451E+02(161)    0.17516E+02(162)    0.17622E+02(163)    0.17770E+02(164)
0.17787E+02(165)    0.17849E+02(166)    0.17965E+02(167)    0.17997E+02(168)
0.18099E+02(169)    0.18179E+02(170)    0.18182E+02(171)    0.18278E+02(172)
0.18307E+02(173)    0.18380E+02(174)    0.18489E+02(175)    0.18520E+02(176)
0.18558E+02(177)    0.18689E+02(178)    0.18726E+02(179)    0.18849E+02(180)
0.18875E+02(181)    0.18937E+02(182)    0.19085E+02(183)    0.19152E+02(184)
0.19190E+02(185)    0.19206E+02(186)    0.19277E+02(187)    0.19342E+02(188)
0.19377E+02(189)    0.19404E+02(190)    0.19495E+02(191)    0.19537E+02(192)
0.19641E+02(193)    0.19662E+02(194)    0.19726E+02(195)    0.19895E+02(196)
0.19916E+02(197)    0.19989E+02(198)    0.20090E+02(199)    0.20121E+02(200)
```

Figure C.10: Eigen Frequencies of Model-10